Optimization of alpha emitter's determination in water. Behavior of radionuclides in water treatment plants

a dissertation submitted to the PhD program on

Nuclear Engineering and Ionizing Radiation

of Universitat Politècnica de Catalunya

in partial fulfillment of the requirements

for the degree of Doctor of Philosophy

Montserrat Montaña Gurrera

June 2013

I certify that I have read this dissertation and that, in my opinion, it is fully adequate in scope and quality as a dissertation for the degree of Doctor of Philosophy, program on Nuclear Engineering and Ionizing Radiation.

_____

(Antonia Camacho García) Principal Advisor

I certify that I have read this dissertation and that, in my opinion, it is fully adequate in scope and quality as a dissertation for the degree of Doctor of Philosophy, program on Nuclear Engineering and Ionizing Radiation.

_____

(Isabel Vallés Murciano) Principal Co-Advisor

Summary

Gross alpha activity measurement is one of the simplest radioanalytical procedures which are widely applied as screening techniques in the fields of radioecology, environmental monitoring and industrial applications. It is used as the first step to perform a radiological characterization of drinking water. According to the WHO guidelines (2011), this screening parameter must be measured in drinking water to ensure that it is safe for consumption.

Different methods are used to measure gross alpha activity. Two of them, the classic ones, are based on evaporation (EPA, 1980) or co-precipitation (EPA, 1984) of the sample, using either a gas proportional counter or a solid scintillator detector. Another alternative method based on concentration of the sample and measurement by liquid scintillation counting (ASTM, 1996), is being increasingly used.

The gross alpha activity of a water sample is an estimate of the actual alpha activity of the water sample (excluding radon). However, it is usually considered that gross alpha activity must be very close to the sum of alpha emitter activities, though in general this is not the case. There are many other factors (e.g., alpha particle energies, calibration standard used, time elapsed from sample preparation to measurement and variability of the results between methods) that affect the gross alpha measurement causing major differences between the gross alpha activity values and the sum of the activities of the main alpha emitters. For this reason, we propose to conduct an eminently experimental study to determine most of the possible factors that may be involved in the above mentioned variability of the results. In addition, we intend to propose a detailed procedure on that basis to establish both their range of validity and the most suitable conditions for their use, thereby ensuring: (A) that the result obtained is the most representative of the sample's real total alpha activity; (B) that it is subject to the lowest technically possible variability; and (C) that this remaining variability is taken into account in determining the

uncertainty associated with the result. In this context, we propose to study these aforementioned considerations using the co-precipitation method.

Aditionally, given the problems with the scarcity and quality of water, the implementation of water treatment plants has been significantly increasing over the last years in several countries. Consequently, large quantities of solid wastes or sludge are generated every year which can be re-used for different applications. These solid wastes may contain all kind of pollutants, including significant levels of radioactivity.

For these reasons, it is considered important studying the occurrence and behavior of radioactivity in water treatment plants. Although radioactivity in water treatment plants has been studied by some authors, we propose an original work analyzing the radioactive temporal evolution in different water treatment plants in which drinking and wastewater are treated. These plants have been selected taking into account both variations in water source and the treatment applied.

This thesis contributes to these goals by analyzing the factors that affect the gross alpha measurement, involving an optimization and validation of the co-precipitation method and studying the behavior of radionuclides in water treatment plants. To this end, Part I provides a comprehensive analysis for the optimization and validation of the gross alpha activity determination using the co-precipitation method. Then, in Part II, we present a set of case studies related to the radionuclide behavior and the temporal evolution of the radioactivity in different drinking water and wastewater treatment plants.

Thesis contributions and structure

The contributions of this thesis are multifold. It is divided into two parts, and a total of 7 chapters as detailed next.

Part I provides a comprehensive analysis for the optimization and validation of the gross alpha activity determination using the co-precipitation method.

<u>Chapter 1</u> presents preliminary considerations related to the co-precipitation procedure as a result of the existence of different versions of this method with some discrepancies among them. This chapter also includes a morphological study of the residue obtained by the co-precipitation method to verify the uniformity of this residue and its mass and efficiency stability as well as a study of the precipitation pH influence, especially on uranium isotopes due to variety of chemical species formed by uranium in solution. Although the co-precipitation is not a new methodology, this chapter is primarily intended to study in detail the procedure by analyzing the critical points that arise due to the discrepancies observed among different versions of the co-precipitation method in order to optimize this methodology and to rewrite a procedure which is presented in Appendix A.

<u>Chapter 2</u> provides mass efficiency curves in ZnS(Ag) and gas proportional detectors using different calibration standards (^{230}Th, ^{nat}U, ^{241}Am, ^{226}Ra and ^{224}Ra). The objective is to benchmark their performance when measuring gross alpha activity using the co-precipitation procedure. Additionally, the following parameters were studied: efficiency dependence on alpha particle energy, and the repeatability of the efficiency and temporal stability of the residue. Part of the results of this chapter as well as those presented in Chapter 1 have been published in the Journal Applied Radiation and Isotopes (Montaña et.al, 2012).

<u>Chapter 3</u> proposes a validation of the co-precipitation method which is optimized using different kinds of water samples (synthetic water, surface water, groundwater and wastewater)

as well as through intercomparisons. Furthermore, a comparative study of gross alpha activity using three different methodologies is also included. Part of the results of this chapter have been published in the Journal of Environmental Radioactivity (Montaña et.al, 2013a).

This part of the Thesis was partially done within the framework of the project entitled "Estudio de la problemática existente en la determinación del índice de actividad alfa total en aguas potables. Propuesta de procedimientos" funded by the Spanish "Consejo de Seguridad Nuclear", and the framework of a four-month internship at Radiochemistry Unit at Wisconsin State Laboratory of Hygiene (WSLH), USA.

Part II applies research related to the radionuclide behavior in different water treatment plants.

Chapter 4 consists on a temporal evolution study for water samples from two conventional drinking water treatment plants (DWTP) located in Spain. This chapter also includes a detailed study related with the reverse osmosis (RO) treatment applied later in one of the DWTPs studied, and which was published in the INSINUME special issue of the Journal of Environmental Radioactivity (Montaña et al. 2013b). Moreover, a seasonal study of radioactivity in the sludge from these DWTPs is presented.

Chapter 5 includes a screening study of the presence of radionuclides in eleven Spanish wastewater treatment plants (WWTPs). This study was published in the Journal of Cleaner of production (Montaña et al., 2011). Additionally, a seasonal study in some of these WWTPs is presented being the main objective the radiological characterization of liquids samples collected in two Spanish WWTPs, where an increase of gross alpha activity had previously been detected. The samples were collected to determine the stage of the treatment where the increase of radioactivity was produced, which radionuclides contribute to gross alpha activity and whether the radionuclides were likely to cause an effect on public health. This study was published in the Journal of Environmental Radioactivity (Camacho, Montaña, et al 2012). It should be highlighted that the study constitutes one of a limited number of publications investigating temporally based sampling to access the behavior of natural radionuclides in WWTP's. Chapter 5 also includes the seasonal study in sludge samples collected, in this case, in three Spanish WWTPs and the results were published in the Journal of Radioanalytical and Nuclear Chemistry (Camacho, Montaña et al., 2013). Finally, on the occasion of the international research stay made in the Radiochemistry Unit at Wisconsin State Laboratory of Hygiene (USA), a preliminary study of a municipal conventional full scale WWTP located in Midwest of the United States (Waukesha-Wisconsin) is also included in this chapter.

Chapter 6 provides an evaluation of the radiological hazards associated with natural radionuclides taking into account the main uses of the sludge generated in the water treatment plants previously studied in Chapters 5 and 6, as well as their evaluation as a NORM. Part of these results were published in the Journal of Radioanalytical and Nuclear Chemistry (Camacho, Montaña et al., 2013).

This part of the Thesis was partially done within the framework of the project SOSTAQUA (CEN2007-1039) led by Aguas de Barcelona and funded by the CDTI (Center for the Development of Industrial) and the framework of a four-month internship at Radiochemistry Unit at Wisconsin State Laboratory of Hygiene (WSLH), USA.

Part III provides general conclusions and future works related to the work made in this thesis. It is worth mentioning that in each chapter is also presented a summary with the conclusions extracted from each study.

x

Acknowledgments

I would like to thank my advisers Dr. Antonia Camacho and Dr. Isabel Vallés for both guiding me throughout the course of these four years and for granting me the opportunity to conduct research within the INTE Research Institute at UPC.

I also have gratitude for the valuable advice and collaboration received from Dr. Mike Ardnt and Lynn West from Wisconsin State Laboratory of Hygiene. I would also like to thank Dr. Ricard Devesa, Dr. Raquel Céspedes-Sánchez from Aguas de Barcelona, Mrs. Montse Marsal and Mr. Isac López from UPC's Department of Materials Science and Metallurgical Engineering, for the fruitful collaborations and the works accomplished together.

I will always remember all the friends and colleagues I happened to meet during this exciting 4-year period, whether in Spain or Wisconsin, it's been fantastic to meet you all: Vanessa, Marta, Maria, Sonia, Antonia, Ma Amor, Natalia, Roger, Isa, Vicente, Vitaly, Ma Carme, Juan Antonio, Alex, Fransesc, Miguel, Claudia, Albert, Loli, Sara, Anna, Arianna, Danielle, Gary, Jack, Dan, Dave, Mike, Julio, Jessie, Lynn, Marla, Ora, Luie (the evil cat!!) ...hope I am not forgetting anyone....

However, it wouldn't have been possible, hadn't been for the unconditional support and patience received from my family: Oscar and family, my parents and my brother! Also my closest friends, thanks for not asking about my thesis!

Contents

5. Behavior of radionuclides in wastewater water treatment plants

6. Evaluation of radiological hazard effects of sludge samples from water treatment plants

Part I

Optimization of alpha emitter's determination in water

Introduction

Gross alpha measurement is one of the simplest radioanalytical procedures which are applied widely as a screening technique in the fields of radioecology, environmental monitoring and industrial applications. It is used as the first step of radiological characterization of drinking water. According to the WHO guidelines (2011), this screening parameter must be measured in drinking water to ensure that it is safe for consumption. In the Spanish Royal Decree on drinking water quality (RD 140/2003) the recommended reference level is 0.1 Bq/L for gross alpha activity. If the measured value is below the reference level of gross alpha activity, the drinking water analyzed is acceptable for human consumption without any further action with respect to its alpha radioactivity. Otherwise, a nuclide specific analysis is required to determine Total Dose Indicative (TDI) using more time-consuming procedures.

Different methods are used to measure gross alpha activity. Two of them, the classic methods, are based on evaporation (EPA, 1980) or co-precipitation (EPA, 1984) of the sample, using either a gas proportional counter or a solid scintillator detector. Another alternative method based on concentration of the sample and measurement by liquid scintillation counting (ASTM, 1996) is being increasingly used.

However, it is usually considered that gross alpha activity must be very close to the sum of the alpha emitter activities that are present in the sample (^{210}Po, radium, and uranium isotopes). Nevertheless, there are several factors (e.g., alpha particle energies, calibration standard used and time elapsed from sample preparation to measurement) that can cause major differences between the gross alpha activity values and the sum of the activities of the main alpha emitters. We therefore propose to conduct an eminently experimental study to determine all the possible factors that may be involved in the above mentioned variability of the results. In addition, we intend to propose a detailed procedure on that basis to establish both their range of validity and the most suitable conditions for their use, thereby ensuring: (A) that the result obtained is the most representative of the sample's real total alpha activity; (B) that it is subject to the lowest

technically possible variability; and (C) that this remaining variability is taken into account in determining the uncertainty associated with the result. In this context we propose to study these considerations above mentioned using the co-precipitation method.

Focusing on the co-precipitation method, such as EPA method (1984), standard methods 7110C (APHA, 1998) or the method described by Suarez-Navarro et al. (2002), the radionuclides of an aliquot of water are co-precipitated with a mixture of barium sulphate and ferric hydroxide. The precipitate is collected onto a filter, which is placed on a planchet. The obtained mass of this precipitate is always around 18 mg because the residue mass is mainly limited by the amount of barium and iron carriers added to the sample and not by the level of dissolved solids. Thus, for samples with high levels of dissolved solids such as wastewater, seawater or groundwater samples, a co-precipitation method would be preferable. Consequently, the MDA achieved with co-precipitation (0.0019-0.0023 Bq/L) is very sensitive and is one order of magnitude lower than that of the evaporation method (0.023-0.031 Bq/L) under the same measuring conditions (Suarez-Navarro et al., 2002). Furthermore, the co-precipitation method produces residues that appear to be relatively uniform and reproducible, though some authors consider that the residue might be hygroscopic (Suarez-Navarro et al., 2002; Jobbágy et al., 2010). Therefore, we propose a morphological study of the residue obtained by the co-precipitation method to verify the uniformity of this residue and its mass and efficiency stability. Additionally, ^{241}Am is recommended as a radionuclide standard for mass efficiency calibration by the co-precipitation method (EPA, 1997), while APHA (1998) recommends the use of ^{230}Th, ^{nat}U, ^{239}Pu, or ^{241}Am. In some countries, the most common calibration standard used up to now is ^{241}Am, but nevertheless, the tendency and recommendation is to use ^{230}Th or ^{nat}U.

For this method, ^{241}Am efficiency curves have been constructed by some authors (Suarez-Navarro et al., 2002; Parsa et al., 2011). Parsa et al (2005; 2011) also drew mass efficiency curves using ^{230}Th as a standard calibration in different proportional gas counters with a residue mass ranging between 20 and 140 mg. As mentioned above, other radionuclides are recommended to be used as a standard calibration and so far ^{nat}U efficiency curves have still not been reported in the literature. We have therefore considered studying the mass efficiency curve using ^{nat}U as a standard calibration in both detection systems (gas proportional counter and ZnS(Ag)) and we have compared it with other standard calibrations (^{230}Th and ^{241}Am). We chose ^{nat}U since it is more likely to be found in natural waters.

The focus of this part of the thesis is therefore set on the study and validation of the co-precipitation method. To be precise, we first propose in Chapter 1 preliminary considerations that we have to take into account to optimize the procedure in order to minimize the variability of the results between gross alpha activity values and the sum of the activities of the main alpha emitters. These considerations are related with some steps of the procedure and they will be

described in different sections of this chapter. Then, Chapter 2 incorporates the calibration of the method in ZnS(Ag) and gas proportional detectors using different calibration standards (^{230}Th, ^{nat}U and ^{241}Am) in order to find out how they performed when measuring gross alpha activity using this procedure. Moreover, this chapter incorporates the determination of ^{224}Ra and ^{226}Ra efficiency curves in gas proportional detectors. This work was done at the Wisconsin State Laboratory of Hygiene (WSLH) at University of Wisconsin in the City of Madison, USA. Finally, Chapter 3 describes and presents the validation of the co-precipitation method taking into account different water matrix samples, to be precise, in synthetic water, drinking water, surface and groundwater, and wastewater matrix samples.

Chapter 1

Gross alpha activity by co-precipitation method

1.1   Introduction and motivation

Some versions related to the co-precipitation method exist with some discrepancies within them. According to the EPA-approved gross alpha co-precipitation procedure (EPA 1984; APHA, 1998), detergent diluted and paper pulp are used in this method. However, in the procedure optimized in this thesis, which is described in greater detail in Appendix A, and the procedure reported by Suarez-Navarro et al. (2002) and the Spanish Nuclear Safety Council (CSN, 2005) no addition of detergent and paper pulp were considered. For this reason, it was considered interesting to study the advantages or drawbacks of diluted detergent and paper pulp addition.

Furthermore, the co-precipitation method produces residues that appear to be relatively uniform and reproducible, though some authors consider that the residue might be hygroscopic (Suarez-Navarro et al., 2002; Jobbágy et al., 2010). Therefore, we propose a morphological study of the residue obtained by the co-precipitation method to verify the uniformity of this residue and its mass and efficiency stability.

On the other hand, one of the co-precipitation steps depends on the pH in order to form the $Fe(OH)_3$ precipitate and thereby we propose to study the precipitation pH influence, specially on uranium isotopes due to variety of chemical species formed by uranium in solution.

And eventually, because of the significant disparities between the elapsed time reported in the different versions of the co-precipitation method (3 hours or two days), it was also considered interesting studying the temporal evolution of the gross alpha activity detected in the blank with the aim to check that no alpha activity contribution there is in the blank.

Although, the co-precipitation is not a new methodology, this chapter is primarily intended to study in detail the procedure analyzing mainly the critical points due to the discrepancies observed among different versions of the co-precipitation method in order to optimize this methodology.

1.2   Diluted detergent and paper pulp addition

As mentioned in the previous section, some versions related to the co-precipitation method exist with some differences between them. One of the main differences between procedures is the use of detergent diluted and paper pulp in order to collect the precipitate. Therefore, this section focuses on the question whether the paper pulp and detergent diluted addition is necessary to obtain good precipitation yields.

Figure 1.1 illustrates the co-precipitation procedure described in Annex I, as well as the procedure using paper pulp and diluted detergent. In general, in the co-precipitaion method such as EPA method (1984), standard methods 7110C (APHA, 1998) or the method described by Suarez-Navarro et al. (2002), the radionuclides of an aliquot of water are co-precipitated with a mixture of barium sulphate and ferric hydroxide ($BaSO_4$ and $Fe(OH)_3$). The precipitate is collected onto a filter, which is placed on a planchet. The obtained mass of this precipitate is always around 18 mg because the residue mass is limited by the amount of barium and iron carriers added to the sample and not by the level of dissolved solids.
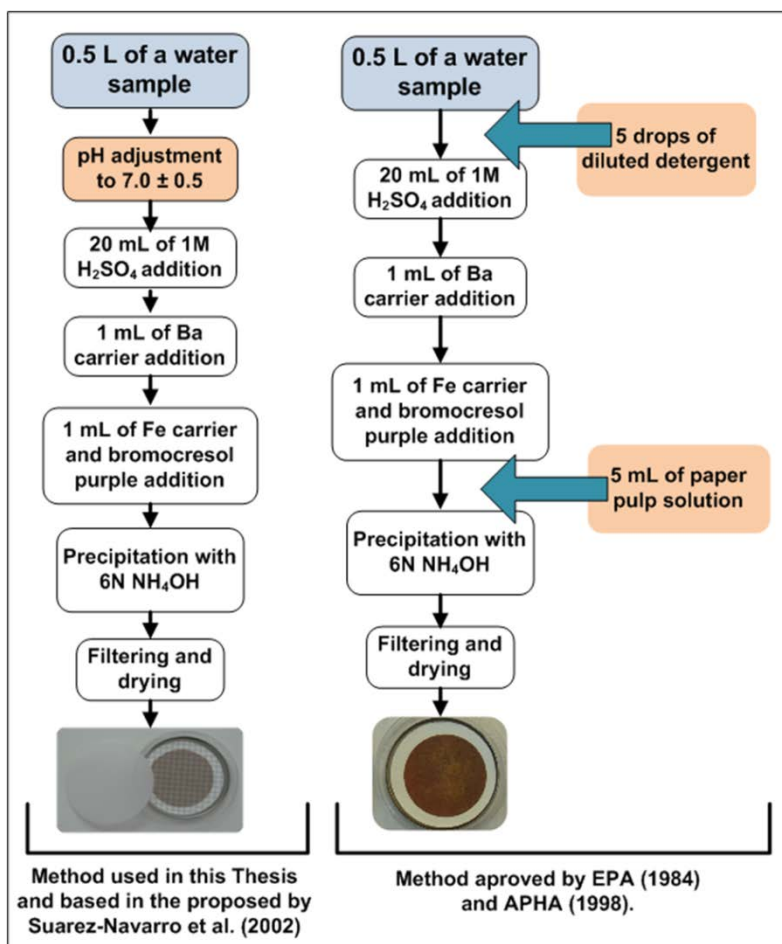
Figure 1.1. Schemes of the co-precipitation procedure used in this thesis (without paper pulp and diluted detergent) and the co-precipitation method using paper pulp and diluted detergent).

Diluted detergent addition

The addition of detergent (or surfactant) in the previous step to the barium sulfate precipitation induces barium sulfate nucleation but it is going to demonstrate that this addition is not necessary obtaining high barium yields. This was accomplished preparing 13 samples spiked with 1 g of 59.280 ± 0.017 Bq/g (*k=2*) [133]Ba traceable solution and measured by gamma spectrometry using a HPGe gamma detector. The chemical yield of barium for each sample (Table 1.1) was determined using the full energy peaks of [133]Ba standard (81, 276.4, 302.85, 356.01 and 383.85 KeV).

As we can see in Table 1.1, [133]Ba yields were about of 100% and therefore, addition of detergent in the co-precipitation method is not strictly necessary. These results are in agreement with those using detergent diluted in the procedure reported by Parsa et al. (2005; 2011).

Table 1.1. Chemical yields obtained for the 13 water samples spiked with [133]Ba without detergent addition.

Sample Code	Yield	Uncertainty[1]
Ba_1	101.1	1.9
Ba_2	102.7	2.0
Ba_3	100.3	1.9
Ba_4	105.6	2.0
Ba_5	96.8	1.9
Ba_6	94.4	1.8
Ba_7	100.1	1.9
Ba_8	98.8	1.9
Ba_9	94.8	1.8
Ba_10	99.2	1.9
Ba_11	102.1	2.0
Ba_12	100.0	1.9
Ba_13	97.8	1.9
Mean	**99.5**	**3.1[2]**

[1]Uncertainty expressed ($k=2$), includes weighted uncertainty of each peak and the uncertainty of [133]Ba standard solution.
[2]Relative Standard Deviation = standard deviation/mean*100.

Paper pulp addition

According to the Standard Methods procedure (APHA, 1998), ion hydroxide precipitates collected on membrane filters without a holding agent flake when dried can be easily lost from the filter, but adding 5 mg of paper pulp fiber to the initial water sample helps to secure the iron hydroxide to the filter.

Our results demonstrate a good adherence of the precipitate onto the cellulose nitrate filter used without paper pulp addition in water sample. Moreover, paper pulp can decrease the efficiency and the homogeneity of the precipitate. Table 1.2 shows [230]Th efficiencies for two residues using either or not paper pulp in the initial water. This was achieved by proportionately varying the amount of barium and iron carriers in the methods (1 and 1.4 mL of each carrier), analyzing aliquots of de-ionized water spiked with [230]Th [activity = 13.2 ± 0.7 (*k=2*) Bq/g]. The precipitates obtained were counted in a gas-flow proportional detector.

Table 1.2. ^{230}Th efficiencies obtained in the co-precipitation method using either or not paper pulp for two different amounts of Ba and Fe carriers.

paper pulp addition	amount added of each carrier (mL)	mass obtained (mg)	^{230}Th efficiency values (cps/dps) in gas-flow proportional detectors (Protean)									
			1	**2**	**3**	**4**	**5**	**6**	**7**	**8**	**9**	**10**
NO	1	17.8	0.147	0.141	0.146	0.138	0.140	0.136	0.138	0.144	0.137	0.127
(our method)	1.4	24.5	0.122	0.121	0.123	0.119	0.116	0.115	0.120	0.120	0.110	0.105
YES	1	22.4	0.135	0.129	0.133	0.127	0.125	0.121	0.125	0.132	0.124	0.117
(5 mg of paper pulp)	1.4	28.8	0.106	0.102	0.107	0.101	0.099	0.100	0.100	0.106	0.100	0.093
efficiency reduction percentage			8%	9%	9%	8%	10%	11%	9%	9%	10%	8%
			13%	15%	13%	15%	15%	13%	16%	12%	9%	11%

The efficiencies obtained using paper pulp are slightly lower than those efficiencies obtained without paper pulp due to the increase in the residue obtained (using the same amount of carriers). The efficiency reduction obtained was between 8% and 16% and therefore paper pulp addition reduces gross alpha efficiency in gas flow proportional detector.

In order to study the homogeneity of the residue, Table 1.3 graphically shows different sample preparations by using, and by not using paper pulp, more specifically, simple preparations using paper pulp and preparations applying the entire co-precipitation methods (by using, and by not using paper pulp). The differences between them are the conditions established with the aim to achieve an uniform distribution onto the filter surface. In Figure 1.2 is presented a schematic procedure of the paper pulp dilution applied to the different experiments briefly presented in Table 1.3. In this figure is also included the conditions which can vary for each experiment.
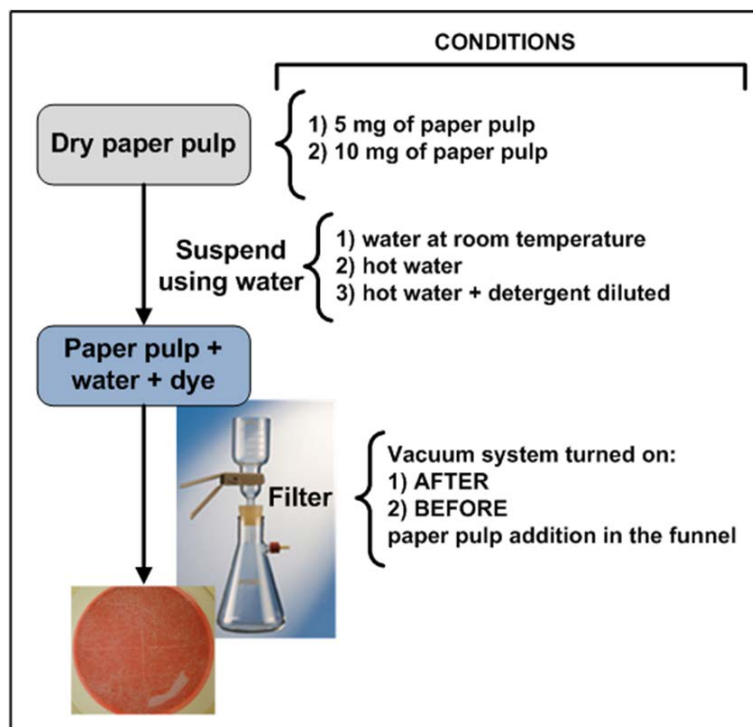
Figure 1.2. Schematic procedure of the paper pulp suspension. Paper pulp or the filter are dyed so that it is easier to see the paper pulp distribution onto the filter.

As it is observed in Table 1.3, several conditions can improve the distribution of the paper pulp onto the filter but the amount of paper pulp established in the co-precipitation procedure by APHA (1998) (5 mg of paper pulp) is not enough to cover evenly the surface filter. The best
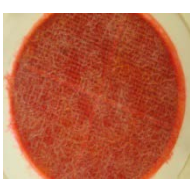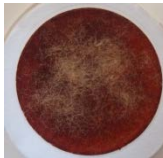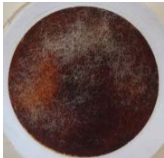
distribution was achieved using 10 mg of paper pulp. On the other hand, using the recommended amount in the procedure approved by APHA (1998) (5 mg), if the paper pulp is mixed with hot water as well as with hot water and diluted detergent at the same time, a better distribution onto the filter is achieved (see work conditions 1 to 5).

Moreover, the way how the precipitate (obtained by the co-precipitation method using paper pulp) is filtered can cause a non-uniform distribution of the paper pulp in the precipitate and this distribution doesn't appear to be reproducible. Therefore we recommend not using paper pulp to avoid both a decrease in gross alpha efficiency and a non-uniform distribution of the paper pulp in the precipitate.

Table 1.3. Brief descriptions and results of different work conditions applied in the co-precipitation method taking into account the paper pulp addition.

Work conditions	Picture	Resutls
1) 5 mg of paper pulp The vacuum system was turned on **before** the paper pulp addition in the funnel.		The paper pulp is not evenly distributed onto the filter.
2) 5 mg of paper pulp The vacuum system was turned on **after** the paper pulp addition in the funnel.		The paper pulp is not evenly distributed onto the filter.
3) 10 mg of paper pulp The vacuum system was turned on **after** the paper pulp addition in the funnel.		The paper pulp is almost evenly distributed onto the filter.
4) 5 mg of paper pulp + hot water The vacuum system was turned on after the paper pulp addition in the funnel.		The paper pulp is evenly distributed onto the filter. It was checked using an optical microscope.
5) 5 mg of paper pulp + hot water + 5 drops of detergent diluted The vacuum system was turned on **after** the paper pulp addition in the funnel.		The paper pulp is evenly distributed onto the filter. It was checked using an optical microscope.
Co-precipitation method (EPA procedure: paper pulp previously stirred and mixed with detergent diluted. Addition of 5 mL of the mixture before precipitation of $Fe(OH)_3$)	 replicate 1 replicate 2	Paper pulp distribution is not reproducible. It is not possible guarantee an uniform distribution onto the filter. Some areas are not covered with paper pulp.
Co-precipitation method used in this Thesis (no paper pulp addition)	 replicate 1 replicate 2	Without addition of paper pulp the precipitate's distribution seems to be uniform.

1.3 Distribution and morphology of the residue

In this section experiments are presented to demonstrate the uniformity of the residue (precipitate) obtained by the co-precipitation method used in this Thesis (without paper pulp and detergent diluted addition).

This method gives visibly uniform residues (Figure 1.3a), but it is important to characterize the geometry of the solid film to some degree of precision. Figure 1.3b represents a visible light micrograph (see Appendix B for the instrumentation) from the 18 mg residue section with 1.25 magnification which enables us to see the precipitate distribution on the filter in detail. It was observed that the precipitate was not a solid continuous film. This is because the solid film is fragmented in the shape of small regions during the drying process and maintains an order that is seen by using visible light threshold micrographs and calculating the equivalent diameter. A threshold was determined visually for each image such that pixels exceeding the threshold coincided with the small areas of precipitate using Buehler Omnimet software. In Figures 1.4a, 1.4b and 1.4c the pixels exceeding the threshold are shown in red.
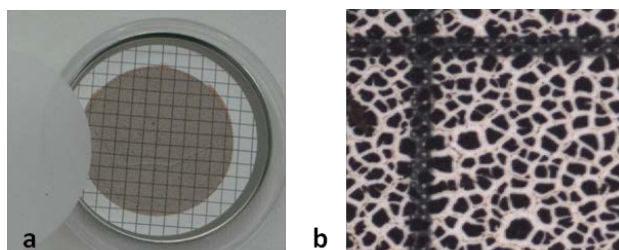
Figure 1.3. a) Picture of a residue obtained by the co-precipitation method. b) Picture with x1.25 magnification obtained by an optical microscope connected to a digital camera.

Figure 1.4a shows the micrograph for the 18 mg residue section, from which the fragment size (equivalent diameter) was found to be in the range 20–135 μm. Figures 1.4b and 1.4c represent the visible light micrograph of the 26.8 and 34.5 mg residue sections, from which we observed that the fragment size (equivalent diameter) ranged from 20 to 270 and 20 to 300 μm. These residues were obtained varying the amount of barium and iron carriers in the method (1.5 and 2 mL of each carrier in order to obtain about 27 and 35 mg of residue respectively). From these figures, we observed that the equivalent diameter for 18 mg residue samples (Figure 1.4a) was smaller than the other two samples. As we have seen in the previous figures, the equivalent

diameter range is more limited in the 18 mg residue. Therefore, the heavier the residue, then the more irregular is the equivalent diameter, while the equivalent diameter differences between heavier residues (26 to 35 mg) are smaller.
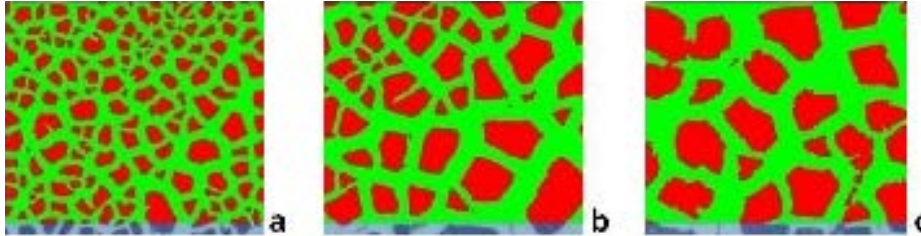
Figure 1.4. a, b and c. Corresponding threshold images from a section of residue pictures of 18.0, 26.8 and 34.5 mg (from left to right).

It is possible to calculate the percentage area of the filter filled with residue or air. Table 1.4 shows the percentage area of the filter filled with residue or filled with air of the samples containing 18.0, 26.8 and 34.5 mg of the precipitate. These values were obtained by calculating the percentage of each coloured area (green for air and red for precipitate area) from figures 1.4a, 1.4b and 1.4c. Another four figures from each sample were used to calculate these areas and to provide different sections of the residue. They also help to improve the area values.

Table 1.4. Percentage of area filled with precipitate and air in each sample with different amounts of precipitate.

| Sample mg | % area filled with | |
	Precipitate (red area)	Air (green area)
18.0 mg	41.4	58.6
26.8 mg	45.3	54.7
34.5 mg	49.1	50.9

There is a tendency to fill more filter area with precipitate when the residue amount increases. From the residues studied, the 18 mg residue presents a percentage area of precipitate of 41%. This value increases up to 50% when the residue mass is 34.5 mg.

According to Ardnt (2010), the precipitate obtained by the co-precipitation method is a heterogeneous mixture of $BaSO_4$ and $Fe(OH)_3$, and there is no guarantee that the spatial distribution of a radionuclide in such a residue is uniform. For this work, the homogeneity of the $BaSO_4$ and $Fe(OH)_3$ mixture was evaluated using a scanning electron microscope (SEM) (see Appendix B for the instrumentation).

Figure 1.5a shows a fragment of the precipitate in which it was possible to identify $BaSO_4$ crystals and $Fe(OH)_3$. The small cubic structure (size: 2μm) is $BaSO_4$, while the other amorphous structure is $Fe(OH)_3$. It was possible to identify each structure using an EDX system. This system is capable of identifying different atoms, in this case barium and iron, using a high-energy beam of electrons which is focused onto the sample being studied. The number and energy of the X-rays emitted from a specimen after being irradiated can be measured by an energy-dispersive spectrometer. The energy of the X-rays is characteristic of the atomic structure of the element from which they were emitted and this allows the elemental composition of the specimen to be measured.

Furthermore, it is possible to obtain a superficial distribution map using this technique. In Figures 1.5b and 1.5c, the superficial distribution of barium atoms from $BaSO_4$ and ferric atoms from $Fe(OH)_3$ can be seen. From these scanning electron micrographs, it is clear that there is an excellent distribution of the barium and ferric salts.
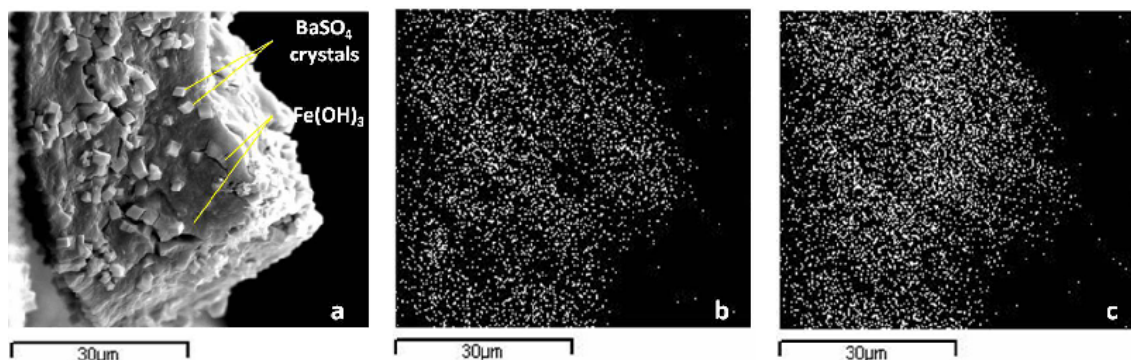
Figure 1.5. a) Scanning electron micrograph of an 18 mg sample fragment; barium and ferric salt identification. b) Barium atom distribution map from $BaSO_4$; c) Iron atom distribution map from $Fe(OH)_3$.

Furthermore, the spatial distribution of the radionuclides had been studied by Parsa and collaborators (2011). In their article they analyzed the radionuclide composition of each precipitate fraction and it was found that alpha radionuclides were recovered in high yields. To be precise, the uranium co-precipitate favours the $Fe(OH)_3$ fraction, while radium favours the $BaSO_4$ fraction. ^{230}Th and ^{241}Am are recovered from either precipitate. ^{133}Ba and ^{59}Fe were used to determine the respective chemical recoveries of $BaSO_4$ and $Fe(OH)_3$ fractions in the mixed precipitate and high yields were obtained. Therefore, it can be stated that the distribution of the mixture and the radionuclides are homogeneous and variations in the gross alpha activity would be minimized.

This study was extended to determine the height of the residue for different amounts of the precipitate in order to understand the mass-efficiency curve behaviour for various calibration standards (^{230}Th, ^{241}Am, ^{nat}U) used in our laboratory routines as well as in order to know the behaviour of ^{226}Ra, ^{224}Ra and their short-lived radionuclides efficiencies.

Figure 1.6 represents the scanning electron micrograph of a transverse section of the 18 mg sample. In this figure a small part of the filter with its precipitate is seen, from which the average height of the precipitate was found to be 32 μm (RSD=8%, n=17). For the residues with 26.8 and 34.5 mg, the average height was 35 and 56 μm, respectively. In Table 1.5 the residue height and the statistical parameters for each residue studied by SEM are presented.
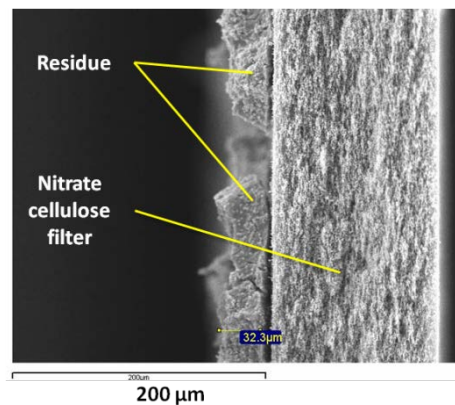
Figure 1.6. Scanning electron micrograph of a transverse section of the 18 mg sample.

Table 1.5. Statistical parameters for the residue height determined in different samples by scanning electron microscopy.

Sample	Residue height (µm)			
(mg)	Minimum	Maximum	Average	RSD (%)
18.0	28	36	32 (17)	8
26.8	26	55	35 (17)	27
34.5	39	78	56 (23)	19

The data used in the calculations is indicated in brackets.
RSD% = Standard deviation*100/average value.

According to the results reported in table 1.5, the height for residues between 18 and 27 mg seem to be constant. Instead, for a 34.5 mg of residue an increase in height is observed. Therefore, take into account the results obtained from Figure 1.4 and Table 1.4, for a 34.5 mg residue, the precipitate cannot fill more the surface of the filter and starts to increase in height.

1.4 Alpha emitters precipitation checking: Uranium recovery at different pH´s.

Co-precipitation is a complex, non-specific process, since there can be various mechanisms responsible for the collection of soluble metal ions including adsorption, inclusion, occlusion, and the formation of a solid solution. When elements are present at very low concentrations in water, as is often the case for natural radionuclides (U, Ra, Th…), the main co-precipitation mechanism is adsorption of the species in solution (Landa, et al., 1995).

The co-precipitaion method studied successfully co-precipitates many radionuclides of interest as it was reported by Suarez et al. (2009) and Parsa et al. (2011). For example, Parsa and collaborators (2011) studied the selectivity of various radionuclides toward the two precipitate components, $BaSO_4$ and $Fe(OH)_3$. It was found that polonium and uranium co-precipitate with the $Fe(OH)_3$ fraction, while radium isotopes favor the $BaSO_4$ portion. Thorium and americium are recovered in high yields from either precipitate.

Considering the natural alpha emitters [210]Po, [224]Ra, [226]Ra, [234]U and [238]U which are the most likely to find dissolved in drinking water samples, uranium isotopes depend strongly on the water's hydrogencarbonate and the pH. Since hydrogencarbonates are removed after H_2SO_4

addition in the co-precipitation method, the problem lies mainly in the $Fe(OH)_3$ precipitation step and, therefore, we propose to study the precipitation pH influence on uranium isotopes.

Thus, it is necessary to take into account the chemical species most frequently formed by uranium in solution. Uranium has different oxidation states : U^{3+}, U^{+4}, UO_2^{2+} (+5) and UO_2^{+2} (+6), of which U^{3+} and UO_2^{2+} (+5) are unstable, and U^{+4} tends to oxidize to the state of maximum oxidation (+6). Consequently in water there fundamentally exists the species UO_2^{+2} (+6), which combines readily with the anions most commonly present , such as Cl^-, NO_3^-, SO_4^{2-}, and CO_3^{2-} (Baeza et al., 2006).

In our case when the co-precipitation methodology is applied, after removing carbonates from the water sample using sulfuric acid, the water is at pH < 2 when the uranyl group in cation form is very stable. From that value of pH, UO_2SO_4(aq) becomes the dominant species due to the great quantity of sulfate in the sample. Then, after 6N NH_4OH addition, above pH 6, the dominant specie is the neutral uranyl $UO_2(OH)_2$(aq) which is efficiently adsorbed by a large amount of $Fe(OH)_3$, phenomena which is accomplished due to the iron carrier addition before neutralizing with 6N NH_4OH. In the proposed method, the pH is controlled using the bromocresol purple indicator (BCP or 5',5"-dibromo-o-cresolsulfophthalein) and the color of the solution is purplish-brown at the endpoint. That endpoint ranges from 5.2 to 6.8 and it is important to ensure that the solution has been neutralized (pH 7 ± 0.5) since between pH 4 and pH 6 there exist no attractive electrostatic interactions between the corresponding predominant specie in solution and the surface layer of the precipitate, whose formation is clearly hindered. Moreover, at pH 8 and pH 10, the phenomenon of adsorption is hindered by the presence of repulsive electrostatic forces and therefore it is recommended not exceeding pH 8.

For these very reasons, we checked the total precipitation of uranium at different pH's, exactly between pH 6.5 and pH 8 in order to establish a defined pH work mainly due to the scarcity of a tracer in the co-precipitation method. Four deionized water samples spiked with [nat]U were co-precipitated at different pH's. The supernatant obtained for each preparation was kept and specific electrodeposition of uranium were done and measured by alpha spectrometry. Table 1.6 shows the uranium activities values obtained in the supernatant of each co-precipitation made at different pH's and their recoveries.

As it is observed on Table 1.6, there are no significant differences among the pH's studied as well as the amounts of precipitate obtained. Therefore, independently of the pH (between 6.5 and 8.0), the total precipitation of uranium is accomplished. Nevertheless, it is recommended a pH value between 7 and 8.

Table 1.6. Uranium activity values obtained in the supernatants and uranium recoveries in the supernatant.

Sample ID	pH	residue (mg)	Uranium added to the sample (Bq)	Uranium remaining in the supernatant			
				^{238}U (Bq)	^{234}U (Bq)	Total uranium (Bq)	Percent recovery (%)
U_1	6.5	17.9	2.36 ± 0.05	0.012 ± 1.6E-03[1]	0.016 ± 1.6E-03[1]	**0.028 ± 0.002**[2]	**1.2**
U_2	7	18.0	2.39 ± 0.05	0.011 ± 1.6E-03[1]	0.010 ± 1.6E-03[1]	**0.021 ± 0.002**[2]	**0.9**
U_3	7.5	17.6	2.38 ± 0.05	0.008 ± 8.5E-04[1]	0.009 ± 8.5E-04[1]	**0.017 ± 0.001**[2]	**0.7**
U_4	8	18.0	2.40 ± 0.05	0.008 ± 7.1E-04[1]	0.008 ± 7.1E-04[1]	**0.016 ± 0.001**[2]	**0.6**

[1] Overall uncertainty (coverage factor k = 2) mainly from counting uncertainties.
[2] Uncertainty for the Total Uranium activity was given as the combined uncertainty of the average uncertainty of each isotope, with a coverage factor *k=2*, corresponding to a level of confidence of 95%.

The pH interval above mentioned was checked on natural samples of which, could contain other chemical species that could modify the bromocresol purple endpoint (Table 1.7). Table 1.7 also shows the temperature of $Fe(OH)_3$ precipitation step because in the optimized method the precipitation of $BaSO_4$ + $Fe(OH)_3$ salts was improved using moderated heat (40-50 ºC). To be able to define the pH work, the experimental endpoint value was checked using a pH meter. 6N NH_4OH solution was used to neutralize and the pH range obtained was 7.1 to 7.7.

According with the results, the preferential pH value for the $Fe(OH)_3$ precipitaion is 7.5 ± 0.5. This value is achieved either using bromocresol purple indicator or, with more precision, using a pH meter

Table 1.7. pH control and temperature of the co-precipitation procedure on natural water samples.

Sample ID	pH	Temperature (˚C)
A	7.58	38.4
B	7.14	50.8
C	7.46	38.6
D	7.71	46.5
F	7.45	38.7
G	7.4	41.7
H	7.3	45.5
I	7.3	44.3
J	7.31	44.3
K	7.2	47.4

1.5   Blank co-precipitation studies

Temporal evolution

Because in the co-precipitation method established by EPA (1984) or APHA (1998), the elapsed time between sample preparation and measurement is 3 hours, it was considered interesting studying the temporal evolution of the gross alpha activity detected in the blank samples with the aim to check that no alpha activity contribution there was in the blank. For that purpose, successive measurements were made after blank preparation during several days. In figure 1.7 it is observed the counts per minute (cpm) variation with the elapsed time between preparation and measurement of 5 different blanks measured in both different time conditions and detector systems. Four of them were measured in ZnS(Ag) detectors and the fifth was measured in a gas flow proportional detector. Measurement conditions of each blank and the detector system used are presented in the chart legend from figure 1.7.
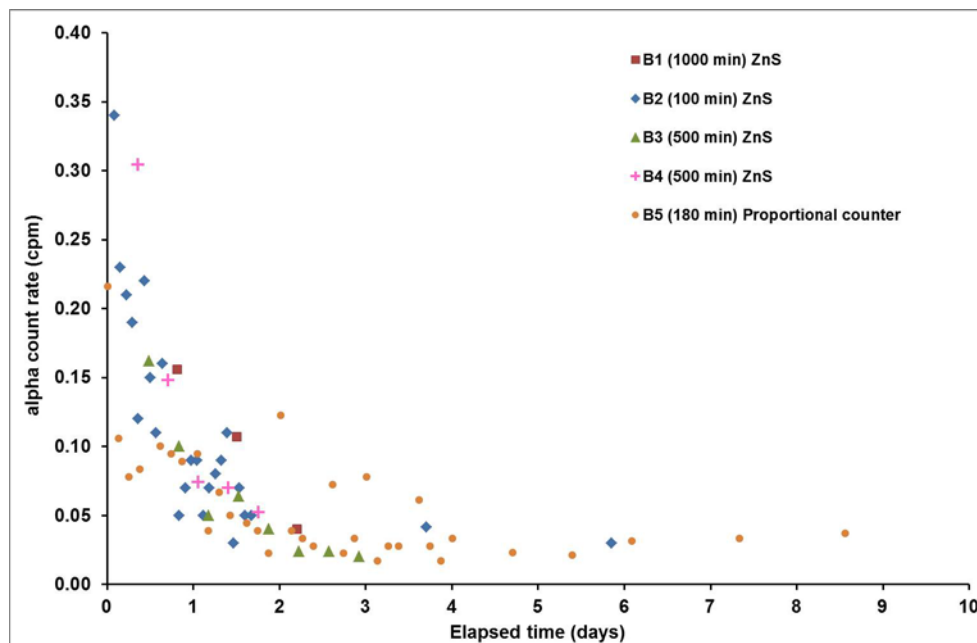
Figure 1.7. Temporal alpha activity detected in co-precipitation blanks measured in ZnS(Ag) and gas flow proportional detectors.

As we can see in Figure 1.7, high values of alpha counts (cpm) were detected for the first two days after preparation and stabilization of alpha cpm was observed after these two days. This phenomena was more evident if the blank were measured in ZnS(Ag) detectors.

Based on these results, it was considered appropriate to detect the presence of possible interferences and to estimate the effect of them.

Evaluation of the interferences

Reagents used in the co-precipitation method were considered as possible radioactive interferences. 1 mL of barium and iron carriers solutions prepared according to the co-precipitation method (Appendix A) were transferred in two different planchets. In addition, in order to evaluate the possible influence of radon decay products, two membrane filters were also measured. One of the filters was measured directly, and the other was measured after passing air for 20 min (estimated time necessary to filter $BaSO_4$ and $Fe(OH)_3$ residue obtained by co-precipitation method). The four samples were dried in a drying oven at 105 ºC for one hour and measured on a gas flow proportional detectors. The results are listed in Table 1.8 and show that planchets with barium and iron carriers and the filter without passing air do not differ from regular alpha background of detectors used. However, the alpha background average value obtained for the filter which the air has passed during 20 min significantly increases.

Table 1.8. Counts per minute (cpm) detected in different reagents used in the coprecipitation method. It is also presented the alpha and beta cpm from the filter and the filter+air (the air passed through the filter for 20 minutes) as well as alpha and beta cpm of the detector background.

Parameters	Gas-flow proportional counter (Berthold)			
	Ba^{2+} carrier	Fe^{3+} carrier	Filter	Filter + air
blank alpha cpm[1] ± u [2]	0.015 ± 0.009	0.012 ± 0.005	0.014 ± 0.008	3.5 ± 5.8 $(18.8 - 0.1)$ [3]
alpha background of the detector (cpm average ± u) [2]	0.015 ± 0.009	0.017 ± 0.009	0.014 ± 0.008	0.021 ± 0.014
blank cpm beta ± u [1]	0.304 ± 0.027	0.319 ± 0.024	0.380 ± 0.024	11.7 ± 21.1 $(69.9 - 1.1)$ [3]
beta background of the detector (cpm average ± u) [2]	0.188 ± 0.075	0.193 ± 0.077	0.347 ± 0.136	0.198 ± 0.085

[1] Mean value (cpm) obtained from 10 measurements over a range between 0 and 3 days of sample preparation.
[2] Uncertainties are expressed as standard deviation of measurements.
[3] The minimum and maximum values are indicated in brackets.

In order to identify the source of interference which causes this increase, Figure 1.8, shows the temporal evolution of alpha cpm detected in the filter with air sample measured in a gas flow proportional detector for three days. Based on this temporal evolution, the disintegration time of alpha emitters which contribute in this increasing was determined. The value obtained was approximately 10 hours and could match with ^{212}Pb (^{212}Pb produces two alpha emitters: ^{212}Bi and ^{212}Po) which belongs to ^{220}Rn progeny. Blanks with different amounts of precipitate (26.8 and 34.5 mg) were measured and a decreasing of ^{220}Rn progeny contribution was observed when the amount of precipitate was increased due to more alpha particle self-absorption.
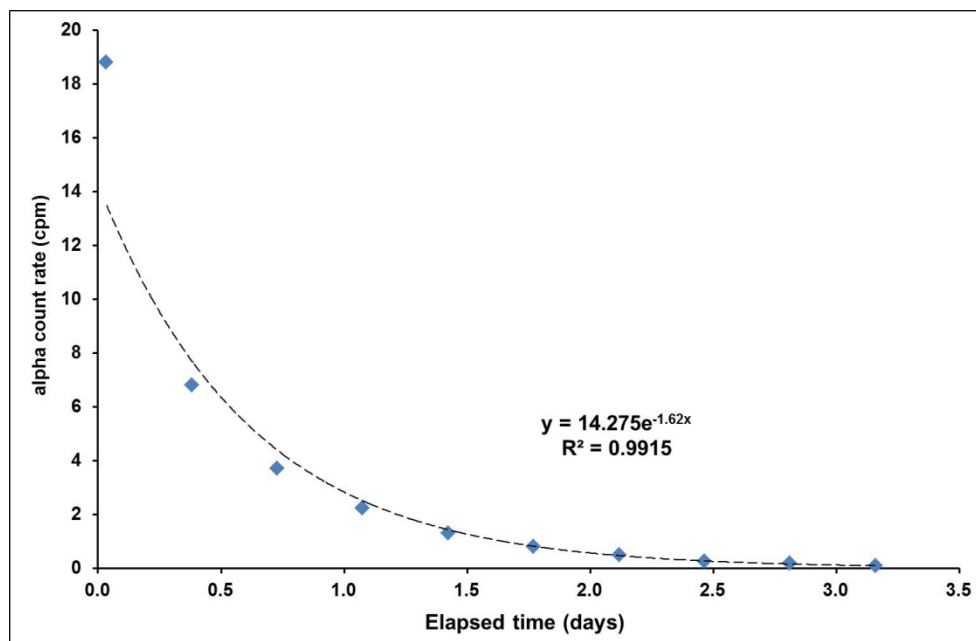
Figure 1.8. Temporal evolution of the filter + air (the air passed through the filter for 20 minutes).

According with the results, during the filtration step in the co-precipitation method, ^{220}Rn and ^{222}Rn from the air, which flows through the filter, is trapped in the precipitate and produces the alpha emitters ^{216}Po and ^{212}Po respectively increasing and varying the alpha contribution in the blank during two days after preparation. For this reason, the elapsed time between sample preparation and measurement should be at least two days, especially relevant in low alpha radioactivity samples. However, if we attempt to measure before two days, the temporal evolution of blanks must be well characterized. In addition, it should be noted that for the

detection systems with background values above 0.05 cpm (gas flow proportional counter), it may not be possible to observe this alpha cpm increasing during the first few days.

Statistical parameters of the blank counts and the background detector

Depending on the detector system and the method used to determine gross alpha activity, the background of the detector can be considered as a blank of the method in order to obtain the alpha net counts (alpha net cpm = alpha cpm of sample – alpha cpm of blank or background).

Several blank samples were prepared in order to determine if the background of the detector can be considered as a blank of the co-precipitation method or the blank sample should be considered as a blank of this method. These blank samples were made using distilled water and the same analytical method. A thin plastic screen of ZnS(Ag) was placed on each blank sample when it was counted in a ZnS(Ag) scintillation alpha detector.

Table 1.9 shows alpha counts (cpm) of different blank samples prepared using the co-precipitation method measured in ZnS(Ag) (ZnS-1 and ZnS-2) and in gas flow proportional counter (AB-10) after two days after preparation. The background cpm values of two detection systems are also included in this table. The measure time of each sample was 1500 minutes.

According to the results obtained in both kinds of detectors the count rate values of blanks were higher than those obtained as backgrounds of the detection systems. Therefore, the count rate of blanks after two days of its preparation should be subtracted from the alpha counts rate of a sample due to the low radioactivity background characteristics in our laboratory.

Table 1.9. Counts per minute (cpm) detected in several blanks in both sulfide zinc solid scintillation and gas flow proportional counter detection systems. It is also presented the cpm of the background.

| Statistical parameters | Solid scintillation | | | | Proportional | |
| | ZnS-1 | | ZnS-2 | | AB-10 | AB-10 |
	blank	background	blank	background	blank	background
mean (cpm alpha)	**0.023**	**0.004**	**0.023**	**0.005**	**0.030**	**0.016**
SD (standard deviation)	0.009	0.002	0.009	0.003	0.008	0.006
RSD %	41	48	40	52	28	37
n (number of samples)	7	67	8	62	5	34

1.6 Summary

In this chapter, we have focused on the discrepancies among the different procedures published for the co-precipitation method.

The main benefit is that no paper pulp and detergent diluted addition are necessary in order to achieve good yields and homogeneous residues.

The morphological study of the precipitate obtained by the co-precipitation method shows that the different salts in the final precipitate are evenly distributed and therefore the final precipitate is consistent in geometry.

The total precipitation of uranium at different pH's indicates no significant differences among the pH's studied. Nevertheless, we recommend a pH value between 7 and 8.

High values of alpha counts are detected for the first two days after preparation in ZnS(Ag) and gas-flow proportional detectors. For this reason, the elapsed time between sample preparation and measurement should be at least two days, especially relevant in low alpha radioactivity samples. Moreover, it should be considered to subtract the alpha count rate of blank from the sample instead to use the background count rate due to the low radioactivity background characteristics in our laboratory.

Finally, according to the results presented in this chapter, a detailed procedure had been described and it is provided for in Appendix A.

Chapter 2

Calibration: Gross alpha efficiency curves

2.1 Introduction and motivation

In order to estimate the gross alpha activity (GAA) of a sample, an appropriate mass efficiency curve has to be defined. Since the various calibration standards have different efficiencies, it is clear that the gross alpha activity depend on the choice of calibration standard. For the co-precipitation method, ^{241}Am and ^{230}Th are recommended as a radionuclide standard for mass efficiency calibration (EPA, 1997), while APHA (1995) recommends the use of ^{230}Th, ^{nat}U, ^{239}Pu, or ^{241}Am.

For this method, ^{241}Am efficiency curves have been constructed by some authors (Suarez-Navarro et al., 2002; Parsa et al., 2011). Parsa et al (2005; 2011) also drew mass efficiency curves using ^{230}Th as a standard calibration in different proportional gas counters with a residue mass ranging between 20 and 140 mg. As mentioned above, other radionuclides are recommended to be used as a standard calibration and so far ^{nat}U efficiency curves have still not been reported in the literature. We have therefore considered studying the mass efficiency curve using ^{nat}U as a standard calibration in both detection systems (gas proportional counter and ZnS(Ag)) and we have compared it with other standard calibrations (^{230}Th and ^{241}Am). We chose ^{nat}U and not ^{239}Pu since it is more likely to be found in natural waters. Aditionally, since ^{226}Ra and ^{230}Th have similar alpha particle energies, 4.781 and 4.684 MeV respectively, their efficiencies should be nearly equal. Moreover, ^{226}Ra efficiency determination allows knowing

the efficiency of their daughters. For the same reason, it was considered interesting to determine ^{224}Ra efficiency curve in order to know the contribution of their daughters on the gross alpha activity.

To summarize, in the course of this chapter, the efficiency curve in ZnS(Ag) and gas proportional detectors using different calibration standards (^{230}Th, ^{nat}U, ^{241}Am, ^{226}Ra and ^{224}Ra) were studied in order to find out how they performed when measuring gross alpha activity using the co-precipitation procedure. Additionally, the following parameters were studied: efficiency dependence on alpha particle energy, the repeatability of the efficiency and the temporal stability of the residue. Parts of these studies have been published in the Journal Apply Radiation and Isotopes (Montaña et.al, 2012).

2.2 ^{230}Th, ^{nat}U and ^{241}Am efficiency curves

2.2.1 Preparation of mass efficiency curves

Traceable solutions of alpha emitting radionuclides of ^{230}Th, ^{nat}U, ^{236}U, ^{241}Am and ^{226}Ra were used in this study (see Appendix C). Their decay properties are listed in Table 2.1 together with other alpha radionuclides, with average alpha energies ranging from 4.2 to 5.8 MeV. ^{226}Ra and ^{236}U standards were also used to study the efficiency temporal stability and the alpha energy dependence of efficiency, respectively.

The analytical procedure used to determine the gross alpha efficiency curves was the co-precipitation method which is described in detail in Appendix A.

Gross alpha particle efficiency curves (efficiency vs. residue mass) were constructed for ^{230}Th, ^{nat}U and ^{241}Am, ranging between 15 to 35 mg. We considered this range since it covered all the samples prepared in our laboratory. This was achieved by proportionately varying the amount of barium and iron carriers in the method (1-2 mL of each carrier), analyzing aliquots of de-ionized water spiked with either ^{230}Th, ^{nat}U or ^{241}Am. Each average residue point was prepared in duplicate or triplicate (between 5 and 7 points-residues) and all standard samples were measured for 180 min and a minimum three times in the two types of detection system (each of the 10 detectors from a gas flow proportional counter and 4 ZnS(Ag) scintillation detector [see Appendix B for the instrumentation]).

Table 2.1. Energy per disintegration (MeV) (Data take from Weast R., 1976).

Radionuclide	^{224}Ra	^{226}Ra	^{234}U	^{238}U	^{210}Po	^{239}Pu[1]	^{236}U	^{230}Th	^{241}Am[1]	^{nat}U [2]
E(MeV)	5.69	4.78	4.77	4.20	5.30	5.14	4.45	4.69	5.46	
	5.45	4.60	4.72	4.15			4.49	4.62		
E average (MeV)	**5.67**	**4.77**	**4.76**	**4.19**			**4.47**	**4.66**		**4.45**
Probability (%)	94.9	94.5	71.4	79	100	100	25.9	76.3	100	100
	5.0	5.5	28.4	20.9			73.8	23.4		

[1] Considered to be other energies.
[2] Average energy between ^{238}U and ^{234}U considering ^{234}U/^{238}U=1.

2.2.2 Results and discussion

Fitting function

No criterion was found in the literature concerning the fitting function. For instance, the efficiency curve vs. residue mass is usually fitted to a power function by Parsa et al. (2005; 2011), while Suarez-Navarro et al. (2002) used a quadratic fit. When the uncertainties are taken into consideration, an exponential function should be choosen because it has fewer parameters to be determined as long as the correlation coefficients are acceptable. It is worth mentioning that Martín Sanchez et al. (2009) considered a two-part mathematical function for the evaporation method. For mass thickness values less than 10 mg/cm^2, experimental values were fitted with an exponential type function and for a mass values greater than 10 mg/cm^2, the efficiency was considered to be constant. In our case the maximum value of mass thickness is 4 mg/cm^2 which means that we can also fit our values with an exponential type function.

The three functions previously mentioned were analyzed and the best correlation coefficient was determined to be the quadratic fit for the three isotopes considered. The exponential fit was the worst and the correlation coefficient wasn't acceptable enough to be considered, as in the case of the power fit. In addition, taking into account the studied range (15 to 35 mg), the best approach was to use a quadratic fit.

The efficiency curve was determined for each of the ten detectors from the proportional counter and for each of the four ZnS(Ag) scintillation detectors by applying a quadratic fitting. For proportional counter detectors, an average quadratic equation was calculated using the different equations of each detector since the fitting coefficients were statistically similar. The same was calculated for the 4 ZnS(Ag) scintillation detectors.

Furthermore, the bias (see equation 1) between the efficiency obtained for each detector and the efficiency obtained using the average equation for different residue masses was calculated for both detection systems.

$$Bias\ (\%) = \left(\frac{\bar{X}_i - Y_i}{Y_i} \right) \cdot 100 \qquad (2.1)$$

where $\bar{X}_i$ is the average efficiency value for one detection system and Y_i is the efficiency obtained in each detector of the same detection system.

The maximum and minimum bias between both efficiency values in two detection systems for ^{230}Th, ^{241}Am and ^{nat}U standard calibrations are presented in Table 2.2. The results show that it is possible to use an average equation for each detection system. The differences were always below 8% in all cases.

Table 2.2. Bias obtained between efficiency obtained from the average equation and equations from each detector for the SZn(Ag) scintillation detectors and the proportional counter.

	Bias (%) [1]					
	SZn(Ag) detectors			Proportional counter		
Standard calibration	min	max	number of data	min	max	number of data
^{230}Th	-6	+3	24	-8	+4	60
^{241}Am	-5	+4	28	-5	+4	70
^{nat}U	-6	+5	24	-6	+6	60

[1] The sign before the number indicates the direction of bias.

The gross alpha particle efficiency curves for ^{230}Th, ^{241}Am and ^{nat}U are presented in Figures 2.1, 2.2 and 2.3 respectively. These curves correspond to the average equations for each detection system. The dashed lines represent the absolute maximum bias presented in Table 2.2. As we can see, in the three standard calibrations, the efficiency varies with respect to the residue mass and the efficiency obtained by ZnS(Ag) detectors was greater than that obtained by the proportional counter detectors. The differences obtained between the ZnS(Ag) detector and the proportional counter efficiencies for an 18 mg residue were 24, 32 and 36% for ^{241}Am, ^{230}Th and ^{nat}U, respectively. Looking at these results, we suggest that there is a relationship between

detectors and the standard calibration energy: when the energy of the standard calibration is higher, there is a lower efficiency difference between the two detection systems.

The experimental efficiency data obtained by [241]Am in ZnS(Ag) detectors are comparable with other authors (Suarez Navarro, 2009). In contrast, [230]Th efficiency curves cannot be compared because the residue mass range is different to that used by Parsa et al. (2005; 2011).
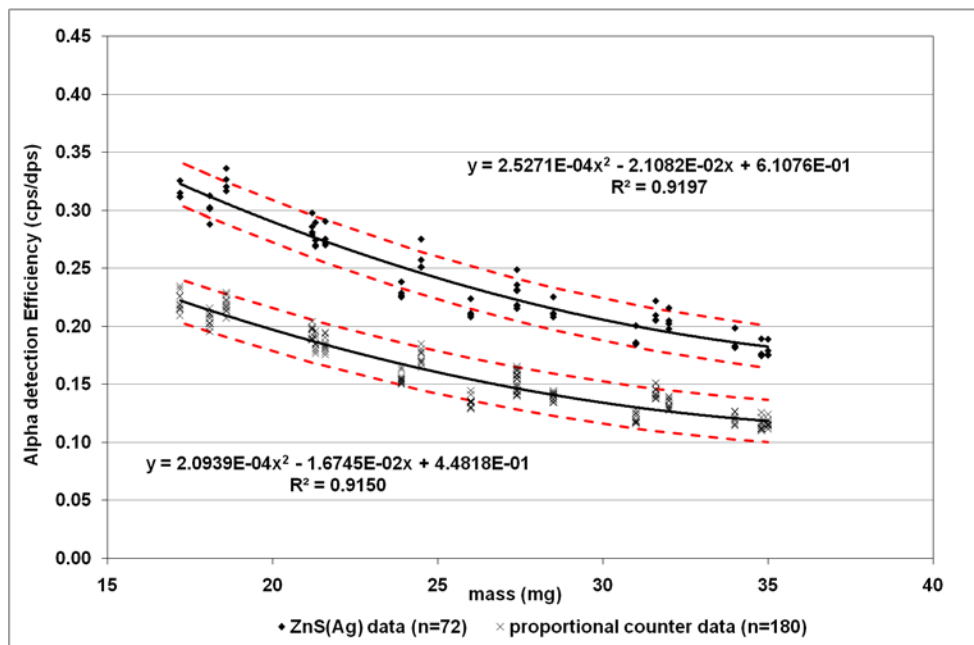
Figure 2.1. Average alpha efficiency detection of [230]Th as a function of the precipitate mass (mg) in four ZnS(Ag) scintillation detectors and in ten proportional detectors.
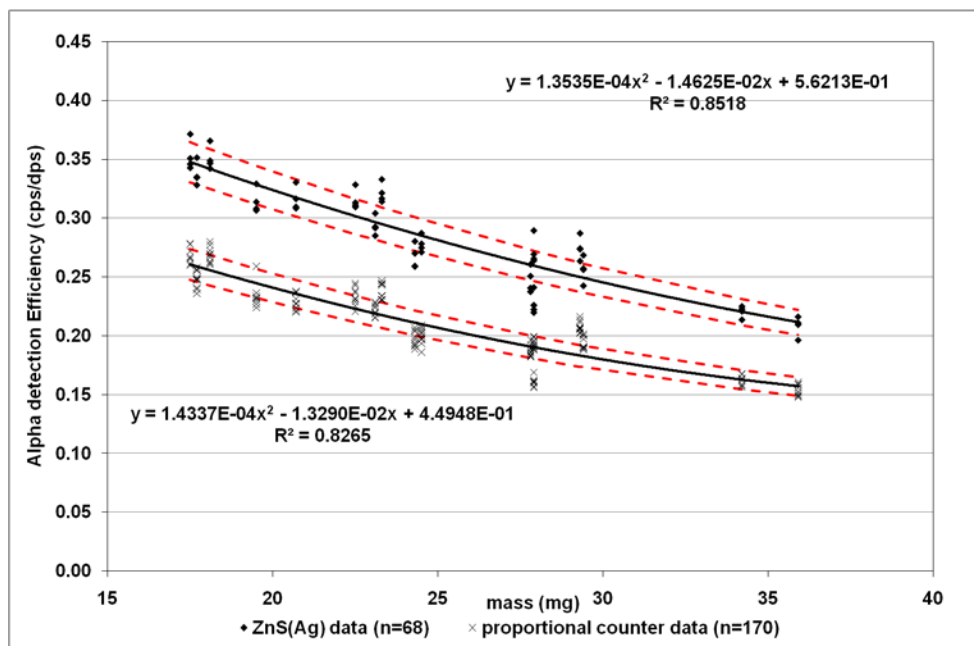
Figure 2.2. Average alpha efficiency detection of [241]Am as a function of the precipitate mass (mg) in four ZnS(Ag) scintillation detectors and in ten proportional detectors.
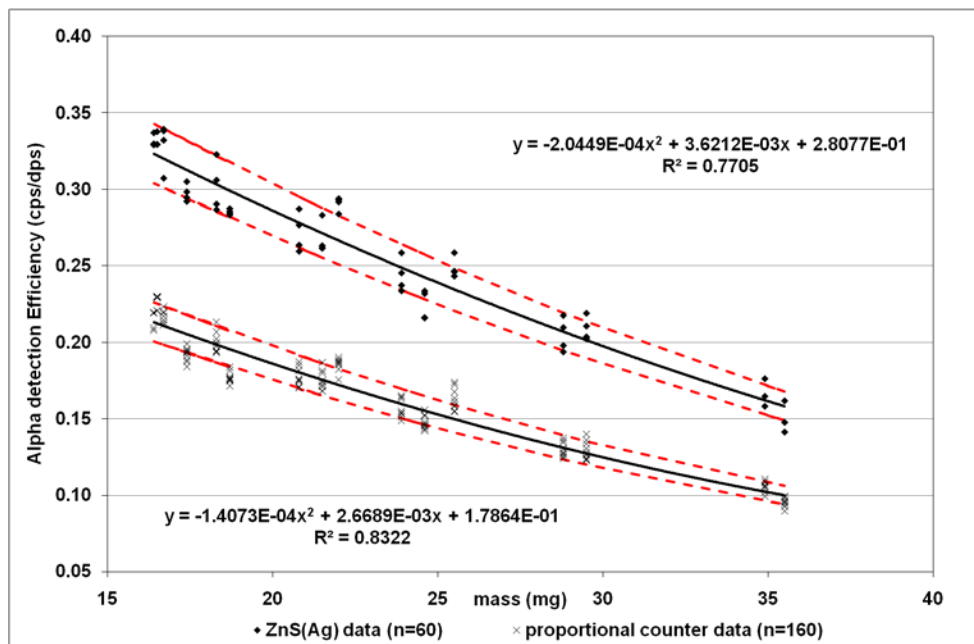
Figure 2.3. Average alpha efficiency detection of [nat]U as a function of the precipitate mass (mg) in four ZnS(Ag) scintillation detectors and in ten proportional detectors.

Efficiency dependence on alpha particle energy

The alpha particle energy dependence of the efficiency was also studied in a proportional counter using [230]Th, [241]Am, [nat]U and [236]U radionuclides and compared with the literature. The data from Figure 2.4 correspond to the efficiency for a residue mass of 18 mg obtained by the co-precipitation method (Section 2.2).

The efficiency data obtained by Monte Carlo simulations in the range 4.2-5.7 MeV studied by Ardnt and West is also presented (2004) with the efficiency data obtained experimentally in the range 4.2-5.8 MeV (Semkov et al., 2004) using the evaporation method. These values were extracted from graphs presented in both papers (Ardnt and West, 2004; Semkow et al., 2004).

For a given residue mass, the efficiency is a linear function of the alpha particle energy and our experimental results show the same tendency, but with higher efficiency values due to the different gas-flow proportional counter used. This fact allows estimation of the efficiency of radionuclides of the studied energy range, such as [210]Po.
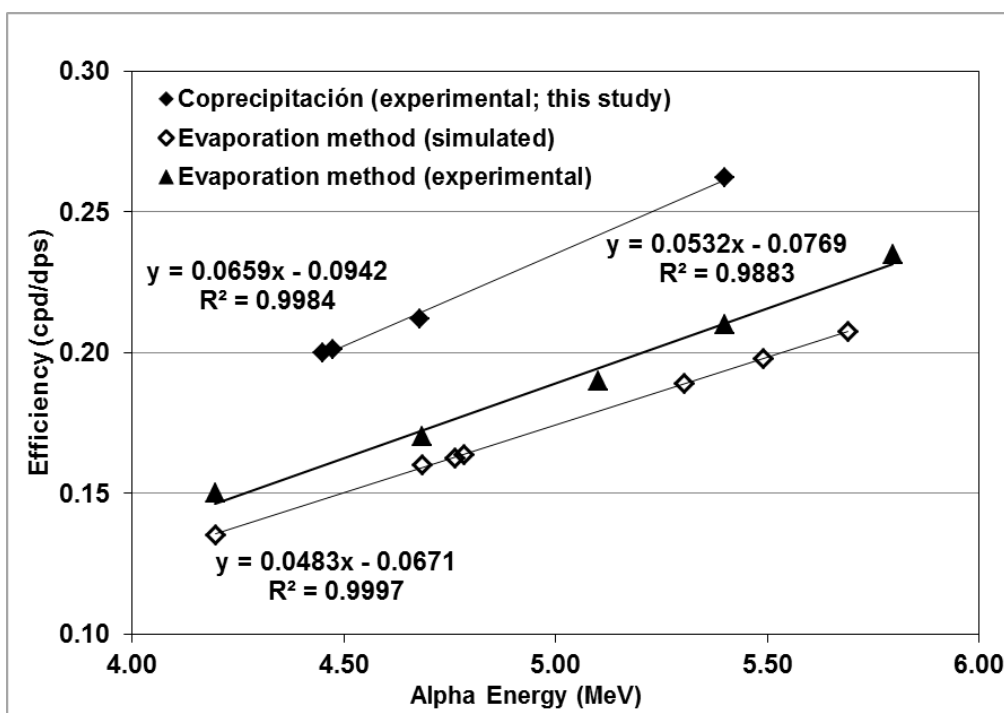
Figure 2.4. Efficiency as a function of alpha energy, for 18 mg residue mass obtained by the co-precipitation method, by the evaporation method (Semkov et al., 2004) and by a theoretical model applied to the evaporation method (Ardnt and West, 2004).

Repeatability of the efficiency

The repeatability of the efficiency was determined for the three standard calibrations and for the two detection systems by equation 1.

$$RSD\ (\%) = \frac{\sqrt{\frac{\sum_{i=1}^{n}(x - \bar{x})^2}{(n - 1)}}}{\bar{X}} \cdot 100 \tag{2.2}$$

The results (Table 2.3) show good repeatability for the three radionuclides standard calibration in both detection systems. The average efficiency repeatability obtained for ^{230}Th, ^{240}Am and ^{nat}U for 18, 20, 23, 25, 28, 30 and 35 mg residues were 6, 4 and 6% respectively in both detection systems and was independent of the residue mass and the radionuclide used for the calibration.

Table 2.3. Repeatability values of the efficiency (RSD in percentages) of different residues for ^{241}Am, ^{230}Th, ^{nat}U calibration standards.

Residue mass (mg)	Gas proportional counter			SZn(Ag)		
	^{230}Th	^{241}Am	^{nat}U	^{230}Th	^{241}Am	^{nat}U
18	4.5 (30)	4.6 (30)	5.7 (30)	4.1 (12)	3.6 (12)	4.0 (12)
20	4.2 (30)	3.7 (20)	3.9 (30)	3.4 (12)	3.0 (8)	5.0 (12)
23	-	4.1 (30)	-	-	4.7 (12)	-
25	11.0 (30)	3.3 (20)	5.4 (30)	9.0 (12)	3.6 (8)	5.8 (12)
28	6.2 (30)	8.2 (30)	-	5.5 (12)	8.6 (12)	-
30	7.6 (30)	4.3 (20)	3.9 (30)	5.9 (12)	5.1 (8)	4.4 (8)
35	4.1 (30)	4.0 (20)	6.3 (30)	4.1 (12)	4.3 (8)	7.9 (6)

The number of data used in calculation is indicated in brackets.

Temporal weight stability

Another parameter studied was the weight variation of the samples. Some authors have suggested that the final precipitate might be hygroscopic (Suarez-Navarro et al 2002; Jobbagy et al 2010), so it is important to know the weight stability over a long period of time. The sample residues prepared with different isotopes (^{230}Th, ^{241}Am, ^{nat}U and ^{226}Ra) were exposed to controlled environmental conditions (temperature of 20 ºC with a humidity of 60-80%) for several days and were weighed periodically. Weight measurements are also included after a long period of time in a desiccator. The relative standard deviation (RSD) of the residue mass was calculated and the average weight of each sample and relative standard deviation for several samples are displayed in Table 2.4.

No statistically significant variation in weight was observed because the relative deviations (RSD) were lower or approximately 1%, which is similar to the expanded uncertainty (1.3%) of the balance for all standard calibrations studied, except for ^{226}Ra.

Table 2.4. Weight variation of some standard calibration samples spiked with ^{nat}U, ^{241}Am, ^{230}Th. Evolution over approximately one year.

Standard sample	Weight after preparation (mg)	Maximum elapsed time since preparation (last measurement) (d)	Average weight (mg)	Standard deviation	RSD (%)
Ra_2	17.4	277	18.1 (10)	1.0	5.3
Th_2	18.6	147	18.9 (8)	0.2	1.0
U_10	18.7	354	18.8 (8)	0.2	1.0
Am_8	27.9	310	27.8 (7)	0.2	0.8

The data used in calculations is indicated in brackets.
RSD% = standard deviation*100/average value

Temporal efficiency stability

Finally, the temporal efficiency variation of the standard calibration samples was also studied. In order to check this temporal stability, different calibration standard samples with varying weights were measured at different times from the time of preparation and the average efficiency of each sample was calculated. Four ^{nat}U, three ^{241}Am and one ^{230}Th and ^{226}Ra samples were measured periodically by the same proportional counter detector. Table 2.5 shows

the average efficiency the standard deviation and the efficiency uncertainty at different times from preparation.

The standard deviation obtained for the radionuclides [241]Am, [230]Th and [nat]U was lower than the expanded uncertainty (*k=2*) and therefore they are considered to be stable during the controlled period (approximately one year). On the other hand, [226]Ra cannot be considered to be stable since its standard deviation was higher than its expanded uncertainty. This is due to the temporal efficiency increase produced by [222]Rn and progeny. However, it is recommended that the calibration standard samples be kept in a dessicator for future measurements in order to protect them.

Table 2.5. Average efficiency obtained at different times and statistical parameters for [241]Am, [230]Th, [nat]U y [226]Ra standard calibration samples.

Standard calibration	precipitate (mg)	Time between preparation and the last measure (d)	Average efficiency	Standard deviation	Efficiency uncertainty (*k=2*)
U-1	17.6	358	0.187 (5)	0.004	0.006
U-10	18.7	342	0.189 (6)	0.004	0.006
U-12	22.0	328	0.174 (4)	0.002	0.006
U-13	25.5	328	0.161 (4)	0.004	0.006
Am-11	17.5	287	0.276 (2)	0.004	0.005
Am-13	23.1	282	0.216 (3)	0.002	0.004
Am-16	34.2	278	0.166 (3)	0.002	0.004
Th-2	18.6	106	0.216 (3)	0.003	0.004
Ra-2	17.4	180	1.089 (4)	0.032	0.012

The number of data used in calculation is indicated in brackets.

2.3 ^{226}Ra and ^{224}Ra gross alpha efficiency curves

This work was done at the Wisconsin State Laboratory of Hygiene (WSLH)-Radiochemistry unit at University of Wisconsin in the City of Madison, USA.

2.3.1 Radium standards conditioning: purification

In order to determine ^{224}Ra and ^{226}Ra efficiencies, part of the co-precipitation procedure should be modified since ^{224}Ra and ^{226}Ra standard solutions are contaminated with their daughters (see Figures 2.5 and 2.6). Therefore, it is necessary to develop a method to accurately spike the residues of the co-precipitation method with an initial ^{226}Ra or ^{224}Ra activities with minimal progeny, especially ^{210}Po (138 d half-life) and ^{228}Th (1.913 y half life).

In the case of ^{224}Ra, because of its short half-life (3.63 days), it proved useful to use an aged ^{228}Ra standard as a source of ^{224}Ra. The determination of the ^{224}Ra activity in the ^{228}Ra standard is given in the section 2.4.2.

This method consists on eliminating radium progeny preparing BaSO$_4$ in the presence of EDTA to keep ^{210}Pb, ^{212}Pb, ^{210}Bi, ^{212}Bi, and ^{210}Po from co-precipitating. This has been proved using 3.5 years old ^{210}Pb standard. Once it has been checked that Pb and Po did not precipitate, the method was used to prepare Ba(Ra)SO$_4$ and Fe(OH)$_3$ residues without radium progeny.
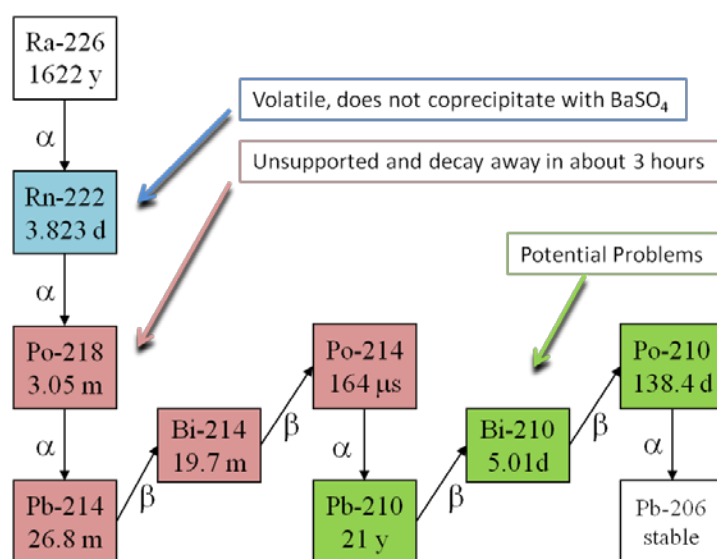
Figure 2.6. ^{226}Ra decay scheme. The initial activities of ^{222}Rn and ^{210}Po in the experiment should be negligible.
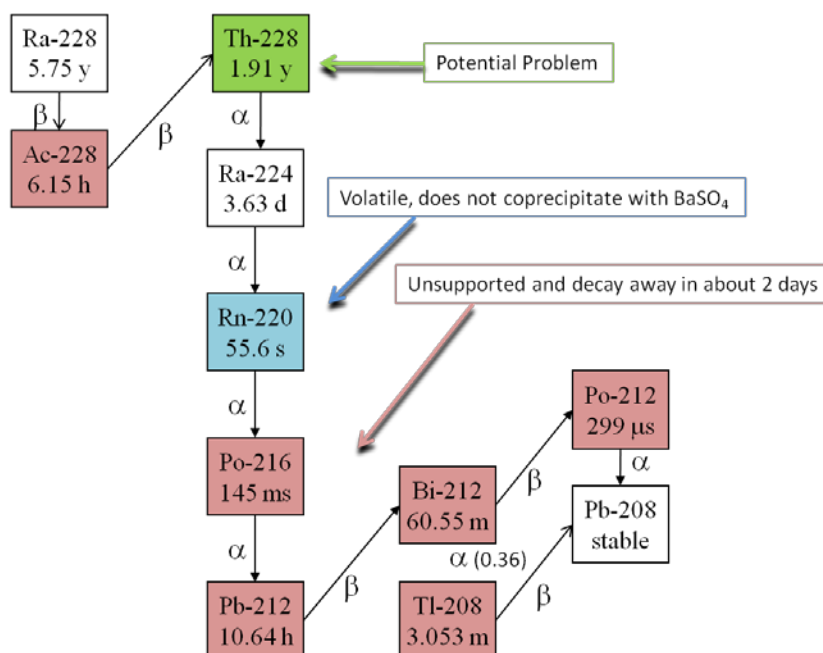
Figure 2.6. ^{228}Ra decay scheme. ^{228}Ra it is considered because of the short half-life of ^{224}Ra, an aged ^{228}Ra standard is used as a source of ^{224}Ra.

The method to prepare Ba(Ra)SO$_4$ without radium progeny is based on that of Goldin (1961), except that the precipitation of the mixed lead-barium sulfate from a basic citrate solution is replaced by a precipitation of BaSO$_4$ from an EDTA solution, which provides an extra decontamination step with EDTA.

Reagents containing sodium (e.g., H$_2$Na$_2$EDTA) led to Ba(Ra)SO$_4$ residues that were hygroscopic, which is undesirable since the efficiencies depend on residue mass. Thus, the only chemicals used to prepare reagents were deionized water , BaCl$_2$·2H$_2$O, H$_4$EDTA, (NH$_4$)$_2$SO$_4$, acetic acid (HOAc), and various concentrations of nitric acid and NH$_4$OH to make pH adjustments, which were made with a pH meter to 0.05 pH units. The reagents prepared were:

Barium carrier: 5 mg/mL Ba^{2+};

EDTA solution (1): 0.05 M EDTA, 0.1 M HOAc (pH=5.5);

EDTA solution (2): 0.1 M EDTA (pH= 9.2);

Precipitant (1): 2 M (NH$_4$)$_2$SO$_4$, 0.1 M HOAc (pH=5.5);

Precipitant (2): 2 M (NH$_4$)2SO$_4$, 1.5 M HOAc;

Wash solution (1): 0.1 M (NH$_4$)2SO$_4$, 0.01 M HOAc (pH=5.5); and

Wash solution (2): 16 M nitric acid.

The reactions in the following procedure were carried out in a 50-mL centrifuge tube. Wherever the tube's contents were mixed, a vortex mixer is used for about 10 s. Afterwards, $Ba(Ra)SO_4$ purified was transferred in a 500 mL beaker in order to form $Fe(OH)_3$ precipitate as described in the co-precipitation method.

Purification procedure

Up to 1.4 mL of barium carrier, 30 mL of EDTA solution (1), and 37 Bq of ^{224}Ra or 5 Bq of ^{226}Ra were added to the tube, and the tube's contents were mixed. $Ba(Ra)SO_4$ was precipitated by adding 2 mL of precipitant (1) and mixing the tube's contents. The tube was centrifuged. The $Ba(Ra)SO_4$ was washed with 20 mL of wash solution (1), and then dissolved with 30 mL of EDTA solution (2). $Ba(Ra)SO_4$ was precipitated by adding 5 mL of precipitant (2) and mixing the tube's contents. The time was recorded. This was the start of the ingrowth of the either ^{224}Ra or ^{226}Ra progeny (time $t= 0$). The tube was centrifuged. The $Ba(Ra)SO_4$ was washed with 20 mL of wash solution (2). Then the $Ba(Ra)SO_4$ was slurried in the tube with 10 mL of wash solution (2) using a vortex mixer, the slurry was poured into a beaker which contained 20mL of 1M H_2SO_4 and 400 mL of deionized water. The solution with $Ba(Ra)SO_4$ was stirred and heated (50ºC). In order to obtain the same precipitate as it is obtained by the co-precipitation method, 1 mL of Fe^{3+} carrier was added to the solution. Bromocresol purple indicator was used to control the pH of the precipitation (about 7±0.5) and 6 N NH_4OH was added dropwise until the precipitate was produced. The solution was continuously stirred without heating for 30 min. Finally, the combined precipitates ($BaSO_4 + Fe(OH)_3$) were cooled to room temperature, filtered and collected on a 0.45 mm, pre-weighed filter using a vacuum filtration system. The filter with the precipitate was placed on a stainless steel planchet, secured with a retaining ring and dried in a drying oven at 105±1 ºC for 1 h. Finally, the combined precipitates were cooled to room temperature.

The figure 2.7 below is a schematic presentation of this procedure.

Several samples were prepared varying the amount of barium and iron carriers in the procedure. This was achieved varying proportionately the amount of both carriers (1 to 2 mL of Ba and Fe carriers; stoichiometric residues) as well as varying but not proportionally (non- stoichiometric residues).
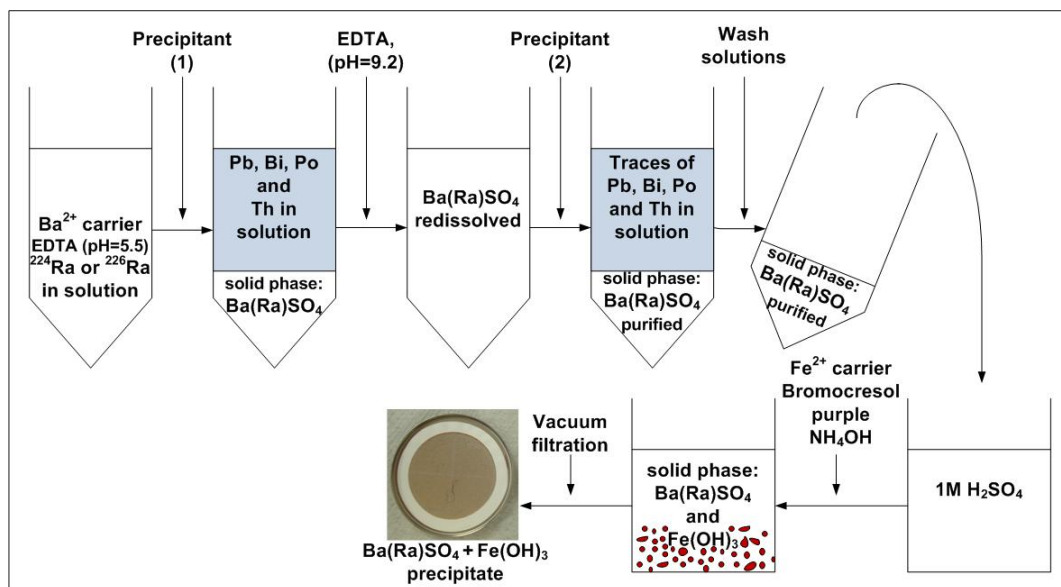
Figure 2.7. Process scheme of the method used to purify and co-precipitate Ra standards in BaSO$_4$-Fe(OH)$_3$ precipitate.

Verification of Pb, Bi, Po and Th removals from Ra standards.

The recoveries of ^{210}Pb, ^{210}Bi and ^{210}Po, using a 3.5-y old ^{210}Pb standard (see Appendix C for the information of the standard), and Th (using a ^{230}Th standard), were checked using the purification procedure, and only obtaining BaSO$_4$ (Arndt and West, 2008) with 1mL of barium carrier. The residues containing BaSO$_4$ were counted immediately following preparation in α-β mode using the gas flow proportional counter (counting time: 300 min). The results for the first step of the precipitation (after the addition of precipitant 1) are given in Table 2.6. The Table includes the activity added, the activity detected in the BaSO$_4$ residue formed and the recovery in percentage.

As shown in Table 2.6, during the first precipitation, Pb, Bi, Po and Th were practically removed given that, in the worst case (Th), only 0.05% remained in the Ba(Ra)SO$_4$ precipitate. Despite the great removal at the first precipitation, the next two precipitations were also done for all residues prepared.

Table 2.6. Radionuclide recoveries in Ba(Ra)SO$_4$ after removing Pb, Bi, Po and Th using EDTA (pH=5.5).

Standard	Activity used (dpm) [1]	Activity detected (dpm) [1]	Percent recovery
^{230}Th	2210	1.015	0.046
^{210}Po	2858	1.200	0.042
^{210}Pb	2858	0.800	0.028
^{210}Bi	2858	0.1143	0.004

[1] dpm: disintegrations per minute

2.3.2 Determination of the efficiencies from ^{224}Ra and its daughters

To measure the two efficiencies of the ^{224}Ra decay chain using the model reported by Arndt and West (2008), three conditions must hold for the Ba(Ra)SO$_4$ residues:

(1) the initial ^{212}Pb and ^{212}Bi activities must be negligible,

(2) the ^{228}Th activity must be negligible during the course of the experiment, and

(3) the initial ^{224}Ra activity must be well-defined.

The data of Table 2.6 shows that condition (1) is fulfilled. Condition (2) is fulfilled because the initial ^{228}Th activity in the residue can be neglected since results on Table 2.6 shows that thorium was removed using the method above mentioned, and, due to its 1.9 years half-life, the production of ^{228}Th from ^{228}Ra over the course of a 24-h experiment is negligible. Condition (3) can be satisfied by using ^{228}Ac activity, from the ^{228}Ra standard, as a tracer for ^{224}Ra.

Yield determination

If at least 40 h have passed since the co-precipitation, the ^{228}Ra and ^{228}Ac activities in the Ba(Ra)SO$_4$ will be equal, and the ^{228}Ac activity can be determined by gamma spectroscopy. Therefore, the chemical yield (γ) of radium, the ratio of the ^{228}Ra activity in the residue to that used in the co-precipitation, can be used to determine the ^{224}Ra yield in the Ba(Ra)SO$_4$ residue as well as its activity (see next page for the activity determination). This chemical yield was determined using the full energy peaks of ^{228}Ac (see Table 2.7).

Table 2.7. Radionuclide full-energy gamma peaks.

Nuclide	Energy (keV)
^{228}Ac	129.24, 209.37, 328.06, 338.35, 409.53, 463.00, 795.03, 835.71, 911.38, 965.01, 969.19,
^{224}Ra	241.07
^{212}Pb	238.73, 300.15
^{208}Tl	583.20, 860.74
^{133}Ba	81.99, 276.39, 302.85, 356.01, 383.85

^{224}Ra activity determination

Firstly, the ^{224}Ra activity from the ^{228}Ra standard was measured. Since ^{228}Ac and ^{228}Ra were in secular equilibrium, the ^{228}Ac activity was equal to the ^{228}Ra value reported in the standard calibration certificate. The full-energy peaks of ^{228}Ac, given above in Table 2.7, were used to generate an energy-efficiency calibration curve for the planar gamma detector. The vial was kept in a distance of 15 cm from the detector end cap to minimize coincidence summing. Since the vial sealed, it was assumed that both ^{212}Pb and ^{208}Tl were in secular equilibrium with ^{224}Ra.

The ^{224}Ra, ^{212}Pb, ^{212}Bi and ^{208}Tl in the standard were measured from the corresponding full-energy peaks given in Table 2.7. The date, time and count duration are given in table 2.8. The weighted ^{224}Ra activity average using these three radionuclides is also given. The separation date between ^{228}Ra and ^{228}Th was 10 October 2005. Using this date, the half-lives and the Bateman equations, the expected ^{224}Ra activity from ^{228}Ra decay was calculated and is given in Table 2.8. Because of the agreement between the calculated and the experimental values, a calculation was used to determine the ^{224}Ra activity in the standard at time t = 0.

Table 2.8. ^{224}Ra activity by gamma spectroscopy and calculation.

Nuclide	Determination
Date	30/04/2012
Count duration (h)	24
^{224}Ra activity (Bq)	1609 ± 31
^{212}Pb activity (Bq)	1577 ± 21
^{212}Bi activity (Bq)	1627 ± 35
^{208}Tl activity (Bq)	555.6 ± 6.6
Weighted ^{224}Ra activity by gamma spectroscopy	**1590 ± 27**
Calculated ^{224}Ra activity using Bateman equations and ^{228}Ra activity from the certificate	**1619 ± 35**
% differences between experimental and calculated activities	**-1.8**

Mass efficiency curves from ^{224}Ra and its daughters

If we look at the decay scheme for ^{224}Ra showed above (see Figure 2.6), the alpha emitters ^{220}Rn and ^{216}Po come into secular equilibrium with ^{224}Ra within 10 min. The beta emitter ^{212}Pb, with a 10.6 h half-life, will be in transient equilibrium with ^{224}Ra within 6 days. The rate of ingrowth of ^{212}Bi is similar to that of ^{212}Pb. About 36% of ^{212}Bi alpha decays to ^{208}Tl; the other 64% beta decays to ^{212}Po. Since its half-life is very short, ^{212}Po is in secular equilibrium with ^{212}Bi almost instantaneously. Thus, in the ^{224}Ra decay chain there are two groups of alpha emitters in secular equilibrium with one another: (1) ^{224}Ra, ^{220}Rn and ^{216}Po, and (2) ^{212}Bi and ^{212}Po. Therefore, it is only necessary to determine two average efficiencies for the two groups of alpha emitters in secular equilibrium with one another and will be referred to as two efficiencies of the ^{224}Ra decay chain.

The following model reported by Ardnt and West (2008) was used to determine this two efficiencies of the ^{224}Ra decay chain in a Ba(Ra)SO$_4$ residue but, this model could be applied to a residue composed of any composition or geometry such as Ba(Ra)SO$_4$ + Fe(OH)$_3$ (residue obtained by the co-precipitation method).

At time $t = 0$, let the ^{224}Ra activity be $A_{1,0}$ and let the ^{224}Ra progeny activities be zero in a sample residue. Then, the ith progeny activity at time t, where i corresponds to one of the radionuclides ^{224}Ra decay chain (^{224}Ra, ^{220}Rn, ^{216}Po, ^{212}Pb, ^{212}Bi and ^{212}Po) is given by the Bateman equations:

$$A_i = \kappa_i \beta_i A_{1,0} \sum_{j=1}^{i} c_{ij} \, exp^{(-\lambda_j t)} \qquad (2 \le i \le 6) \qquad \qquad (2.3)$$

where the factor κ_i (≤ 1) accounts for volatilization and recoil loss from the residue, λ_j is the decay constant of the jth radionuclide, β_i is the alpha-decay branching ratio, and

$$c_{ij} = \frac{\lambda_2 \lambda_3 \dots \lambda_{i-1} \lambda_i}{\prod_{\substack{k=1 \\ k \neq j}}^{i} (\lambda_k - \lambda_j)} \qquad \qquad (2.4)$$

If about 10 min have passed since $t = 0$, then the second and third exponential terms in eqn (2.3) are negligible relative to the first, fourth, fifth, and sixth terms, and

$$A_i = \kappa_i A_{1,0} exp^{(-\lambda_1 t)} \qquad (i = 1, \dots, 3) \qquad \qquad (2.5)$$

$$A_5 = \beta_5 \kappa_5 A_{1,0} \left[c_{51} exp^{(-\lambda_1 t)} + c_{54} exp^{(-\lambda_4 t)} + c_{55} exp^{(-\lambda_5 t)} \right] \qquad \qquad (2.6)$$

$$A_6 = (1 - \beta_5) \kappa_6 A_{1,0} \left[c_{51} exp^{(-\lambda_1 t)} + c_{54} exp^{(-\lambda_4 t)} + c_{55} exp^{(-\lambda_5 t)} \right] \qquad \qquad (2.7)$$

where $\kappa_1 = 1$, $\beta_5 = 0.3594$, $c_{51} = 1.153$, $c_{54} = -1.260$ and $c_{55} = 0.1077$.

The number of counts dN induced in the detector in time dt is given by

$$\frac{dN}{dt} = \varepsilon_1 A_1 + \varepsilon_2 A_2 + \varepsilon_3 A_3 + \varepsilon_4 A_4 + \varepsilon_5 A_5 + \varepsilon_6 A_6 \qquad \qquad (2.8)$$

where ε_i is the efficiency of the ith alpha emitter in the residue. Substituting eqns (2.5), (2.6), and (2.7) into eqn (2.8) yields

$$\frac{dN}{dt} = A_{1,0} \left\{ k_1 \, exp^{(-\lambda_1 t)} - k_2 \left[exp^{(-\lambda_4 t)} + \frac{c_{55}}{c_{54}} exp^{(-\lambda_5 t)} \right] \right\} \qquad \qquad (2.9)$$

where

$$k_1 = \varepsilon_1 + k_2\varepsilon_2 + k_3\varepsilon_3 + \beta_5 c_{51}k_5\varepsilon_5 + (1 - \beta_5)c_{51}k_6\varepsilon_6 \qquad (2.10)$$

$$k_2 = -\beta_5 c_{54}k_5\varepsilon_5 - (1 - \beta_5)c_{54}k_6\varepsilon_6 \qquad (2.11)$$

Integrating both side of eqn (2.9) with respect to t from t to $t + \Delta t$ gives

$$\Delta N = A_{1,0}\left[k_1 I_1 - k_2\left(I_4 + \frac{c_{55}}{c_{54}}I_5\right)\right] \qquad (2.12)$$

where ΔN is the number of alpha counts accumulated from t to $t + \Delta t$ and

$$I_i = \frac{1}{\lambda_i}\{exp^{(-\lambda_i t)} - exp^{[-\lambda_i(t+\Delta t)]}\}$$

Rearranging terms in eqn (2.12) gives

$$\frac{\Delta N}{A_{1,0}I_1} = k_1 - k_2\frac{1}{I_1}\left(I_4 + \frac{c_{55}}{c_{54}}I_5\right) \qquad (2.13)$$

In the coprecipitation experiments, $A_{1,0} = \gamma A_{1,S}$, where γ are the chemical yield of radium in Ba(Ra)SO$_4$ + Fe(OH)$_3$ residue and $A_{1,S}$ is the ^{224}Ra activity used in the coprecipitation. Eqn (2.13) shows that a plot of $\Delta N/(\gamma A_{1,S}\ I_1)$ vs. $[I4 + (c_{55}/c_{54})I_5]/I_1$ is a line with slope $-k_2$ and intercept k_1.

The parameters k_1 and k_2 can be related to the two efficiencies:

$$\varepsilon_{ave,1} = \frac{\varepsilon_1 + k_2\varepsilon_2 + k_3\varepsilon_3}{1 + k_2 + k_3} \qquad (2.14)$$

$$\varepsilon_{ave,2} = \frac{\beta_5 k_5\varepsilon_5 + (1 - \beta_5)k_6\varepsilon_6}{\beta_5 k_5 + (1 - \beta_5)k_6} \qquad (2.15)$$

which are weighted averages of the efficiencies for ^{224}Ra, ^{220}Rn, and ^{216}Po and the efficiencies for ^{212}Bi and ^{212}Po, respectively. Let

$$K_1 = \frac{1}{3}(1 + k_2 + k_3), \qquad K_2 = \beta_5 k_5 + (1 - \beta_5)k_6$$

Then the ε_i from eqns (2.14) and (2.15) can be eliminated from eqns (2.10) and (2.11) to give

$$K_1 \varepsilon_{ave,1} = \frac{1}{3}\left(k_1 + \frac{c_{51}}{c_{54}}k_2\right) \tag{2.16}$$

$$K_2 \varepsilon_{ave,2} = -\frac{k_2}{c_{54}} \tag{2.17}$$

The quantities $K_1\varepsilon_{ave,1}$ and $K_2\varepsilon_{ave,2}$ will be referred to as the two efficiencies of the ^{224}Ra decay chain, since these are the quantities that can be measured experimentally.

Eqns (2.16) and (2.17) can be solved simultaneously to give

$$k_1 = 3K_1 \varepsilon_{ave,1} + c_{51}K_2 \varepsilon_{ave,2} \tag{2.18}$$

$$k_2 = -c_{54}K_2 \varepsilon_{ave,2} \tag{2.19}$$

In order to determine the two efficiencies of the ^{224}Ra decay chain, a total of 12 samples were prepared varying the amount of barium and iron carriers in the method. The residues obtained ranged between 17 and 30 mg. To obtain the efficiencies, all standard samples were measured for 30 min several times during 4 days in a gas-flow proportional counter (4 detectors).

Figure. 2.8 is a plot of $\Delta N/(\gamma A_{1,S} I_1)$ vs. $[I4 + (c_{55}/c_{54})I_5]/I_1$, from eqn (2.13), for eight residues for data taken within 24h of t = 0 and it is seen that each plot conforms well to a line. The radium yields, determined from the ^{228}Ac full-energy peaks, ranged from 80 to 100%.
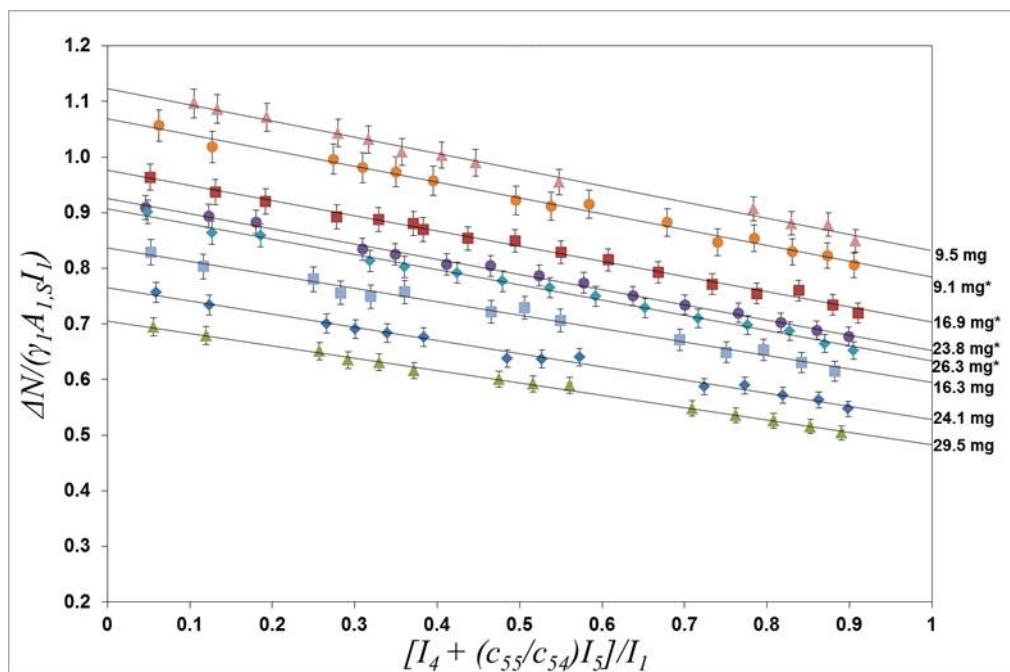
Figure 2.8. Plots of $\Delta N/(\gamma A_{1,S} I_1)$ vs. $[I_4 + (c_{55}/c_{54})I_5]I_1]$ for eight $Ba(Ra)SO_4 + Fe(OH)_3$ residues. In this plot are plotted residues containing different amounts [stoichiometric (indicated by star) and non-stoichiometric] of Ba and Fe carriers.

As we can see in Figure 2.8, the lines observed appear to be parallel between them (equal slope). Therefore, according to equation (2.13) and (2.17), no variation of $K_2\varepsilon_{ave,2}$ should be observed in the range of residues studied. Moreover, the behavior of the stoichiometric residues (indicated by star in Figure 2.8) seems to be different than the non- stoichiometric ones. Below, it is considered a refined analysis splitting between stoichiometric and non-stoichiometric residues as well as splitting between the amount of $BaSO_4$ and $Fe(OH)_3$ obtained.

Related to this behavior difference found, a tendency it is observed between the amount of Fe carrier and the intercept obtained: the more Fe carrier amount (16.3, 24.1 and 29.5 mg of residue plotted in Figure 2.8) added the less intercept value.

Values of k_1 (intercept) and k_2 (-slope) were obtained from the lines and used to calculate $K_1\varepsilon_{ave,1}$ and $K_2\varepsilon_{ave,2}$ in eq.(2.16) and (2.17). Plots of $K_1\varepsilon_{ave,1}$ and $K_2\varepsilon_{ave}$ vs. residue mass are given in Figure 2.9. The values obtained for $K_1\varepsilon_{ave,1}$ and $K_2\varepsilon_{ave,2}$ ranged between 0.167 to 0.286 and 0.176 to 0.279 respectively.
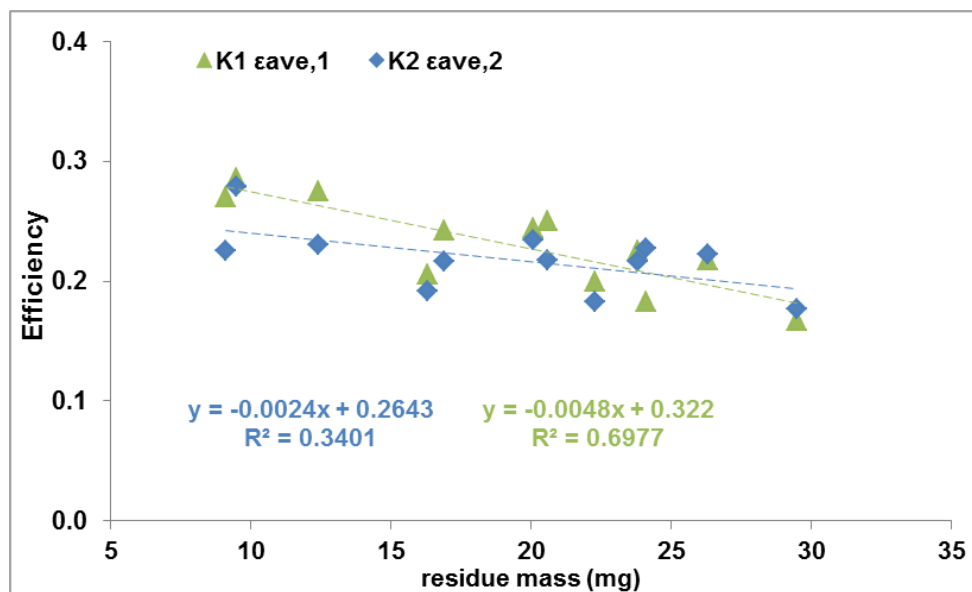
Figure 2.9. The efficiencies $K_1\varepsilon_{ave,1}$ and $K_2\varepsilon_{ave}$ of ^{224}Ra decay chain vs. residue mass.

From Figure 2.9, it is clear that no tendency between the efficiencies and the residue mass exist for the range studied. For some residue mass, ^{224}Ra efficiencies $(K_1\varepsilon_{ave,1})$ are higher than efficiencies from decay products $(K_2\varepsilon_{ave,2})$. Nevertheless, ^{224}Ra efficiencies $(K_1\varepsilon_{ave,1})$ would be lower than efficiencies from decay products $(K_2\varepsilon_{ave,2})$ to be coherent with their energies.

On the other hand, if we plot only the stoichiometric points (same amount added of both carriers) (Figure 2.10) $K_1\varepsilon_{ave,1}$ (green triangles) decreases, but $K_2\varepsilon_{ave,2}$ (blue diamonds) remains constant, probably due to the higher energies of decay products, so they can reach better the detector. Therefore, it appears that exists some dependence between $K_1\varepsilon_{ave,1}$ with $Fe(OH)_3$ and $BaSO_4$ masses. For stoichiometric residues, $K_1\varepsilon_{ave,1}$ decreases when $BaSO_4$ and $Fe(OH)_3$ residues increase (see Figure 2.11).

The efficiencies $K_1\varepsilon_{ave,1}$ and $K_2\varepsilon_{ave,2}$ vs mL of Fe or Ba carriers added were also studied and the results showed the best correlation between amount of Fe added and $K_1\varepsilon_{ave,1}$ (Figure 2.12). A $K_1\varepsilon_{ave,1}$ decreasing is observed when the amount of Fe carrier added increases. On the other hand, $K_2\varepsilon_{ave,2}$ efficiency curve didn't show a good correlation with Fe added as well as $K_1\varepsilon_{ave,1}$ and $K_2\varepsilon_{ave,2}$ with Ba added.
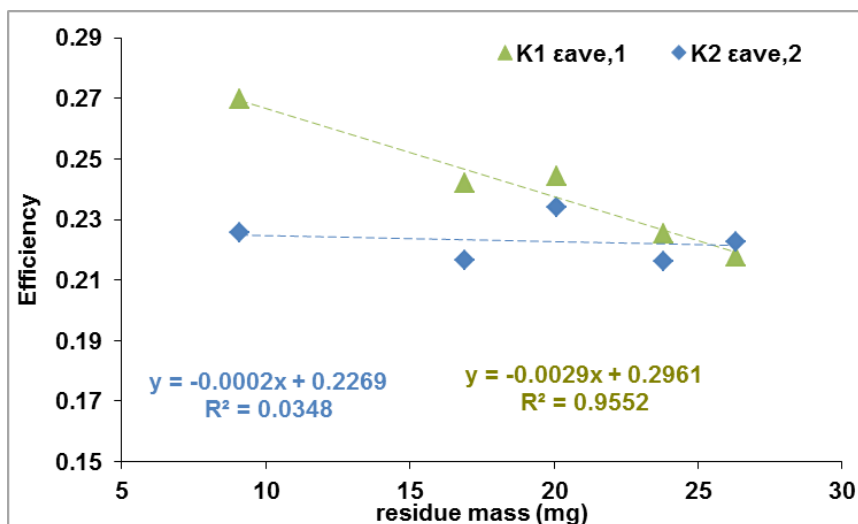
Figure 2.10. The efficiencies $K_1\varepsilon_{ave,1}$ and $K_2\varepsilon_{ave,2}$ for the stequiometric points vs residue mass.
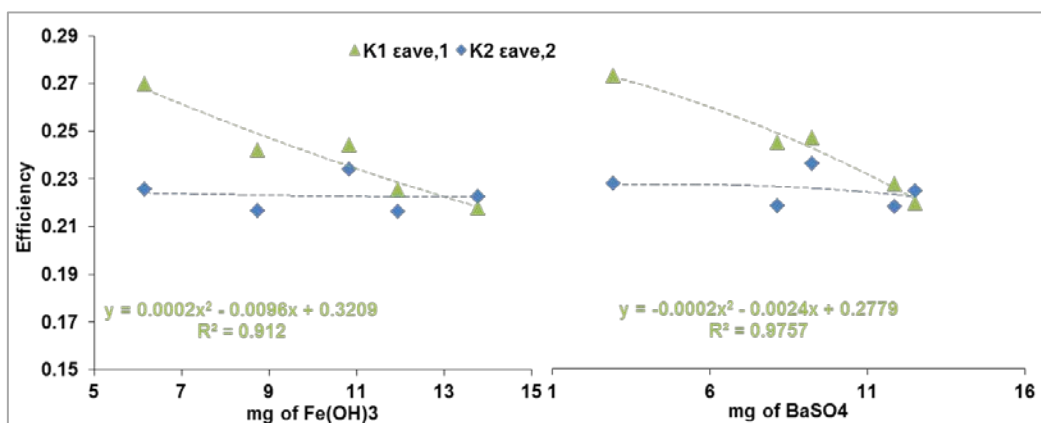
Figure 2.11. The efficiencies $K_1\varepsilon_{ave,1}$ and $K_2\varepsilon_{ave,2}$ for the stequiometric points vs $Fe(OH)_3$ and $BaSO_4$ masses.
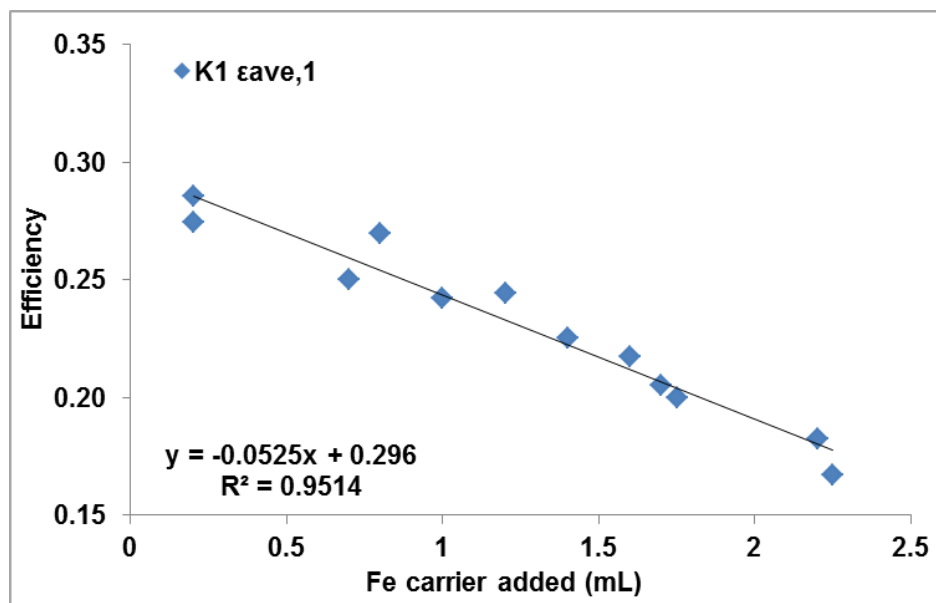
Figure 2.12. $K_1\varepsilon_{\text{ave},1}$ vs. volume of Fe carrier added.

2.3.3 Determination of the efficiencies from ^{226}Ra and its daughters

The same method was also used to prepare Ba(Ra)SO$_4$ residues for the determination of the ^{226}Ra efficiency and the average efficiency of ^{222}Rn, ^{218}Po, and ^{214}Po. The only requirement was that the initial activities of ^{222}Rn and ^{210}Po in the Ba(Ra)SO$_4$ be negligible (Arndt and West, 2007), which was the case since the amount of radon that coprecipitates with BaSO$_4$ was negligible (Sill and Williams, 1969). In this case, the chemical yield of ^{226}Ra was determined using the full energy peaks of ^{133}Ba standard (see Table 2.7 presented in section 2.4.2).

Mass efficiency curves from ^{226}Ra and its daughters

The efficiency of ^{226}Ra and the average efficiency of ^{226}Ra progeny ^{222}Rn, ^{218}Po and ^{214}Po for each residue were determined as described below using the Bateman equations.

Let the ^{226}Ra and its alpha emitting progeny be labeled sequentially from zero to four so that the ^{226}Ra activity is A_0, the ^{222}Rn activity is A_1, the ^{218}Po activity is A_2, and the ^{214}Po activity is A_3. We will assume that A_0 is constant and that the initial activities of the progeny are zero. Let t be the time between a measurement on the gas-flow proportional counter and the co-precipitation step. If the progeny activities are zero at $t = 0$, then at some later time the progeny activities are given by

$$A_i = A_0\left[1 - exp^{(-\lambda t)}\right] \tag{2.20}$$

where λ_1 is the decay constant of ^{222}Rn. (It is assumed that ^{214}Po and ^{218}Po are in secular equilibrium with ^{222}Rn, which will be the case at $t = 3$ hr.

If ε_0 is the ^{226}Ra detector efficiency, then the contribution of ^{226}Ra to the alpha-particle count rate is given by

$$\varepsilon_0 A_0 \tag{2.21}$$

Since progeny can be lost from the residue by emanation or recoil, it is assumed that the fraction of the ith progeny that stays in the residue is κ_i ($i = 1, 2, 3$). Then the contribution of a progeny to the alpha count rate is

$$\varepsilon_i \kappa_i A_i = \varepsilon_i \kappa_i A_0\left[1 - exp^{(-\lambda_1 t)}\right] \tag{2.22}$$

where ε_i is the detector efficiency of the ith progeny. Combining terms (2.21) and (2.22), the total instantaneous alpha count rate C is given by

$$C = \varepsilon_0 A_0 + \left(\sum_{i=1}^{3} \kappa_i \varepsilon_i\right) A_0\left[1 - exp^{(-\lambda_1 t)}\right] \tag{2.23}$$

Let $\langle \kappa\varepsilon \rangle$ denote the average of the three progeny $\kappa_i \varepsilon_i$ terms so that

$$\langle \kappa\varepsilon \rangle = \frac{1}{3}\sum_{i=1}^{3} \kappa_i \varepsilon_i \tag{2.24}$$

This result and Eqn. (2.23) give

$$C = \varepsilon_0 A_0 + \langle \kappa\varepsilon \rangle A_0\left[1 - exp^{(-\lambda_1 t)}\right] \tag{2.25}$$

Dividing this equation by A_0 and integrating the result from time t to time $t + \Delta t$ gives

$$\Delta N = A_0(\varepsilon_0 + 3\langle\kappa\varepsilon\rangle)\Delta t + \frac{3\langle\kappa\varepsilon\rangle}{\lambda_1}A_0 exp^{(-\lambda_1 t)}\left[exp^{(-\lambda_1\Delta t)} - 1\right] \qquad (2.26)$$

where ΔN is the integral number of counts collected from time t to time $t + \Delta t$. Dividing this equation by $A_0\Delta t$ gives

$$\frac{\Delta N}{A_0\Delta t} = \varepsilon_0 + 3\langle\kappa\varepsilon\rangle + 3\langle\kappa\varepsilon\rangle\frac{exp^{(-\lambda_1 t)}\left[exp^{(-\lambda_1\Delta t)} - 1\right]}{\lambda_1\Delta t} \qquad (2.27)$$

In the coprecipitation experiments, $A_0 = \gamma A_{1,S}$, where γ are the chemical yield of radium in $Ba(Ra)SO_4 + Fe(OH)_3$ residue and $A_{1,S}$ is the ^{226}Ra activity used in the coprecipitation.

This equation shows that a plot of

$$\frac{\Delta N}{A_0\Delta t} \qquad (2.28)$$

versus

$$\frac{exp^{(-\lambda_1 t)}\left[exp^{(-\lambda_1\Delta t)} - 1\right]}{\lambda_1\Delta t} \qquad (2.29)$$

gives a straight line with slope $3\langle\kappa\varepsilon\rangle$ and intercept $\varepsilon_0 + 3\langle\kappa\varepsilon\rangle$. Thus, both ε_0 and $\langle\kappa\varepsilon\rangle$ can be determined by the plot.

In term (2.29), let $t = 0$ and take the limit as Δt approaches zero

$$\lim_{\Delta t\to 0}\frac{exp^{(-\lambda_1 t)}\left[exp^{(-\lambda_1\Delta t)} - 1\right]}{\lambda_1\Delta t} = -1 \qquad (2.30)$$

This result shows that the minimum possible value for term (2.28) is ε_0. Also, as $t \to \infty$, term (2.29) approaches zero and term (2.28) approaches $\varepsilon_0 + 3\langle \kappa\varepsilon \rangle$. Thus, a plot would look like that in Figure 2.14.
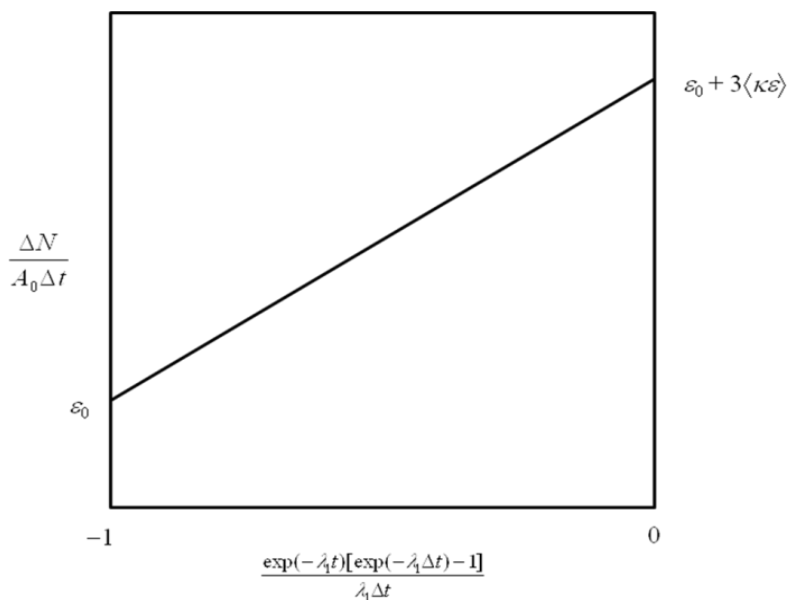
Figure 2.14. Plot of the equation 24.

Since the first measurement would take place at about $t = 3$ hr, the value of first data point would be somewhat larger than ε_0. Further, since term (2.29) is not a linear function of t, making measurements at equally spaced values of t would not correspond to equally spaced values of term (2.29). For good statistics, it is desirable to have at least 10,000 counts in any one measurement, and it is desirable to have equally spaced values for term (2.29). To obtain the points equally spaced, different counting times between 180 and 30 min during 30 days were made, decreasing the counting time over time.

Figure 2.15 is a plot of terms (2.28) and (2.29) for five residues. For 13 samples the correlation coefficients of the plotted lines ranged from 0.9948 to 0.9997. From this figure, it is observed a decreasing of the slope value in function of the residue mass. This would mean that the difference between ^{226}Ra and the average efficiency of its decay products decreases as the residue mass increases.
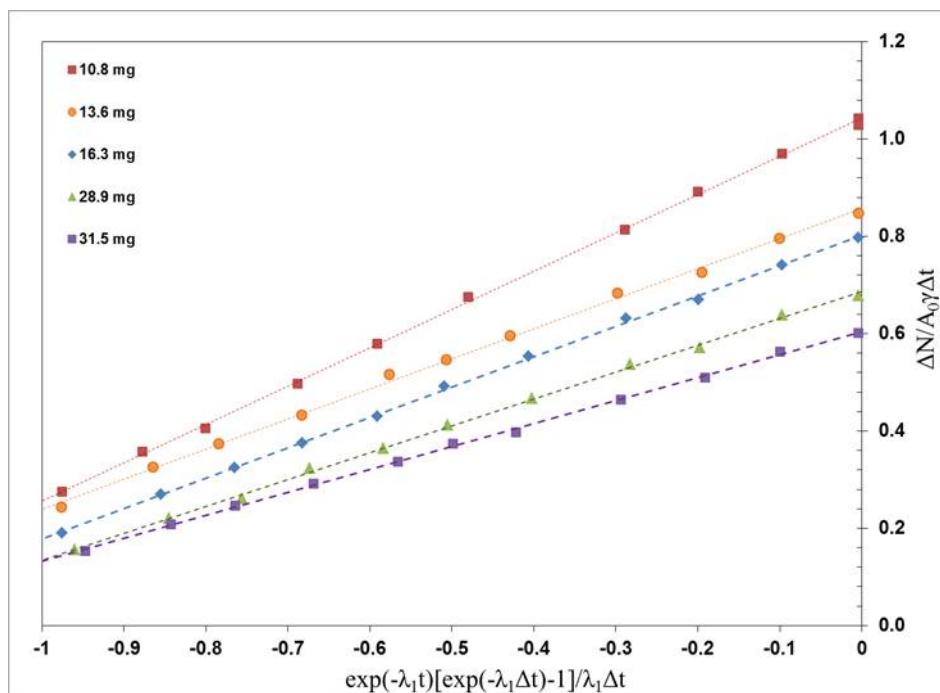
Figure 2.15. Plots of five residues obtained by the co-precipitation method for the determination of ε_0 and $3\langle \kappa\varepsilon \rangle$.

The values of the ^{226}Ra efficiencies (ε_0) and the average progeny efficiencies ($3\langle \kappa\varepsilon \rangle$) were determined from the intercepts and slopes from the lines and used to obtain the efficiency curve of ^{226}Ra and the average efficiency of the ^{226}Ra progeny ^{222}Rn, ^{218}Po and ^{214}Po (Figure 2.16). In Figure 2.16 the solid circles are values of ε_0 and the solid squares are values of $3\langle \kappa\varepsilon \rangle$ vs residue mass. The solid triangles are ^{230}Th efficiency data obtained for co-precipitation residues and using the same gas-flow proportional detector.

It is seen that values of ^{226}Ra efficiencies are slightly scattered, which is due to the variable geometry of these residues (different amounts of Ba and Fe carriers in the same residue). This phenomenon is more pronounced for $3\langle \kappa\varepsilon \rangle$. ^{230}Th and ^{226}Ra data overlap relatively well. The agreement between the ^{226}Ra and ^{230}Th data shows that it is reasonable to use ^{230}Th efficiency curve to obtain estimates of the gross alpha activity for samples containing ^{226}Ra using the co-precipitation method.
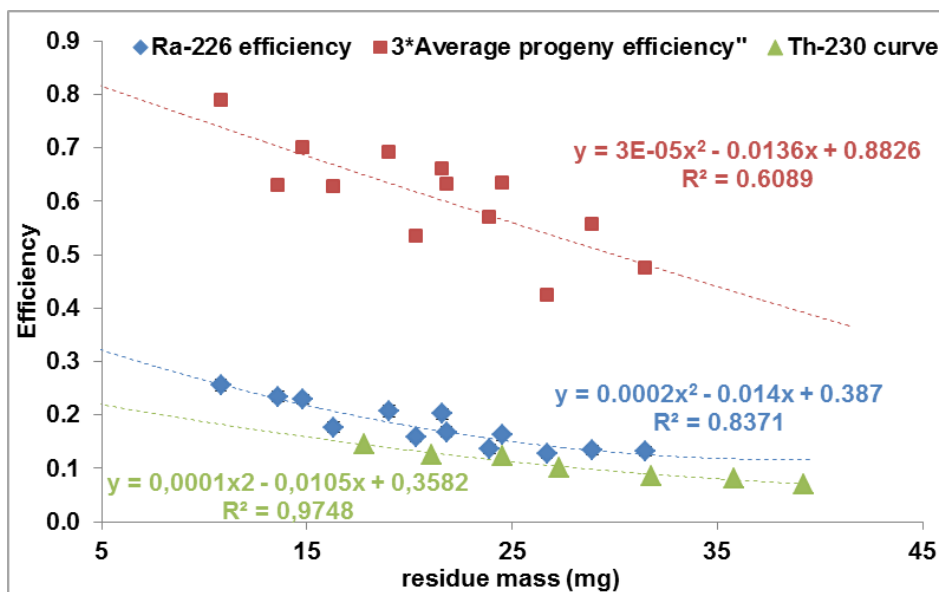
Figure 2.16. ^{226}Ra(ε_0) and 3times ^{226}Ra progeny ($3\langle\kappa\varepsilon\rangle$) and ^{230}Th efficiencies vs. residue mass.

From the high alpha particle energies of the ^{226}Ra progeny, it might be expected that $\langle\kappa\varepsilon\rangle$ is comparable to ε_0, suggesting some loss of ^{222}Rn due to recoil and volatilization, since this loss would be more prominent at lower masses (Figure 2.17). For example, for a residue mass of 10.8 mg $\langle\kappa\varepsilon\rangle$ and ε_0 are 0.263 and 0.255 respectively (3% of bias). Instead, for a residue mass of 23.9 mg $\langle\kappa\varepsilon\rangle$ and ε_0 are 0.190 and 0.136 (40% of bias). The only difference between both residues is the amount of Fe carrier added. When the amount of Fe carrier increases less differences between average ^{226}Ra progeny and ^{226}Ra efficiencies are observed. Therefore, there is a dependence between average ^{226}Ra progeny efficiencies and the amount of Fe(OH)$_3$ in the residue.

In Figure 2.18 is presented the average ^{226}Ra progeny efficiencies vs. mg of BaSO$_4$ and Fe(OH)$_3$ precipitated respectively. The blue diamond series includes all data while red circle series only includes the stoichiometric data (same amount of both carriers added). As we can see in this figure, the dependence between average ^{226}Ra progeny efficiencies and the amount of Fe(OH)$_3$ in the residue is confirmed. On the other hand, the amount of Ba carrier added does not suggest a correlation with the average ^{226}Ra progeny efficiencies. Therefore, the amount of Fe(OH)$_3$ in the precipitate is which causes a diminution of the efficiency.
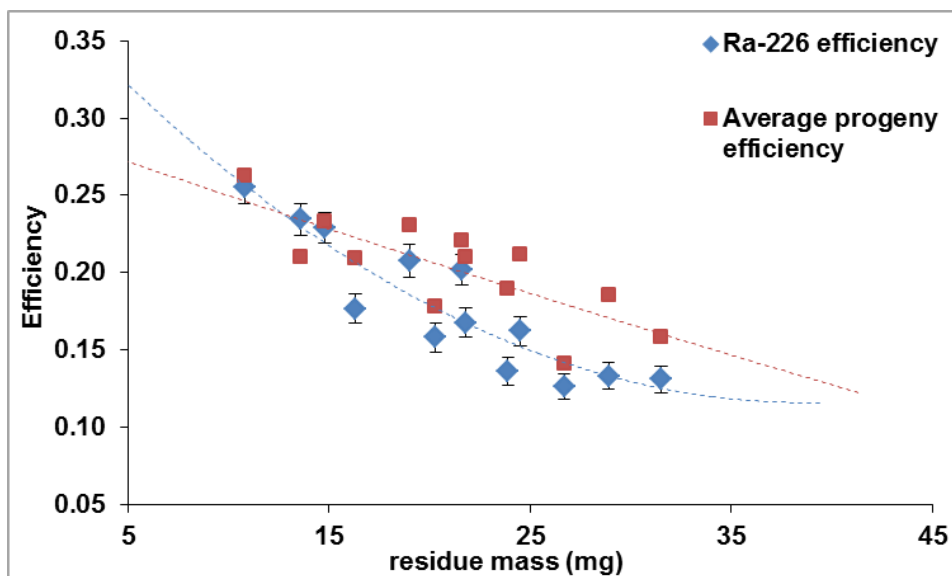
Figure 2.17. ^{226}Ra(ε_0) and average ^{226}Ra progeny ($\langle\kappa\varepsilon\rangle$) efficiencies vs. residue mass.
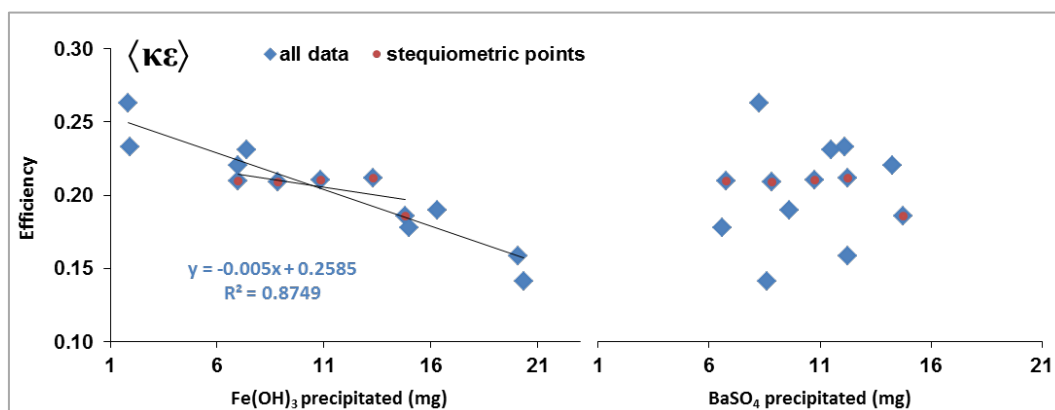
Figure 2.18. From left to right: average ^{226}Ra progeny efficiencies vs. Fe(OH)$_3$ mass and BaSO$_4$, respectively.

If we look at the stoichiometric data points (same amount added of both carriers), ^{226}Ra progeny efficiency practically remains constant for the range of residues studied. When ^{226}Ra decays, the recoiling ^{222}Rn nucleus may travel far enough to leave BaSO4 residue fraction and be lost to volatilization. But Fe(OH)$_3$ fraction causes that ^{222}Rn is trapped avoiding its volatilization. There seems to be a ^{226}Ra progeny efficiency decreasing when a substantial amount of Fe(OH)$_3$ is in the residue (15 mg). This suggests that the height of the precipitate obtained starts increasing suggesting that higher alpha particles don't reach the detector and ^{222}Rn is more trapped in the precipitate. Therefore another influential factor seems to be the height of the

precipitate. This is particularly evident when the average mass efficiency of ^{226}Ra progeny is plotted as function of both residues at the same time. In Figure 2.19 the efficiency curve in function of the residue mass of both salts ($BaSO_4$ and $Fe(OH)_3$) is displayed in three dimensions (black spheres). A 2D surface fit is also drawn, showing that the efficiency falls faster with $Fe(OH)_3$ mass than $BaSO_4$ mass. Because the surface fitting, some of the spheres are underneath the surface plot (six of the thirteen residues prepared).
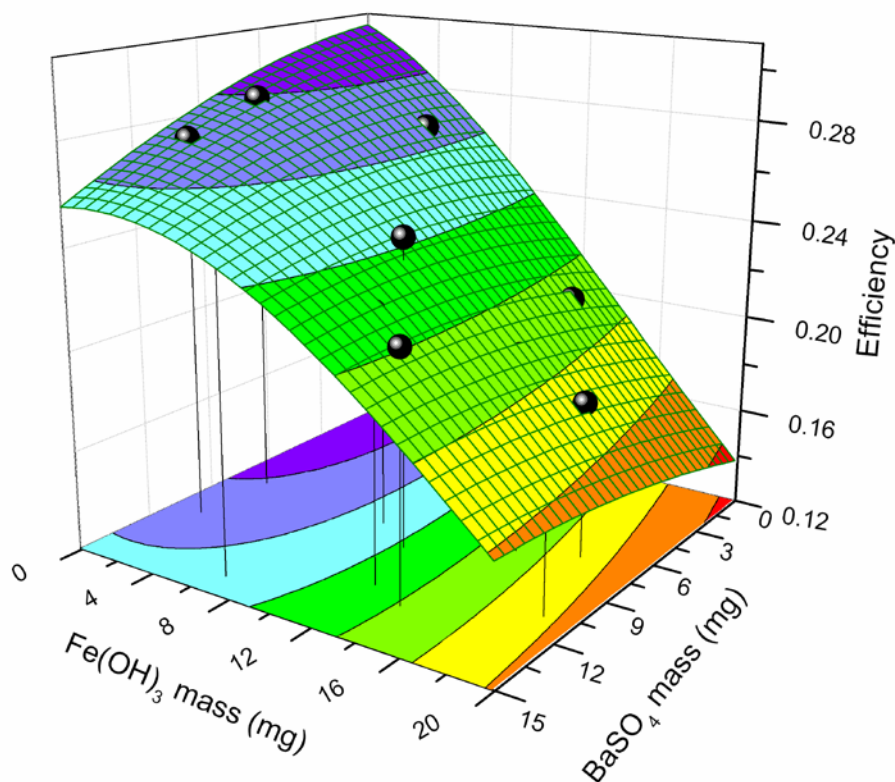
Figure 2.19. Plot of the average mass efficiency of ^{226}Ra progeny ($\langle\kappa\varepsilon\rangle$) as a surface in function of both residues ($BaSO_4$ and $Fe(OH)_3$).

2.4 Summary

The main objective of this chapter has been the efficiency determination of some alpha emitters that can be used as calibration standards in order to estimate the GAA by the co-precipitation method.

An efficiency curve was constructed for each detector (10 proportional counter detectors and 4 ZnS (Ag) detectors) using ^{230}Th, ^{241}Am and ^{nat}U. The best correlation coefficient was achieved using a quadratic fit in the studied mass range (15–35 mg).

For these alpha emitters, an average equation for the two detection systems was also calculated to obtain differences between individual curves and the average curve below 8%. Hence, it was possible to use an average equation for each detection system. The efficiency obtained with ZnS (Ag) scintillation detectors was higher than that obtained with the proportional counter detectors.

The alpha energy dependence of the efficiency was also studied in a proportional counter using ^{230}Th, ^{241}Am, ^{nat}U and ^{236}U radionuclides. The results demonstrated a linear dependence if when considering a residue mass obtained by the co-precipitation method.

The repeatability of the efficiency determination was studied and the results indicated good repeatability in all residue groups for the standard calibration samples analyzed.

The temporal study of the efficiency showed that the different standard calibrations (^{nat}U, ^{230}Th and ^{241}Am) are stable for at least one year. Therefore, the same preparations could be used to calibrate new equipment. Moreover, the precipitate obtained by the co-precipitation method is not hygroscopic. The weight of the precipitate was practically constant for the period studied (one year). Despite its stability, it is recommended to keep the calibration standard samples in a desiccator for future measurements and also in order to protect them due to time-consuming preparation and measurement.

In addition the ^{226}Ra ^{224}Ra and their decay products efficiencies using the co-precipitation method were also investigated during the stay at the Wisconsin State Laboratory of Hygiene (WSLH).

For ^{224}Ra and its progeny, two average efficiencies were experimentally determined for different residues containing $BaSO_4$ and $Fe(OH)_3$. The result indicate a dependence of ^{224}Ra-^{220}Rn efficiency ($K_1\varepsilon_{ave,1}$) with the amount of $Fe(OH)_3$ in the residue. Instead, $K_2\varepsilon_{ave,2}$ remains practically constant for the range of residue mass studied.

The agreement between the ^{226}Ra and ^{230}Th data shows that it is reasonable to use ^{230}Th efficiency curve to obtain estimates of the gross alpha activity for samples containing ^{226}Ra using the co-precipitation method. From the high alpha particle energies of the ^{226}Ra progeny, it

was observed a dependence between average ^{226}Ra progeny efficiencies and the amount of Fe(OH)$_3$ in the residue suggesting ^{222}Rn is more trapped when the Fe(OH)$_3$ amount increases in the final precipitate.

The alpha energy dependence of the ^{226}Ra ^{224}Ra and their decay products efficiencies were also studied in a proportional counter. In this case there was no linear dependence.

Chapter 3

Validation

3.1 Introduction and motivation

The ISO definition of validation is the process of defining analytical requirements and confirming that the method under consideration has performance capabilities consistent with what the application requires (ISO, 1994), method validation is the process of providing an analytical method acceptable for its intended purpose. Therefore, this chapter makes an attempt at presenting a validation of the co-precipitation method.

According to the results obtained in Chapter 2, the method validation was made taking into account the three calibration standards (^{241}Am, ^{230}Th and ^{nat}U) with the aim of establishing, if it is possible, one of them as providing more accurate Gross Alpha Activity (GAA) results.

Two types of validation were applied, internal and external validation, in order to obtain accurate results. The internal validation includes, preparation and analysis synthetic water samples spiked with different alpha emitters in order to study the isotope effect on the GAA. It was of interest to study the GAA placing utmost importance on the elapsed time between sample preparation and measurement with the intention to establish a maximum of this elapsed time to get comparable results. From these results an estimation of the ^{226}Ra content was also performed using the samples spiked with ^{226}Ra. Furthermore, the validation was carried out on natural water samples of very different radioactive characteristics from Spain and USA. For these samples, uranium (^{238}U, ^{235}U, and ^{234}U), radium (^{226}Ra and ^{224}Ra), ^{210}Po, and ^{232}Th isotopes were also assayed using radiochemical separation and alpha spectrometry in order to determine

the sum of activities of these alpha emitters [Total Alfa Activity Concentration (TAAC)]. The precision was calculated for this method.

This chapter also includes an external validation by participating in different proficiency test and intercomparisons organized by different institutions. In addition, a comparison of results obtained between different methods available to determine the GAA of a water sample (evaporation, co-precipitation and total evaporation by liquid scintillation counting) was made with the aim of checking whether these results are representative of the sum of the activities of the alpha emitters present in water samples. The differences among these methods were also statistically studied using ANOVA and 't' tests in order to consider whether there was significant variability among the three methods. The comparative study among methods has been published in the Journal of Environmental Radioactivity (Montaña et.al, 2013a).

3.2   Materials: water samples studied

3.2.1 Synthetic water samples

A synthetic water sample containing 95 mg /L Ca^{2+}, 51 mg /L Mg^{2+}, 38 mg /L Na^+, 2 mg /L K^+, 227 mg /L SO_4^{2-}, 149 mg /L Cl^- and 138 mg /L HCO_3^- was used. It was acidified by HNO_3 to pH = 1. The water composition selected is representative of Spanish waters (CSN, 2012) and it was prepared by the Laboratory de Radiologia Ambiental-Universitat de Barcelona. Several aliquots of this synthetic water sample were spiked with natural isotopes ^{226}Ra, ^{nat}U and ^{210}Po with similar alpha total activity. For each different radioactive composition six replicates were prepared (30 samples).

In order to estimate the ^{226}Ra contribution on the gross alpha activity of a sample, nine extra aliquots of the synthetic water sample were spiked with ^{226}Ra and ^{nat}U with different composition (increasing ^{226}Ra contribution). Because ^{226}Ra standard contains supported ^{210}Po, these samples also contain ^{210}Po, which was determined by gamma spectroscopy (0.7 Bq of ^{210}Po:1Bq of ^{226}Ra). In order to obtain synthetic samples with only ^{226}Ra contribution, the standard was purified following the procedure described in section 2.4.1. The composition of these solutions is shown in Table 3.1. In order to simplify the Table 3.1, the activity of only one replicate of each composition is presented containing the rest of replicates the same activity order for each composition.

Table 3.1. ^{nat}U, ^{226}Ra, ^{210}Po and total activity concentrations (Bq/L) in the synthetic water samples.

ID	^{nat}U	^{226}Ra	^{210}Po [1]	Total Alpha Activity concentration (TAAC)	Composition U:Po:**Ra** (%)
U	0.228 ± 0.005	---	---	0.228 ± 0.005	100:0:**0**
Ra	---	0.210 ± 0.003	---	0.210 ± 0.003	0:0:**100**
Po	---	---	0.172 ± 0.003	0.172 ± 0.003	0:100:**0**
Ra:Po	---	0.210 ± 0.004	0.156 ± 0.002	0.367 ± 0.004	0:43:**57**
	0.160 ± 0.003	0.0520 ± 0.0007	0.0390 ± 0.0005	0.252 ± 0.003	64:16:**21**
	0.116 ± 0.002	0.1050 ± 0.0014	0.0780 ± 0.0010	0.299 ± 0.003	39:26:**35**
U:Ra:Po	0.0577 ± 0.0011	0.0855 ± 0.0012	0.0825 ± 0.0001	0.2256 ± 0.0016	25:37:**38**
	0.0850 ± 0.0017	0.260 ± 0.003	0.193 ± 0.003	0.538 ± 0.005	16:36:**48**
	0.160 ± 0.003	1.55 ± 0.02	1.157 ± 0.016	2.87 ± 0.03	6:40:**54**

[1] The indicated activity of ^{210}Po includes ^{210}Po activity from ^{210}Pb and, as well as from ^{226}Ra standards when samples containing both radionuclides.

3.2.2 Natural water samples

A total of eight natural waters from different parts of Spain, with different radioactive levels, and with a wide range of dissolved solids, were analyzed. Table 3.2 lists the type of water, residue, conductivity, original pH, sulfates and the reservoir geology of the Spanish waters studied. Additionally, 15 more Spanish waters and six natural waters from USA were analyzed in order to further the validation of the method. The six natural waters from USA were analyzed during the stay in that country. Table 3.3 lists the type of waters studied from USA and the other Spanish ones. No information about these waters was available due to the confidentiality.

To preserve the water samples, they were acidified with HNO$_3$ (1.25 mL/L). The origins of the samples were surface water (SF), wastewater (WW) while the other samples were groundwater (GW). All the samples were treated water except GW-4, GW-8, GW-9, GW-10, GW-11 and GW-17 which were raw water.

Table 3.2. Summary of the types, dry residue, conductivity, original pH, sulphate amount and reservoir geology of the Spanish waters studied.

Sample code	Type of water	Residue (g/L)	Conductivity (mS/cm)	Original pH	Sulfate (mg/L)	Reservoir geology
GW-1	groundwater	1	1.225	7.2	79	Granitic
GW-2	groundwater	0.5	0.700	7.0	51	Gypsum-bearing rocks
GW-3	groundwater	4.7	1.295	7.1	32	Basaltic
GW-4	groundwater	2.1	2.145	7.1	458	old lignite mines
SF-1	surface	1.5	1.318	7.8	116	Detrital
SF-2	surface	0.4	0.214	7.7	22	Detrital
SF-3	surface	0.9	1.896	7.7	73	Detrital
SF-4	surface	0.7	0.415	7.8	113	Calcareous

Table 3.3. Summary of the types of the additional waters studied from US and Spain.

Sample code	Type of water, country	Sample code	Type of water, country
GW-5	groundwater, USA	SF-6	surface, Spain
GW-6	groundwater, USA	SF-7	surface, Spain
GW-7	groundwater, USA	SF-8	surface, Spain
GW-8	groundwater, USA	GW-11	groundwater, Spain
GW-9	groundwater, USA	GW-12	groundwater, Spain
GW-10	groundwater, USA	GW-13	groundwater, Spain
WW-1[1]	wastewater, Spain	GW-14	groundwater, Spain
WW-2[1]	wastewater, Spain	GW-15	groundwater, Spain
WW-3[1]	wastewater, Spain	GW-16	groundwater, Spain
WW-4[1]	wastewater, Spain	GW-17	groundwater, Spain
SF-5	surface, Spain		

[1] The origin of wastewater is mainly from surface water.

3.3 Results and discussion

3.3.1 Validation on synthetic water samples

To evaluate the influence of radionuclides and salts that may be present in water samples, a synthetic water sample was prepared containing the most common dissolved salts in natural water and spiked with ^{226}Ra, ^{nat}U and ^{210}Po standards. A temporal evolution study was made in order to know the behavior of the different alpha emitters present in water samples as well as to evaluate the importance of the elapsed time between sample preparation and measurement. Five samples with different radiochemical compositions were prepared: three of them with an only one alpha emitter and the other two samples with alpha emitter's mixtures. Three replicates were made for each sample and were measured at several time points after the sample preparation. At least, eight measurements were made with counting times between 500 and 1000 min. The elapsed time studied was until one month.

By way of example, in figures 3.1 and 3.2 the temporal evolution of the GAA by co-precipitation referred to ^{241}Am, ^{230}Th and ^{nat}U standards (used in the calibrations presented in Chapter 2) for samples containing ^{nat}U and ^{226}Ra respectively are plotted. ^{224}Ra and ^{226}Ra mass efficiency curves were not considered in this study since they were obtained in a different detector system that measurements obtained for synthetic samples. As we can see, samples containing ^{nat}U (Figure 3.1) no significant variation of the GAA over the elapsed time is observed and the GAA referred to ^{241}Am underestimate the TAAC of the sample. Samples containing ^{210}Po present the same behavior (no GAA variation over time). However, in this case GAA referred to ^{241}Am match better than GAA referred to both ^{230}Th and ^{nat}U (see Table 3.7).

On the other hand, in samples containing ^{226}Ra (figure 3.2), GAA vary considerably depending on the elapsed time between sample preparation and its measurement. Furthermore, none of the three standards considered (^{241}Am, ^{230}Th and ^{nat}U) matched with the TAAC. At zero days, the GAA overestimates the TAAC (see Tables 3.6 and 3.8).

In order to quantify the influence of this ingrowths' factor, the mean GAA and the standard deviation are presented in Table 3.4. These values were achieved measuring the samples several times over the period of one month and calculating the GAA referred to the three standards used.
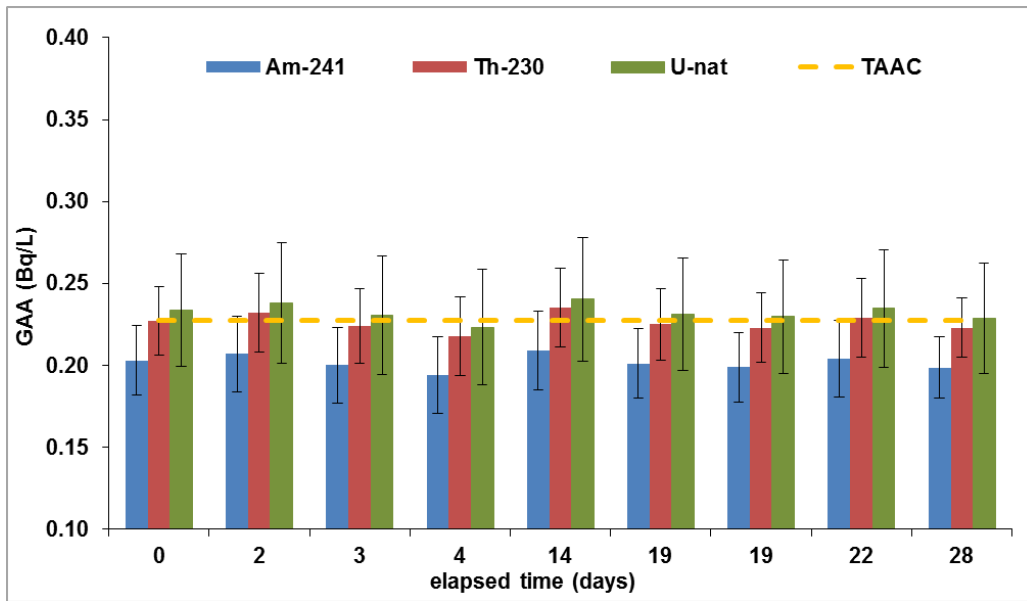
Figure 3.1. GAA temporal evolution for the synthetic water sample containing ^{nat}U (0.228 ± 0.005 Bq/L). GAA is referred to ^{nat}U, ^{230}Th and ^{241}Am standards.
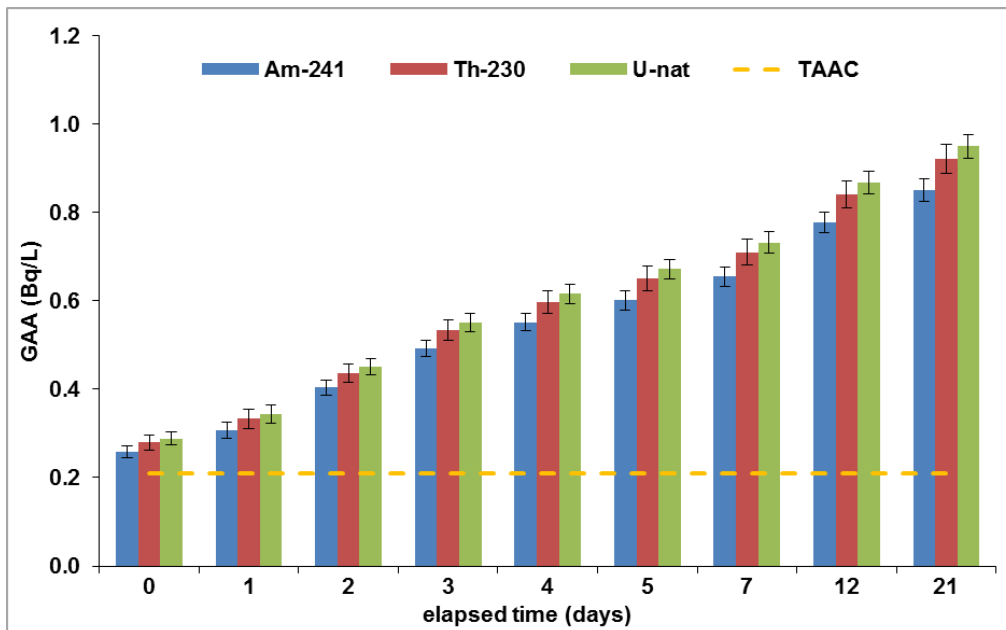
Figure 3.2. GAA temporal evolution for the synthetic water sample containing ^{226}Ra (0.210 ± 0.003 Bq/L). GAA is referred to ^{nat}U, ^{230}Th and ^{241}Am standards.

Table3.4. Temporal variability of the GAA on simple synthetic samples spiked with either ^{nat}U, ^{210}Po and ^{226}Ra.

Sample identification:	Gross Alpha Activity (average ± standard deviation)			Detector [1]
	Referred to ^{241}Am	Referred to ^{230}Th	Referred to ^{nat}U	
U_1	0.209 ± 0.005	0.226 ± 0.005	0.232 ± 0.005	ZnS-3 (9)
U_2	0.212 ± 0.008	0.238 ± 0.009	0.243 ± 0.009	ZnS-2 (8)
U_4	0.176 ± 0.005	0.208 ± 0.005	0.212 ± 0.006	ZnS-2 (5)
U_3	0.181 ± 0.006	0.220 ± 0.008	0.231 ± 0.008	AB-2 (16)
U_5	0.196 ± 0.004	0.261 ± 0.005	0.265 ± 0.006	AB-1 (9)
U_6	0.188 ± 0.006	0.248 ± 0.008	0.258 ± 0.008	AB-3 (9)
Ra_1	0.54 ± 0.19	0.59 ± 0.21	0.60 ± 0.21	ZnS-1 (13)
Ra_2	0.51 ± 0.19	0.57 ± 0.22	0.59 ± 0.23	ZnS-4 (11)
Ra_4	0.45 ± 0.16	0.57 ± 0.21	0.58 ± 0.21	ZnS-4 (9)
Ra_3	0.55 ± 0.16	0.67 ± 0.19	0.73 ± 0.20	AB-4 (16)
Ra_5	0.61 ± 0.16	0.75 ± 0.20	0.82 ± 0.22	AB-4 (17)
Ra_6	0.51 ± 0.14	0.64 ± 0.18	0.71 ± 0.19	AB-9 (16)
Po_1	0.168 ± 0.006	0.187 ± 0.006	0.192± 0.006	ZnS-2 (8)
Po_2	0.175 ± 0.005	0.190 ± 0.005	0.193± 0.006	ZnS-3 (8)
Po_4	0.165 ± 0.003	0.186 ± 0.004	0.185 ± 0.004	ZnS-3 (8)
Po_3	0.176 ± 0.006	0.212 ± 0.007	0.221 ± 0.007	AB-3 (16)
Po_5	0.162 ± 0.006	0.209 ± 0.008	0.219 ± 0.008	AB-6 (15)
Po_6	0.158 ± 0.007	0.195 ± 0.008	0.209 ± 0.009	AB-8 (15)

[1] Number of measurements.
AB: gas-flow proportional counter.
ZnS: zinc sulfide solid scintillation counter.

According to the results presented in Table 3.4, standard deviation of measurements from samples spiked with ^{nat}U or ^{210}Po were below than 4 percent, independently of the standard used in the calibration. This value was below to measurement uncertainty which was in the order of 7 percent at the 95 percent confidence level ($k=2$). These results indicate GAA stability over time on samples containing ^{nat}U and ^{210}Po.

For synthetic samples containing ^{226}Ra, standard deviation of measurements was around of 30 percent while, as mentioned above, the measurement uncertainty was in the order of 7 percent. Given that, there is a substantial variation of the GAA over time on samples containing ^{226}Ra.

For samples containing a mixture of radionuclides being one of them ^{226}Ra, the obtained results were equivalent to those obtained on synthetic samples spiked with ^{226}Ra. GAA on samples

containing mixtures of ^{226}Ra, ^{210}Po and ^{nat}U were increasing over time due to the ^{226}Ra daughters contribution.

^{226}Ra contribution: GAA relationship between 10 and 2 days measurements

A study of the GAA temporal evolution on samples containing different percentage of ^{226}Ra was made, in order to establish a duplicate counting to estimate the ^{226}Ra contribution on the GAA. To evaluate the ^{226}Ra contribution in the evolution profiles, synthetic samples with similar gross alpha values but increasing the percentage of ^{226}Ra on the sample were prepared. Figure 3.3 shows the GAA temporal evolution referred to ^{241}Am measured in a gas-flow proportional counter for synthetic samples containing different amounts of ^{226}Ra. Error bars represents the overall uncertainty of GAA at the 95 percent confidence level.
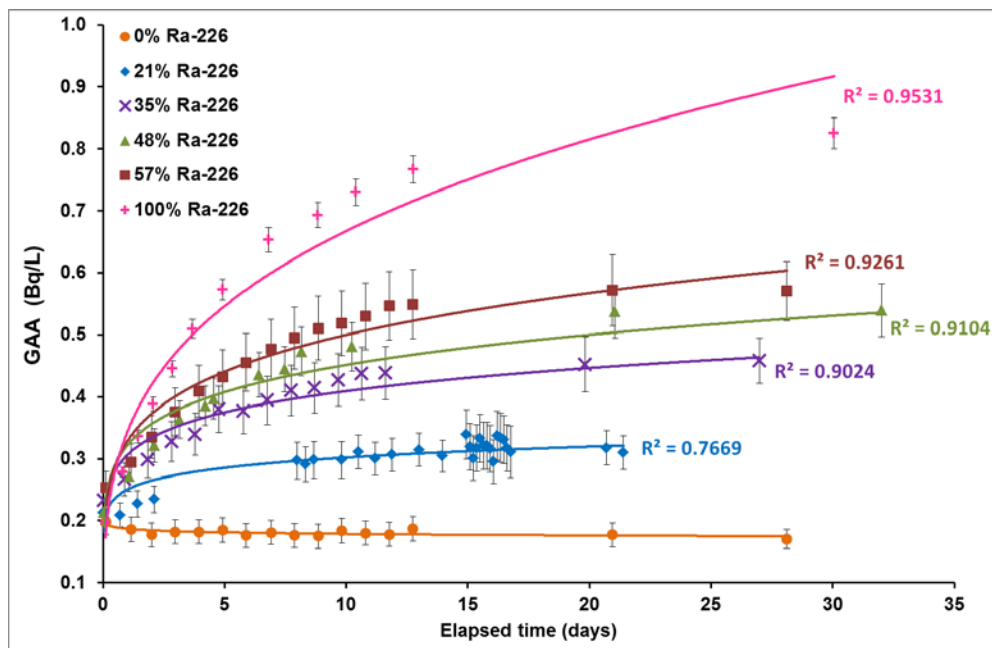
Figure 3.3. Evoulution of the GAA over time for samples containing different of ^{226}Ra content. Solid lines represent the exponential adjustment. Error bars represent the overall uncertainty (coverage factor $k = 2$).

As shown in figure 3.3, the GAA of zero percent of ^{226}Ra remains constant, and instead, GAA of samples containing 21 percent until 100 percent of ^{226}Ra increases over time. The temporal

evolution data for each sample composition can be adjusted to growth curves which are parallel between them and the more [226]Ra proportion in the mixture synthetic sample, the more radioactivity growth. In addition, the more [226]Ra contribution, the more exponential growth curve tendency.

Building on the activities obtained during different times, it was estimated the relationship of the GAA obtained between ten and two days after sample preparation. It was considered this interval in order to ensure sufficient radioactive growth of [226]Ra activity, without reaching the radioactive equilibrium. The theoretical GAA ratio between ten and two days was determined using Bateman equations and was 1.84. The measurements were made in three different detectors (two in ZnS and one in gas-flow proportional detectors) obtaining the plots presented in Figure 3.4. The GAA ratio between ten and two days for the synthetic samples containing 100% of [226]Ra was 1.88 ± 0.18.
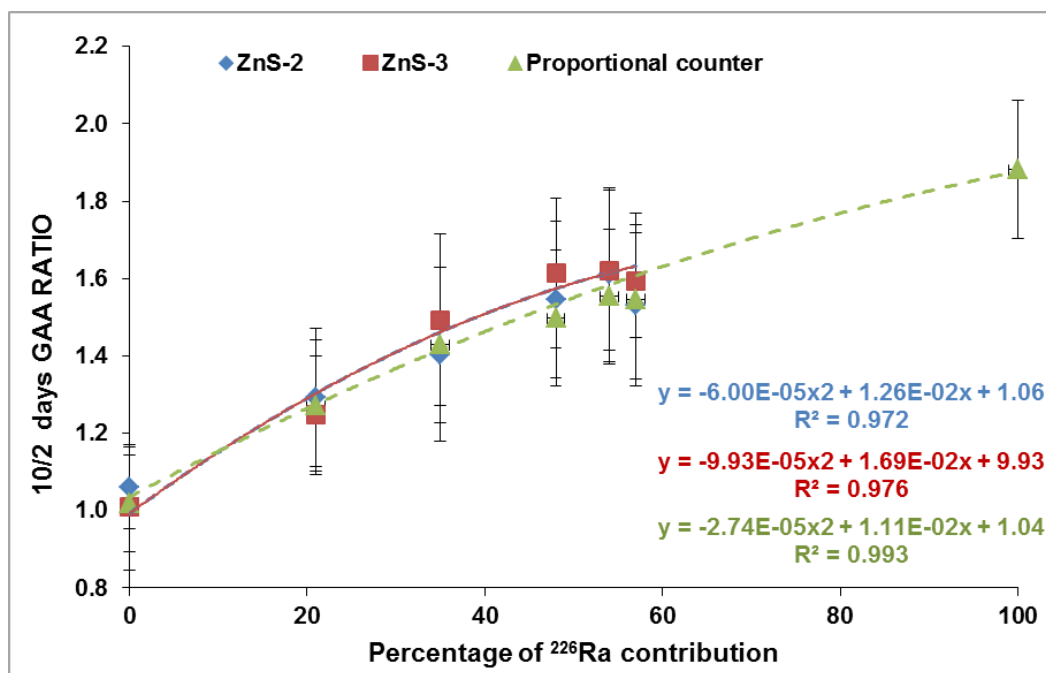
Figure 3.4. 10/2 days GAA RATIO vs. [226]Ra content in percentage. Dashed lines represent the quadratic adjustment for each detector. Error bars represent the combined/overall uncertainty of the two GAA values used to obtain the ratio (coverage factor k = 2).

It should be noted that, since this ratio is a relationship between GAA values, the plots presented in Figure 3.4 are independent of the standard calibration used as well as the rest of alpha

emitters present on the sample (^{nat}U, ^{210}Po). Therefore, it is possible to identify and estimate ^{226}Ra content in water samples without any further specific calibration.

According to the results obtained for the different detectors, an average quadratic equation was calculated using all data. The ^{226}Ra content estimation curve is presented in Figure 3.5. The dashed lines represent the uncertainty in percentage calculated with 95% confidence level using the MATLAB program. This equation could be used to estimate the ^{226}Ra content in real samples which are measured at two and ten days.
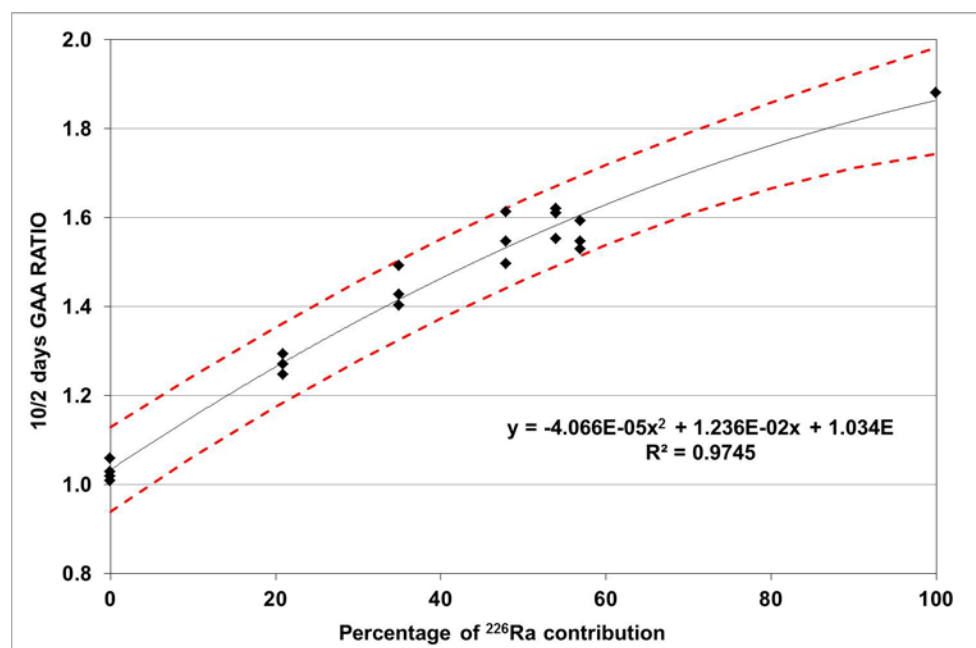
Figure 3.5. Average quadratic function of 10/2 days GAA RATIO as a function of the ^{226}Ra content in percentage. Dashed lines represent the uncertainty (around 9%) obtained using the 95% confidence bounds provided to MATLAB program.

Assessment of results: Precision and Bias

The data from the synthetic studied samples were tested by the EURACHEM guide (1998). According to this guide, precision is a measure of how close results are to one another. The most common precision measure within a single laboratory is 'repeatability'. Repeatability will give an idea of the sort of variability to be expected between results when sample is analyzed in duplicate. If a sample is analyzed by different equipment, different analysts, etc., this is known as 'intermediate precision'. Precision is usually stated in terms of standard deviation or relative standard deviation which describes the spread of the results (see equation 3.1).

$$RSD = \sqrt{\frac{\sum_{i=1}^{n}(x-\bar{x})^2}{(n-1)}}\Big/ \bar{X} \cdot 100 \qquad (3.1)$$

where $\bar{X}$ is the mean of the individual results for sample and X_i is the individual value (GAA value).

The bias of a method is how close the mean of a set of results (produced by the method) is to the true value and was determined by equation 3.2:

$$Bias\ (\%) = \left(\frac{\bar{X}_i - Y_i}{Y_i}\right) \cdot 100 \qquad (3.2)$$

where $\bar{X}_i$ is the mean of the individual results for sample and Y_i is the reference (true) value.

Summaries of precision (repeatability and intermediate precision taking into account the different equipment used) and bias evaluation of the GAA results for the synthetic samples as calculated with the three standard counting efficiencies are given in Tables 3.5 through 3.8. The GAA values reported in these tables are values obtained measuring the samples at two days after sample preparation. For sample containing mixtures of radionuclides, results from one of the different composition samples were presented.

Table 3.5. Statistical parameters for synthetic samples containing 100% of Natural Uranium.

Synthetic sample 1 (100% of ^{nat}U)	GAA (two days after sample preparation) referred to		
Parameter	^{241}Am	^{230}Th	^{nat}U
Y (Bq/L), true value	0.228 ± 0.003	0.228 ± 0.003	0.228 ± 0.003
$\bar{X}$ (Bq/L), GAA value	0.180 ± 0.013	0.225 ± 0.019	0.230 ± 0.015
Bias (%)[1]	-17.7 ± 1.5	-1.4 ± 0.1	0.9 ± 0.06
Repeatibility (%) (RSD$_{ZnS}$)	12.5	13.2	12.3
Repeatibility (%) (RSD$_{proportional}$)	4.8	5.9	3.9
Intermediate precision (RSD)	9.9	9.1	8.3

[1] The bias uncertainty is the relative standard deviation of the replicates.

Table 3.6. Statistical parameters for synthetic samples containing 100% of ^{226}Ra.

Synthetic sample 2 (100% of ^{226}Ra)	GAA (two days after sample preparation) referred to		
Parameter	^{241}Am	^{230}Th	^{nat}U
Y (Bq/L), true value	0.209 ± 0.007	0.209 ± 0.007	0.209 ± 0.007
$\bar{X}$ (Bq/L), GAA value	0.370 ± 0.029	0.441 ± 0.033	0.487 ± 0.037
Bias (%)[1]	76.9 ± 6.0	110.9 ± 8.3	133.1 ± 10.0
Repeatibility (%) (RSD$_{ZnS}$)	11.3	4.1	16.5
Repeatibility (%) (RSD$_{proportional}$)	9.4	9.2	8.7
Intermediate precision (RSD)	10	9	13

[1] The bias uncertainty is the relative standard deviation of the replicates.

Table 3.7. Statistical parameters for synthetic samples containing 100% of ^{210}Po.

Synthetic sample 3 (100% of ^{210}Po)	GAA (two days after sample preparation) referred to		
Parameter	^{241}Am	^{230}Th	^{nat}U
Y (Bq/L), true value	0.170 ± 0.003	0.170 ± 0.003	0.170 ± 0.003
$\bar{X}$ (Bq/L), GAA value	0.158 ± 0.011	0.191 ± 0.016	0.197 ± 0.014
Bias (%)[1]	-6.6 ± 0.5	12.9 ± 1.1	16.2 ± 1.1
Repeatibility (%) (RSD$_{ZnS}$)	4.2	5.9	6.5
Repeatibility (%) (RSD$_{proportional}$)	4.0	3.8	2.5
Intermediate precision (RSD)	3.9	5.1	6.8

[1] The bias uncertainty is the relative standard deviation of the replicates.

Table 3.8. Statistical parameters for synthetic samples containing ^{nat}U, ^{210}Po and ^{226}Ra (39:26:35).

Synthetic sample 4 (39% ^{nat}U, 26% ^{210}Po and 35% ^{226}Ra)	GAA (two days after sample preparation) referred to		
Parameter	^{241}Am	^{230}Th	^{nat}U
Y (Bq/L), true value	0.297 ± 0.006	0.297 ± 0.006	0.297 ± 0.006
$\bar{X}$ (Bq/L), GAA value	0.358 ± 0.022	0.441 ± 0.032	0.453 ± 0.023
Bias (%)[1]	20.4 ± 41.3	48.5 ± 3.5	52.2 ± 2.7
Repeatibility (%) (RSD$_{ZnS}$)	6.6	6.4	7.3
Repeatibility (%) (RSD$_{proportional}$)	8.7	8.8	10.1
Intermediate precision (RSD)	7.1	7.7	9.2

[1] The bias uncertainty is the relative standard deviation of the replicates.

According to the results presented on Tables 3.5 to 3.8, the repeatability obtained for samples measured in ZnS detectors has been comprised between 4 and 17%. For samples measured in gas-flow proportional detectors was between 2 and 10%. These values were very similar to those obtained by Whitaker (1986) which were between 10 and 15%. Furthermore, the assay intermediate precision has been compressed between 4 and 11%.

The bias obtained in samples containing only ^{nat}U or ^{210}Po were less than 20%, independently the standard used in the calibration. On samples containing ^{nat}U (Table 3.6) the ^{241}Am calibration standard underestimates the reference value by 18%. On the contrary, samples containing only ^{210}Po (Table 3.7), ^{nat}U standard calibration overestimates the reference value by 16%.

Bias for samples containing ^{226}Ra (simple and mixed synthetic samples) has been between 20 and 133% above the reference value due to the presence of ^{226}Ra decay products.

According to the results obtained, and taking into consideration other previously published studies, the selection of one of the calibration standards studied is discussed below.

It is clear that samples containing only ^{nat}U, GAA values with less bias were obtained using ^{230}Th and ^{nat}U as calibration standards. GAA (two days after preparation) of samples containing ^{226}Ra will be overestimated in function of the percentage of ^{226}Ra in the sample as well as the standard used in the calibration.

However, at present it cannot yet be said with certainty that ^{230}Th is the suitable standard to use in the calibration for the co-precipitation method since ^{241}Am has not presented enough bias to discard its use as a calibration standard. ^{nat}U has also not presented enough bias to discard it. But from now, ^{nat}U standard will be discarded as standard calibration due to mainly for three

reasons: The first one is the lack of amount certified of both ^{238}U and ^{234}U in the certificate; the second one is because most of natural water samples present disequilibrium between ^{238}U and ^{234}U isotopes which their alpha energies are quite different (^{234}U: 4.76 MeV and ^{238}U: 4.20 MeV). The different energy of both isotopes and their amount may change substantially the GAA value (Arndt, 2010). Finally the third reason is the only selectivity of uranium towards to Fe(OH)$_3$ precipitate instead of ^{241}Am and ^{230}Th selectivity towards to both Fe(OH)$_3$ and BaSO$_4$ precipitate components (Parsa et al. 2011).

Another noteworthy conclusion is the good degree of precision obtained for this method independently the standard used in the calibration as well as the equipments used (10%, maximum value obtained from GAA results referred to ^{230}Th and ^{241}Am).

3.3.2 Validation through intercomparisons

Samples provided by different institutions were analyzed in order to obtain an external validation of the co-precipitation method. They were water samples with a known concentration of gross alpha activity that has been established by the reference laboratory. In some cases the reference value established corresponds to an average value derived from the results obtained by the participating laboratories. Samples were provided by International Atomic Energy Agency (IAEA), the European Commission (EC) and the Spanish Nuclear Safety Council (CSN). Samples were prepared and measured in duplicate by the co-precipitation method in ZnS(Ag) detectors. The co-precipitation method was evaluated by averaging the results obtained using ^{241}Am and ^{230}Th as standard calibrations.

Table 3.9 shows the results obtained and the corresponding Bias values for GAA estimated referred to ^{230}Th and ^{241}Am. As can be observed the method improved for determining GAA provided satisfactory results. GAA values using ^{241}Am as standard of calibration provided accurate results with a maximum bias (in absolute value) of 15. Only one of the GAA results obtained using ^{230}Th as standard of calibration exceeded 25%. For all the rest using ^{230}Th, the bias obtained was less than 7%.

Table 3.9. Results obtained in the intercomparisons exercises organized by IAEA, EC and CSN.

Organization (year)	Radionuclide used for spiking	Activity concentration in water (Bq/L)	Gross alpha activity estimated referred to the (Bq/L)		Bias (%)	
			^{230}Th	^{241}Am	^{230}Th	^{241}Am
IAEA (2009; 2010)	blank	< 0.2	0.15 ± 0.05	0.13 ± 0.04	---	---
	^{230}Th	3.93 ± 0.08	3.26 ± 0.24	2.92 ± 0.23	-7	-14
	^{230}Th	7.68 ± 0.15	7.29 ± 0.047	6.71 ± 0.35	-5	-13
	N.A.	4.8 ± 0.1	6.1 ± 0.5	5.5 ± 0.5	27	15
	N.A.	8.5 ± 0.2	8.4 ± 0.6	7.5 ± 0.6	-2	-11
EC (2012)	^{241}Am	0.95 ± 0.08	0.96 ± 0.05	0.89 ± 0.03	1	-7
CSN (2011)	^{230}Th, ^{nat}U, ^{210}Po, ^{226}Ra, ^{241}Am, ^{238}Pu	2.50 ± 0.45 [1]	2.38 ± 0.17	2.186 ± 0.126	-5	-13

N.A.: information not available.
[1] The reference value corresponds to an average value derived from the results obtained by the participating laboratories.

Figure 3.7 displays a least-squares linear regression analysis of GAA using ^{230}Th and ^{241}Am as standard calibration and the reference value (TAAC) of water samples from the intercomparisons. It shows a high correlation coefficient (0.98), for GAA values using ^{230}Th and ^{241}Am. Note that ^{230}Th line regression (red dashed line) overlap the solid line plotted with the reference values.

According to these results, ^{230}Th and ^{241}Am can be used in order to estimate the total alpha activity of a water sample by co-precipitation method.
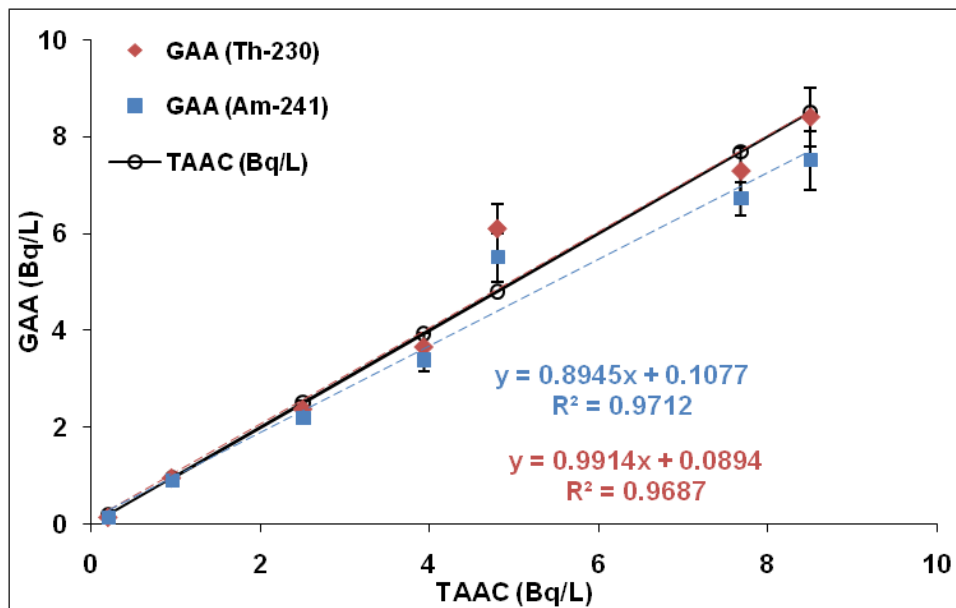
Figure 3.6. A plot of lest-squares linear regression analysis of gross alpha activity using ^{230}Th and ^{241}Am as standard calibration and the reference values of water samples from different intercomparisons. The reference value (TAAC) of these samples is also presented (black solid line with circles).

3.3.3 Validation on natural water samples

The validation with natural samples was carried out on several water samples of different radioactive characteristics. This validation was made splitting into two groups all the samples studied according to the available data and the studies conducted with them.

The first group consists of the eight Spanish natural waters presented above in Table 3.2 (subsection 3.2.1). It is noteworthy that for these samples other laboratories participated applying other methods to determine the GAA (CSN, 2012). For the eight Spanish water samples, uranium (^{238}U, ^{235}U, and ^{234}U), radium (^{226}Ra and ^{224}Ra), ^{210}Po, and ^{232}Th isotopes were assayed using radiochemical separation and alpha spectrometry (see Appendix B) in order to determine the sum of activities of these alpha emitters (Total alpha activity concentration: TAAC). This value will be the reference value used in order to compare with the GAA by co-precipitation method. TAAC was calculated by summing the quantified specific alpha emitter activity. If the activity was lower than the minimum detectable activity, this value was not used to calculate TAAC. Activities were expressed in mBq/L because of the very low values for some radionuclides detected (^{210}Po and ^{232}Th). Additionally, for these eight natural waters, a temporal evolution study of the GAA was conducted in order to establish a maximum elapsed

time between sample preparation and measurement of the GAA. Taking advantage of the measurements made for a period of one month, the [226]Ra content estimation using GAA measured at ten and two days was determined for these samples and compared to [226]Ra concentration reference value obtained by radiochemical separation.

The second group consists of 21 natural waters from Spain and from USA, these last ones analyzed in the WSLH (Table 3.3, subsection 3.2.1). All these samples were used to extend the validation taking into account the maximum elapsed time established based on the study conducted in the eight Spanish natural waters. Therefore, the temporal evolution of the gross alpha activity for this second group of samples was not studied. Additionally, [232]Th concentrations were not determined since thorium presents a very low solubility. Only the major contributors to the alpha activity were determined for this group of samples, taking into account previous information available related to these samples and provided by each laboratory (LARA and WSLH).

In short, it was considered studying in more detail the eight Spanish water samples and the second group were only considered in order to expand the validation of the method with natural waters.

Radiochemical characterization of the eight Spanish natural waters

The results of the activity concentration of specific alpha emitters in the eight Spanish waters (SF-1 to SF-4 and GW-1 to GW-4) are given in Table 3.10. According to the results presented in for the eight Spanish waters, groundwater showed higher TAAC than surface waters. In fact, all the studied groundwater presented gross alpha activities above the screening level of 100 mBq/L, while only one of the four studied surface waters exceeded this value.

The activity concentration (mBq/L) of [234]U, [235]U and [238]U in the natural waters varied from 18 to 2900, from < 1 to 90 and from 8 to 3000, respectively. The high activity concentration of uranium observed in the GW-4 sample was due to the rock present in the reservoir which was mainly lignite containing elevated levels of uranium. The arithmetical mean of the [234]U/[238]U activity ratio for all samples resulted in 2.0 ± 1.5 (relative standard deviation, RSD = 73%) thus confirming a different disequilibrium in the samples studied.

The fact that [226]Ra concentration in groundwater was higher than in surface water was also observed. The minimum [226]Ra activity concentration was 2.3 mBq/L (SF-2) and the maximum value was 550 mBq/L (GW-2). Significant activity concentration of [224]Ra was also measured in the four selected groundwater samples.

^{210}Po activity concentration was determined for most of the samples, but its contribution to Alpha Total was below 2.5%. The minimum activity concentration of ^{210}Po was 0.6 mBq/L and the maximum activity concentration was 110 mBq/L (GW-4).

Contribution of ^{232}Th was insignificant due to its low solubility in water and it was not detected in most of the studied waters.

In summary, Uranium and radium isotopes are the main contributors to the TAAC in these samples and produced more than 90% of the activity. Uranium isotopes (^{238}U+^{234}U) were usually present to a higher percentage (more than 70 %) compared with ^{226}Ra (usually less than 20 %). The exceptions were GW-2 and GW-3 with 40% and 80 % of ^{226}Ra, respectively.

Table 3.10. ^{238}U, ^{235}U, ^{234}U, ^{232}Th, ^{226}Ra, ^{224}Ra,^{210}Po activity concentrations (mBq/L) in the eight Spanish natural waters.

Sample code	Alpha activity concentration (mBq/L)							
	^{238}U [1]	^{235}U [1]	^{234}U [1]	^{232}Th [1]	^{226}Ra [1]	^{224}Ra [1]	^{210}Po [1]	Total Alpha activity concentration (Σ isotopes) [2]
GW-1	240 ± 20	10 ± 3	1330 ± 90	< 5	470 ± 60	80 ± 20	36 ± 4	2200 ± 200
GW-2	370 ± 60	13 ± 6	390 ± 60	< 8	550 ± 40	40 ± 10	28 ± 3	1400 ± 200
GW-3	8 ± 4	< 1	18 ± 5	< 9	210 ± 20	27 ± 6	0.6 ± 0.4	260 ± 40
GW-4	3000 ± 200	90 ± 20	2900 ± 200	< 10	130 ± 10	17 ± 4	110 ± 10	6200 ± 600
SF-1	70 ± 10	< 2	90 ± 10	9 ± 5	5 ± 1	< 2	< 0.3	170 ± 30
SF-2	11 ± 5	< 3	21 ± 6	8 ± 5	2.3 ± 0.4	< 1	1.0 ± 0.3	40 ± 10
SF-3	20 ± 5	< 2	34 ± 6	< 5	4.0 ± 0.8	< 2	0.8 ± 0.4	60 ± 15
SF-4	34 ± 8	< 2	48 ± 9	< 5	2.6± 0.7	< 2	1.2 ± 0.5	90 ± 20

[1]The overall uncertainty (coverage factor k = 2) was given as the average uncertainty for individual results, corresponding to three replicates prepared for each sample. This arose mainly from counting uncertainties.

[2] Uncertainty for the Alpha Total activity was given as the combined uncertainty of the average uncertainty of each isotope, with a coverage factor k = 2, corresponding to a level of confidence of 95%.

Temporal evolution of gross alpha activity

For these eight natural waters, their temporal evolution in gross alpha activity was studied to evaluate the influence of elapsed time from sample preparation to measurement in the gross alpha results. Different measurements, between 0 and 30 days, were performed.

By way of example, Figure 3.7 shows the gross alpha activities measured repeatedly for up to one month for water sample GW-3 (80% ^{226}Ra) using co-precipitation method.

In Figure 3.7, as might be expected for samples with ^{226}Ra, it is clear that gross alpha activity varies with time and therefore can be overestimated depending on the elapsed time between sample preparation and measurement. Gross alpha activity reached 660 mBq/L (2.6 times the TAAC value) after 21 days since preparation.
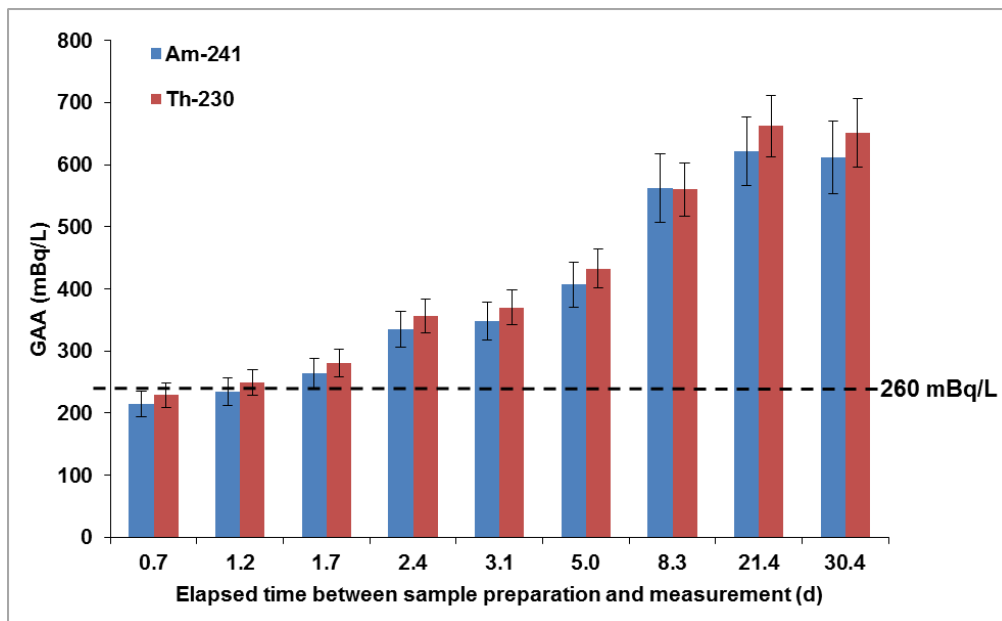
Figure 3.7. Temporal evolution of gross alpha activity in the GW-3 sample by co-precipitation method using ^{230}Th and ^{241}Am as standards of calibration. The dashed line is the TAAC in the sample. The error bars represent the overall uncertainty (coverage factor k = 2).

The ratio calculated by dividing the measured GAA and the TAAC (reference value) ranged from 0.9 to 2.6 (elapsed time between 1 and 21 days). This range is not surprising since three alphas are decaying in the ^{226}Ra decay chain.

By way of example, table 3.11 shows some statistical parameters (arithmetic mean, relative standard deviation, minimum and maximum values and the number of data) for gross alpha activity obtained by the co-precipitation method and using ^{230}Th as standard of calibration in the temporal evolution study (0-30 days) in the eight selected Spanish waters. The ratio GAA 10d/2d values are also presented in table 3.11 in order to estimate the ^{226}Ra contribution.

Uncertainty corresponds to average uncertainty for individual measurements which mainly arises from counting statistics, and RSD gives information about temporal variation in the measured activity. Both parameters are compared and if no differences between them are found, no gross alpha activity variations occur over time. However, this time should be considered as an important factor that needs to be defined. High uncertainties are associated with low activities (SF-2 or SF-3) with values near the MDA.

On the other hand, RSDs for radioactivity in groundwaters were usually higher than the mean uncertainty. One characteristic of studied groundwater is the presence of significant ^{226}Ra activities. Ingrowth of ^{226}Ra daughters means that elapsed time has an influence on count rate and ideally would require measurements to be carried out as soon as possible. However, one must decide on a compromise between the theoretically ideal time and each laboratory's work routine. Consequently, to limit the variability associated with the elapsed time after source preparation, an optimal range for measurement delay should be established. It is recommended that the elapsed time for co-precipitation method be after two days and before a maximum of five days. The differences between the values for the same sample obtained at two and five days (Figure 3.7) were calculated and found to be 21%.

Nevertheless, the recommendation to measure samples after two days of their preparation does not provide satisfactory results for this sample (GW-3). But it is important to consider three points. First; using ^{230}Th as a calibration standard for samples with significant amounts of ^{226}Ra will tend to overestimate gross alpha activity because ^{226}Ra and its daughters emit higher energy alpha particles than does ^{230}Th. On the other hand, samples containing ^{226}Ra can be measured immediately after preparation, but this recommendation carries some drawbacks under routine laboratory work. Finally, in a previous investigation (CSN, 2012) it was observed that natural waters in Spain with non-negligible ^{226}Ra content are unusual. Therefore, the initial recommendations are suitable for most natural waters in Spain.

Table 3.11. Average of gross alpha activity (mBq/L) obtained at different elapsed time and statistical parameters for the co-precipitation method using ^{230}Th as standard calibration. GAA values at two and ten days after sample preparation and 10/2 days ratio are also presented.

Statistical parameters	GW-1	GW-2	GW-3	GW-4	SF-1	SF-2	SF-3	SF-4
Mean (uncertainty) [1]	2451 (± 8%)	2144 (± 5%)	550 (± 8%)	5374 (± 8%)	151 (± 9%)	7 (± 28%)	51 (± 12%)	87 (± 10%)
Range (min-max)	(1935-3259)	(1249- 2805)	(229-1070)	(4562-6113)	(126-175)	(3-18)	(44-79)	(49-113)
RSD (data)	16% (55)	21% (78)	35% (62)	7% (56)	8% (55)	58% (52)	17% (49)	22% (69)
GAA ± SD [2] (two days)	2249 ± 109 (4)	1605 ± 138 (4)	361 ± 4 (4)	5353 ± 510 (4)	145 ± 12 (4)	5 ± 3 (4)	53 ± 8 (4)	80 ± 18 (4)
GAA ± SD [2] (ten days)	2872 ± 126 (4)	2357 ± 131 (4)	625 ± 39 (4)	5748 ± 598 (4)	151 ± 12 (4)	6 ± 4 (4)	57 ± 14 (4)	85 ± 22 (4)
Ratio GAA (10d/2d)	1.28	1.47	1.73	1.07	1.04	1.01	1.08	1.06

[1] all data average uncertainty $k=2$.
[2] standard deviation of replicates.
The number of data used in calculation is indicated in brackets.

Additionally, if there is a non-negligible presence of ^{226}Ra in samples with activities around 0.1 Bq/L, not enough time has passed for its descendants to significantly increase the gross alpha count rate in that maximum elapsed time proposed.

A large variation in gross alpha activity (RSD) was also observed for sample SF-2 which had detectable activity at or slightly above the MDA.

Accuracy

A comparison of the gross alpha activity results referred to ^{241}Am and ^{230}Th, excluding SF-2, and the TAAC was also reported as a bias (Figure 3.8). The reference value for each sample is the TAAC.
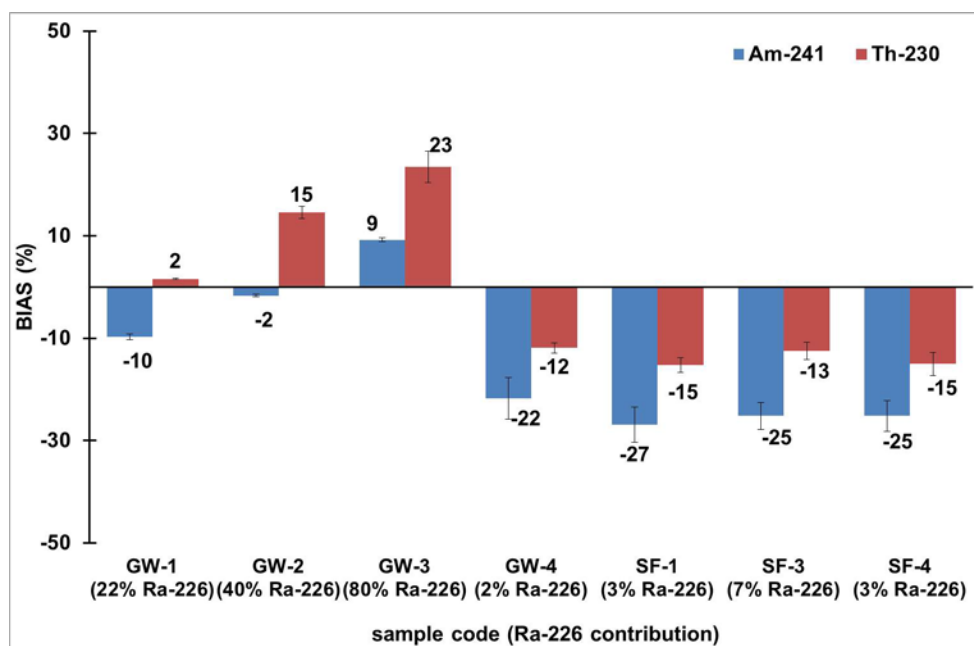
Figure 3.8. Bias (%) obtained by co-precipitation method using ^{241}Am and ^{230}Th as standards of calibration and the TAAC for the natural water samples studied. The error bars represent the standard deviation of the replicates.

Significant bias (positive) on the GAA using ^{230}Th was shown for sample GW-3 due to the significant contribution of ^{226}Ra, 80% of the TAAC. Samples containing less ^{226}Ra contribution,

(less than 40%) their GAA values using [230]Th as a calibration standard match with TAAC. Results obtained for the other samples presented an acceptable bias (less than 15%).

Using [241]Am as a standard of calibration, biases are greater than 20% except when samples containing an important [226]Ra contribution (GW-2 and GW-3) in which [241]Am gives the most accurate results for these samples (2% and 9% respectively).

Gross alpha activity determined by the co-precipitation method has a bias below 25 % for the eight samples irrespectively of the activity and the standard used in the calibration. Therefore, there are no reasons for selecting one of the two calibration standards if it is considered a 25% tolerance level (the worst relative uncertainty value obtained from TAAC results).

Despite this, in Spain, only 20 % of samples contain [226]Ra and 80% mostly contain uranium isotopes (CSN, 2012). Therefore, if we should decide for one of them, in accordance with the statistical data, [230]Th would be the calibration standard providing most accurate results.

[226]Ra content estimation

According to the results obtained in Section 3.3.1, two GAA measurements, one at two days and one at ten days, were used to estimate the [226]Ra content of a water sample. Table 3.11 presented above also contains both activities measured at two and ten days after sample preparation and their GAA ratio. The values presented are the mean of four replicates. The following equation discussed above in the subsection 3.3.1 permits this estimation and was used to calculate the [226]Ra content for the eight natural water samples.

$$Ratio\left(\frac{GAA_{10\ days}}{GAA_{2\ days}}\right) = -4.066 \cdot 10^{-5} \boldsymbol{Ra}(\%)^{\boldsymbol{2}} + 1.236 \cdot 10^{-2} \boldsymbol{Ra}(\%) + 1.034$$

The [226]Ra content estimation and the [226]Ra reference value for the eight natural water samples are showed in Figure 3.9. As we can see, it is possible obtaining a good estimation of the [226]Ra content. For samples GW-1, GW-2 and GW-3 that contain an important [226]Ra contribution presented bias around 3% respect to the reference content. For samples containing around 5% of [226]Ra content, the bias obtained was more than 30%. These last results agreed within the uncertainties obtained for these results.
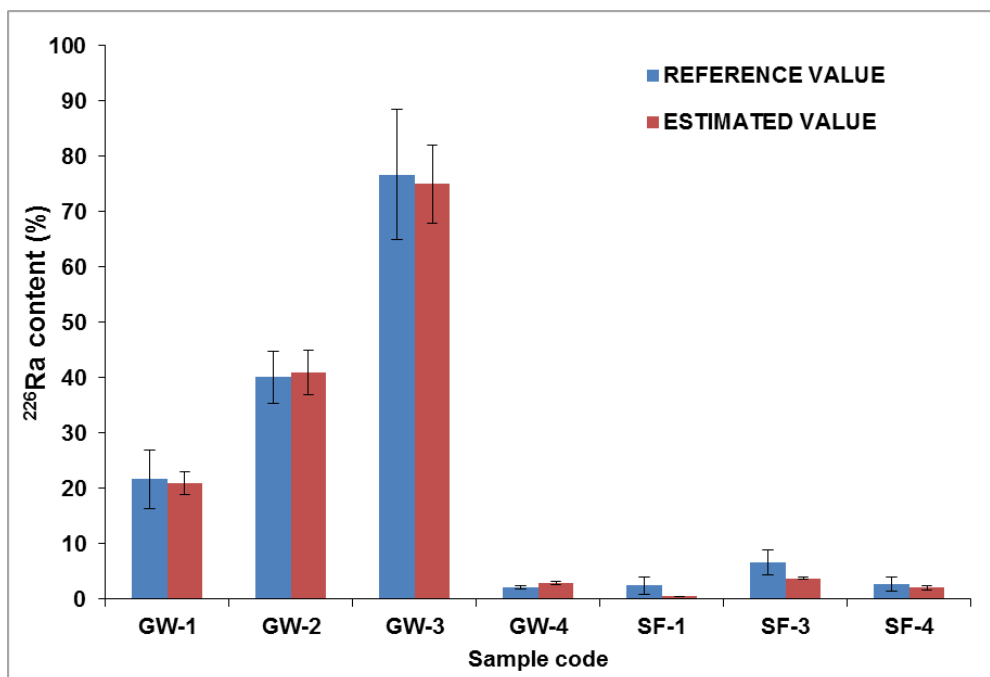
Figure 3.9. Reference and calculated [226]Ra content values in percentage for the eight natural water samples. The error bars represent the uncertainty due to the replicates and the estimation of the curve.

Extended Validation

21 additional natural water samples have been used in order to expand the validation. Tables 3.12 and 3.13 contain their radiological characterization. As it is observed on tables 3.12 and 3.13, the validation was extended including mainly groundwater samples and some wastewater and surface water samples.

For surface waters and wastewater samples, the most common radionuclides are Uranium isotopes whereas in ground water samples were both Uranium and Radium isotopes.

Taking into account the geographical location of the groundwater samples studied, the most common radionuclides in Spanish water samples were uranium isotopes (CSN, 2012). On the other hand, water samples from USA presented more variety of radiological composition finding uranium and radium isotopes and [210]Po. GW-8, GW-9 and GW-10 samples contain significant amounts of [210]Po unsupported which have been extensively studied before (Outola et al., 2008).

Therefore, we can say that this study contains samples with different radionuclide composition.

Table 3.12. ^{238}U, ^{235}U, ^{234}U, ^{226}Ra, ^{224}Ra, ^{210}Po activity concentrations (mBq/L) in the natural waters of the 2nd group (groundwater samples).

Sample code	Alpha activity concentration (mBq/L)						
	^{238}U [1]	^{235}U [1]	^{234}U [1]	^{226}Ra [1]	^{224}Ra [1]	^{210}Po [1]	Total Alpha activity concentration (Σ isotopes) [2]
GW-5	5 ± 2	7 ± 2	23 ± 4	116 ± 16	759 ± 49	< 0.1	911 ± 52
GW-6	944 ± 41	68 ± 7	1920 ± 78	< 10	< 20	< 3	2932 ± 88
GW-7	124 ± 9	9 ± 2	353 ± 18	58 ± 4	81 ± 23	< 5	625 ± 31
GW-8	< 2	< 1	< 4	< 12	< 23	881 ± 67	793 ± 67
GW-9	< 13	< 9	< 5	< 2	< 15	859 ± 36	859 ± 36
GW-10	15 ± 5	5 ± 3	7 ± 4	<10	<26	1301 ± 52	1328 ± 52
GW-11	122 ± 6	6 ± 1	126 ± 6	276 ± 6	33 ± 2	---	563 ± 11
GW-12	320 ± 9	35 ± 3	273 ± 8	50 ± 2	<5	---	678 ± 13
GW-13	165 ± 5	8 ± 1	185 ± 5	---	---	---	357 ± 7
GW-14	155 ± 6	8 ± 1	172 ± 6	---	---	---	335 ± 8
GW-15	55 ± 3	2.3 ± 0.6	89 ± 4	---	---	---	146 ± 5
GW-17	387 ± 14	19 ± 0.3	571 ± 17	---	---	---	977 ± 22
GW-18	54 ± 4	5 ± 1	88 ± 5	---	---	---	147 ± 6

[1] The Overall uncertainty (coverage factor k = 2) was given as the average uncertainty for individual results, corresponding to one replicate. This arose mainly from counting uncertainties.
[2] Uncertainty for the Alpha Total activity was given as the combined uncertainty of the average uncertainty of each isotope, with a coverage factor k = 2, corresponding to a level of confidence of 95%.

Table 3.13. ^{238}U, ^{235}U, ^{234}U, ^{226}Ra, ^{224}Ra, ^{210}Po activity concentrations (mBq/L) in the natural waters of the 2nd group (surface and wastewaters).

Sample code	^{238}U [1]	^{235}U [1]	^{234}U [1]	^{226}Ra [1]	^{224}Ra [1]	^{210}Po [1]	Total Alpha activity concentration (Σ isotopes) [2]
				Alpha activity concentration (mBq/L)			
SF-5	41 ± 3	3 ± 1	120 ± 5	---	---	---	164 ± 6
SF-6	55 ± 4	4 ± 1	97 ± 5	---	---	---	156 ± 6
SF-7	76 ± 4	3 ± 1	117 ± 5	---	---	---	196 ± 6
SF-8	78 ± 5	3 ± 1	110 ± 6	---	---	---	191 ± 8
WW-1	12 ± 4	<	16 ± 5	---	---	---	28 ± 6
WW-2	27 ± 3	1.4 ± 0.6	37 ± 3	---	---	---	66 ± 4
WW-3	26 ± 3	2 ± 1	42 ± 4	---	---	---	69 ± 6
WW-4	320 ± 9	35 ± 3	273 ± 8	---	---	---	628 ± 13

[1] The Overall uncertainty (coverage factor k = 2) was given as the average uncertainty for individual results, corresponding to one replicate. This arose mainly from counting uncertainties.
[2] Uncertainty for the Alpha Total activity was given as the combined uncertainty of the average uncertainty of each isotope, with a coverage factor k = 2, corresponding to a level of confidence of 95%.

A comparison of the gross alpha activity results referred to [241]Am and [230]Th and the TAAC was reported as a bias (Figure 3.10 and 3.11). Samples from USA (GW-5 to GW-10) did not presented bias for [241]Am calculations due to the lack of [241]Am calibration during the stay at WSLH.
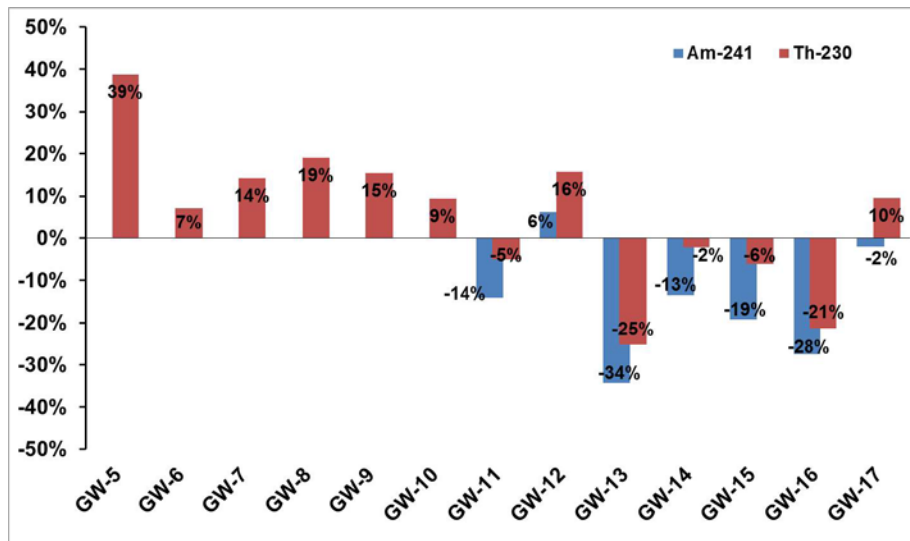
Figure 3.10. Bias (%) obtained by co-precipitation method using [241]Am and [230]Th and the TAAC for the second group of groundwater samples studied.

GW-5 mainly contains [224]Ra and GAA using [230]Th is overestimated by 39%. In samples that contain [224]Ra and their short lived, high-energy progeny, the GAA often greatly exceeds the TAAC of the sample. The overestimation in this sample is because the short-lived progeny of [224]Ra, account for the bulk of the GAA. This is because the alpha-particle energies of these short lived progeny are relatively high so that their corresponding efficiencies are high. This is readily seen from the results presented in Chapter 2 (section 2.4.2). In addition, Parsa et al. (2000) found that the GAA of some replicate water samples analyzed within 48 h of collection could vary by over an order of magnitude and showed the variation to be due to [224]Ra, [212]Pb, and/or [214]Pb/[214]Bi.

For sample GW-5, during the stay at WSLH, it was possible to analyze another sample from the same water utility except that this was analyzed immediately after sample collection. The GAA for this sample was ten times greater than TAAC and it was due to [224]Ra and its descendants. As was the case of sample GW-5, it is usual for a sample to be in storage at least one week or two before a GAA analysis is performed on it. Over this period of time some of [224]Ra will have

decayed away and therefore the GAA would excess less than in the case when sample is prepared immediately after sample collection. According to these results, it is seen that the time between sample collection and preparation can determine variability of the GAA.

For GW-6 which contains mainly Uranium isotopes, GAA using ^{230}Th gives an accurate result (7% of bias).

GW-7 contains 11% of ^{226}Ra , 13% of ^{224}Ra and its main contribution is due to uranium isotopes. In this case GAA using ^{230}Th gave a reasonable result (14% of overestimation) being the bias lower than the precision of the method.

Samples containing ^{210}Po unsupported (GW-8, GW-9 and GW-10), ^{230}Th subestimates GAA of the sample, mainly due to higher alpha-particle energy of ^{210}Po than ^{230}Th. When samples containing ^{210}Po, ^{241}Am should give the most accurate results, as it is demonstrated before in section 3.3.1.

The rest of the groundwater samples (GW-11 to GW-17), containing mainly uranium isotopes, GAA using ^{230}Th and ^{241}Am are overestimated by up to 16 and 6 percent and underestimated by up to -25 and -34 percent respectively.

For surface water samples (Figure 3.11), in all cases, except SF-5, the alpha activity using both ^{241}Am and ^{230}Th are underestimated.
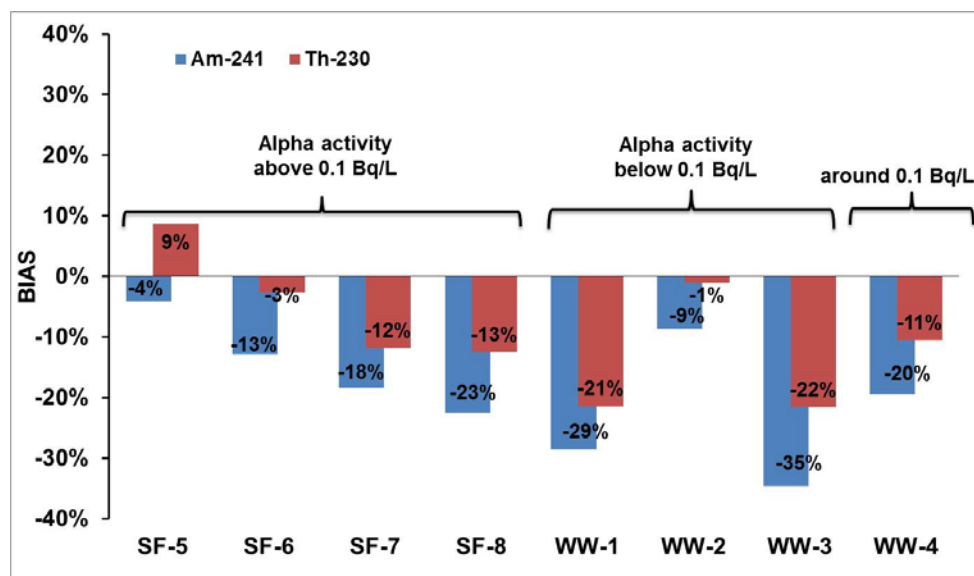
Figure 3.11. Bias (%) obtained by co-precipitation method using ^{241}Am and ^{230}Th and the TAAC for the second group of natural water (surface and wastewater) samples studied.

In general and typically, water samples containing uranium isotopes are enriched in ^{234}U relative to ^{238}U, being alpha-particle energies of ^{234}U higher than alpha-particle energies of ^{238}U. It is seen that the alpha particle energies for ^{234}U and ^{230}Th are relative close, and since most of the activity in these samples is from ^{234}U, using ^{230}Th as the calibration standard gives the most accurate results. Only three exceptions were found, giving ^{241}Am the most accurate results (SF-5, GW-12and GW-17).

For wastewater samples, the alpha activity levels were below or around 0.1 Bq/L and, by definition, bias obtained for samples with a low alpha activity using the co-precipitation method can be greater than those obtained for samples with higher alpha activity. Since these samples contain uranium isotopes as main contributors to the TAAC, the GAA calculated using ^{230}Th gave the most accurate results.

In short, all these rates do not yet allow selecting one of both standards in order to obtain the most accurate results of the GAA, mainly due to the small differences found between GAA results using ^{230}Th and ^{241}Am (around 10%).

3.3.4 Comparative study of gross alpha natural water samples determined by different procedures

With the aim to expand the validation, the GAA by different procedures applied by different Spanish laboratories were compared. Three accredited laboratories (ISO/IEC 17025) took part in the study: the *Laboratorio de Radiactividad Ambiental-Universidad de Extremadura* (LARUEX), the *Laboratori de Radioactivitat Ambiental-Universitat de Barcelona* (LRA-UB) and our laboratory LARA. A specific method for gross alpha determination was assayed by each laboratory and radiochemical procedures for specific alpha emitters were applied by the three laboratories. The comparison study was made between evaporation, co-precipitation and total evaporation/LSC methods (see Appendix B for evaporation and total evaporation/LCS methods description). Our laboratory used the co-precipitation method, while two others used evaporation (LARUEX) and total evaporation/LSC methods (LRA-UB) (CSN, 2012; Montaña et al., 2013a). Evaporation and total evaporation/LSC methods have been also optimized by these laboratories mentioned above in the same way as optimized the co-precipitation method.

Table 3.14 shows the data for the eight Spanish waters (samples from Table 3.2) studied and presents a comparison among gross alpha activities measured by the three methods. Additionally, the average activity among the three methods is given.

As the optimal elapsed time between sample preparation and measurement is different for each method (Montaña et al., 2013a), the gross alpha activity after two days of measurement for evaporation and co-precipitation and after two hours for total evaporation/LSC are presented in order to compare results among these methods. The results were obtained with ^{230}Th as the efficiency calibration standard for evaporation and co-precipitation, while ^{236}U was used for the concentration method.

RSD between methods was less than 30% with the exception of sample SF-3, whose gross alpha activity is near the minimum detectable activity for the total evaporation/LSC method. In order to test if this deviation entails a no significant variation, an ANOVA test was applied.

Table 3.14. Gross alpha activity obtained for each method in Bq/L. The mean value obtained among the three methods is also presented.

Sample code	evaporation			co-precipitation			total evaporation/LSC			Average activity among methods		
	activity	unc. [1]	RSD (%)	activity	unc. [1]	RSD (%)	activity	unc. [1]	RSD (%)	activity	unc. [2]	RSD (%)
GW-1	1860	460	17 (3)	2235	193	8 (4)	1970	70	9 (3)	2020	190	9
GW-2	1120	280	28 (3)	1604	134	9 (4)	1320	60	6 (3)	1350	243	18
GW-3	380	200	20 (3)	321	30	11 (4)	210	30	9 (3)	310	90	29
GW-4	3780	920	8 (3)	5591	295	15 (4)	6830	250	2 (3)	5170	1278	25
SF-1	150	70	17 (3)	144	13	9 (4)	180	30	5 (3)	160	20	13
SF-2	<MDA			<MDA			<MDA					
SF-3	60	40	5 (3)	52	7	18 (4)	30	20	55 (3)	50	16	33
SF-4	60	40	16 (3)	76	9	25 (4)	100	20	26 (3)	80	18	23

The number of data used in each calculation is indicated in brackets.

[1] Uncertainty is given as average uncertainty, corresponding to three replicates for each sample which arises mainly from counting uncertainty.

[2] Uncertainty is given as a standard deviation, corresponding to the three methods.

ANOVA results

In order to test statistically whether there was significant variability among the three methods, an ANOVA test was applied to the results from the eight natural water samples. SF-2 was excluded because its activity was below the MDA for all three methods. This test was applied to the data obtained at the optimal elapsed time for each method (two days for evaporation and co-precipitation and two hours for total evaporation/LSC). The conclusions derived from this test involve only the methods when the measure is performed at this optimal elapsed time. The ANOVA results are presented in Table 3.15.

Table 3.15. ANOVA test results for the natural water samples.

Sample code	F_{cal}	F'	Differences between methods	Degrees of freedom
GW-1	1.60	4.75	No diff.	9
GW-2	4.10	4.75	No diff.	9
GW-3	5.78	6.59	No diff.	7
GW-4	17.38	4.75	Sig. Diff	9
SF-1	2.95	4.75	No diff.	9
SF-2	-	-		
SF-3	4.85	4.75	Sig. Diff	9
SF-4	4.55	5.41	No diff.	8

F_{cal}: Calculated value from de F distribution
F': 0.05 critical value from de F distribution

For five of the seven water samples tested there were no significant differences among the three studied methods. There were significant differences among methods for samples SF-3 and GW-4. In order to find the cause of these differences a t-test was applied comparing the results of each of the studied methods with the TAAC. This test was done for three replicated (evaporation and total evaporation/LSC) and four replicated (co-precipitation) samples.

Table 3.16 showed the t-test results. In general, for all water samples, the results obtained for the studied methods (evaporation, co-precipitation or total evaporation/LSC) were not significantly different for alpha spectrometry determination. This finding is concordant with the ANOVA test results. However, there were differences between the evaporation method and the alpha spectrometry determination for sample GW-4. This allows us to attribute to the evaporation method the significant differences detected between the three methods using the

ANOVA test. The inability of the evaporation method to determine gross alpha activity in sample GW-4 was due to the high residue of the sample. A high saline content in the sample is a drawback for the evaporation method as it implies a high mass residue which increases autoabsorption. Moreover, the high sulfate content in sample GW-4 (unusual in natural waters in Spain) generated residues with an autoabsorption greater than that obtained with the nitrates matrix used in the calibration. This fact involves an underestimation of the gross alpha content.

Table 3.16. T test between each sample for each method and the alpha spectrometry results.

Sample code	evaporation			co-precipitation			evaporation/LSC		
	t_{cal}	t'	equal to α spect.	t_{cal}	t'	equal to α spect.	t_{cal}	t'	equal to α spect.
GW-1	1.407	3.182	Equal	0.508	4.715	Equal	1.133	3.182	Equal
GW-2	1.267	3.182	Equal	1.525	4.527	Equal	0.606	3.182	Equal
GW-3	2.102	3.182	Equal	1.368	4.551	Equal	1.778	3.182	Equal
GW-4	6.457	3.182	Sig. Diff	1.034	4.337	Equal	0.167	3.182	Equal
SF-1	1.615	3.182	Equal	2.357	4.724	Equal	0.223	3.182	Equal
SF-2	-	-		-	-		-	-	
SF-3	0.226	3.182	Equal	0.734	4.603	Equal	1.954	3.182	Equal
SF-4	2.468	3.182	Equal	1.659	4.773	Equal	0.044	3.182	Equal

t_{cal}: Calculated value from de t distribution
t': 0.05 critical value from de t distribution (evaporation and evaporation/LSC 3 degrees of freedom, co-precipitation 4 degrees of freedom).

However, for sample SF-3 there were differences between methods but there were no differences between each method and the TAAC. This apparent contradiction could be justified on the basis of the MDA of the methods, since the evaporation/LSC method has a MDA one order of magnitude higher than the other two methods, and similar to the level of activity of sample SF-3. This means that the differences between methods were detected by the ANOVA test but in the comparison of each method with the TAAC, the high dispersion in the total evaporation/LSC method provides the non-significant result.

Precision and accuracy

A comparison of the gross alpha activity results, excluding SF-2, for each method and the TAAC was also reported as a bias (Figure 3.12).

Total evaporation/LSC has usually the lowest bias (generally <10%) with the exception of GW-

3 and SF-3. SF-3 presented gross alpha activity close to the MDA of this method. On the other hand, significant biases (positive) in the evaporation and co-precipitation methods were shown for sample GW-3 due to the significant contribution of ^{226}Ra, 80% of the TAAC.
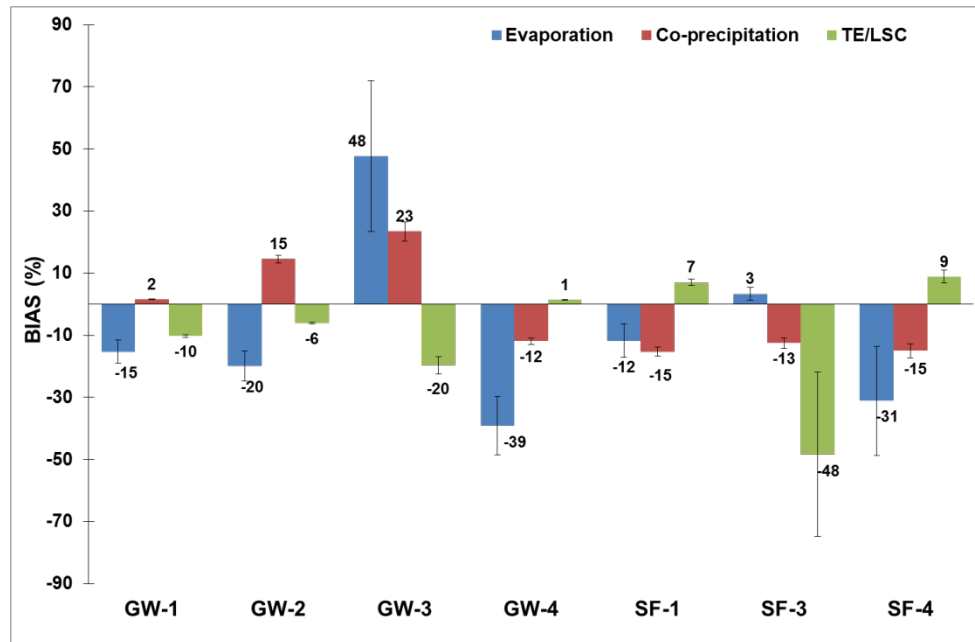
Figure 3.12. Bias (%) obtained by the three methods (evaporation, co-precipitation and total evaporation/LSC) and the TAAC for the natural water samples studied. The error bars represent the overall uncertainty (coverage factor k = 2).

Results obtained for the other samples presented an acceptable bias (less than -20%) for the three methods. When the bias is greater than 20% it is due to low activity levels, as in samples SF-1, SF-3 and SF-4.

Gross alpha activity determined by the evaporation method is often underestimated as a negative bias was obtained for most of the samples. Gross alpha activity determined by the co-precipitation method has a bias below 25 % for all the samples irrespectively of the activity. Gross alpha activity determined by the total evaporation/LSC method and the TAAC were comparable when the samples contained significant activity.

3.4 Summary

The co-precipitation method has been validated using synthetic samples spiked with different alpha emitters. Related to the temporal evolution study, synthetic samples containing uranium and polonium no significant variation of the GAA over the elapsed time was observed. Taking into account the standard used in the calibration, samples containing uranium the GAA using ^{230}Th and ^{nat}U gave the most accurate results. ^{241}Am underestimate the reference value, whereas GAA referred to ^{241}Am of samples containing polonium give most accurate results.

On the other hand, samples containing ^{226}Ra (figure 3.2), GAA vary considerably depending on the elapsed time between sample preparation and its measurement. Furthermore, none of the three standards considered (^{241}Am, ^{230}Th and ^{nat}U) matched with the TAAC. At zero days, the GAA was overestimated the TAAC.

A study of the GAA temporal evolution on samples containing different percentage of ^{226}Ra was made, in order to establish a duplicate counting to estimate the ^{226}Ra contribution on the GAA. From the GAA ratio values obtained between 10 and two days for the synthetic samples containing different amounts of ^{226}Ra, an average quadratic equation was calculated. This equation was applied on natural water samples giving accurate results when samples contain important ^{226}Ra content. The presence of uranium and polonium did not bias the ^{226}Ra content estimation neither for natural samples studied containing ^{224}Ra.

According to the results for natural water samples, uranium and radium isotopes are the main contributors to TAAC in natural surface water and groundwater samples from different regions of Spain and USA, each with different radioactive characteristics. Groundwater show higher gross alpha activities than do surface waters.

For practical uses, especially because radiological laboratories sometimes process a large number of samples in a small window of time, gross alpha measurements should be carried out after two days and preferably before five days after sample preparation in order to obtain results which are not largely overestimated, especially in waters in which the main contributor is ^{226}Ra.

Gross alpha activity determined by the co-precipitation method has a bias around 25 % for all natural water samples studied irrespectively of the activity and the standard used in the calibration. Therefore, there are no reasons for selecting one of the two calibration standards if it is considered a 25% tolerance level.

Despite this, in Spain, only 20 % of samples contain ^{226}Ra and 80% mostly contain uranium isotopes. If we should decide for one of them, in accordance with the statistical data, ^{230}Th would be the calibration standard providing most accurate results.

For natural water samples containing uranium isotopes, ^{230}Th curve generate a more conservative value.

ANOVA tests were used to identify differences among evaporation, co-precipitation and total evaporation/LSC methods. For the samples with the most common radiochemical characteristics there were no significant differences among the three studied methods. However differences were detected for samples with a high saline content or with a very low activity level.

For the comparative study among methods, precision (as RSD) was below 28 % for evaporation and below 18 % for co-precipitation, while in the case of total evaporation/LSC it was below 10 % for samples with TAAC above 0.1 Bq/L. For samples below 0.1 Bq/L the precision obtained for the total evaporation/LSC was around 50%.

The comparison of results for gross alpha activity obtained by the three methods (evaporation, co-precipitation and total evaporation/LSC) show an acceptable deviation (RSD less than 30 %). For the same study, the biases obtained by the evaporation, co-precipitation, and total evaporation/LSC methods were lower than 40%, 25% and 20%, respectively.

Part II

Behavior of radionuclides in water treatment plants

Introduction

The water has an importance in environmental studies because of its daily use for human consumption and its ability to transport pollutants. The occurrence of natural radionuclides in drinking water poses a problem of health hazard, when these radionuclides are taken into the body by ingestion. Additionally, the natural water resource availability can sometimes be lower than the water demand in some areas, so securing supplies of drinking water of a standard quality is becoming more and more difficult. It is thus indispensable to perform frequent and extensive analyses to guarantee that there is minimal or zero contamination of drinking water and to implement drinking water treatment processes to reduce pollutants when it is necessary.

In addition, another media that it should be taking into account are the wastewater treatment processes. Their construction is becoming increasingly important in order to accomplish an integrated water resources management and also due to population growth since more both restrictive environmental regulations are applied and wastewater re-use was demanded.

Drinking water treatment plants (DWTP) are used to treat raw water in order to produce water that is pure enough for the most critical of its intended uses, usually for human consumption. Conventional drinking water treatment plants have a fairly standard sequence of processes which essentially consist in solids separation using physical processes such as settling and filtration, and chemical processes such as coagulation and disinfection.

Levels of natural radionuclides in drinking water may be increased by a number of human activities. The most important radionuclides to be considered are ^{40}K, as well as the radionuclides of the radioactive series, particularly ^{238}U and ^{232}Th (UNSCEAR, 2000). Radionuclides from the nuclear fuel cycle, from medical and from other uses of radioactive materials may also enter into the drinking water supplies. However, the contribution to these

sources is normally limited by regulatory control and it is through this regulatory mechanism that remedial action should be taken in the event that such sources cause concern by contaminating drinking water (Ehmann and Vance, 1991).

In recent years, estimates have appeared in the scientific literature about the effects of radionuclides in water on human health and its elimination. Fortunately, conventional methods for treating raw waters for some other contaminants, such as mentioned above, are also effective in removing radionuclides found in water. For instance, there are some studies about the influence of conventional treatments (coagulation, flocculation, ion exchange, among others) applied at drinking water treatment plants (DWTP) to reduce radioactivity (Sorg, 1990;Gafvert et al., 2002; Jiménez and De la Montaña 2002; Wisser, 2003; Baeza et al., 2006; Baeza et al., 2008; Palomo et al., 2010a). In these works it was found that uranium and radium removal were very sensitive to the pH, the coagulant used and also showed important influence of other ions presented in the waters. Salonen (2006) evaluates the removal capacity of levels of uranium and radium isotopes by anion exchange applied at drinking water treatment plant in Finland. The results showed 98% of uranium reduction. In contrast, the radium removal was less effective. Kleinschmidt and Akber (2008) examined radioactivity concentrations of ^{238}U, ^{232}Th, ^{226}Ra, ^{222}Rn and ^{210}Po in water at both pre- and post-treatment under typical water treatment operations in Australia. The results indicate that radiological properties of all water tested were within Australian drinking water guideline values. Pilot plants have been also constructed in order to analyze the removal capacity, in terms of radioactivity, at different stages of the global treatment plant process (Salas. 2005; Baeza et al., 2008)).

Regarding the artificial radionuclides, Gäfvert et al. (2002) also investigated the removal of plutonium, cesium and strontium, and found that conventional processes were effective to remove plutonium but neither cesium nor strontium. Nevertheless, there are currently methods to remove these artificial radionuclides (Smith et al. 2001). In addition, Baeza and collaborators studied the effectiveness of potable water treatment processes in eliminating gamma-emitting man-made radioisotopes of cesium, strontium and americium from different natural waters. The resulting decontamination was found to depend on the chemical behavior of each radionuclides considered, on the pH at which the process of coagulation is carried out, and the concentration of the other stable cations present (Baeza et al., 2004).

The occurrence of radionuclides in sludge samples from drinking water treatment plants has been also studied by some authors to evaluate their impact on human exposure. For instance, in the U.S., groundwater, which often contains more radioactivity, is generally used in water treatment processes to produce drinking water, and consequently, EPA has already published several technical reports on this topic. One of them summarizes data on the radioactive constituents and levels found in sewage sludge with the aim of evaluating any potential health

concerns in the future together with recommendations on management of radioactive materials in sewage sludge (Bastian et al. 2005). In another study reported by Wisser (2003), relatively high activity concentrations for natural radionuclides were found in sludge samples from a water treatment plant in Canada. Kleinschmidt and Akber (2008) also examined radioactivity concentrations in solid wastes derived from DWTPs and elevated residual concentrations were identified in these waste products. Palomo et al., (2010b) have been recently reported results of liquid and sludge samples from a Spanish DWTP. This study revealed that the major contribution to radioactivity in sludge samples was made by natural sources (97% of total activity).

In addition, recent advances suggest that many issues involving water quality could be resolved or greatly ameliorated by using ultrafiltration (UF), nanofiltration (NF), reverse osmosis (RO), electrodialysis (ED) or electrodialysis reversal (EDR) processes.

UF and NF membrane filtration processes work by excluding contaminants using pore size constrains when water under pressure is forced to pass through a semi-permeable membrane with different pore sizes. Both the pore size and applied pressure must be adequate for the required purposes. RO membrane works as a molecular filter that rejects positively and negatively charged ions based on molecular weight when pressurized water is forced through the membrane. In contrast, the driving force for separation in ED and EDR processes is an electric potential, and an applied current is used to transport ionic species across selectively permeable membranes. The principal difference between ED and EDR is that EDR includes the additional step of a change in electrode polarity every 15 to 20 minutes, thus causing a reversal in ion movement. This step minimizes scale buildup on the membranes which means that EDR can operate for longer time periods between cleanings.

Membrane technology is also appropriate for the elimination of natural radioisotopes present in drinking waters. Van der Bruggen and Van der Casteele (2003) have reviewed the use of NF to remove cations, natural organic matter, biological contaminants, organic pollutants, nitrates and arsenic from groundwater and surface water. The UF process is also used for purification of water contaminated by toxic metal ions, radionuclides, organic and inorganic solutes, bacteria and viruses. For example, UF assisted by complexation has been used to reduce uranium concentration (Kryvoruchko et al., 2004). A NF pilot plant experiment was set up to determine the uranium removal efficiency and for most experiments the uranium removal was about 95% (Raff and Wilken, 1999). In another study (Favre-Réguillon et al., 2008) demonstrated that uranium rejection depended on the uranyl species. RO effectively removes many inorganic contaminants, including heavy metals and radionuclides, such as radium and uranium (Huikuri et al., 1998). RO can remove 87 to 98% of radium from drinking water and similar elimination can be achieved for alpha, beta and gamma emitters (EPA, 1998). Uranium and its complexes

are very heavy, which allows the RO process to effectively remove (95 to 99%) uranium complex such as uranyl carbonate (Hansen, 2004).In principle, removal of radionuclides by ED/EDR is similar to RO. ED/EDR does not remove neutral species, such as UO_2CO_3, as it removes relatively small amounts of ions that have low mobility. As with RO, a prefiltration step may be necessary before both membrane processes (Ardnt, 2010).

Wastewater treatment plant (WWTP) may also need to be considered in this context. Sewage treatment is the process of removing contaminants from wastewater which includes physical, chemical and biological processes. Its objective is to produce a disposable effluent and solid waste or sludge suitable for discharge or re-use back into the environment without causing harm to communities or pollution. A conventional wastewater treatment plant (WWTP) provides pre-treatment, primary and secondary treatment and sometimes a tertiary treatment. Pre-treatment removes materials that can be easily collected from the raw wastewater before it damages or clogs the pumps and skimmers of primary treatment clarifiers. Primary treatment involves physical settling of the raw wastewater and secondary treatment consists of a biological process that is followed by physical settling. The purpose of tertiary treatment is to provide a final treatment stage to raise the effluent quality using disinfection before it is discharged to the receiving environment.

Sludge processing is complex and can consist of a variety of operations including: sludge thickening, sludge stabilization by lime addition or digestion (either aerobic or anaerobic), sludge de-watering, and, ultimately, disposal by landfill, composting, land application, or incineration. In most plants, primary and secondary sludge are combined, thickened by sedimentation or flotation, stabilized, and de-watered by the use of a belt filter press or centrifuge.

The wastewater treated ends up most frequently within the aquatic environment (river or sea), but it may also be further used, for instance, as irrigation water in agriculture and ground water recharge, which necessitates enhanced treatment to remove nutrients (nitrogen and phosphorus), suspended solids, and other contaminants. Evaluation of its quality is therefore essential to protect human health and the environment.

Levels of naturally occurring radionuclides of ^{238}U series, the ^{232}Th series and ^{40}K are present in soil and water used for drinking and industrial processes. These isotopes may be introduced into the sewerage system from ground and surface water as well as from potential industrial discharges. Another possible source of radioactivity at WWTPs is the authorized release of man-made radionuclides into the system. In most regions, the level of radionuclide contamination in wastewater results from weapons testing, accidents, industrial applications,

research institutions and medical uses. The radionuclides most commonly used in biotechnology, hospital and medical facilities are ^{3}H, ^{99}Tc and radioiodines.

On the other hand, ^{7}Be (of a cosmogenic origin) and ^{210}Pb (radon progeny) are natural radionuclides present in surface airborne particulate matter and are subject to wet and dry deposition onto the ground (Cailet et al., 2001).

Wastewater is transported to the sewage plant where solids and pollutants are removed using a simultaneous biological-chemical precipitation method. Radioactive elements represent a special case of inorganic pollutants and they show similar environmental behavior to their stable chemical isotopes. Radionuclides released into the sewage systems may be concentrated in digested sludge or released to the recipient surface waters. It has been shown previously that sewage sludge is a very sensitive indicator for radioactive materials released from hospitals and an indicator of radionuclides in general (Sundell-Bergman et al. 2008).

As mentioned at the beginning of the introduction, in the literature there are several studies related to radioactivity in drinking water treatment plants. However, the number of wastewater studies that can be found in the literature is limited. Stetar et al. (1993) and Ipek et al. (2004) studied the removal of some artificial radionuclides in secondary treatment and radioactivity behavior in biological treatment. These studies have shown that radioactivity in wastewater is reduced by biological treatment and the authors conclude that radioactivity removal could occur by adsorption to the activated sludge. Rodriguez and collaborators (Rodriguez et al. 2009) recently completed a study which analyzed the removal efficiency of reverse osmosis in wastewater. The results indicate that reverse osmosis is able to reduce the concentration of gross alpha and gross beta activity and produce high quality water.

By contrast, the occurrence of radionuclides in sludge samples for different WWTPs has been studied more by some authors to evaluate their potential danger. Initially, the studies were focused on artificial radionuclides as a result of the Chernobyl accident and nuclear tests. A Swedish study by Erlandsson et al. (1983) analyzed radionuclides from global fallout and local sources in ground level air and sewage sludge. Imhoff et al. (1988) sampled sewage sludge from 10 WWTPs in Ruhrverband (Germany). The results indicate that a sudden increase of radioactivity was observed with an initially high fraction of ^{131}I due to the Chernobyl accident and the presence of long-life fission products.

Research was later focused on other potential sources such as medical and industrial waste and the water treatment process. Note that some of these sources may contain both natural and artificial radionuclides. Miller and collaborators (1996) analyzed sludge samples from 25 municipal WWTPs to determine if sewage effluents from nuclear facilities had levels of radioactivity above those expected from the environment and the sludge samples had maximum

values of 2 Bq/Kg of ^{137}Cs and 3 Bq/Kg of ^{60}Co. Puhakainen (1998) found gamma activities between 24 and 250 Bq/Kg in sludge samples from a WWTP in Finland and detected their origin due to medical applications and industrial processes. Martin and Fenner (1997) measured radioactivity levels in sludge at one WWTP next to a medical complex which carries out radioiodine treatments with the aim of determining concentrations of ^{131}I and estimating radiation doses to employees and the public. A similar investigation it has been recently carried out by Jiménez and colleagues (Jiménez et al. 2011).

Additionally, water treatment plants have been also considered by some authors as NORM industries (Gäfvert et al., 2002; IAEA, 2003; EPA, 2004; Kleinschmidt and Akber, 2008, Casacuberta et al., 2009). Examples of NORM containing residues from water treatment plants are radioactive contaminated sludge and solids including filter sludge, spent ion exchange resins, spent granular activated carbon, as well as waters from filter backwash. The radioactive concentrations can vary considerably because of the varying geological characteristics of different water sources in different regions of a country. In some cases, these concentrations can be substantial (Hofmann et al., 2008). However, the vast majority of residues from water treatment are in the form of sludge and their disposal is likely to be the greatest concern. Depending on the concentration levels found in the sludge, special considerations may need to be given to the re-use or disposal of this waste. For this reasons various countries have regulated these practices over the last few years or are in the process of doing so (European Commission, 2012).

In Spain, Direct discharge of radioactive material into the sewerage system and NORM materials are regulated by the Spanish Royal Decree 783/2001 (RD 2001), revised as RD 1439/2010 (RD 2010), which corresponds to the transfer of European Council Directive 96/29 of 13th May (EC, 1996). This standard regulates "Natural Sources of Radiation" and the need to study activities in which workers or members of the public could be exposed to significant doses of radiation.

In 2011 the Nuclear Safety Council (CSN) published the technical Instruction IS-33, defining the radiological criteria for protection against exposure to natural sources of radiation. In the Annex of this instruction, work activities are mentioned in which operators or leaders must perform studies required by the Regulation on Protection against Ionizing Radiations (783/2001). One of the activities mentioned is related to facilities where groundwater is treated and stored. Since in some cases the precise origin of the water treated in WWTPs is unknown, this kind of facilities must also be considered

The USEPA has addressed disposal management options for waste generated by water treatment (EPA, 1990) and also indicates that NORM residues from drinking water treatment may be disposed in landfills or lagoons or can also be used as agricultural conditioners. However, in some cases it may be necessary to dispose of the residues in a licensed radioactive waste disposal facility (EPA, 1994).

It should be pointed out that, up until now, there exist no official regulations or recommendations for the detection and assessment of radionuclides in the liquid effluents from WWTPs. Nevertheless, the default screening values (gross alpha and beta activities) entered in the Spanish Royal Decree 140/2003 for drinking water are used as a reference value for the discussion of the results related to the studies in liquids from Spanish WWTPs. In the case of the wastewater studied in the USA the default screening values entered in the United States Environmental Protection Agency (EPA) regulations for drinking water are used (EPA, 2000).

The focus of this part of the thesis is therefore to investigate the occurrence of radioactivity in liquid and sludge samples from different water treatment plants located in Spain and one located in Wisconsin in the USA. This part is divided into three different chapters. We propose in Chapter 4 and Chapter 5 the occurrence of radioactivity in liquid and sludge samples from different DWTPs and WWTPs located in Spain, respectively. Additionally, Chapter 5 provides a screening study of a WWTP located in Waukesha which was made during the stay in the USA. Finally, Chapter 6 presents an evaluation of radiological hazard effects of the sludge generated in drinking water and wastewater treatment plants previously studied in Chapters 4 and 5.

Chapter 4

Behavior of radionuclides in drinking water treatment plants

4.1 Introduction and motivation

Levels of radionuclides in drinking water may be increased by a number of human activities and later can be accumulated in the sludge generated in the process of removing pollutants in water.

For these very reasons, it is considered important studying the occurrence and behavior of radioactivity in drinking water treatment plants (DWTPs). Though radioactivity in DWTP has been studied by some authors, as has already been mentioned before in the introduction, we propose an original work studying the temporal evolution in different DWTPs. These plants have been selected taking into account both variations in water source and the treatment applied.

This chapter is organized as follows. Section 4.2 consists on a temporal evolution study for water samples from two conventional DWTPs. A study related to the water contribution from wells in DWTP-1 has been also presented in order to determine their influence in the treated water. In this section, we show that conventional treatment applied in DWTPs does not enough effective to remove radioactivity and membrane technologies are necessary to remove them. Therefore, a detailed study related with the RO treatment applied later in the DWTP-1 was done and the results are described in Section 4.3. This study was presented as a poster in the INSINUME 2012 conference (www.insinume2012.com) and has also been published as an article in the INSINUME special issue of the Journal of Environmental Radioactivity (Montaña

et al. 2013b). In <u>Section 4.4</u> we provide a seasonal study of radioactivity in the sludge from DWTPs previously studied in section 4.2. Finally, a summary is presented in <u>Section 4.6</u>.

4.2 Temporal evolution of radionuclides in water from conventional drinking water treatment plants

Two full-scale DWTPs (1 and 2) located in Northeast Spain were studied during the period 2007-2010 in order to carry out a temporal evolution of radionuclides in water and their removal using a conventional treatment.

4.2.1 Plants characteristics

DWTP-1

The DWTP-1 treats water from the Llobregat River. At that point, the river has received effluents from industrial and urban WWTPs, influence of agricultural and mining activities. The high anthropogenic influence of the water makes it necessary to add an ozone treatment in order to remove several organic and inorganic compounds which cannot be efficiently removed with the more common treatments as flocculation or activated carbon.

The treatment plant has a maximum treatment capacity of 5.5 m^3/s, and provides almost 50% of the annual drinking water in Barcelona metropolitan area (population equivalent of the plant: 4,856,579). The treatment process is composed by the following phases and is showed in Figure 4.1:

1. Water collecting: The water intake can be from the Llobregat River or groundwater from the wells in Cornellà and Sant Feliu (see Table 4.1). These wells are near the DWTP-1 and are used mainly in periods of drought or on isolated days when river flow is not sufficient to provide the water demand. They are also used when episodes of river water pollution prevent water catchment, in that it fails to reach the standards laid out in legislation on human drinking water or water company quality control requirements. These episodes are usually due to rains causing some rivers and collectors of polluted water to overflow. Under normal conditions, this polluted water by-passes the treatment plant and is returned to the river down-stream. Occasionally, pollution is caused by industrial dumping. This additional groundwater from wells is added after the sand filters point which is previously treated by 'stripping' to remove organic pollutants.

As indicated in Table 4.1, sampling campaigns included all the different kinds of samples that are treated in this DWTP: only water from river, only water from wells or mixture water from river and wells.

2. Pre-treatment: Only the water coming from the river needs pre-treatment, since the water coming from the wells is considered to be naturally filtrated.

    a. Chlorination: Chlorine is dosed in order to remove the major part of ammonia which is present in the water, by producing chloramines. The chlorination can also be done with chlorine dioxide, which has the advantage of producing fewer THM (trihalomethanes) compounds than the molecular chlorine.

    b. Sand removal: the water flows at lower speed, facilitating the sedimentation of sand particles, down to a particle diameter of 0.5 mm.

    c. Particles separation: The water is pumped to the clarifiers, previously adding coagulant ($FeCl_3$) and flocculant reagents, where the smaller particles are separated by precipitation. To finish the separation process, the water goes through a sand filter, which retains all the particles that did not precipitate before.

3. Post-treatment: Water from both the pre-treatment and the wells is pumped by four Archimedes' screws.

    a. Ozonisation: The water is treated with ozone, which reduces the content in organic compounds, and substantially improves the organoleptic qualities of the water.

    b. Activated carbon: After the ozonisation, the water is directed to granular activated carbon beds (GAC). The activated carbon process has three objectives: remove any possible suspended solids, remove organic matter, and eliminate any virus, microorganisms or bacteria from water.

4. Post-chlorination: The treated water is chlorinated with chlorine gas and kept in a 10,000 m^3 storage tank. This way there is a constant presence of residual chlorine, in order to ensure the disinfection of water before its distribution.

5. Storage and Pumping station: The treated water is kept in two 4,000 m^3 storage tanks from where the water is pumped to different distribution points.

DWTP-2

The DWTP-2 treats water from the Ter River (Figure 4.1). The treatment plant has a maximum treatment capacity of 0.27 m^3/s, and provides the annual drinking water in 16 towns in which the main human activity is agriculture and stockbreeding (population equivalent of the plant:

45,000). In this case the treatment process is simpler than the process of DWTP-1. The process consists on water collecting, pre-treatment with chlorination, coagulation (aluminium polychloride) and activated carbon (GAC), post-chlorination and storage in two different tanks located in different points from the DWTP, from where the water is pumped to the 16 towns. Figure 4.1 shows the schematic diagram of the studied conventional DWTPs and the points where the water samples were taken are indicated by star.
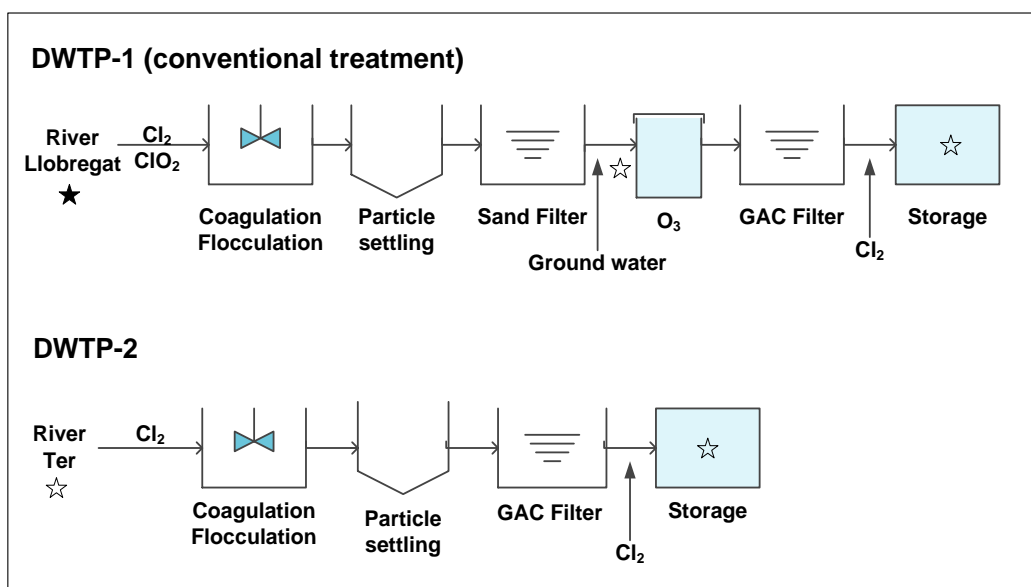
Figure 4.1. Schematic diagram of the studied DWTPs. The points where the samples were taken are indicated by star.

4.2.2 Sampling collection

The sampling was carried out according to established sampling protocols and locations defined by 'Aguas de Barcelona'. Composite liquid samples were collected using the ISCO GLS Compact Composite Sampler with an integrated 5 L glass bottle. The sampling program was set to collect 0.1 L of liquid every 30 min during 24 h. Liquid samples (unfiltered) were later transferred to 2 L polyethylene bottles for radioactivity determination. Composite raw water, after sand filters and final effluent drinking water samples were sampled taking into account the hydraulic retention time (HRT) in the DWTP. HRT was calculated using the inflow arriving to the DWTP the sampling campaign and the volume of the tanks used in all the processes of the DWTPs.

The HRT is the time the water takes to pass through DWTP. As the HRT depends on the quantity of raw water to be treated, the sampling campaigns were chosen in different seasons in order to consider the changes due to storm occurrence.

In order to preserve the liquid samples prior to the radioactivity analysis, the unfiltered liquid samples were acidified with concentrated nitric acid (at pH 2) and later they were filtered through 0.45 μm membrane filters. Therefore it should be highlighted that the results in liquid samples refer to dissolved radioactivity levels according to the pretreatment.

Table 4.1. Dates, inflow and HRT of each sampling campaigns in the DWTPs

Campaign	Month of sampling campaign	DWTP-1		DWTP-2	
		Inflow (m3/h)	HRT (h)	Inflow (m3/h)	HRT (h)
C-1[1]	July 2007	6300	12.8	250	2.0
C-2[1]	October-November 2007	4860	8.0	250	2.0
C-3	November-December 2007	9810	6.8	250	2.0
C-4[2]	February 2008	-	-	-	
C-5[1]	June 2008	4860	7.3	250	2.0
C-6[1]	September 2008	14761	4.6	250	1.5
C-7	November 2008	18000	3.9	250	1.0
C-8	April 2009	18000	4.0	250	1.0
C-9[3]	May 2009	-	-		
C-10[4]	September 2009	12240	6.2	-	-
C-11[3]	November 2009			-	-

[1] In these campaigns samples from DWTP-1 contain mixture of water from river and wells.
[2] In campaign C-4 there wasn't water sampling, only sludge sampling in DWTP-1.
[3] In these campaigns samples from DWTP-1 contain only water from wells.
[4] In this campaign samples from DWTP-1 only contain water from river. A sample which only contains water from wells was also collected.

For up to 11 sampling campaigns carried out over the period 2007-2009, 43 water samples were collected. Seven campaigns were analyzed for the DWTP-1 (C-1 to C-3 and C-5 to C-8), where samples in different points of the treatment were collected (influent, after sand filters and final effluent). Seven water samples from wells, which represent three additional campaigns (C-9 to C-11), were collected in order to determine their radioactivity content. In the campaign C-4 a sludge sample from DWTP-1 was only collected (see Section 4.5). For the DWTP-2, only the

influent and final effluents were sampled in seven campaigns (C-1 to C-3 and C-5 to C-8) due to the simplicity of the process. Table 4.1 shows the dates of the different campaigns.

For the 43 water samples collected, gross alpha and beta activities and the potassium content were determined. For gross alpha activity the co-precipitation method was used (see Appendix A), while gross beta activity was determined by evaporation method (see Appendix B for this method, for the potassium determination and all the instrumentation used).

4.2.3 Results and discussion related to DWTP-1

Gross alpha activity in water samples

The origin of alpha activity in the Llobregat river basin has been previously investigated and it was established that it was mainly due to ^{234}U, and ^{238}U (Camacho et al., 2010). Total Uranium activity after the treatment in DWTP-1 was 0.08 ± 0.02 during the period 2007-2009 (data source: internal report from our laboratory).

Figure 4.2 shows the temporal evolution of the gross alpha activity values obtained for the analyzed samples in DWTP-1 between C-1 and C-8 campaigns. As can be observed in this figure, water from river (in) was not resulted notably constant throughout the different campaign and therefore, there is absolutely point in carrying out a temporal evolution study and to see the effectiveness of removing the radioactivity in this DWTP. As it is shown in comments from Table 4.1, we can easily be distinguished two different types of waters from DWTP-1. When water only came from the river, the treatment did not reduce gross alpha activity (C-3 and C-8). There was only a substantial reduction in campaign C-7, however, there was not detected any significant anomaly in this campaign nor on the other two campaigns (C-3 and C-8) during the sampling protocol.

On the other hand, it should be highlighted that the gross alpha activity measured in some campaigns (C-1, C-2 and C-5) was higher after the treatment (out). As confirmed below (Figure 4.3), this is due the water contribution from wells, because surface water catchment from the Llobregat is occasionally complemented by water from wells in the aquifers of the river delta, as has already been mentioned (campaigns C-1, C-2, C-5 and C-6).
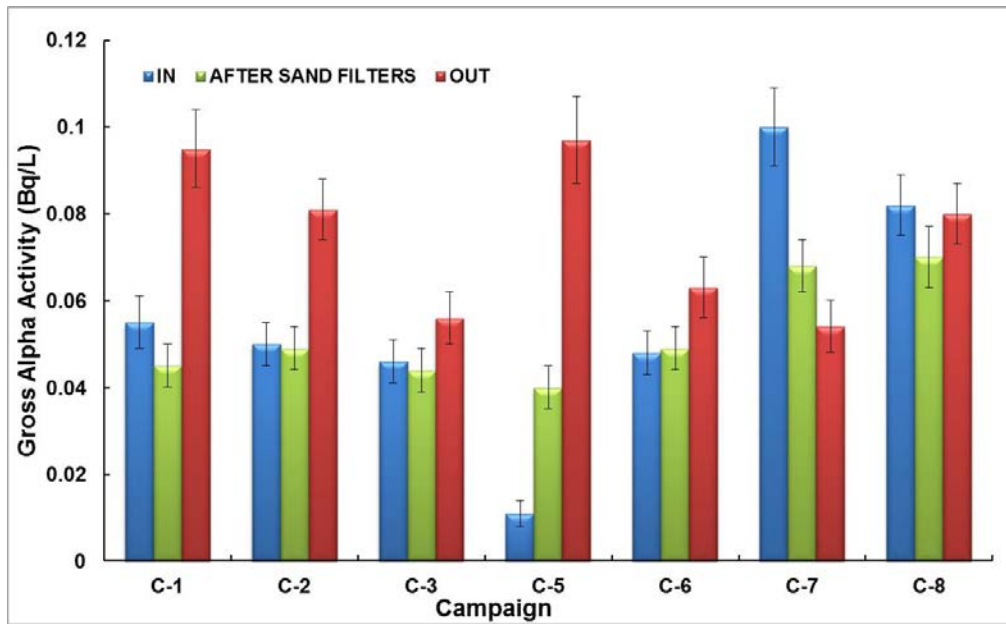
Figure 4.2. Temporal evolution of the gross alpha activity in liquid samples from DWTP-1. The error bars are the uncertainty of the method (*k=2*).

The water from these wells is groundwater which often shows slightly higher levels of mineralization and radioactivity as reported before by some authors (Cothern and Rebers, 1990; Ruberu et al., 2005).

Figure 4.3 shows gross alpha ratio parameter and the groundwater from wells contribution in percentage. The gross alpha ratio parameter was used in order to confirm the groundwater from wells influence in the gross alpha activity. This ratio parameter was calculated dividing effluent (out) by influent (in) values of gross alpha activity for each campaign. If the ratio parameter is >1 a gross alpha increase is produced. The gross alpha ratio parameter is positively correlated with the groundwater content (R^2=0.95). Therefore, the gross alpha activity increase was due to the radioactive contribution of water from wells. This increase was produced after sand filters treatment where groundwater is introduced in the WTP. The maximum gross alpha ratio (8.8) was produced for the maximum contribution of water from wells (57% of groundwater from wells) in campaign C-5. An additional study in the groundwater from wells was done and presented below.
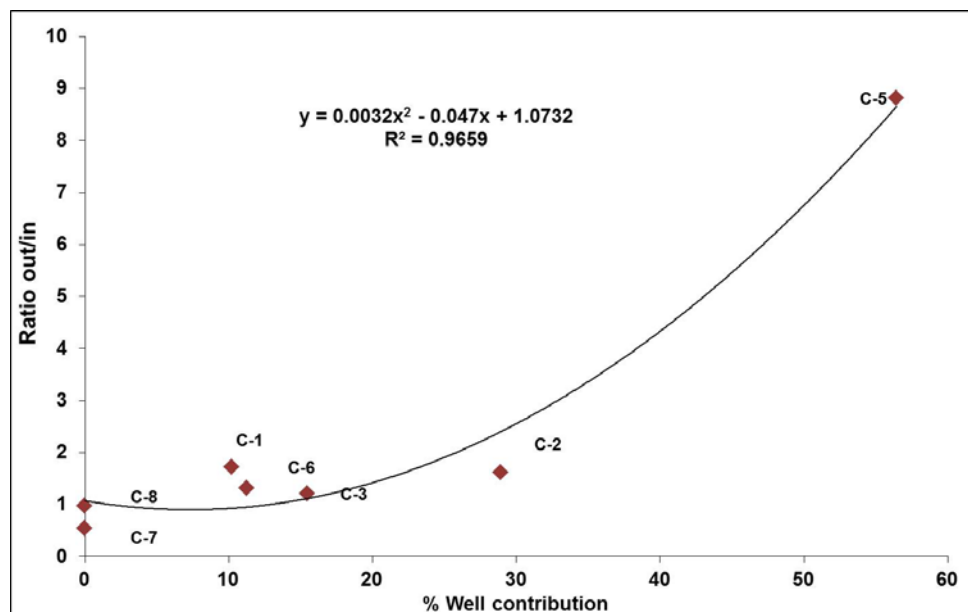
Figure 4.3. Variation of the gross alpha ratio parameter in liquids from DWTP-1 with the contribution of groundwater from wells.

Gross alpha activity in groundwater from wells

The radioactive content of the groundwater from wells was studied during the sampling campaigns C-9, C-10 and C-1. Two wells with different origin but located in the Llobregat basin supplied ground water in DWTP-1, wells from Sant Feliu and well from Cornellà. In Figure 4.4 is presented the results obtained for the gross alpha activity and the gross alpha average values from river water for the year when groundwater samples from campaigns C-9, C-10 and C-11 were sampled (2009).

The mean value and the range for the gross alpha activity obtained in samples from wells analyzed were 0.09 ± 0.02 and $[0.07-0.12]$ Bq/L respectively, clearly higher value than the average value of river sample and its range (0.05 ± 0.02 Bq/L and $[0.03-0.07]$). It is obvious that this explains the increase in gross alpha activity if water from wells is used during the treatment in DWTP-1.

118
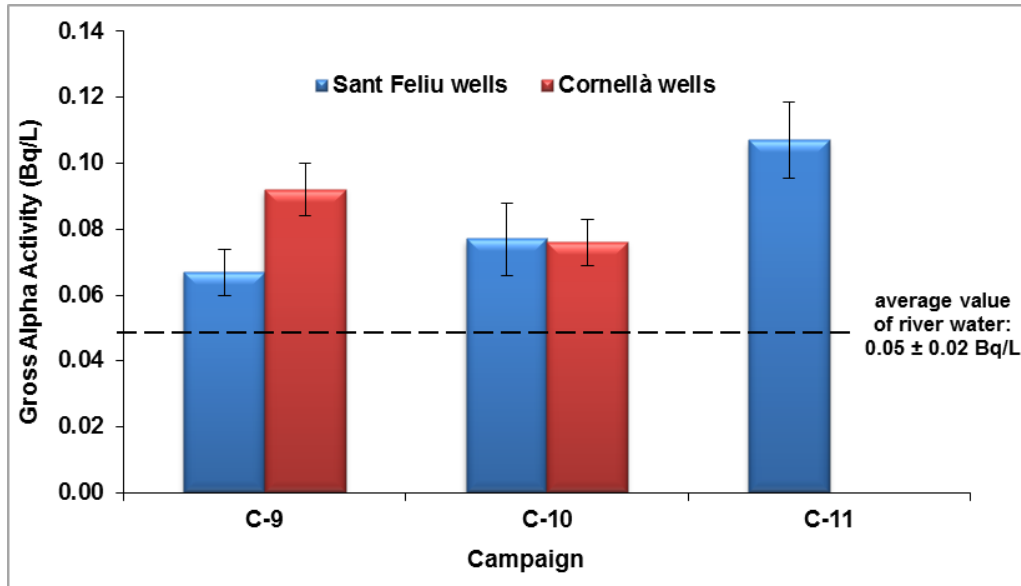
Figure 4.4. Gross alpha activity in ground water from wells used in the DWTP-1. The error bars are the uncertainty of the method (*k=2*).

Gross beta activity in water samples

The origin of beta activity in the Llobregat river basin has also been previously investigated and it was established that it was mainly due to ^{40}K. Other beta emitters were tested (^{3}H and Sr) and were not detected (Vallés et al., 2007).

Figure 4.5 shows gross beta activities (including ^{40}K) measured in influent, effluent and after the sand filters in the DWTP-1. None of the sample presented 'rest beta' (adjusted beta) activity (a term used in Spanish legislation which refers to gross beta activity excluding ^{40}K) above the screening level in drinking water of 1 Bq/L (RD, 2003). Thus, it can be stated that gross beta was mainly due to the ^{40}K content of the samples which is highly soluble in water so remain into the water more than alpha emitters (Baeza et al., 1995).

Comparing gross beta activity values measured in the influent and effluent water samples, gross beta activity increases when water from wells contribution is higher than 50% (C-5). For the rest of the campaigns, neither an increasing nor a decreasing is observed for gross beta activity values. Therefore the conventional treatment applied at DWTP-1 did not reduce the gross beta activity due to ^{40}K content.

119
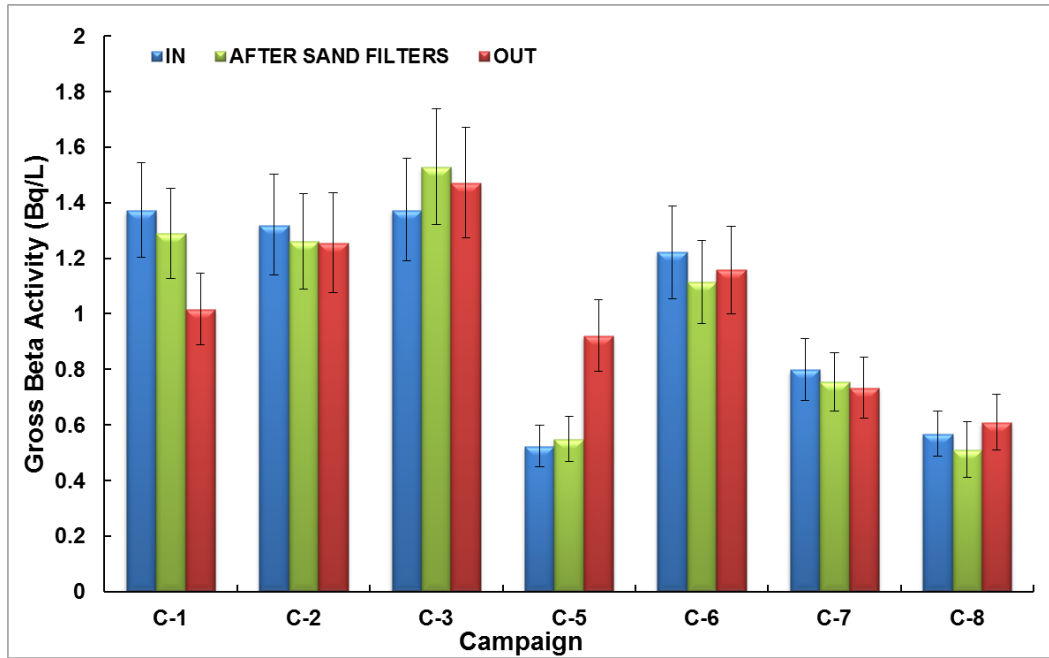
Figure 4.5. Temporal evolution of the gross beta activity in liquid samples from DWTP-1. The error bars are the uncertainty of the method (*k=2*).

Gross beta activity in groundwater from wells

In Figure 4.6 is presented the results obtained for gross beta activities and the gross beta average value from river water for the year when groundwater samples from campaigns C-9, C-10 and C-11 were sampled (2009).

Mean and range gross beta values from wells, 0.99 ± 0.06 and [0.87-1.07] Bq/L, were also slightly higher than values for river samples during the May-November period of 2009 (0.8 ± 1.0 and [0.70-0.99] Bq/L). None of the samples presented 'rest beta'. As previously mentioned, the groundwater catchment did not substantially influence to gross beta growth unless there was at least 50% of contribution of this groundwater. Instead, in the case of gross alpha activity did substantially influence when groundwater contribution was higher than 25%.
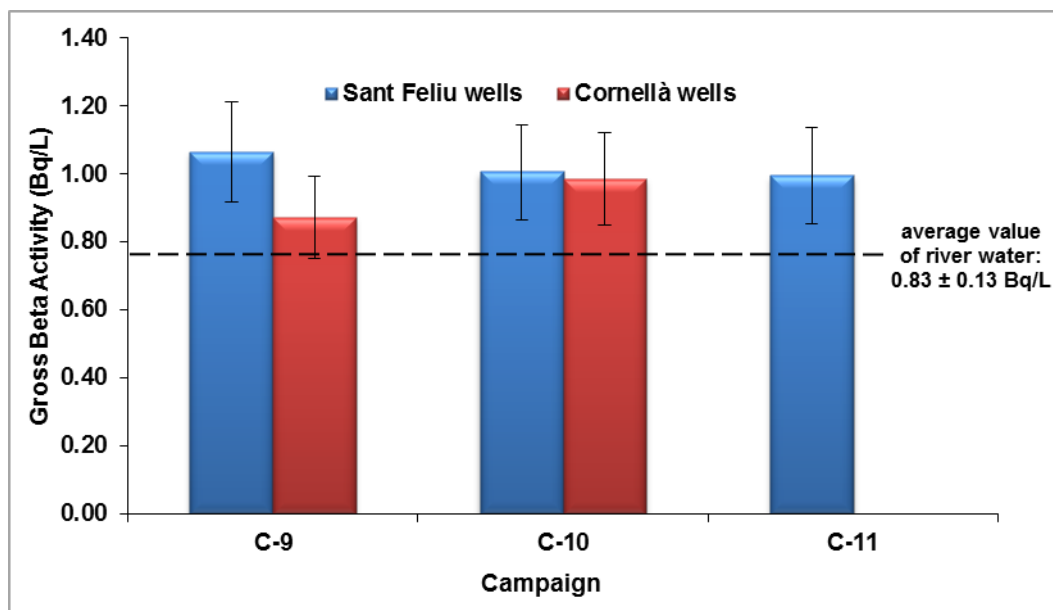
Figure 4.6. Gross beta activity in ground water from wells used in the DWTP-1. The error bars are the uncertainty of the method (*k=2*).

4.2.4 Results and discussion related to DWTP-2

Gross alpha activity in water samples

Figure 4.7 shows the temporal evolution of the gross alpha activity values obtained for all the analyzed samples from DWTP-2. Through the results shown in this figure, the general trend is a decrease of the gross alpha activity values (in a percentage of 22-40%) in the samples taken from effluent with respect samples taken from the river. This can be attributed to the fact that some alpha emitting radioisotopes are removed during the water treatment procedure. Some studies (Gäfvert et al., 2002; Baeza et al., 2006) have reported that alpha activities from uranium and thorium decay chains are removed from the water by sedimentation after the addition of a coagulant in conventional treatment plants. As described previously, the DWTP-2 procedure consists of following steps: coagulation, flocculation, settling, GAC filtration and chlorination as is usually in a conventional treatment process.

However, if we take into account the uncertainties associated to the gross alpha activity determination (error bars in Figure 4.7), it can only be stated that exists an alpha activity decrease in two of the eight campaigns analyzed. Thus there is insufficient data to ensure that a decrease of the alpha activity exist due to the conventional treatment applied.

Gross alpha activities detected in the final effluent (out) not exceed the maximum gross alpha activity (0.1 Bq/L) allowed by Spanish legislation (RD, 2003) in waters for human consumption and were low than the values obtained in DWTP-1. In this case, gross alpha activity is also due to Uranium, being the Total Uranium activity of the treated water 0.019 ± 0.004 Bq/L during the period 2007-2009 (data source: internal report from our lab). No radium was detected after the treatment.
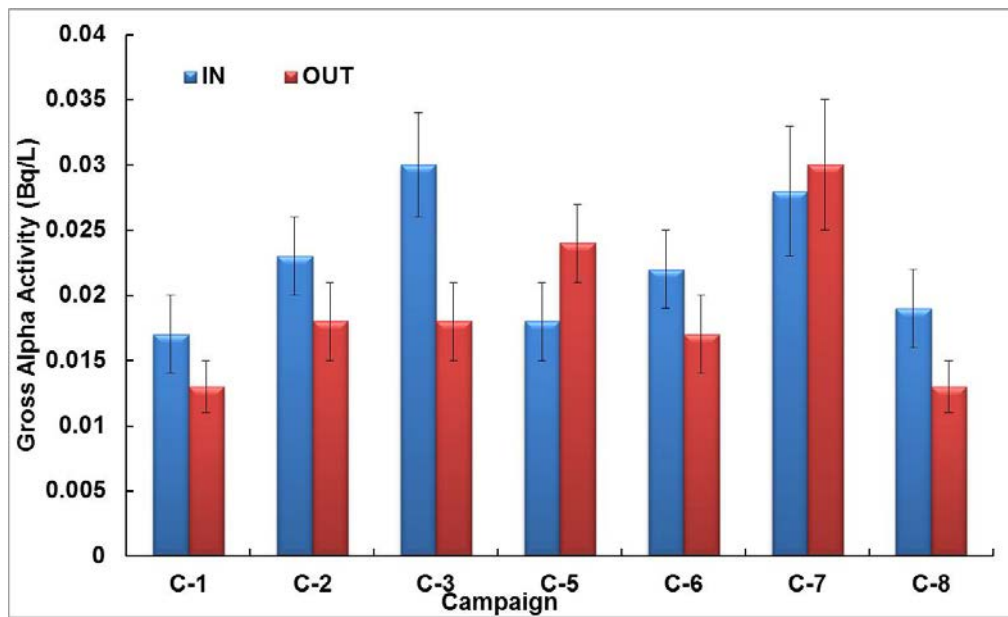
Figure 4.7. Temporal evolution of the gross alpha activity in liquid samples from DWTP-2. The error bars are the uncertainty of the method ($k=2$).

Gross beta activity in water samples

Figure 4.8 shows gross beta activities (including [40]K) measured in influent and effluent in the DWTP-2. None of the sample presented 'rest beta' (adjusted beta) activity (a term used in Spanish legislation which refers to gross beta activity excluding [40]K) above the screening level in drinking water of 1 Bq/L (RD, 2003). Thus, it can be stated that gross beta was mainly due to the [40]K content of the samples as happens in DWTP-1.

Comparing gross beta activity values measured in the influent and effluent water samples neither an increasing nor a decreasing was observed for gross beta activity values in all campaigns.
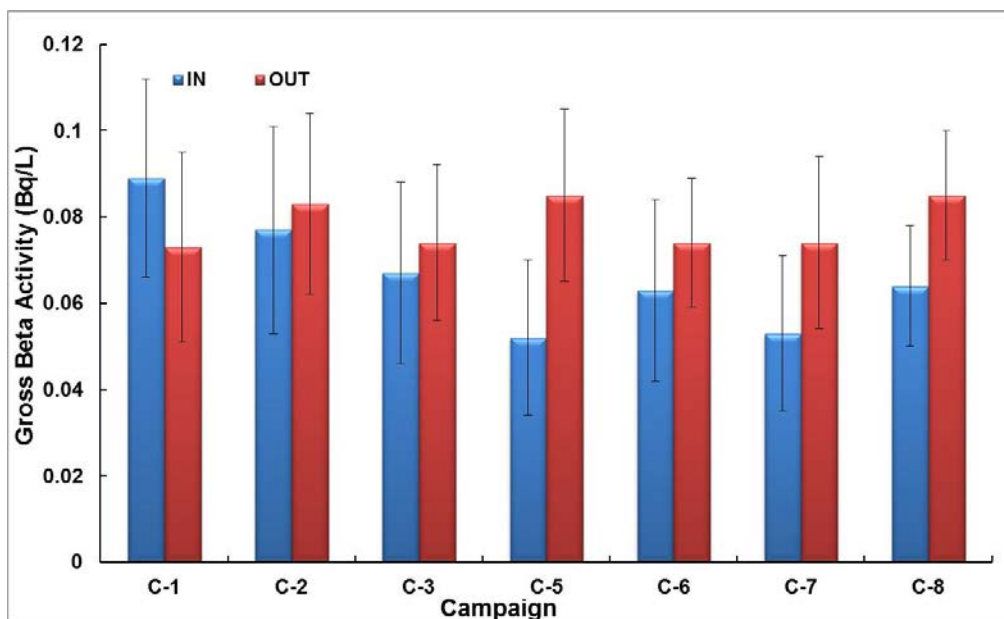
Figure 4.8. Temporal evolution of the gross beta activity in liquid samples from DWTP-2. The error bars are the uncertainty of the method (*k=2*).

4.2.5 Comparison of the results between both DWTPs

If we compare gross alpha and beta activity values from both DWTPs, it seems that values from DWTP-2 are lower than values from DWTP-1. This is due mainly to water treated in DWTP-1 can be groundwater which usually contains more radioactivity levels. Moreover, the water treated in both plants is from different rivers (Llobregat River in DWTP-1 and Ter River in DWTP-2) in which the salinity is very different. This is due to the different geological properties of the basin, where the Llobregat basin presents high values of potassium content (34 ± 12 mg/L) (Ortega et al., 1996). The average value for potassium content during the period 2007-2009 on DWTP-2 outlet was 2.0 ± 0.5 mg/L. Water from Llobregat River has higher salinity which is related to the mining activities at the large salt deposits located in the upper part of the basin. Fernández-Turiel et al. (2000) states that the raw water quality variability of both the Llobregat River and the Ter River could be related to the seasonal variations of the Mediterranean climate. However, the Sau-Susqueda reservoir system minimizes the influence of these effects on the Ter's raw water increasing their quality.

This is reflected by the gross alpha and beta variations in the different campaigns carried out in raw water from Llobregat River where the range values for gross alpha and beta activities were [0.01-0.1] and [0.5-1.4] Bq/L respectively. In contrast, in raw water from the Ter River these

range values were smaller ([0.02-0.03] and [0.05-0.09] Bq/L for gross alpha and beta respectively) than those found in raw water from Llobregat River.

However, comparing gross alpha activity values between raw water and treated water, it is difficult to assess a radioactivity diminution in both conventional DWTPs.

It can be concluded that the final effluent in both DWTPs fulfils the requirements set by Spanish legislation for water intended for human consumption regarding gross alpha and beta parameters.

4.3   Membrane technology implementation at DWTP-1

This section presents radioactivity results from two studies. Firstly, results from a pilot plant with four different designs or scenarios are presented. Secondly, results from the full-scale treatment plant built according to the findings of the pilot study are commented on.

Before the implementation of this improved process, a pilot plant had been built to test the behavior of ultrafiltration (UF), reverse osmosis (RO), and electrodialysis reversal (EDR) in order to improve the quality of the water from the Llobregat River and test which of these membrane technologies was the most suitable for DWTP-1 (Devesa et al., 2010).

In 2009 an improved process at this DWTP started operating. The new process is based in membrane technology, and treats 50% of the water flow with ultrafiltration (UF) and reverse osmosis (RO). This process is placed after the sand bed filtration, where the flow is split: 50% is treated with the new process, and the rest 50% will follow ozonisation and granular activated carbon filtration as before. Finally, the water is blended with the stream coming from the conventional process, and the post-chlorination treatment is applied before storage and pumping. The conventional process and the new process flowsheets are represented after in Figure 4.11.

4.3.1 Scenarios of the study

Pilot plant

The pilot plant was located within the DWTP-1 which catches water from the final stretch of the Llobregat river basin. As previously mentioned, the conventional full-size DWTP-1 has the

following treatment stages: pre-chlorination, coagulation-flocculation, sand filtration, ozonation, granular activated carbon (GAC) filtration and post-chlorination.

This pilot plant was set up with three membrane modules: UF, RO and EDR (Table 4.2). In addition, it also had a module which reproduced the polishing treatment (ozonation plus GAC filtration) used at the DWTP-1. The operating conditions of the latter were adapted to coincide, as far as possible, with those of the full-size plant (ozone dosage, 3 mg/L; GAC, Chemviron F-40; contact time in carbon filters, 9 minutes).

Table 4.2: Main characteristics of the membrane modules (pilot plant).

	UF	RO	EDR
Capacity (L/s)	3,5	1,7	1,5
Membrane	ZeeWeed 500B	BW30LE-440	AQ-X
Manufacturer	Zenon	Filmtec	Ionics
Stages	1	1	2

Four different scenarios were studied in the pilot plant using the following configurations (Figure 4.9):

Scenario 1: composed of the following stages: pumping of raw water from the Llobregat River, UF of the whole flow, and subsequently two parallel treatments: RO and conventional (ozonation and GAC filtration) treatments. This scenario produced two final effluents, one after the RO treatment and another after GAC filtration. For the radiochemical study, four effluents were sampled: raw water and after UF, RO and GAC treatments.

Scenario 2: was analogous to the previous one but RO was replaced by EDR. The effluents were the same: raw water and after UF, EDR, and GAC treatments.

Scenario 3: is arranged completely in series: catchment of raw water, UF, EDR and GAC filtration.

Scenario 4: analogous to scenario 3 but UF was replaced by sand filters, which is the conventional treatment at the DWTP-1: catchment of raw water, sand filters, EDR and GAC filtration.

Two samples per sampling point (1, 2, 3 and 4 in Figure 4.9) for each scenario were taken, at the raw water, after UF, after RO, after EDR and after GAC filtration. All samples were

analyzed for gross alpha activity and gross beta activity. Uranium content was tested in some samples.

There was a sequential arrangement of the scenarios in time, so feed water characteristics suffered from some fluctuations.
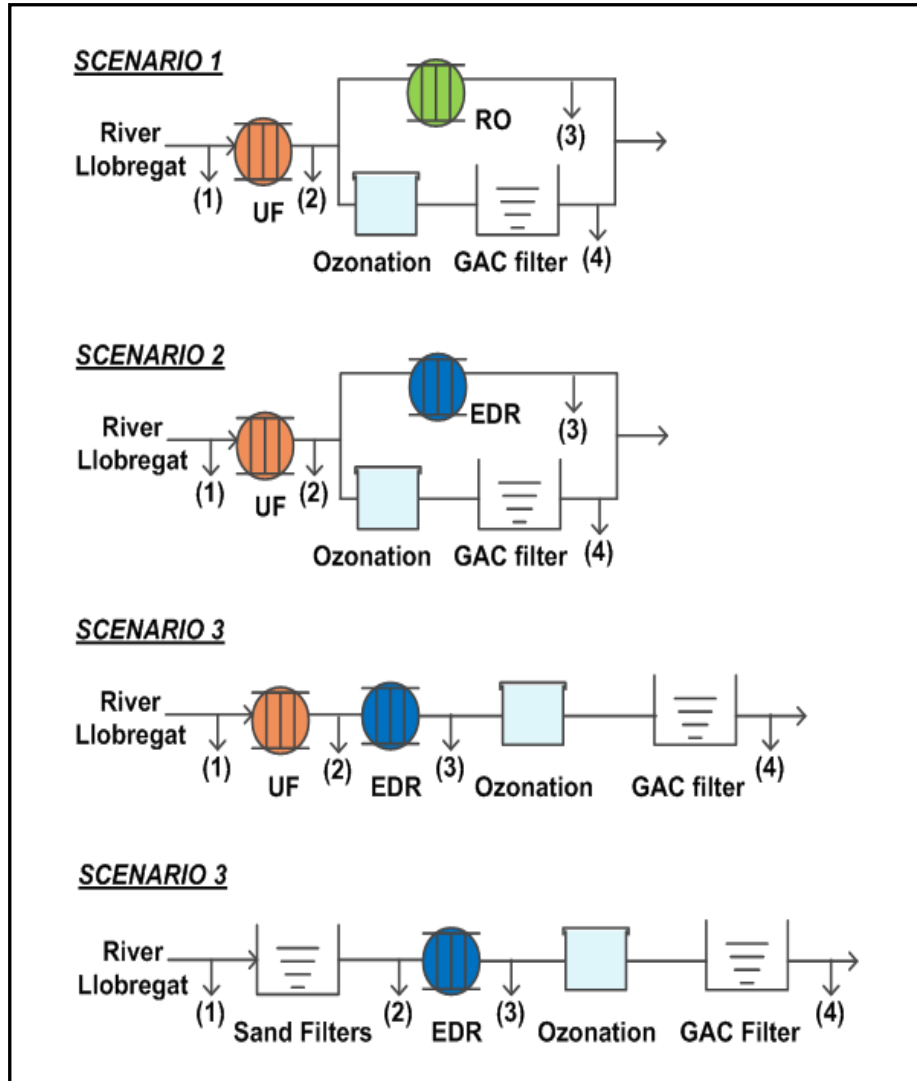
Figure 4.9. Treatment layouts for the four scenarios studied in the pilot plant. Sampling points are represented by numbers in brackets.

Full-scale treatment plant

The study of the performance of the different scenarios of the pilot plant showed that the best results (radiological, chemical, biological and aesthetic) were obtained with scenario 1. On the other hand, operational and maintenance considerations required that the UF modules were fed with sand-filtered water. Therefore, the final design of the new part of the process applied at DWTP-1 is as shown in Figure 4.10. The flow of sand-filtered water is divided into two parts: one for conventional treatment and the other for two lines with UF and RO membranes, which were basically identical. The maximum capacity for the membranes modules was 50 % of the nominal capacity of the plant.
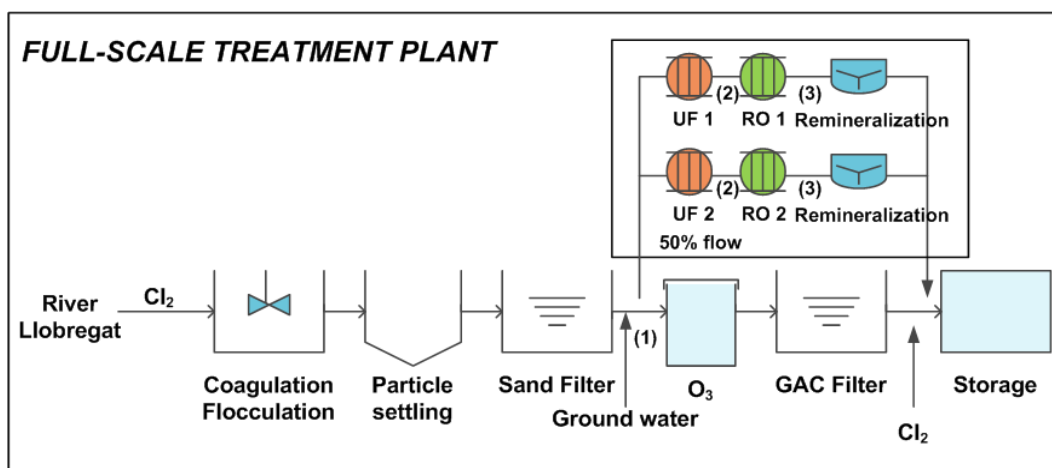
Figure 4.10. Schematic diagram of the improved full-scale DWTP-1. Sample points are represented by numbers in brackets.

4.3.2 Sampling collection and details

All samples were collected according to water company's internal protocols to ensure adequate sampling, preservation and transportation to the laboratory. The samples were collected and kept in polyethylene containers, and were acidified with concentrated HNO_3 (1mL per liter).

Pilot plant

Two water samples were sampled in two different days, identified as "A and B", for each scenario (1, 2, 3 and 4), giving a total of 32 samples. In this case samples were not composite

water samples. The evaporation method was used to determine both gross alpha and gross beta activities. Total uranium activity by alpha spectrometry was also determined for some of these samples. The total number of analysis was 77 (see Appendix B for test methods and instrumentation).

Full-scale treatment plant

In order to make sure that the actual reductions of radioactivity levels were those forecast in the pilot plant, seven monitoring events from different sources, only in the new part of the process (UF + RO), were performed covering three years of operation (2009-2011), as shown in Table 4.3.

A total of 21 water composite samples from the current SJD WTP were taken at three different points: before UF (1), after UF (2) and after RO (3) as depicted in Figure 4.10. In this case, samples were analyzed with respect to gross alpha by co-precipitation method, and gross beta and beta rest activities by evaporation method, giving a total of 63 analyses.

As mentioned above (section 4.3), the composition of the water of the river and, consequently, the radioactive levels, change in time. The water from wells is more stable and shows slightly higher levels of mineralization and radioactivity.

Table 4.3. Sampling campaigns and sources carried out in order to study only the new part (UF + RO) implemented at the DWTP-1

| Monitoring events | day | Source water | |
		River (%)	Wells (%)
February 2009	1	-	100
	2	94	6
September 2009	1	100	-
	2	-	100
December 2009	1	-	100
January 2012	1	85	15
	2	80	20

Additionally, a screening study related with the final design of the treatment (conventional + membrane processes) eventually implemented in the DWTP-1 was done with the aim to assess the influence of this treatment. Three sampling monitoring campaigns were done (C-10, C-12

and C-12bis) with a total of eight composite samples collected. These samples were taken at the beginning of the process (raw water), after RO and after the final process (50% RO + 50% conventional). The differences between C-12 and C-12bis are the composition of the water in order to confirm the influence of groundwater from wells in this new process. These water samples were only from wells (15/06/10) or a mixture of water from the LLobregat River and wells (29/06/10). The main characteristics of these campaigns are indicated in table 4.4. In this case, samples were also analyzed with respect to gross alpha by co-precipitation method (Appendix A), and gross beta and beta rest activities by evaporation method, giving a total of 24 analyses (see Appendix B for test methods and instrumentation).

According to the sampling campaigns, the RO treatment was available since campaign C-9 for C-12bis. Nevertheless, samples from campaigns C-9 and C-11were not considered in this study since those samples corresponding to the radiological characterization of ground water from wells previously studied in section 4.3.2.

Table 4.4. Dates, inflow and HRT of each sampling campaigns in the improved DWTP-1 with membrane technologies.

Campaign	Month of sampling campaign	Inflow (m3/h)	HRT (h)
C-10[1]	September 2009	12240	6.2
C-12[2]	June 2010 (15-06-2010)	18000	4.2
C-12bis[3]	June 2010 (29-06-2010)	-	-

[1] In this campaign samples from DWTP-1 only contain water from river.
[2] In this campaign samples from DWTP-1 only contain water from wells.
[3] In this campaign samples from DWTP-1 contain mixture of water from river and wells.

4.3.3 Results and discussion

Pilot plant

The results of activity measurements are presented in Table 4.5. Two samples, identified as "A and B", were analyzed for each scenario (1, 2, 3, 4).

Minimum Detectable Activities MDA were between 0.001 and 0.03 Bq/L for gross alpha activity, while for gross beta activity they ranged from 0.002 to 0.04 Bq/L and they were 0.0005 Bq/L for uranium determination. Variations were due to the volume of sample used in preparation which changed depending on the total dissolved solids. It should be highlighted that

very low activities were detected in RO and EDR samples because volumes of liquid between 0.5 and 1 L were used for preparing the samples.

Table 4.5. Gross alpha (evaporation method), gross beta and total uranium activities by scenario points in the pilot plant. Overall uncertainty at the 95 percent confidence level (*k=2*).

Sc.	Reference	Sampling point	Gross alpha (Bq/L) by Evaporation	Total uranium (Bq/L)	Gross beta (Bq/L) by Evaporation
	A(1)	Inlet	0.04 ± 0.02	0.052 ± 0.006	0.71 ± 0.09
	A(2)	UF	0.02 ± 0.02	0.025 ± 0.005	0.64 ± 0.08
	A(3)	RO	< 0.001	< 0.0005	0.013 ± 0.002
	A(4)	CONVENTIONAL	< 0.03	---	0.56 ± 0.07
1					
	B(1)	Inlet	0.05 ± 0.02		1.22 ± 0.15
	B(2)	UF	0.04 ± 0.02		1.20 ± 0.15
	B(3)	RO	< 0.003		0.023 ± 0.007
	B(4)	CONVENTIONAL	0.04 ± 0.03		1.16 ± 0.14
	A(1)	Inlet	0.06 ± 0.03		0.79 ± 0.10
	A(2)	UF	0.05 ± 0.02		0.82 ± 0.11
	A(3)	EDR	0.007 ± 0.004		0.22 ± 0.04
	A(4)	CONVENTIONAL	0.04 ± 0.02		0.72 ± 0.09
2					
	B(1)	Inlet	0.07 ± 0.03	0.074 ± 0.011	0.78 ± 0.10
	B(2)	UF	0.05 ± 0.02	0.066 ± 0.006	0.71 ± 0.09
	B(3)	EDR	0.02 ± 0.02	0.033 ± 0.006	0.27 ± 0.04
	B(4)	CONVENTIONAL	0.06 ± 0.02	---	0.67 ± 0.09
	A(1)	Inlet	0.06 ± 0.03	0.054 ± 0.005	1.34 ± 0.17
	A(2)	UF	0.05 ± 0.03	0.056 ± 0.007	1.23 ± 0.15
	A(3)	EDR	< 0.02	0.009 ± 0.003	0.32 ± 0.04
	A(4)	Outlet	< 0.02	0.002 ± 0.001	0.38 ± 0.05
3					
	B(1)	Inlet	0.04 ± 0.03		0.76 ± 0.10
	B(2)	UF	0.04 ± 0.03		0.65 ± 0.09
	B(3)	EDR	< 0.009		0.13 ± 0.02
	B(4)	Outlet	< 0.02		0.19 ± 0.03
	A(1)	Inlet	0.04 ± 0.02		1.05 ± 0.14
	A(2)	SAND FILTERS	0.06 ± 0.02		1.06 ± 0.13
	A(3)	EDR	0.013 ± 0.007		0.27 ± 0.04
	A(4)	Outlet	< 0.008		0.30 ± 0.04
4					
	B(1)	Inlet	0.06 ± 0.02	0.073 ± 0.004	1.10 ± 0.14
	B(2)	SAND FILTERS	0.05 ± 0.02	0.057 ± 0.006	1.10 ± 0.14
	B(3)	EDR	0.012 ± 0.009	---	0.55 ± 0.07
	B(4)	Outlet	0.008 ± 0.006	0.003 ± 0.001	0.42 ± 0.06

Sc.=scenario, Inlet=Raw water; UF=water after UF treatment; RO=water after RO treatment; EDR=water after EDR treatment; CONVENTIONAL=water after conventional treatment; Outlet=water leaving the pilot plant.

According to the results presented in table 4.5, gross alpha activities were produced by the uranium content in the analyzed samples. Application of the t-test for independent samples to gross alpha and uranium content showed a significance value (2-tailed) of 0.912, and therefore no statistically significant differences between groups were found. Rest beta activities were not measured in any samples over the MDA of 0.03 Bq/L so it can be assumed that gross beta was mainly due to the ^{40}K content of the samples.

In general, UF, sand filtration (point 2 in scenario 4), and conventional treatment (point 4 in scenarios 1 and 2) did not reduce gross alpha or gross beta activities as it was reported in the previous section. GAC has been widely used as an adsorbent for contaminants, especially for organic removal, but it is less effective for uranium (Coleman et al. 2003). This was confirmed statistically by using the t-test for independent samples to examine gross alpha at points 1 and 2 and at points 1 and 4 in scenarios 1 and 2. There was a significance value (2-tailed) of 0.222 and 0.321 respectively so there were no statistically significant differences between the groups.

On the other hand, the membrane techniques (RO and EDR) showed a significant decrease in radioactivity levels. To quantify the reduction obtained, removal rates were calculated by comparing the influent (point 2) and the effluent (point 3) activity values using the following equation:

$$RE\ (\%) = \frac{(activity\ in\ the\ influent - activity\ in\ the\ effluent)}{activity\ in\ the\ influent} \times 100 \qquad (\mathbf{4.1})$$

The results for gross alpha, beta and total uranium activity are shown in Figure 4.11. Scenario 1 presented the best removals for gross alpha, gross beta and total uranium activities. The removal rate during RO treatment (scenario 1) was higher than 90% for gross alpha, gross beta and total uranium activities. In the scenarios where EDR treatment was applied (2, 3 and 4) the removal for gross alpha was higher than 70%, removal for gross beta was higher than 60% and for total uranium activity the value was between 55 and 84% depending on the scenario. Furthermore, the results from EDR technology were less reproducible as greater error bars were obtained. As uranium is the main isotope which produces gross alpha in raw water from the Llobregat River, this means that EDR shows a lower efficiency in reducing both gross alpha and uranium at this water treatment plant.

The best results for radioactivity reduction were obtained in scenario 1 (scenario with RO technology), in agreement with the global behavior of the chemical, biological and aesthetic parameters. As a consequence, scenario 1 was taken as a reference in the design of the new full-scale treatment plant.
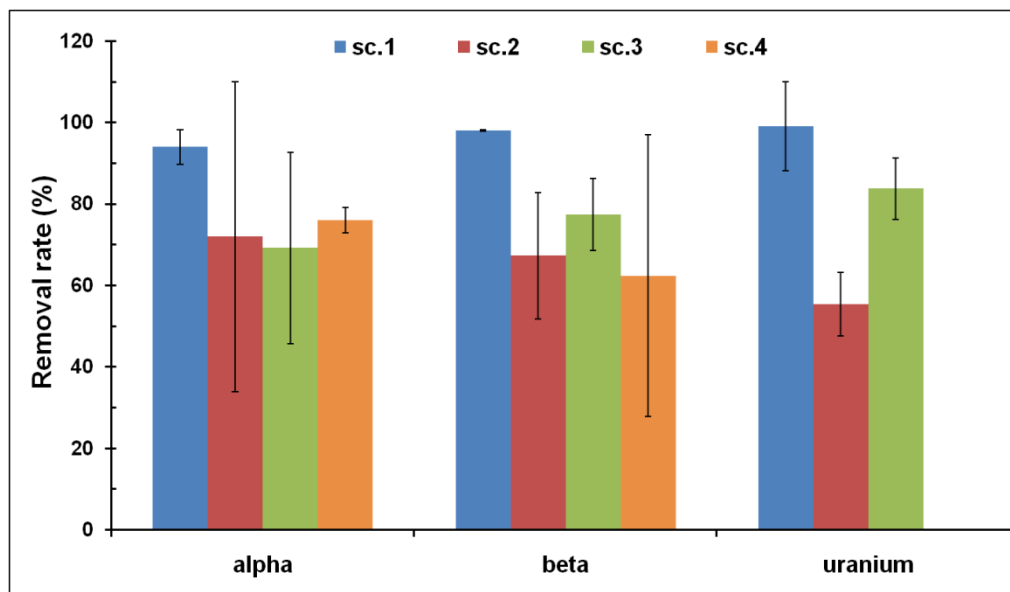
Figure 4.11. Removal rates for gross alpha, gross beta and total uranium activities in four scenarios (sc.) from the pilot plant by different membrane treatments. Error bars are two times the standard deviation.

Full scale treatment plant (only UF +RO treatment lines)

The summary statistics for gross alpha and beta activity and the removal rate for the membranes lines are presented in Table 4.6. The co-precipitation method was used to measured gross alpha activities in order to reduce uncertainties. Four campaigns (2009-2012) took place during catchment of a blend of surface water from Llobregat River (minimum 80%) and wells, while the other three corresponded to extraction of 100% groundwater (7 samplings in total).

A close relation between water source (river and/or wells) and gross alpha activity was observed. The results for gross alpha activity from waters coming from the wells presented higher activities (0.099 Bq/L) than water coming mainly from the Llobregat River (0.075 Bq/L). Furthermore, both gross alpha and beta activities in waters from the Llobregat River showed a temporal variation ([0.01-0.1] and [0.5-1.4] Bq/L for gross alpha and beta respectively during 2009-2012 (data obtained from internal report from our laboratory) in accordance with the Mediterranean regime of the river.

Table 4.6. Gross alpha, gross beta activities and summary statistics of the full scale treatment applied in the SJD WTP.

Source	Point	Gross alpha activity (Bq/L)				Gross beta activity (Bq/L)			
		Mean	**MIN**	**MAX**	**Removal rate (%)**	**Mean**	**MIN**	**MAX**	**Removal rate (%)**
River (>80 %)	Before UF	0.075	0.050	0.093		0.86	0.56	1.06	
	After UF 1	0.074	0.050	0.084	1	0.90	0.57	1.11	-5
	After UF 2	0.077	0.073	0.086	-2	0.91	0.61	1.14	-7
	After RO 1	0.005	0.004	0.007	93	0.06	0.02	0.16	93
	After RO 2	0.005	0.004	0.005	94	0.08	0.01	0.16	91
Wells	Before UF	0.099	0.093	0.107		0.93	0.83	0.98	
	After UF 1	0.093	0.074	0.106	7	0.90	0.86	0.98	3
	After UF 2	0.102	0.098	0.105	-3	0.96	0.92	1.03	-4
	After RO 1	0.004	0.002	0.005	96	0.05	0.03	0.06	95
	After RO 2	0.004	0.002	0.005	96	0.05	0.05	0.06	95

Both treatment lines (with UF and RO treatments) presented similar behavior. As occurred in the pilot plant, UF treatment did not reduce gross alpha and beta activities, and the mean removal by RO membrane for these parameters was higher than 90 % in the studied period in agreement with results obtained in wastewater treatment plants in Australia (Rodriguez et al., 2009). The RO membrane works as a molecular filter that rejects positively and negatively charged ions based on molecular weight. Uranium and their complexes are very heavy, which allows the RO process to effectively remove uranium complexes such as uranyl carbonate.

Individual gross alpha and beta activities for the campaigns are shown in Figures 4.12 and 4.13 respectively. Errors bars represent combined uncertainties corresponding to a confidence level of 95 % and include counting, efficiency and volume of sample uncertainties. Data without errors bars are MDA values. Gross alpha activities after RO were usually below the MDA (0,005 Bq/L) in the analyzed samples.

The results show that UF did not change gross alpha and beta activities while RO treatment reduced these parameters more than 90 % in all the campaigns. Given that gross alpha activity was produced by natural uranium and gross beta activity was due to ^{40}K content, we can conclude that these radionuclides are efficiently removed from water by RO, regardless of its origin (surface or groundwater).
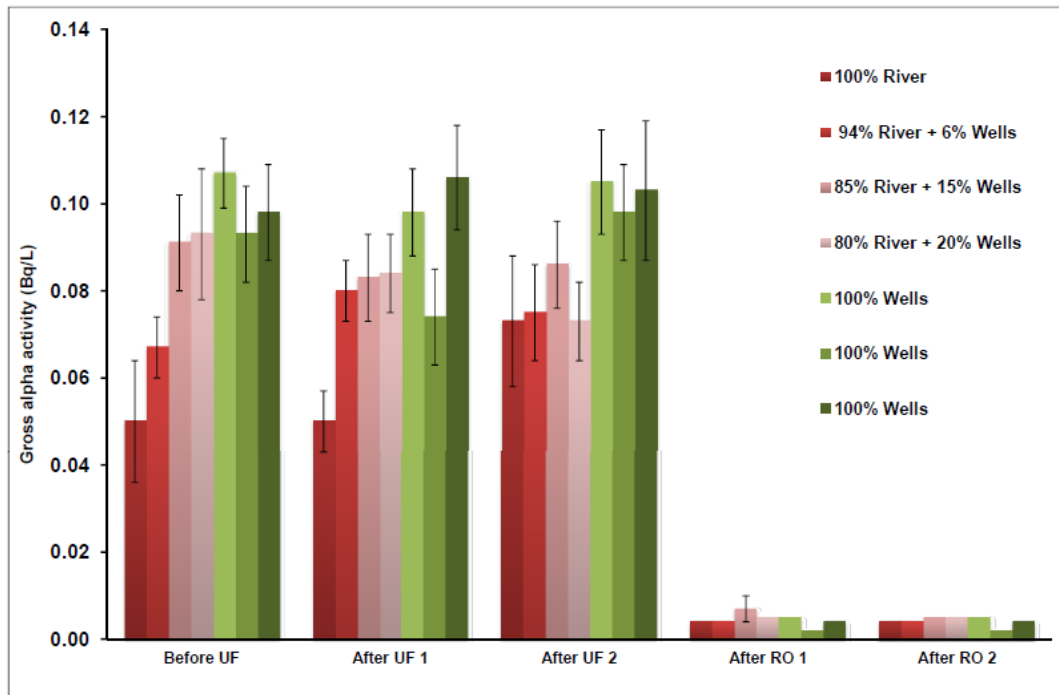
Figure 4.12. Gross alpha activity for different stages at the SJD WTP depending on the amount of water, from both river and wells. The error bars are the uncertainty of the method (*k=2*).
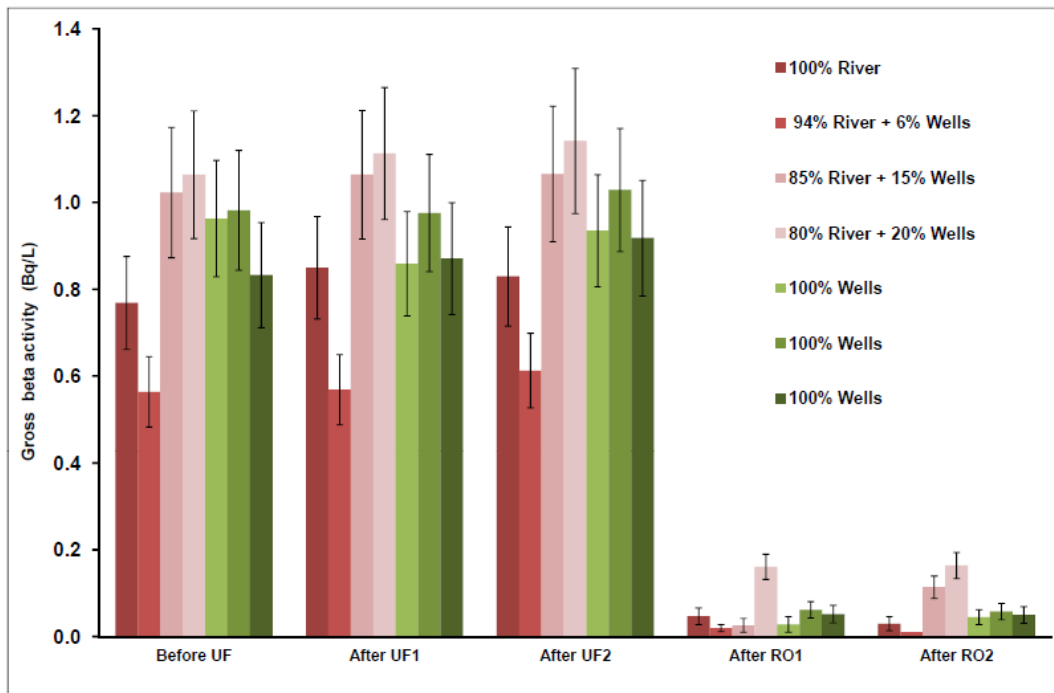
Figure 4.13. Gross beta activity for different stages at the SJD WTP depending on the amount water, from both river and wells.

Screening study of the full scale treatment plant (global treatment)

A screening study related with the RO treatment eventually implemented in the DWTP-1 was done with the aim to assess the influence of this treatment in the global ones. In this study all the process, from the river (in) to the water purified (out) bearing in mind that 50% of water is only treated through the conventional treatment has been analyzed.

Figure 4.15 shows the temporal evolution of the gross alpha activity values obtained between campaigns C-10 and C-12bis in the DWTP-1. It should be pointed out that in these campaigns; the intermediate sample was after Reverse Osmosis (RO) treatment instead of sand filters treatment. For this reason, in these campaigns it is observed an important decreasing after RO treatment but there was an increasing after the intermediate sampling, because only a 50% of water from the DWTP-1 was treated by RO (see campaign C-12 and C-12bis in Figure 4.14).
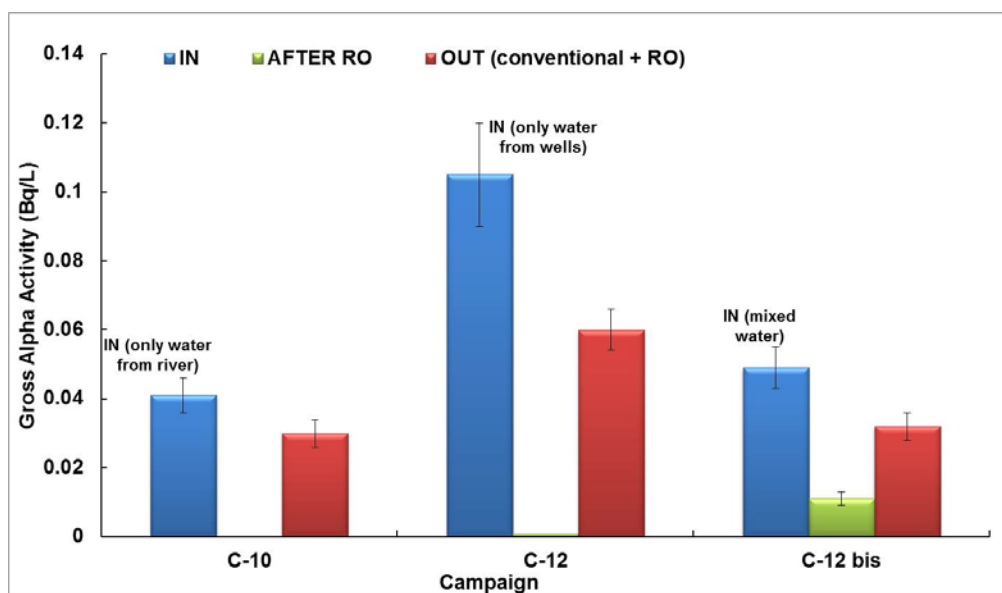
Figure 4.14. Gross alpha activity in liquid samples from DWTP-1, in which the RO treatment was applied.

From Figure 4.14 it can be seen that the gross alpha and beta activity were reduced after RO treatment. Although, in the final effluent, when 50% of water treated by the conventional process was added the gross alpha and beta increased.

4.4   Temporal evolution of radionuclides in sludge from drinking water treatment plants

Sludges from the two full-scale DWTPs (1 and 2) previously studied in section 4.2 were also analyzed during the period 2007-2010 in order to carry out a temporal evolution of radionuclides present in these sludges.

4.4.1 Sampling collection

The temporal study was made taking into account the particular conditions in Spain, at least one sampling campaign per season which correspond to the same campaigns as those with the study presented in section 4.4.

The sludge from DWTP-1 consists on sludge produced by the decanter cleaning process (after the clarification step), in the wash water of the different filters and the washing of the calcite beds. All this sludge is sent to a homogenization tank before being dried and atomized in order to market for future applications. Instead, the sludge produced in DWTP-2 corresponds to sewage from the decanter cleaning process and is sent to a sludge line from a wastewater treatment plant.

Table 4.7 shows the pH range during the sampling campaigns. The coagulant used in the treatment and the sludge production of the studied DWTPs.

Table 4.7. Some characteristics of the studied DWTPs and pH range values during the sampling campaigns.

	DWTP-1	DWTP-2
Sludge production (t/year, dry)	10,950	-
coagulant	Iron chloride	Aluminum polychloride
Retention time of decantation and flocculation	2 hours and 14 min	1 hour and 37 min
pH sludge	10.4-12.3	7.1-7.9

13 sludge samples were obtained from DWTP-1 (7) and DWTP-2 (6) located in Northeast Spain in the period July 2007–March 2009. The sludge samples from DWTP-1 and DWTP-2 were analyzed to determine gross alpha, gross beta and gamma activities, giving a total of 39 analyses.

4.4.2 Results and discussion

Statistical parameters

Gross alpha activity in the sludge ranged from 331 to 533 Bq/kg and gross beta activity from 667 to 1076 Bq/kg. Table 4.8 shows some statistical parameters for the gross alpha and gross beta activities in the DWTPs studied. Similar average values were obtained in both DWTPs.

Some statistical parameters for gamma emitting isotopes detected in the sludge samples analyzed for the period under study (July 2007-March 2009) are also given in Table 4.8.

It should be mentioned that Table 4.8 shows two values for ^{210}Pb (^{210}Pb$_d$ and ^{210}Pb$_u$) where ^{210}Pb$_d$ is the total ^{210}Pb activity measured for each sample and ^{210}Pb$_u$ is unsupported ^{210}Pb which refers to an excess of this radionuclide in the ^{226}Ra content of the samples. The unsupported ^{210}Pb (^{210}Pb$_u$) gives an estimate of ^{210}Pb arising from "rain-out" or wet deposition of atmospheric radionuclides onto the surface of the sludge. ^{210}Pb$_u$ was determined by establishing the ^{226}Ra content of the sample and subtracting this value from the ^{210}Pb$_d$ content. Note that if it's assumed that secular equilibrium was established the ^{210}Pb from the ^{238}U series is equal to the ^{226}Ra activity.

^{226}Ra and ^{232}Th activities were established indirectly by their decay products. In the case of ^{226}Ra, its daughter ^{214}Pb was used because ^{222}Rn and its progeny (^{214}Pb, ^{214}Bi) were in secular equilibrium with ^{226}Ra after 20 days of sealing. Furthermore, we found that ^{214}Pb and ^{214}Bi were present with similar values which agreed with the secular equilibrium that existed between them. For ^{232}Th activities we used ^{228}Ac as a daughter of ^{228}Ra and ^{212}Pb as a daughter of ^{224}Ra. We also checked that ^{224}Ra daughters (^{212}Pb, ^{212}Bi and ^{208}Tl) reached equilibrium because ^{212}Pb and ^{208}Tl activities were within theoretical values (^{208}Tl activities were about 0.36 ^{212}Pb activities due to the branching in ^{212}Bi).

Table 4.8. Statistical parameters for the gross alpha, gross beta activities and gamma emitting radionuclides detected in sludge from DWTPs analyzed.

Radionuclide	DWTP-1				DWTP-2			
	minimum	maximum	average	RSD (%)	minimum	maximum	average	RSD (%)
^{238}U series								
^{234}Th	34.1	88.4	57.5 (7)	33	19.8	102.8	54.4 (6)	59
^{214}Pb	28.5	35.5	32.2 (7)	8	21.4	36.1	27.1 (6)	19
^{214}Bi	25.9	32.9	29.5 (7)	10	17.3	36	25.5 (6)	25
^{210}Pb$_d$	39.0	64.8	53.2 (6)	45	56.1	128.9	87.3 (6)	30
^{232}Th series								
^{228}Ac	33.9	43.5	37.3 (7)	10	32.1	50	42.3 (6)	15
^{212}Pb	30.3	42.8	36.3 (7)	12	29.2	53	36.9 (6)	25
^{212}Bi	34.4	43.6	39.8 (7)	9	36.4	65.5	46.8 (4)	28
^{208}Tl	8.9	12.7	11.2 (7)	12	10.1	18.4	12.5 (5)	27
other								
^{210}Pb$_u$	4.5	31.5	21.2 (6)	47	32.2	102.7	60.2 (6)	41
^{40}K	457	728	598 (7)	17	430	773	539 (6)	23
^{7}Be	28	93	64 (6)	43	68	269	177 (4)	47
^{137}Cs	1.2	2.7	1.9 (7)	29	3	9.1	5.0 (4)	55
Gross alpha	405	533	471 (6)	11	331	522	441 (6)	16
Gross beta	666	988	849 (6)	14	666	1075	814 (6)	18

Data correspond to activity expressed in Bq/kg dry weight.

The number of data used in calculations is indicated in brackets.

RSD (%): relative standard deviation in percentage = standard deviation x 100/average value.

Naturally gamma emitters from the natural ^{238}U series, the ^{232}Th series and other natural gamma emitters such as ^{7}Be or ^{40}K were detected in the sludge samples. In the case of man-made radionuclides small amounts of ^{137}Cs were measured (less than 10 Bq/kg). This could be due to the presence of low levels of ^{137}Cs in Catalan soils long after Chernobyl accident (26-4-1986) (Llauradó, 1990; Coll, 2005). No ^{137}Cs activity values in DWTPs have been reported in the literature yet.

Temporal evolution

Related to naturally gamma emitters, Figure 4.15 shows the temporal evolution for the ^{238}U series activities (mean activity using ^{234}Th and ^{226}Ra values) in the two DWTPs. Arithmetic mean of both activity concentrations of ^{238}U series in Spanish soils (Quindos et al., 1994) and sludge from DWTP studied by Kleinschmidt and Akber (2008) are also plotted in this figure. Figure 4.16 shows the temporal evolution for the ^{232}Th series activities (mean activity using ^{228}Ra and ^{224}Ra values) in the two DWTPs and the arithmetic mean of both activity concentrations of ^{232}Th from the literature above mentioned.
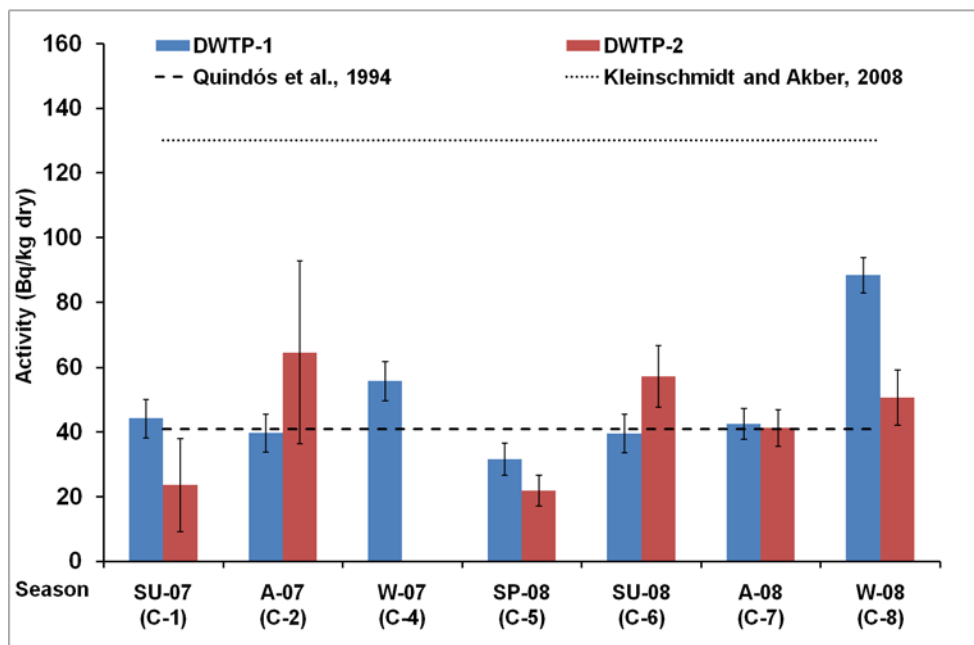
Figure 4.15. Temporal evolution of ^{238}U series in sludge from the DWTPs. Arithmetic mean of both activity concentrations of ^{238}U series in Spanish soils (Quindós, et al., 1994) and sludge from DWTPs studied by Kleinschmidt and Akber (2008).
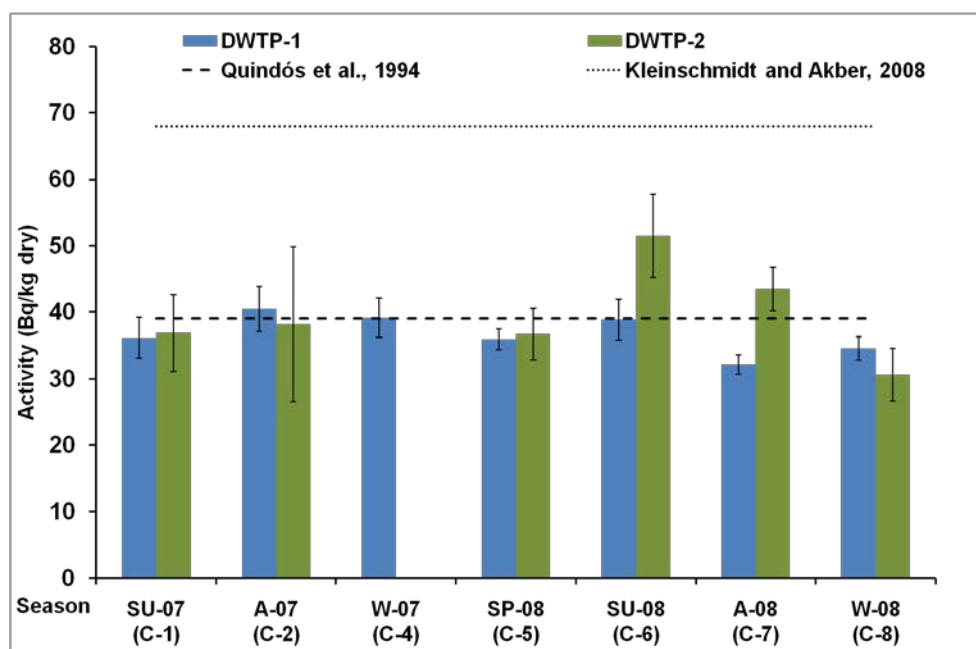
Figure 4.16. Temporal evolution of ^{232}Th series in sludge from the DWTPs. Arithmetic mean of both activity concentrations of ^{232}Th series in Spanish soils (Quindós, et al., 1994) and sludge from DWTPs studied by Kleinschmidt and Akber (2008).

In studied sludge ^{238}U and ^{232}Th activities are similar or below the arithmetic mean found in Spanish soils so no increase in natural radiation are produced by the uses of these sludges. We can see that no seasonal tendency could be observed in the studied period for both series because of the uncertainties associated with the results.

Mean values for gamma-emitted radionuclides in sludge samples were 30 Bq/kg for ^{226}Ra (^{214}Pb), 40 Bq/kg for ^{232}Th (^{228}Ac), 569 Bq/kg for ^{40}K and 120 Bq/kg for ^{7}Be. In all the samples the main contribution from natural gamma radionuclides was produced by ^{40}K (maximum value: 773 Bq/kg) and ^{7}Be (maximum value: 269 Bq/kg). It should be pointed out that a moderate relative standard deviation (RSD) was obtained for ^{7}Be and ^{210}Pb$_u$ (around 45%). If the RSD value is higher than the uncertainties of the measurement, a temporal variation is observed as occurred with ^{7}Be and ^{210}Pb$_u$. These are the radionuclides that are normally associated with airborne surface particles. This particulate matter is subject to wet and dry deposition to the terrestrial surface and it is greatly influenced by rainfall events (Cailet et al., 2001; González-Gómez et al., 2006; Ioannidou and Papastefanou, 2006). The results obtained for gamma emitters from ^{232}Th and ^{238}U series are in the range of those found by Palomo et al. (2010) in other Spanish DWTP and also the values found in Spanish soils (Quindós, et al. 1994) but under the values found by Kleinschmidt and Akber (2008) in Australia. It appeared that isotopes

belonging to the ^{232}Th series are in secular equilibrium whilst isotopes belonging to the ^{238}U series do not, being ^{234}Th activity higher than ^{226}Ra activity.

Application of the t-test for independent samples to the ^{238}U series and ^{232}Th series activities in the two DWTPs showed that no differences were found between the activities in the sludge. Despite water samples from DWTP-1 present higher levels of radioactivity than water samples from DWTP-2, the ^{238}U series mean values of sludge samples from both DWTPs are very similar. It is important to note that the correlation between the uranium concentration and the salinity has been the subject of previous study by Salas (2005). In that study, it was observed that a high salt concentration decreases the uranium absorption onto the particulates and, consequently, when water has a high salinity it reveals lower uranium activities in the sludge. Another noteworthy fact is the difference between coagulants used. As shown in Table 4.6, DWTP-1 uses FeCl$_3$ as coagulant whereas DWTP-2 uses aluminum polichloride. Gäfvert et al. (2002) stated that, as a general trend, iron coagulant has slightly lower removal efficiency than aluminum coagulant. This statement is also accomplished where FeCl$_3$ used in DWTP-1 did not remove efficiently the uranium from water decreasing the uranium accumulation in the sludge.

Correlation analysis

A correlation analysis between radioactivity levels in sludge was performed and the results are presented in Table 4.9. All statistical analyses were carried out using SPSS-V17 software. Positive relationship (r>0) was obtained for all the correlated parameters.

Firstly, the correlation study was focused analyzing all data without taking into consideration the origin of those data (DWTP-1 and DWTP-2). On the other hand, the disaggregation of data by treatment plant characteristics (DWTP-1 and DWTP-2) allows determine more correlations at DWTP-2 in which its conditions (e.g. inflow and HRT) are more stable than conditions in DWTP-1. For instance, the treatment inflow in DWTP-1 ranges between 4860 - 18000 m^3/h (RSD = 54%) and also this plant treats groundwater, whilst in DWTP-2 the treatment inflow was always 250 m^3/h. Consequently, no correlations were found in DWTP-1 due to the variability of the conditions in the treatment.

Considering all data, gross beta activities were highly (r = 0.8) correlated with ^{40}K and ^{232}Th. As occurred in soils, we found a correlation between the activities of ^{40}K and ^{232}Th (Quindós et al., 1994; Khan et al., 2011), but it is usually to find also correlation with ^{238}U series.

The members of the same series were also positively correlated as in the cases of ^{214}Bi with ^{214}Pb or ^{212}Pb with ^{212}Bi and ^{208}Tl. The Pearson's correlation coefficients were higher than 0.87 and close to 1 as should occur if there is equilibrium between them.

No correlations were found among natural radionuclides associated with surface airborne particles such as ^{7}Be and ^{210}Pb$_u$. However, correlations between ^{137}Cs and ^{7}Be and ^{210}Pb$_u$ were found. A positive correlation was also found between ^{137}Cs and ^{7}Be in depositional fluxes by Ioannidou and Papastefanou (2006).

As regards chemical characteristics, we found that, ^{238}U series were positively correlated with sludge pH, which suggested that high pH stimulated the accumulation of these radionuclides in the sludge. Similar conclusion was obtained in drinking water treatment plants where the influence of the pH of the coagulation was study in order to know the removal of uranium and radium (Baeza et al., 2006) from natural water.

Table 4.9. Correlation studies between radioactivity and other parameters in sludge from DWTPs.

Correlated parameters	Level of significance	Pearson's coefficient
All data		
Gross Beta/^{40}K activities (12)	99	0.832
Gross Beta/^{232}Th activities (12)	99	0.825
^{40}K/^{232}Th activities (13)	99	0.871
^{214}Bi/^{214}Pb (13)	99	0.927
^{212}Pb/^{212}Bi (11)	99	0.872
^{212}Bi/^{208}Tl activities (11)	99	0.939
^{137}Cs/^{7}Be activities (10)	95	0.684
^{137}Cs/^{210}Pb$_u$ activities (10)	95	0.670
pH sludge/^{238}U activities (12)	95	0.589
DWTP-2 data		
^{40}K/^{232}Th activities (5)	99	0.981
^{40}K/^{238}U activities (6)	95	0.898
^{214}Bi/^{228}Ac (6)	99	0.938
^{214}Pb/^{228}Ac (6)	95	0.871
^{214}Pb/^{214}Bi (6)	99	0.947
^{7}Be/rainfall[1] (4)	95	0.961

The number of correlated data is in brackets.
Rainfall data source: www.meteo.cat

By contrast, correlations with ^{40}K and ^{238}U series and ^{232}Th were found in DWTP-2 when data were separated into DWTP-1 and DWTP-2. Furthermore, radionuclides belonging to the ^{238}U and ^{232}Th series were also positively correlated in this case (only DWTP-2). For example, ^{214}Pb was positively correlated with ^{228}Ac and ^{228}Ac was positively correlated with ^{214}Bi. Similar correlations were found in a study carried out in soil samples (Quindós et al., 1994) and they were explained by the fact that the ^{238}U and ^{232}Th series commonly appear together in nature.

We found correlation between ^{7}Be activity and rainfall during the month because the main factor controlling the removal of this radionuclide was wet deposition (Cailet et al., 2001; Ioannidou and Papastefanou, 2006; González-Gómez et al., 2006; Jury Ayub et al., 2009)).

4.5   Summary

4.5.1 Temporal evolution of radionuclides in water samples from conventional DWTPs

Two conventional DWTPs with different levels of radioactivity and different treatments were studied. The results of this study showed that gross alpha activities after the conventional treatment in both DWTPs were below the screening level of 0.1 Bq/L and none of them presented 'rest beta' activity above the screening level of 1 Bq/L for drinking water.

The conventional treatments applied at both DWTPs did not influence gross beta activity (produced by the ^{40}K activity). Nevertheless, gross alpha activity after the treatment in DWTP-1 increased, in a variable manner depending on the campaign, due to the water contribution from wells. In the case of gross alpha activity did substantially influence when groundwater contribution was higher than 25%. This contribution instead, was at least 50% to increase substantially gross beta activity.

The temporal evolution of gross alpha and beta activities at DWTP-2 were constant and lower than values detected in water samples from DWTP-1. Any seasonal variation in the studied period was found at DWTP-2.

Comparing gross alpha activity values between raw water and treated water, it is difficult to assess a radioactivity diminution in both conventional DWTPs and therefore, conventional treatments are not suitable to remove gross alpha activity (due to uranium).

4.5.2 Removal of radionuclides in drinking water by membrane treatment

A pilot plant was built to test the behaviour of different membrane techniques, UF, RO and EDR, using four different scenarios. The plant was fed with water from the Llobregat River, where gross alpha activity is due to uranium, while gross beta activity is mainly a consequence of ^{40}K. In general, UF, sand filtration and conventional treatment (ozonation and GAC filtration) did not reduce gross alpha and gross beta activities. However, the membrane techniques, RO and EDR, produced a significant decrease in radioactivity levels.

The removal rate during the RO treatment (scenario 1) was higher than 90% for gross alpha, gross beta and total uranium activities. In the scenarios where EDR treatment was applied (2, 3 and 4), the removal for gross alpha was higher than 70%, for gross beta higher than 60% and for total uranium activity between 55 and 84% depending on the scenario. The radioactivity results for the different scenarios followed the overall performance for chemical, biological and aesthetic factors, which indicates, that scenario 1 with a RO treatment was the best option from the analytical point of view.

In addition, seven sampling campaigns were performed in order to evaluate the decrease in radioactivity levels achieved in the current full-scale SJD WTP. The campaigns covered a three year period under two different operating conditions at the plant: catchment of mostly surface water (80-100%) and full use of water from wells. The results obtained at the current plant were in agreement with those from the pilot plant: UF does not significantly reduce gross alpha and gross beta activities, while RO shows great efficiency in doing so. The removal rates obtained for both cases (the pilot plant and the full-scale plant) were over 90%.

4.5.3 Temporal evolution of radionuclides in sludge samples from DWTPs

With regard to sludge samples, naturally gamma emitters from the natural ^{238}U series, the ^{232}Th series, ^{7}Be, ^{210}Pb$_u$ and ^{40}K were detected. The activities were similar to other published values and the main contribution was produced by the ^{7}Be and the ^{40}K activities.

In the case of man-made radionuclides, small amounts of ^{137}Cs (less than 10 Bq/kg) were measured which may be due to the resuspension process long after Chernobyl accident. No ^{137}Cs activity values in sludge from DWTPs have been reported in the literature yet. Activities for all gamma emitters in the sludge samples from DWTP-1 were similar to the activities

detected in the sludge from DWTP-2. Gross alpha and beta activities instead, are very similar in both DWTPs.

Correlations were found between radionuclides with the same origin in DWTP-2, whilst in DWTP-1 no correlations were found due to the variability of the conditions during the treatment in all campaigns. Considering all data (both DWTPs), the natural ^{232}Th series was highly correlated with ^{40}K and gross beta activities but, as occurred in soils, it is usually to find also correlation between ^{40}K and ^{238}U series. This fact is accomplished in DWTP-2 when data from both DWTPs were separated.

Correlations between members of the same series were positively correlated being the Pearson's correlation coefficients higher than 0.87 as should occur if there is equilibrium between them.

No correlations between radionuclides associated with surface particulate matter such as ^{7}Be and ^{210}Pb$_u$ were found. However, as regards man-made radionuclides, correlations between ^{137}Cs and ^{7}Be and ^{210}Pb$_u$ were found.

In both DWTPs, ^{238}U series were positively correlated with the sludge pH, which suggested that high pH stimulated the accumulation of these radionuclides in the sludge.

Chapter 5

Behavior of radionuclides in wastewater treatment plants

5.1 Introduction and motivation

Because little is known about the transport and behavior of natural radioactive materials in wastewater treatment plants (WWTPs), we undertook the following studies to improve the knowledge in this topic.

This chapter is organized as follows. Section 5.2 consists on a screening study of the presence of radionuclides in eleven Spanish WWTPs. In this study we found that conventional treatment often efficiently removes a high percentage of alpha emitters but, in some cases, an increase of gross alpha activity in liquid samples during the treatment process was observed. This study was published in the Journal of Cleaner of production (Montaña et al., 2011). In Section 5.3 a seasonal study in some WWTPs is presented in order to know if this fact was only produced in that sampling campaign or was repeated temporally in other campaigns. The main aim of the study presented in this section is the radiological characterization of liquids samples collected in two Spanish WWTPs where an increase of gross alpha activity was measured earlier. The samples were collected in order to find out the step of the treatment where the increase of radioactivity was produced, which radionuclides contribute to gross alpha activity and whether the radionuclides were likely to cause an effect on public health.

It should be highlighted that in previous studies (Section 5.2 and the literature previously mentioned in the introduction of part II) there was no information on the sampling procedure applied during liquid sampling or whether the hydraulic retention time (HRT) in the plant was considered. In this study liquid samples were composite samples and were sampled taking into account the hydraulic retention time in the WWTP. In addition, the study constitutes one of a limited number of publications investigating temporally based sampling to access the behavior of natural radionuclides in WWTP's. This study was published in the Journal of Environmental Radioactivity (Camacho, et al 2012a). The seasonal study was also made in sludge samples collected, in this case, in three Spanish WWTPs (WWTP-1, WWTP-2 and WWTP-3). The WWTP-3 was not considered in the radiological characterization of liquid samples since radioactivity levels were not found in the previous study presented in section 5.3. In this case, the sludge study has been published in the Journal of Radioanalytical and Nuclear Chemistry (Camacho et al., 2012b). A preliminary study of a municipal conventional full scale WWTP located in Midwest of the United States (Waukesha-Wisconsin) is presented in Section 5.4 by the reason of the research stay made in the WSLH. Finally, the conclusions of all studies presented in this chapter are gathered in Section 5.5.

5.2 Screening study of the presence of radionuclides in wastewater treatment plants in Spain

The aim of the present work is to investigate the occurrence of radioactivity both in the inlet and outlet waters and sludge at 11 WWTPs in Spain, working under a variety of conditions, with the objective of studying their levels of radioactivity in the resulting treated water and sludge and their removal in the treatment plant.

5.2.1 Plants characteristics and sampling collection

The plants were located in two different areas of Spain, in the north east (Catalonia) and the north west of Spain (Galicia) and the selection was carried out by taking into account the fact that plants were in different geological areas and that they used different treatment processes. The wastewater included domestic water, fruit and vegetable washing water, hospital effluent, other varieties of wastewater and rainwater.

The sewage sludge samples correspond to a mix of primary and secondary sewage, which was anaerobically digested and then dehydrated using press filters. The conventional treatment for sewage effluent basically employs: mechanical filtration, gravity settling, biological oxidation and chemical treatment. Sludge generated in these plants is essentially organic, although measurable quantities of metals, minerals and other compounds are present.

Table 5.1 summarizes some characteristics of the investigated WWTPs. The effluents are aerated in an open-air tank and subsequently segregated into the water and sludge phases.

A total of 22 water samples from the influent and effluent and 11 sewage sludge samples from 11 conventional municipal WWTPs in Spain were collected.

The influent wastewater samples were collected in the pre-treatment building and the effluent wastewater samples were taken after the secondary treatment at WWTP-1, WWTP-3, WWTP-4, WWTP-5, WWTP-7, WWTP-8, WWTP-10 and WWTP-11, and after the tertiary stage in the other ones (WWTP-2, WWTP-6 and WWTP-9). The liquid samples were collected in sterile polyethylene containers with a capacity of 3 L. After collection, the samples were immediately transported to our laboratory where they were acidified with nitric acid 1/1000 to pH<2 and filtered through 0.45μm pore cellulose nitrate filters.

The sludge samples were taken from the centrifuge and water was removed by decantation. The dehydrated sludge samples were collected in clean polyethylene containers with a capacity of 3L. Liquid samples from the influent and final effluent and sludge were sampled together in order to obtain sludge samples which were representative of the water samples.

For water samples, the analytical procedures used to determine the gross alpha activity were the co-precipitation method (Appendix A) and the evaporation method (Appendix B). The evaporation method was also used for gross beta and rest beta activity determination. The potassium content was also determined for these samples (analysis in total: 66).

The sludge samples were analyzed to determine pH, gross alpha, gross beta and gamma activities, giving a total of 33 analyses.

Table 5.1. Characteristics of the investigated treatment plants.

ZONE	WWTP	Average daily plant design flow (m³/d)	Primary Treatment	Secondary Treatment	Tertiary Treatment
North east	**WWTP-1**	35000	Y	AS with N/D (medium load)	N
	WWTP-2	47500	Y	AS (medium load)	Coagulation Filtration and Chloration
	WWTP-3	34560	Y	AS with N/D (medium load) and P	N
	WWTP-10	1500	Y	Biological films	N
	WWTP -11	20000	Y	AS with N/D (medium load) and P	n.d.
North west	**WWTP -4**	24640	Y	AS (medium load)	N
	WWTP -5	54560	Y	AS (medium load)	N
	WWTP -6	4320	N	AS with N/D (extended aeration)	Filtration and UV disinfection
	WWTP -7	10800	N	AS with N/D and P(extended aeration)	N
	WWTP -8	2000	N	AS (extended aeration or medium load depending on season)	N
	WWTP -9	6250	N	AS (extended aeration)	Filtration and disinfection UV

Y= yes   AS: activated sludge; AS with N/D: activated sludge with Nitrification and De-nitrification.
N= no   P=phosphorus
n.d.: no data.   UV= Ultraviolet light

5.2.2 Results and discussion

Activity in liquid samples

Gross alpha and beta activity, potassium concentration, dry residue and pH in the influent and effluent of the 11 WWTPs are given in Table 5.2. Gross alpha activity was measured by both evaporation and co-precipitation methods.

As regards the method used to determine gross alpha activity, the co-precipitation method provides a lower MDA and alpha activity is detected. Evaporation methodology does not seem to be appropriate for determination of low levels of alpha activity in wastewater.

Gross alpha and beta analysis of wastewater showed huge variations of activity for the different plants. A wide range of gross alpha activities (3 to 144 mBq/L, co-precipitation method) and gross beta activities (151 to 1422 mBq/L) in liquid samples was obtained. This variation can be due to different geological zones and different treatments at the WWTPs.

From Table 5.2 it can be seen that the gross alpha activity (co-precipitation method) in the liquids after treatment, decreases in some WWTPs (6 of 11 WWTPs). This may be explained by the fact that this activity is associated with particles that are removed from the water by sedimentation during treatment (Gäfvert et al. 2002). In some cases an increase of concentration was seen (WWTP-1, WWTP-2, WWTP-6, WWTP-9 and WWTP-10) and two of them were selected in order to study in detail in Section 5.4.

Gross beta radioactivity of waste water does not show significant differences between influent and effluent liquids. The results of gross beta activity for all the plants are in agreement with potassium concentration. In this case, the main contribution to gross beta activity is due to ^{40}K, which is highly soluble in water.

The rest beta activity in the liquid samples does not exceed the MDA, consequently the gross beta activity was due to ^{40}K.

Gross beta activity in Zone 2 is generally lower than gross beta activity in Zone 1 which agreed with the potassium content. Quindós et al (1994) studied the concentrations of ^{226}Ra (from the uranium series) and ^{232}Th (from the thorium series) in soils all around the country, dividing Spain into three main regions. The highest values of the mentioned isotopes are found in Zone 2, where granitic formations are prevalent.

Table 5.2. Gross alpha and beta activity, potassium concentration, dry residue and pH in the influent (in) and effluent (out) of the 11 WWTPs. Overall uncertainty at the 95 percent confidence level ($k=2$).

ZONE	WWTP	Alpha in (mBq/L)		Alpha out (mBq/L)		Beta in (mBq/L)	Beta out (mBq/L)	Dry residue (mg/L)		Potasium (mg/L)		pH	
		Evap.	Coprecipitation	Evap.	co	Evap.		in	out	In	out	in	out
North east	WWTP-1	< 54[1]	46 ± 7	87 ± 46	63 ± 7	640 ± 92	621 ± 89	1897	1934	23.0 ± 0.4	21.7 ± 0.4	7.07	7.48
	WWTP-2	< 59 [1]	80 ± 10	95 ± 52	110 ± 11	648 ± 86	632 ± 84	1816	1930	20.1 ± 0.4	20.4 ± 0.4	7.04	7.08
	WWTP-3	< 64 [1]	13 ± 3	< 61 [1]	3 ± 2	1364 ± 170	1422 ± 178	2125	1878	46.9 ± 0.8	46.4 ± 0.8	6.82	6.96
	WWTP-10	< 39 [1]	21 ± 4	< 44 [1]	34 ± 5	625 ± 90	507 ± 73	1324	1627	19.7 ± 0.4	17.7 ± 0.3	6.97	7.51
	WWTP-11	< 83 [1]	48 ± 6	< 81 [1]	36 ± 6	869 ± 122	784 ± 110	3858	3461	25.1 ± 0.5	24.1 ± 0.4	7.21	7.75
North west	WWTP-4	< 24 [1]	144 ± 14	< 23 [1]	15 ± 3	263 ± 52	230 ± 50	298	270	7.9 ± 0.2	9.2 ± 0.2	6.88	6.23
	WWTP-5	20 ± 10	24 ± 4	< 14 [1]	14 ± 2	182 ± 33	236 ± 38	165	232	4.6 ± 0.2	7.2 ± 0.2	6.66	6.27
	WWTP-6	< 28 [1]	15 ± 3	< 62 [1]	27 ± 4	480 ± 69	778 ± 106	868	2141	16.6 ± 0.3	27.6 ± 0.5	6.77	6.71
	WWTP-7	< 16 [1]	29 ± 4	< 17 [1]	5 ± 2	172 ± 32	224 ± 38	242	285	6.0 ± 0.2	7.3 ± 0.2	6.81	7.01
	WWTP-8	41 ± 16	134 ± 13	< 13 [1]	12 ± 3	431 ± 64	151 ± 29	799	190	12.6 ± 0.3	5.5 ± 0.2	4.24	6.55
	WWTP-9	< 18 [1]	8 ± 3	< 16 [1]	20 ± 4	470 ± 68	338 ± 51	446	372	16.2 ± 0.3	12.7 ± 0.3	6.62	8.09

[1] Minimum detectable activity.

Evap. = evaporation

Copr = co-precipitation

Removal rate

In this study we employed the removal rate in order to determine alpha and beta activity removal during wastewater treatment. Removal rates (RE) were calculated by comparing the load of each parameter in influent and effluent waste using the next equation:

$$RE\ (\%) = \frac{(activity\ in\ the\ influent - activity\ in\ the\ effluent)}{activity\ in\ the\ influent} \times 100 \tag{5.1}$$

Positive removals in liquids for gross alpha and beta activity indicated in Figures 5.1 and 5.2, respectively, varied from rather low (for gross beta activity) to high rate values (for gross alpha activity). For gross alpha activity, the removal rate from WWTPs varied from 25 to 91%. WWTP-4 and WWTP-8 presented the highest removal rate values for gross alpha activity (90 and 91% respectively) and low pH for ingoing and outgoing water (the solubility of alpha-emitters might decrease if pH is low and isotopes are removed from the water by sedimentation).

Apart from the WWTP-8 plant, no significant differences were observed in gross beta activities for influent and effluent water, with values of removal rate from 2 to 28%. These values are the same order of magnitude as the uncertainty of the gross beta activity determination and therefore there is no reduction on gross beta activities. In this case the main contribution to gross beta activity is due to ^{40}K, which is highly soluble in water, so these isotopes remain within water more than alpha emitters (Baeza et al. 1995).

The removal rate could be related to the composition of influent waters, operating conditions of the plant and physicochemical properties of the radionuclides.

The removal rate is strongly related to the type of treatment at each plant and the physicochemical properties of the radionuclides. This could be due to changes in the composition of influent waters and operating conditions of the plant.

The negative values of removal rates for gross alpha activity are due to an increase in the concentration of alpha activity during treatment (higher activity in the effluent than in the influent water samples). This phenomenon of "negative removal" for some alpha emitters has not been reported in the literature.

The explanation for this can be found in sampling protocols because they could be inadequate. Furthermore, negative removal can also be explained by the physical-chemical mechanism of desorption of the uranium and radium in the sludge layer and the partition of alpha isotopes within solution (Retallack et al. 2007).
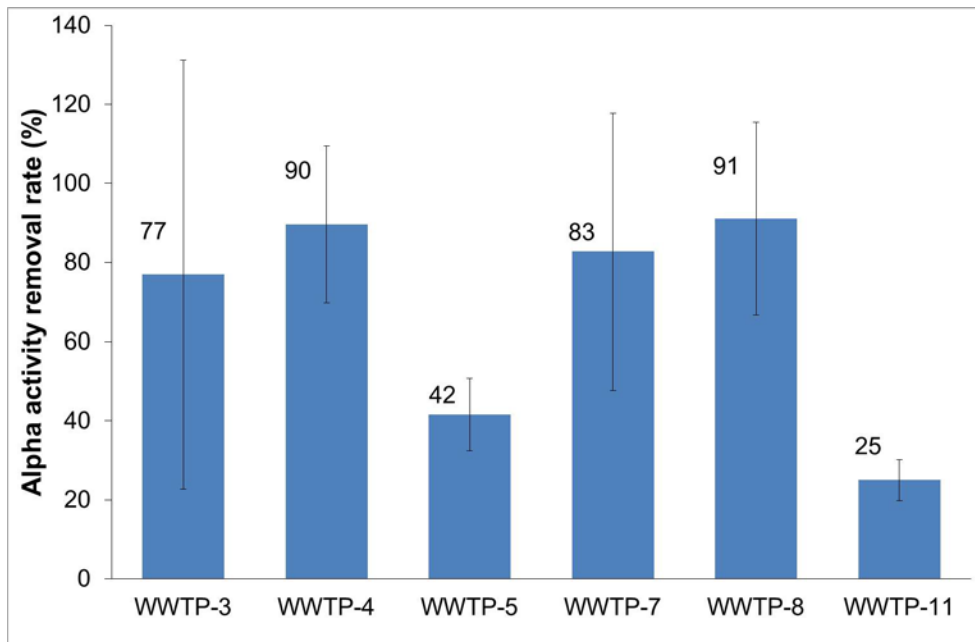
Figure 5.1. Alpha activity removal rate in liquid samples from WWTP-3, WWTP-4, WWTP-5, WWTP-7, WWTP-8 and WWTP-11. Error bars are the overall uncertainty (*k=2*).
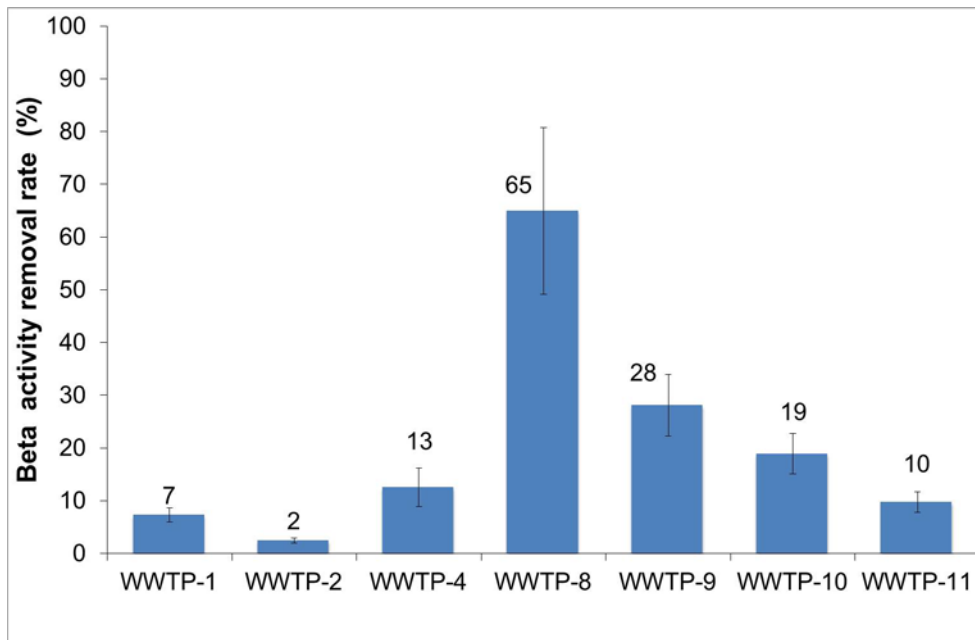
Figure 5.2. Beta activity removal rate in liquid samples from WWTP-1, WWTP-2, WWTP-4, WWTP-8, WWTP-9, WWTP-10 and WWTP-11. Error bars are the overall uncertainty (*k=2*).

When the values of removal rate are compared, it can be concluded that some alpha radionuclides are removed in the WWTPs and a fraction of the radioactivity may be concentrated in the sludge generated during the water treatment process (Ipek et al. 2004; Palomo et al. 2010b).

Activity in sludge samples

Gross alpha and beta radioactivity in the solid waste from the 11 WWTPs are given in Table 5.4. Gross alpha concentration in the sludges ranged from 80 to 861 Bq/kg with an average of 276 Bq/kg. Gross beta activity varied from 172 to 1463 Bq/kg with an average of 582 Bq/kg. WWTP-4 and WWTP-8 presented the highest values of gross alpha and beta activity in the sludge and it should be pointed out that these WWTPs also presented high levels of alpha and beta removal rate in wastewater. Solid waste presenting high levels of gross alpha and beta activity also show low values of pH (5.42 and 5.32) (Table 5.4). Thus under these conditions solubility decreases and the isotopes can precipitate.

Table 5.3 shows the activity of gamma radionuclides in sludge samples from wastewater treatment plants. Natural gamma radiation emitted from natural ^{238}U and the ^{232}Th series, natural gamma emitted with an origin in atmospheric deposition (^{7}B, ^{210}Pb$_u$), with a terrestrial origin (^{40}K) and an anthropogenic origin (^{131}I and ^{137}Cs) are presented.

Mean values for gamma-emitted radionuclides in sludge samples were 37 Bq/kg for ^{226}Ra (^{214}Pb), 36 Bq/kg for ^{232}Th (^{228}Ac), 278 Bq/kg for ^{40}K and 255 Bq/kg for ^{7}Be. The main contribution to natural gamma radioisotopes was made by ^{7}Be (maximum value: 517 Bq/kg) and ^{40}K (maximum value: 478 Bq/kg) and a few activities were measured from artificial radionuclides from nuclear testing fallout (^{137}Cs, 2.6 Bq/kg). ^{131}I, which is widely used in nuclear medicine, was only reported in sludge from WWTP-4 (640 Bq/kg), which treats water from institutions with nuclear medicine programs. This sludge would not be expected to produce a significant population dose when it is used as a soil conditioner because the time required for processing exceeded the 8 days (half - life of ^{131}I).

The highest concentrations of gamma isotopes were for WWTP-4 and WWTP-8 and it is seen that in the sludge from zone 2 the activity values were, in general, higher than the sludge from zone 1. This is because of the differences in the geology of each zone where granitic formations are prevalent in zone 2 as well as in the type of treatment plant.

The results obtained are quite similar to those found by Bastian et al. (2005) in the USA and Jiménez et al. (2011) in Spain.

Table 5.3. Activity of gamma radionuclides, gross alpha and gross beta and pH in sludge from wastewater treatment plants. Overall uncertainty at the 95 percent confidence level ($k=2$).

Radionuclides	North east zone					North west zone					
	Activity ± uncertainty ($k=2$) (Bq/kg dry weight)										
	WWTP-1	WWTP-2	WWTP-3	WWTP-10	WWTP-11	WWTP-4	WWTP-5	WWTP-6	WWTP-7	WWTP-8	WWTP-9
^{228}Ac	11 ± 2	23 ± 3	22 ± 3	28 ± 5	21 ± 3	73 ± 3	43 ± 4	45 ± 3	39 ± 4	77 ± 6	29 ± 3
^{212}Pb	5.6 ±1.0	7.3 ± 1.2	15 ± 2	26 ± 3	13 ± 2	54 ± 1	30 ± 3	19 ± 2	22 ± 1	48 ± 5	24 ±1
^{212}Bi	< 8.1 [2]	< 14.1 [2]	22.8 ± 8.0	21 ± 13	17 ± 6	66 ± 9	40 ± 10	21 ± 7	18 ± 12	64 ± 14	30 ± 8
^{208}Tl	1.9 ± 0.6	2.2 ± 0.8	5.2 ± 0.7	7 ± 1	2.4 ± 0.9	16.5 ± 0.8	8.4 ± 1.1	6.0 ± 0.7	8 ± 1	14 ± 1	7.3 ± 0.8
^{234}Th	39 ± 8	85 ± 11	58 ± 10	46 ± 14	41 ± 12	387 ± 13	60 ± 14	80 ± 10	78 ± 14	164 ± 18	32 ± 10
^{214}Pb	12 ± 2	15 ± 3	16 ± 3	16 ± 3	17 ± 3	132 ± 3	56 ± 7	22 ± 3	29 ± 2	64 ± 8	20 ± 2
^{214}Bi	11 ± 1	14 ± 2	15 ± 2	15 ± 3	14 ± 2	121 ± 3	50 ± 3	18 ± 1	26 ± 2	57 ± 3	19 ± 2
^{210}Pb$_{(d)}$	37 ± 11	42 ± 12	71 ± 14	119 ± 25	88 ± 17	202 ± 12	156 ± 27	65 ± 14	111 ± 14	225 ± 36	73 ±10
^{219}Pb$_{(u)}$	25 ± 7	27 ± 7	55 ± 5	103 ± 5	71 ± 5	70 ± 1	100 ± 4	43 ± 5	82 ± 3	161 ± 4	53 ± 3
^{7}Be	75 ± 16	91 ± 19	169 ± 23	324 ± 28	129 ± 11	233 ± 10	435 ± 104	198 ± 20	517 ± 37	479 ± 40	147 ± 17
^{40}K	133 ± 13	205 ± 20	211 ± 19	313 ± 33	151 ± 18	478 ± 19	221 ± 22	325 ± 26	308 ± 21	347 ± 31	369 ± 19
^{131}I	n.d. [1]	n.d. [1]	n.d. [1]	n.d. [1]	n.d. [1]	640 ± 386	n.d. [1]	n.d. [1]	n.d. [1]	n.d. [1]	n.d. [1]
^{137}Cs	< 0.6 [2]	<1.1	0.9 ± 0.5	2.6 ± 1.0	n.d. [1]	1.8 ± 0.3	1.4 ± 0.3	< 0.6 [2]	n.d. [1]	2.0 ± 0.3	1.1 ± 0.5
Gross alpha	97 ± 37	95 ± 41	80 ± 32	122 ± 45	89 ± 38	861 ± 233	455 ± 128	163 ± 55	160 ± 54	699 ± 192	211 ± 67
Gross beta	172 ± 44	397 ± 68	253 ± 51	584 ± 92	310 ± 60	1463 ± 213	604 ± 99	523 ± 85	582 ± 93	1011 ± 153	504 ± 85
pH	5.57	5.96	7.17	7.03	6.39	5.42	7.48	6.14	6.08	5.32	5.63

[1] n.d.: not detected

[2] Minimum detectable activity.

5.3 Temporal evolution of radionuclides in wastewater treatment plants

The main aim of the study presented in this section is the radiological characterization and the temporal evolution of liquids samples collected in two Spanish WWTPs where an increase of gross alpha activity was observed in the previous section. The temporal study in the sludge samples was also presented.

5.3.1 Wastewater treatment plants characteristics

Fig. 5.3 shows the schematic diagram of the studied WWTPs and the points where the liquid samples were taken are also indicated by a star. The liquid treatment consisted of pre-treatment, primary settling, and biological treatment followed by secondary settling at WWTP-1 and WWTP-3, while at WWTP-2 there was a tertiary treatment which included coagulation/flocculation and chlorination. The treatment steps were done in the open air with the exception of pre-treatment in WWTP-2, which was done inside a building. In WWTP-1, the sludge generated from primary and secondary clarifiers was thickened and blended and fed into an anaerobic digester system and dewatered by a centrifuge. In WWTP-2 the gravity-thickened (primary sludge) and flotation-thickened waste activated sludge are mixed and dewatered by a centrifuge and sent for composting. In WWTP-3 the sludge mixture proceeding from the primary and secondary settlers is thickened by gravity, treated by anaerobic digestion and dewatered on a belt filter press.

WWTP-1 treats both industrial and municipal wastewater which includes hospitals effluents and WWTP-2 influent is predominantly residential wastewater. Both WWTPs are designed to handle runoff so they are influenced by storm occurrence. It should be pointed out that WWTP-2, which shows a huge variation in the influent flow for the different sampling campaigns is located next to a touristic town and is affected by a seasonal increase of population. This fact greatly influences the quantity of wastewater to be treated and consequently the HRT.

Table 5.4 shows the main characteristics of these three plants and Table 5.5 presents some specific chemical characteristics of water samples in sampling campaigns from WWTP-1 and WWTP-2. It can be seen that the chemical characteristics of the water samples varied significantly in the sampling campaigns so the results obtained refer to different chemical scenarios.
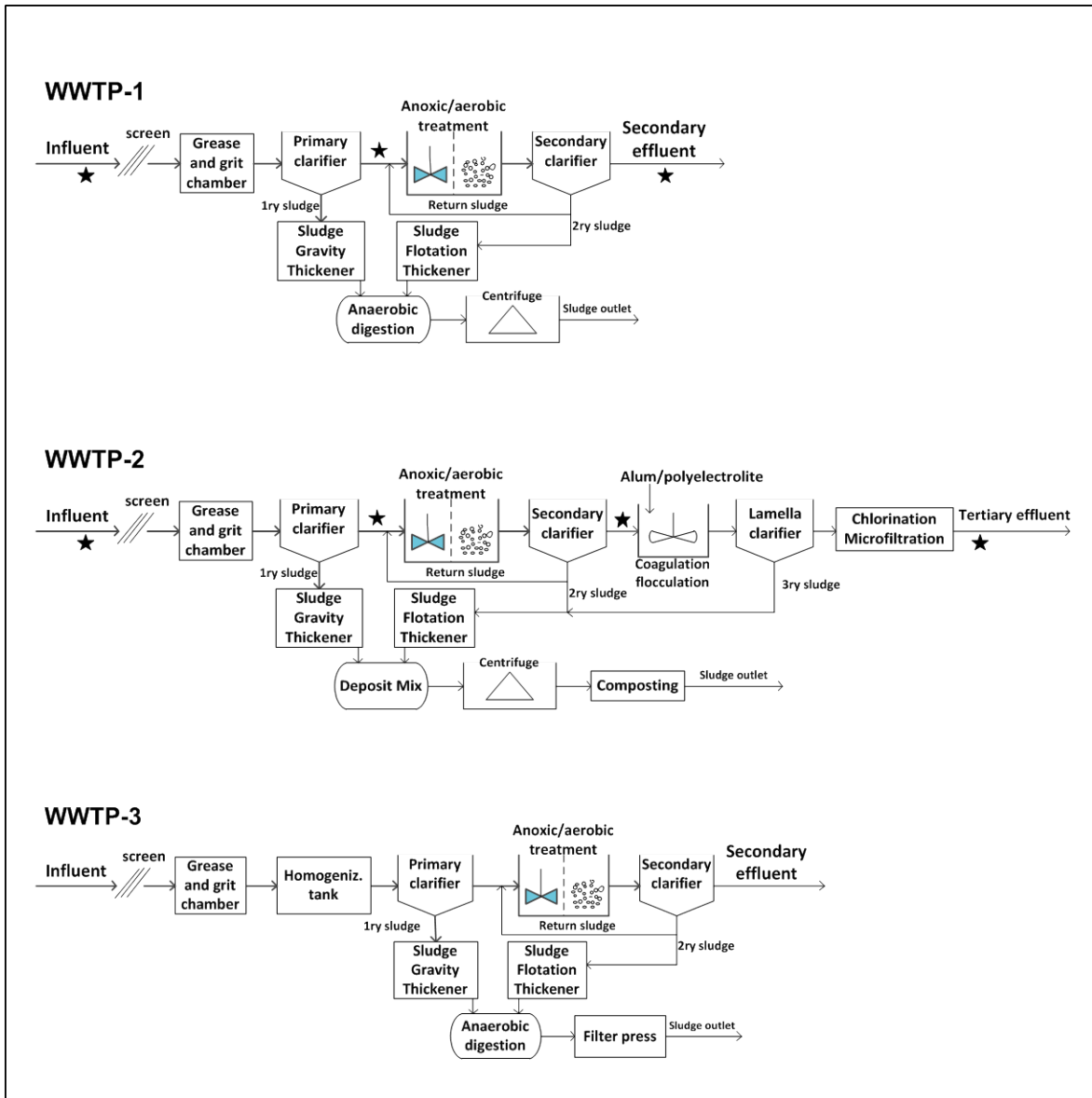
Figure 5.3. Schematic diagram of the studied WWTPs. The points where the liquid samples were taken from WWTP-1 and WWTP-2 are indicated by star.

Table 5.4. Main characteristics of the studied WWTPs and range of values for some specific parameters during the sampling campaigns (2007-2010).

WWTP	WWTP-1	WWTP-2	WWTP-3
Type of treatment	Biological	Biological and tertiary	Biological with P and N removal
Designed treatment capacity (m^3/day)	35,000	47,500	25,000
Average flow (m^3/day)[a]	28,500	27,140	20,750
Population equivalent	175,000	210,600	204,166
Sludge treatment	Anaerobic digestion, drying	Anaerobic digestion, drying	Anaerobic digestion, drying
Disposal of sludge	Agricultural usage	Agricultural usage, disposal to soil	Controlled disposal to landfill, incineration
Sludge production (t/year, wet)[1]	8,786	9,800	8,853
Inflow (m3/day)[1]	960-1,550	230-2,000	690-1,070
HRT (h)[2]	14-22	16-142	41-63
Sludge production (t/month, wet)[2]	255-1008	579-1460	615-1051
Sludge retention time (d)[2]	4.5-7.2	No data	6.9-25.4
pH_{sludge}[3]	5.2-6.8	5.5-8.0	6.0-7.2

Sources: website of the Catalan Water Agency (http//aca-web.gencat.cat/aca) and information from WWTP as personal communication
[1] Average values for the period 2007-2010
[2] These ranges refer to the temporal variation in the parameters for the different sampling campaigns
[3] Data measured by our research group

Table 5.5. Chemical caracteristics of the liquids from WWTP-1 and WWTP-2 in sampling campaigns.

WWTP	WWTP-1	WWTP-2
Suspended particulate matter (in)	340-1076	95-272
Suspended particulate matter (in)	7-86	6-23
Biochemical oxygen demand (in)	396-825	128-298
Biochemical oxygen demand (out)	14-37	7-21
Chemical oxygen demand (in)	759-1633	51-603
Chemical oxygen demand (out)	68-179	7-58

In= influent; out= final effluent
[a] These ranges refer to the temporal variation in the parameters for the different sampling campaigns.

5.3.2 Sampling collection

Composite liquid samples from two municipal conventional full-scale WWTPs (WWTP-1 and WWTP-2) and sludge samples from three WWTPs (WWTP-1, WWTP-2 and WWTP-3) located in Northeast Spain in the period 2007-2010 were obtained in order to carry out a temporal study.

The sampling was carried out according to established sampling protocols and locations defined by 'Aguas de Barcelona', and occupational health and safety regulations were followed.

Composite liquid samples were collected using the ISCO GLS Compact Composite Sampler with an integrated 5 L glass bottle. The sampling program was set to collect 0.1 L of liquid every 30 min during 24 h. Liquid samples (unfiltered) were later transferred to 2 L polyethylene bottles for radioactivity determination. Composite water samples were sampled taking into account the hydraulic retention time (HRT) in the WWTPs. HRT was calculated using the inflow arriving to the WWTP, the sampling campaign and the volume of the tanks used in primary and secondary treatment.

The HRT is the time the wastewater takes to pass through WWTP. As the HRT depends on the quantity of wastewater to be treated, the sampling campaigns were chosen in different seasons in order to consider the changes due to storm occurrence or tourism period.

In order to preserve the liquid samples prior to the radioactivity analysis, the unfiltered liquid samples were acidified with concentrated nitric acid (at pH 2) and later they were filtered through 1mm glass fiber filters followed by 0.45 μm membrane filters. Therefore it should be highlighted that the results in liquid samples refer to dissolved radioactivity levels according to the pretreatment.

For up to 12 sampling campaigns carried out over the period 2007-2010, 56 samples including influent, primary effluent, secondary effluent and final effluent (if tertiary treatment was also applied) wastewater from two municipal WWTPs were sampled.

22 sludge samples were obtained from three municipal full-scale conventional WWTPs (WWTP-1, WWTP-2 and WWTP-3) located in Northeast Spain in the period July 2007–March 2009. The sewage sludge samples correspond to a mix of primary and secondary sewage which were dehydrated and were taken from the centrifuge (WWTP-1 and WWTP-2) or taken from the filter press (WWTP-3).

The temporal study was made taking into account the particular conditions in Spain (at least one sampling campaign per season). Note that in Spain both the rain and tourism vary seasonally and greatly influence the quantity of wastewater to be treated and also the quantity of produced sludge. The season and year of the sampling campaigns are indicated in Figs. 5.4 and 5.5 .

For the 56 water samples collected, gross alpha and beta activities and the potassium content were determined. The evaporation method was used to determine both gross alpha and gross beta activities. The co-precipitation method (Appendix A) was also used to determine gross alpha activities. Total uranium activity by alpha spectrometry was also determined for some of these samples. The 22 sludge samples were analyzed to determine gross alpha, gross beta and gamma activities (see Appendix B for test methods and instrumentation).

5.3.3 Results and discussion related to activity in water samples

Statistical parameters

Table 5.6 shows some statistical parameters (arithmetic mean, the relative standard deviation, the minimum and maximum values and the number of data) for radioactivity and chemical characteristics of liquid samples from WWTP-1 and WWTP-2 (period 2007-2010). The 'Ratio parameter' for gross alpha and beta, dry residue and potassium content is also included in this table. These ratio parameters were calculated by dividing effluent by influent values for each campaign and their statistics are also presented in Table 5.6. The results are discussed below.

Gross alpha activity was measured using both the evaporation and the co-precipitation methods. One of the disadvantages of the evaporation method is that you can't use large amounts of water if the total dissolved solids are high because of the self-shielding of the sample which would be unacceptable to detected low activities. The co-precipitation method enabled lower gross alpha activities to be measured than the evaporation method (see the mean MDA of each method in Appendix B) and for this reason we detected gross alpha activity in 100% of the liquid samples, while only 29% was detected when the evaporation method was used. According to these results, the evaporation method is not suitable for measuring the low activities that were present in the studied wastewaters. Table 5.6 shows the statistics for the co-precipitation values.

In effluent wastewater gross alpha activity ranged between 31 and 90 mBq/L at WWTP-1 and between 27 and 129 mBq/L at WWTP-2. These values are similar to those measured in Australia (Rodriguez et al., 2009).

Gross beta (including ^{40}K) in effluent from WWTP-1 ranged between 554 and 878 mBq/L and in WWTP-2 effluents from 477 to 696 mBq/L. None of the samples presented 'rest beta' activity (a term used in Spanish legislation which refers to gross beta activity excluding ^{40}K activity) above the screening level in drinking water of 1 Bq/L (Spanish Royal Decree 140/2003). 'Rest beta' was not measured in any samples over the MDA of 40 mBq/L so it can be stated that gross beta was mainly due to the ^{40}K content of the samples.

Table 5.6. Statistical parameters for radioactivity and chemical characteristics in liquid samples from WWTP-1 and WWTP-2 (2007-2010).

Chemical parameter	Statistical parameter	WWTP-1			WWTP-2		
		Influent	Final effluent	Ratio parameter	Influent	Final effluent	Ratio parameter
Gross alpha activity (mBq/L)	Arithmetic mean	25	57	2.5	34	84	2.9
	RSD	42	30	43	57	42	60
	Minimum	15	31	1.4	15	27	1.4
	Maximum	46	90	5.0	80	129	7.2
	n	10	10	10	12	12	12
Gross beta activity (mBq/L)	Arithmetic mean	753	696	0.94	583	555	0.96
	RSD	17	16	10	10	12	11
	Minimum	559	554	0.77	506	477	0.76
	Maximum	983	878	1.09	667	696	1.14
	n	10	10	10	12	12	12
Dry residue (mg/L)	Arithmetic mean	1765	1713	0.97	2114	2082	0.99
	RSD	16	15	6	20	15	6
	Minimum	1272	1292	0.85	1800	1722	0.88
	Maximum	2193	2185	1.03	3238	2862	1.07
	n	10	10	10	12	12	12
Potassium content (mg/L)	Arithmetic mean	24.3	22.5	0.93	20.7	18.9	0.92
	RSD	13	13	9	15	9	12
	Minimum	19.6	16.9	0.76	16.2	16.3	0.71
	Maximum	29.2	28.2	1.02	28.1	22.1	1.14
	n	10	10	10	12	12	12

RSD = Relative standard deviation (%) = standard deviation x 100/arithmetic mean.

Beta emitting radionuclides used in medical therapies such as ^{131}I or ^{99m}Tc were not measured in gross beta activities because the elapsed time between sampling and measurement was more than two weeks. Furthermore the sample preparation method, which uses acidification of the liquid sample and evaporation, is not suitable for the consistent retention of radioiodine. In addition, although ^{131}I is usually found in sludge of WWTPs which treat wastewater from hospitals using radiotherapies this radionuclide was not observed in effluents (Martin and Fenner, 1997; Jiménez et al., 2011; Montaña et al., 2011).

RSD was low for both gross beta activities and potassium content, with similar values in effluent and influent wastewater, and as high as the total uncertainties.

The 'Ratio parameter' was used as an indicator of the removal efficiency of the treatment applied in the WWTPs. We found that Gross alpha activities (arithmetic mean 'Ratio parameter' >2.5) show a different behavior compared to gross beta, potassium or dry residue (arithmetic mean 'Ratio parameter' $\simeq$ 1) and are influenced by the treatment applied at the studied WWTPs.

Application of the Student t-test for independent samples to gross beta activity, residue and potassium content in influent and effluent samples showed a significance value (2-tailed) greater than 0.05 which demonstrated that no statistically significant differences between groups (influent versus effluent) existed. This is in agreement with the previous results for the 'Ratio parameter' so the treatment applied at these WWTPs did not influence gross beta activity, potassium content or the residue as it was also observed in the previous screening in other Spanish WWTPs (Montaña et al., 2011).

These results disagree with those obtained in the study carried out in Turkey (Ipek et al., 2004) which found that alpha radioactivity in liquids decreased by 52-90% and beta radioactivity decreased by 62-92%. It is worth pointing out that about 50% of the gross beta activity in the Turkish samples came from radionuclides such as ^{129}I, ^{137}Cs and ^{90}Sr. However, in the liquids analyzed in this study gross beta activity was produced by ^{40}K. There was no information given about the radionuclides that produced gross alpha activity in the Turkish work. However, no elimination or even an increase of some compounds during wastewater treatment was also found in a few pharmaceuticals and/or personal care products (Teijón et al., 2010; Jelic et al., 2011).

Temporal behavior of gross alpha activity

As explained in the previous section, gross alpha activities are influenced by the treatment applied in the WWTPs and for this reason are further studied.

Figures. 5.4 and 5.5 show gross alpha activities measured in liquid samples fromWWTP-1 and WWTP-2 respectively for the different sampling campaigns at different sampling points within the treatment plants. In the case of WWTP-1 the samples were taken before pre-treatment (influent), after primary treatment (primary effluent) and after secondary settling (final effluent). For WWTP-2 there was a difference between samples after secondary settling (secondary effluent) and after tertiary treatment (final effluent).
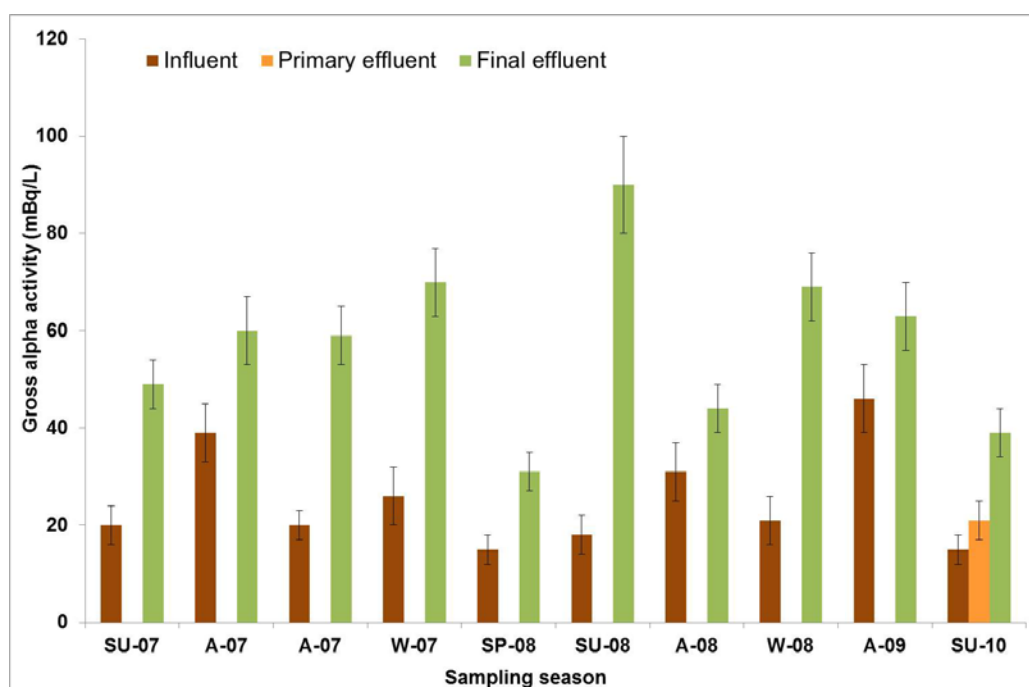
Figure. 5.4. Gross alpha activity in liquid samples from WWTP-1 (2007-2010).

In Spain, wastewaters do not have to comply with any legislation regarding radioactive levels, but these waters are usually treated lately by potable water treatment plants so we take as reference the values published by the Spanish legislation for potable waters (Spanish Royal Decree 140/2003). Liquid samples fromWWTP-1 (influents or effluent) did not present gross alpha activity higher than the screening value for drinking water (0.1 Bq/L; Spanish Royal Decree 140/2003), but about 18% of the liquid samples fromWWTP-2 exceeded this value.

These values (0.108-0.129 Bq/L) were always measured in effluent samples and usually in samples obtained in the autumn season which also show the higher 'Gross alpha ratio' (7.2-3.3). A seasonal tendency was found in effluent from WWTP-2 with maximum values in autumn and winter. These variations could be associated with seasonal changes in the inflow and the chemical characteristics of the liquids which are studied below.

In all the sampling campaigns we detected higher gross alpha activities in the final effluent (after secondary treatment for WWTP-1 or after tertiary treatment for WWTP-2) than in the influent. So we found that the increase in gross alpha activity was produced every sampling campaign and was independent of the environmental conditions.
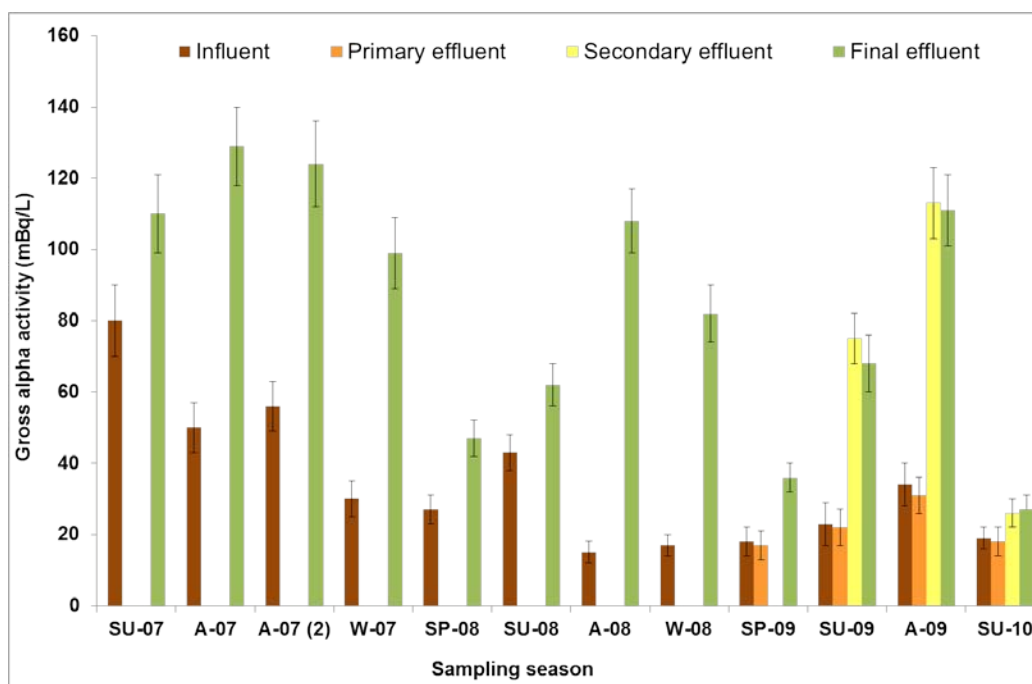
Figure 5.5. Gross alpha activity in liquid samples from WWTP-2 (2007-2010).

In order to find out where the increase in gross alpha activity was produced, primary effluent and secondary effluent were also analyzed in recent campaigns (see results in Figures. 5.4 and 5.5). No variation in gross alpha activities between influent and primary effluent or secondary effluent and final effluent in WWTP-2 were observed. Thus, according to the results presented in Figures. 5.4 and 5.5 the increase in gross alpha activity was produced during secondary treatment.

To identify which radionuclide produced the gross alpha activity, uranium (^{238}U, ^{234}U and ^{235}U) and Radium (^{226}Ra and ^{224}Ra) isotopes were analyzed in some liquid samples. Radium isotopes were not detected in any of the samples. Table 5.7 shows gross alpha activity, total uranium activity (^{234}U+^{235}U+^{238}U) and ^{234}U/^{238}U activity ratio in liquid samples from different sampling campaigns and steps within the treatment plants. As occurred in waters from the Llobregat Basin in NE Spain, the total uranium activity is higher than the global average river water uranium (2.3 mBq/L) (Camacho et al., 2010) nevertheless these values are much lower than the guidance levels presented in the WHO guidelines for ^{238}U (10 Bq/L) and ^{234}U (1 Bq/L) in drinking water (WHO, 2011).

Application of the t-test for independent samples to gross alpha activity and uranium content presented in Table 5.8 showed a significance value (2-tailed) of 0.871 so no statistically significant differences between groups were found.

We can therefore affirm that uranium isotopes produced gross alpha activity in the analyzed liquid samples and dissolving or desorption of this element occurred during the secondary treatment. This statement agrees with the fact that under aerobic condition, which occurs during the biological treatment in the secondary step, the uranyl ion (UO_2^{+2}, the uranium soluble oxidation state) is formed and therefore U^{+4} present in the solid material could be dissolved.

As we can observe in table 5.7, the isotopic ratio values between ^{234}U/^{238}U show that uranium is out of secular radioactive equilibrium, exhibiting an enrichment of ^{234}U relative to ^{238}U. The mean ^{234}U/^{238}U activity ratio and the standard deviation were 1.32 ± 0.07 for the samples from WWTP-1 and 1.6 ± 0.1 for the samples from WWTP-2. This enrichment observed is probably due to its instability in crystalline lattices after recoil following alpha emission from ^{238}U. In this process, the chemical bond is weakened and the ^{234}U oxidation changes from tetravalent to a more soluble hexavalent form. High uranium isotopes disequilibrium was measured in the liquid samples and these values were in the range reported in the literature for surface waters from the Llobregat River (Camacho et al., 2010).

Table 5.7. Gross alpha activity and Total Uranium activity (mBq/L) at different steps into the WWTPs.

Sampling campaign	Sample	WWTP1			WWTP2		
		Gross alpha[1]	Total uranium[1]	^{234}U/^{238}U	Gross alpha[1]	Total uranium[1]	^{234}U/^{238}U
Nov-07(2)	**Influent**	20 ± 3	28 ± 6	1.31 ± 0.36	56 ± 7	69 ± 12	1.61 ± 0.27
	Final Effluent	59 ± 6	66 ± 9	1.36 ± 0.18	124 ± 12	134 ± 10	1.81 ± 0.13
Nov-09	**Influent**				34 ± 6	36 ± 3	1.62 ± 0.12
	Primary effluent				31 ± 5	33 ± 3	1.52 ± 0.14
	Secondary effluent				113 ± 10	120 ± 8	1.57 ± 0.10
	Final effluent				111 ± 10	117 ± 8	1.53 ± 0.10
Jul-10	**Influent**	15 ± 3	9 ± 2	1.23 ± 0.26	19 ± 3	18 ± 2	1.37 ± 0.16
	Primary effluent	21 ± 4	11 ± 3	1.40 ± 0.32	18 ± 4	11 ± 2	1.60 ± 0.23
	Secondary effluent				26 ± 4	22 ± 3	1.38 ± 0.18
	Final effluent	39 ± 5	47 ± 4	1.28 ± 0.12	27 ± 4	28 ± 2	1.49 ± 0.12

[1] Total uncertainty $k=2$.

Correlation analysis

A correlation analysis between radioactivity in liquid samples and the performance characteristics of the WWTPs was performed and the results are presented in Table 5.8. All statistical analyses were carried out using SPSS-V17 software.

Table 5.8. Correlation studies between radioactivity in wastewater liquid samples and the performance characteristics of the WWTPs.

Correlated parameters	Level of significance	Pearson's coefficient
Gross beta activity IN/OUT (21)	99	0.811
Potassium content IN/OUT (21)	99	0.734
Dry residue IN/OUT (21)	99	0.946
Gross beta activity IN/Potassium IN (21)	99	0.779
Gross beta activity OUT/Potassium OUT (22)	99	0.893
Gross alpha activity/Total Uranium (15)	99	0.992
Gross alpha activity/COD OUT (22)	95	-0.428
Total Uranium/COD (10)	95	-0.680
Gross Alpha ratio parameter/Inflow (22)	99	-0.561
Gross Alpha ratio /HRT (22)	99	0.592

The number of correlated data is indicated within parenthesis.
IN=Influent; OUT= Final effluent
COD=Chemical Oxygen Demand

The parameters gross beta, potassium content and dry residue in influent and effluent samples were all positively correlated with correlation coefficients higher than 0.7. This agrees with the treatment not having any influence on these variables.

Gross beta results both in influent and effluent samples were positively correlated with the potassium content of the same samples. This confirms the fact that gross beta activity was mainly produced by ^{40}K in the sample and it explains why no 'rest beta' was measured in any of the samples.

Both Gross alpha and total uranium were negatively correlated with the Chemical Oxygen Demand (COD). If COD tells us the quantity of oxygen needed to oxidize some compounds and uranium is present in the highest oxidation state (U^{+6} as uranyl ion UO_2^{+2}), a negative correlation should be expected because no further oxidation state is possible.

Gross alpha activity is positively correlated with the total uranium content of the samples (Pearson coefficient 0.99) which agrees with the fact that no differences between these parameters were found in the previous section.
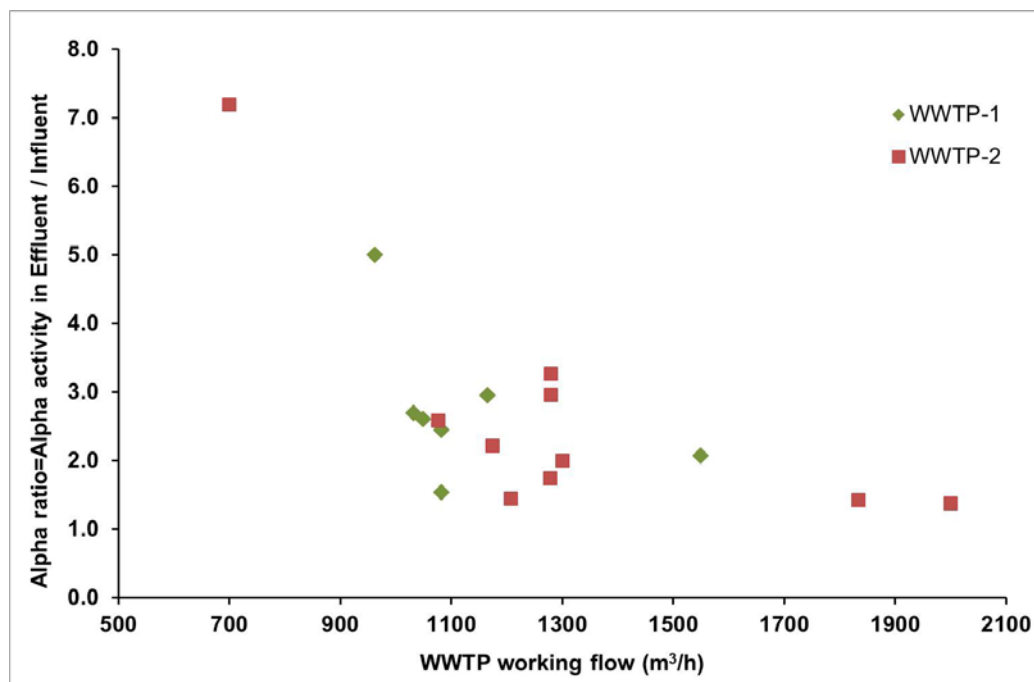
Figure 5.6. Variation of the gross alpha ratio parameter in liquids from WWTPs with the inflow.

We found a negative correlation between the gross alpha activity 'Ratio parameter' and the inflow and a positive correlation with the hydraulic retention time in the WWTP. The working characteristics of the WWTPs during the sampling campaigns therefore greatly influenced the gross alpha behavior. Figure. 5.6 shows the gross alpha 'Ratio parameter' in liquid samples and the inflow at both WWTPs. The maximum gross alpha ratio (7.2) was produced for the minimum inflow (700 m3/h) and the minimum gross alpha ratio (1.4) for the maximum inflow (2000 m3/h), both values measured in samples from WWTP-2. Most of the inflow values are between 1000 and 1300 m3/h and show gross alpha ratio values in the range 1.6-3.3. These results show the importance of considering the hydraulic retention time of the liquids in theWWTP when sampling. In previous studies no information about this factor has been included.

5.3.4 Results and discussion related to activity in sludge samples

Statistical parameters

Gross alpha activity in the sludge ranged from 32 to 203 Bq/kg and gross beta activity from 149 to 625 Bq/kg. The lowest average gross alpha activity was found in WWTP-3, which also showed the lowest gross alpha activity in the liquid samples (<0.015 Bq/L, (Montaña et al., 2011)). However, similar gross beta activities were measured in the three WWTPs. These values were in the range of activities measured in the national survey carried out in the USA (Bastian et al., 2005).

Naturally gamma emitters from the natural ^{238}U series (such as ^{234}Th, ^{214}Pb, ^{214}Bi, ^{210}Pb), the ^{232}Th series (such as ^{228}Ac, ^{212}Pb, ^{212}Bi and ^{208}Tl), other natural gamma emitters such as ^{7}Be, ^{210}Pbu or ^{40}K and anthropogenic gamma emitters such as ^{137}Cs and ^{131}I were detected in the sludge samples.

Some statistical parameters for the natural and artificial isotopes detected in the sludge samples analyzed for the period under study (July 2007–March 2009) are given in Table 5.9.

It should be mentioned that Table 5.9 shows two values for ^{210}Pb (^{210}Pb$_d$ and ^{210}Pb$_u$) where ^{210}Pb$_d$ is the total ^{210}Pb activity measured for each sample and ^{210}Pb$_u$ is unsupported ^{210}Pb which refers to an excess of this radionuclide in the ^{226}Ra content of the samples. The unsupported ^{210}Pb (^{210}Pb$_u$) gives an estimate of ^{210}Pb arising from ''rain-out'' or wet deposition of atmospheric radionuclides onto the surface of the sludge. ^{210}Pbu was determined by establishing the ^{226}Ra content of the sample and subtracting this value from the ^{210}Pbd content. Note that if it's assumed that secular equilibrium was established the ^{210}Pb from the ^{238}U series is equal to the ^{226}Ra activity. ^{226}Ra and ^{232}Th activities were established indirectly by their decay products. In the case of ^{226}Ra, its daughter ^{214}Pb was used because ^{222}Rn and its progeny (^{214}Pb, ^{214}Bi) were in secular equilibrium with ^{226}Ra after 20 days of sealing. Furthermore, we found that ^{214}Pb and ^{214}Bi were present with similar values which agreed with the secular equilibrium that existed between them. For ^{232}Th activities we used ^{228}Ac as a daughter of ^{228}Ra and ^{212}Pb as a daughter of ^{224}Ra. We also checked that ^{224}Ra daughters (^{212}Pb, ^{212}Bi and ^{208}Tl) reached equilibrium because ^{212}Pb and ^{208}Tl activities were within theoretical values (^{208}Tl activities were about 0.36 ^{212}Pb activities due to the branching in ^{212}Bi).

In all the samples the main contribution from natural gamma radionuclides was produced by ^{7}Be (average activity 167 Bq/kg) and ^{40}K (average activity 172 Bq/kg) activities. It should be pointed out that a high RSD was obtained for ^{7}Be and ^{210}Pb$_u$ (higher than 75 %). These are the radionuclides that are normally associated with airborne surface particles. This particulate matter is subject to wet and dry deposition to the terrestrial surface and it is greatly influenced

by rainfall events (Caillet, et al., 2001; Ioannidou and Papastefanou, 2006; Gónzalez-Gómez et al., 2006).

On the other hand, the high RSD calculated for ^{40}K in WWTP-2 should be discussed. This RSD was due to the high activities measured in samples taken in autumn 2007(A 07). We measured two samples taken at the beginning and end of November and we found the same values. During this month there were point source discharges of detergents which could explain these anomalous values.

The ^{238}U series (mean value of 31 Bq/kg dry using ^{234}Th and ^{226}Ra activities) and the ^{232}Th series (mean value of 14 Bq/kg dry using ^{228}Ra and ^{224}Ra activities) were present as low activities because their values were always lower than 10 times the MDA for each radionuclide (values of MDA are listed in the Appendix B). Furthermore, low activities usually presented high uncertainties in their values.

Table 5.9. Statistical parameters for the gamma emitting radionuclides detected in sludge from the WWTPs analyzed.

Radionuclide	WWTP-1				WWTP-2				WWTP-3			
	Minimum	Maximum	Average	RSD%	Minimum	Maximum	Average	RSD%	Minimum	Maximum	Average	RSD%
Gross alpha	58	163	**98** (8)	36.8	67	203	**116** (8)	42.5	32	45	**38** (6)	11.2
Gross beta	149	398	**281** (8)	31.4	256	625	**391** (8)	36.5	234	415	**327** (6)	21.6
U-238 series												
Th-234	27	51	**37** (7)	25.2	37	86	**64** (8)	29.6	41	58	**48** (7)	13.0
Pb-214	5.6	28.0	**14.4** (7)	50.0	4.0	25.0	**12.3** (8)	65.6	7.0	16.3	**11.1** (7)	30.5
Bi-214	4.9	23.9	**12.8** (7)	47.0	3.4	24.5	**11.4** (8)	71.1	5.5	14.8	**10.0** (7)	32.7
Pb-210$_d$	18	124	**66** (7)	59.4	34	141	**59** (8)	58.3	42	103	**55** (7)	30.0
Th-232 series												
Ac-228	9.2	22.1	**15.5** (7)	31.8	15.9	33.1	**23.2** (8)	24.5	12.9	21.6	**18.1** (7)	15.4
Pb-212	3.1	11.7	**7.3** (7)	43.8	4.4	12.9	**8.1** (8)	34.9	8.2	18.4	**13.7** (7)	27.5
Bi-212	6.8	15.8	**10.2** (5)	42.0	5.3	14.1	**9.2** (4)	45.0	7.5	22.9	**17.7** (7)	36.7
Tl-208	1.3	3.6	**2.3** (7)	38.1	1.2	3.9	**2.4** (8)	34.4	2.9	5.4	**4.2** (7)	25.0
Be-7	45	500	**185** (7)	90.6	55	316	**141** (8)	75.5	44	465	**174** (7)	79.0
Pb-210$_u$	4.4	107	**51.2** (7)	75.4	9.5	133.2	**47.3** (8)	82.4	32.1	94.2	**54.0** (7)	36.5
K-40	89	157	**122** (7)	23.1	105	497	**214** (8)	74.3	109	213	**179** (7)	22.5
Cs-137	0.5	0.7	**0.6** (2)	23.6	n.d.				0.4	0.9	**0.7** (6)	28.0
I-131	58	883	**290** (4)	136.8	n.d.				64	98	**81** (2)	30.0

Data correspond to activity expressed in Bq/kg dry weight.

The number of data used in calculation is indicated in brackets.

n.d.: no detected.

RSD%=Relative standard deviation in percentage=Standard deviation*100/Average value.

Temporal behavior of gamma emitting radionuclides

Figure 5.7 shows the temporal evolution for the ^{238}U series activities (mean activity using ^{234}Th and ^{226}Ra values) in the 3 WWTPs. Arithmetic mean of both activity concentrations of ^{238}U series in Spanish soils (Quindós et al., 1994) and sludge from several wastewater treatment plants studied by Bastian et al. (2005) are also plotted in this figure. Figure 5.8 shows the temporal evolution for the ^{232}Th series activities (mean activity using ^{228}Ra and ^{224}Ra values) in the three WWTPs and the arithmetic mean of both activity concentrations of ^{232}Th from the literature mentioned above in Figure 5.7. In studied sludge ^{238}U activities are similar or below the arithmetic mean found in Spanish soils but ^{232}Th content are much lower than the values found in Spanish soils so no increase in natural radiation are produced by the uses of these materials. We can see that no seasonal tendency could be observed in the studied period because of the high uncertainties associated with the results. Nevertheless, WWTP-2 shows higher ^{40}K and ^{232}Th series activities in samples taken in summer (SU) and autumn (A) of 2007. These results could be in accordance with the high values of surfactants in detergents found in both campaigns (SU and A of 2007) as above mentioned.

Application of the t test for independent samples to the ^{238}U series and ^{232}Th series activities in the different WWTPs showed that no differences were found between the ^{238}U activities in the sludge from the 3 selected WWTPs. However, some differences between the ^{232}Th activities in the sludge from WWTP-3 and the values in sludge from WWTP-1 and WWTP-2 were detected. Nevertheless, compared with the results obtained from other sites and countries, the values were similar to other published activities (Bastian et al., 2005; Palomo et al., 2010b; Jiménez et al., 2011).

In the case of man-made radionuclides small amounts of ^{137}Cs were measured (less than 1 Bq/kg), while important amounts of ^{131}I (between 58 and 883 Bq/kg) were detected in some samples (6/22, 66.7 %, in sludge fromWWTP-1).There are many studies on the presence of ^{131}I in sludge in WWTPs when sewerage from health centers is treated (Martin and Fenner, 1997; Puhakainen, 1998; Jiménez et al., 2011) and our results are similar to the values obtained in these studies.
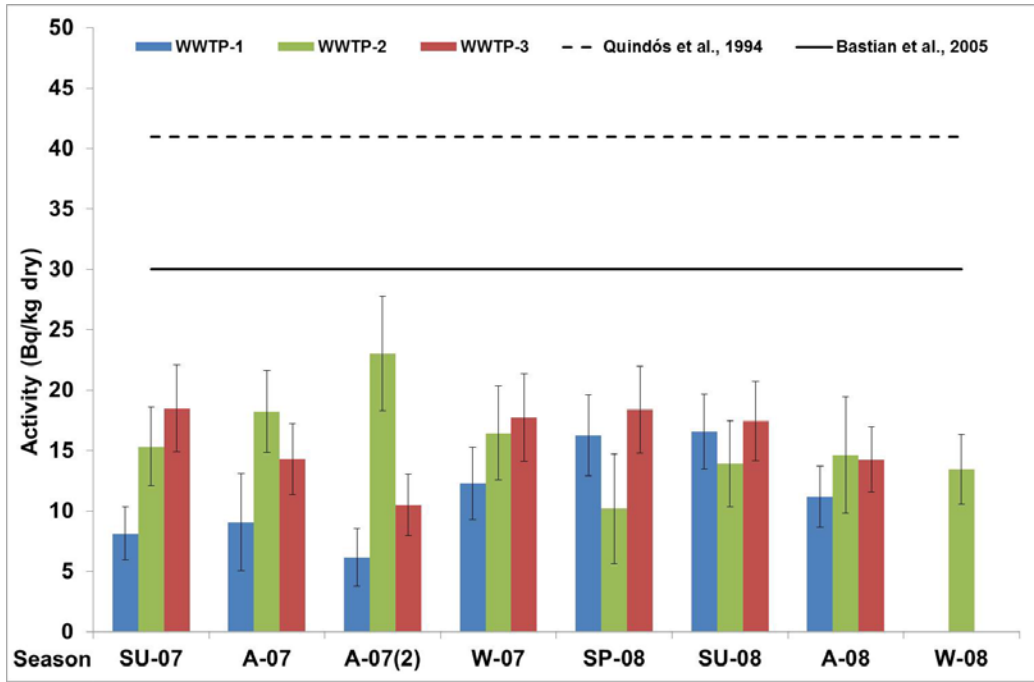
Figure. 5.7. Temporal evolution of ^{238}U series in sludge from the WWTPs. Arithmetic mean of both activity concentrations of ^{238}U series in Spanish soils (Quindós et al., 2005) and sludge from several WWTPs studied by Bastian et al. (2005).
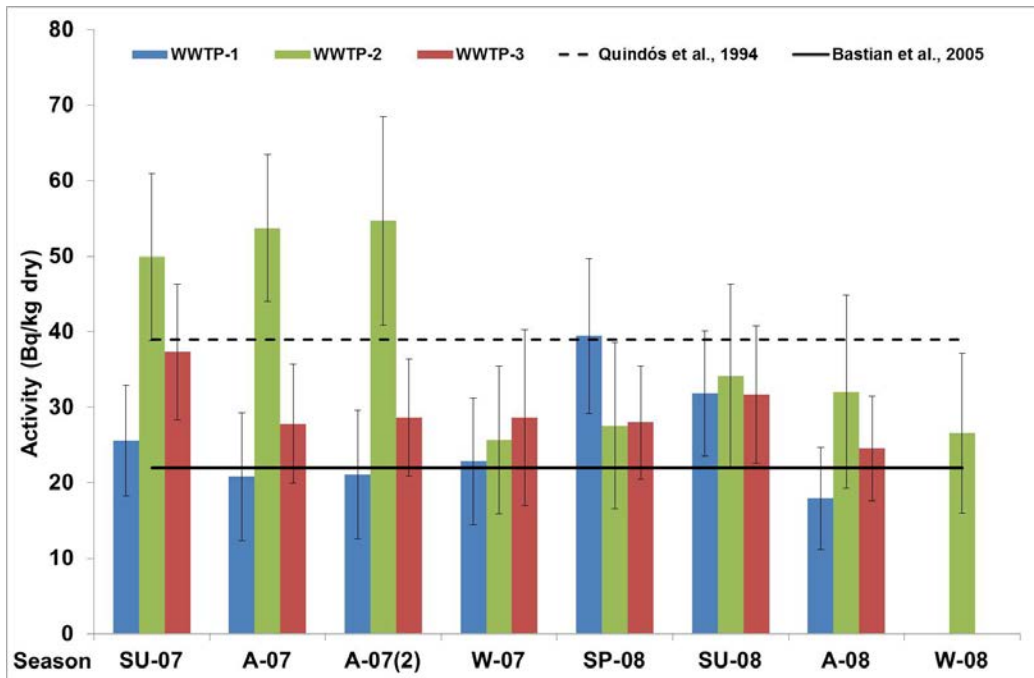
Figure. 5.8. Temporal evolution of ^{232}Th series in sludge from the WWTPs. Arithmetic mean of both activity concentrations of ^{232}Th series in Spanish soils (Quindós et al., 2005) and sludge from several WWTPs studied by Bastian et al. (2005).

Correlation analysis

A correlation analysis between radioactivity levels in sludge was performed and the results are presented in Table 5.10. All statistical analyses were carried out using SPSS-V17 software. Positive relationship ($r > 0$) was obtained for all the correlated parameters.

Table 5.10. Correlation studies between radioactivity in sludge from WWTPs.

Correlated parameters	Level of significance	Pearson's coefficient
Gross Alpha/Gross Beta activities (22)	99	0.612
Gross Alpha/^{238}U activities (21)	99	0.584
Gross Beta/^{40}K activities (21)	99	0.881
Gross Beta/^{238}U activities (21)	99	0.720
Gross Beta /^{232}Th activities (21)	95	0.498
^{40}K/^{238}U activities (22)	99	0.798
^{40}K/^{232}Th activities (22)	95	0.457
^{234}Th/^{228}Ac activities (22)	99	0.790
^{214}Bi/^{228}Ac activities (22)	95	0.514
^{234}Th/^{214}Bi activities (22)	95	0.514
^{214}Bi/^{214}Pb activities (22)	99	0.989
^{212}Pb/^{212}Bi activities (16)	99	0.858
^{212}Pb/^{208}Tl activities (22)	99	0.974
^{7}Be/^{210}Pb$_u$ activities (22)	99	0.824
^{7}Be/rainfall (22)	95	0.490
^{210}Pb$_u$/rainfall (22)	99	0.540
pH sludge/^{232}Th activities (21)	99	0.669
pH sludge/^{40}K activities (21)	95	0.519
pH sludge/^{238}U activities (21)	95	0.471

The number of correlated data is in brackets.

Gross alpha activities were moderately ($0.5<r<0.7$) correlated with ^{238}U activities and gross beta activities were highly ($0.7<r<0.9$) correlated with ^{40}K and ^{238}U and moderately correlated with ^{232}Th.

As occurred in soils, we found a correlation between the activities of ^{40}K and ^{238}U and ^{232}Th (Quindós et al., 2005; Khan et al., 2011). Furthermore, radionuclides belonging to the ^{238}U and ^{232}Th series were also positively correlated. For example, ^{234}Th was positively correlated with ^{228}Ac and ^{228}Ac was positively correlated with ^{214}Bi. Similar correlations were found in a study

carried out in Valladolid (Spain) (Jiménez et al., 2011) or in soil samples (Khan et al., 2011) and they were explained by the fact that the ^{238}U and ^{232}Th series commonly appear together in nature.

The members of the same series were also positively correlated as in the cases of ^{214}Bi with ^{214}Pb or ^{212}Pb with ^{212}Bi and ^{208}Tl. The Pearson's correlation coefficients were higher than 0.85 and close to 1 as should occur if there is equilibrium between them.

On the other hand, natural radionuclides associated with surface airborne particles such as ^{7}Be and ^{210}Pb$_u$ were also correlated. Nevertheless, they did not correlate with other radionuclides detected because these isotopes have an atmospheric origin. The similar temporal variation found for ^{7}Be and ^{210}Pb$_u$ is shown in Figure. 5.9, which presented, as example, the temporal variation of these radionuclides in WWTP-1. We found correlation between ^{7}Be and ^{210}Pb$_u$ activities and rainfall during the month because the main factor controlling the removal of these radionuclides was wet deposition (Caillet, et al., 2001; Ioannidou and Papastefanou, 2006; Gónzalez-Gómez et al., 2006). Consequently, we could suggest that the presence of these radionuclides in sludge could be used to evaluate their removal from atmosphere (Erlandsson et al., 1989).
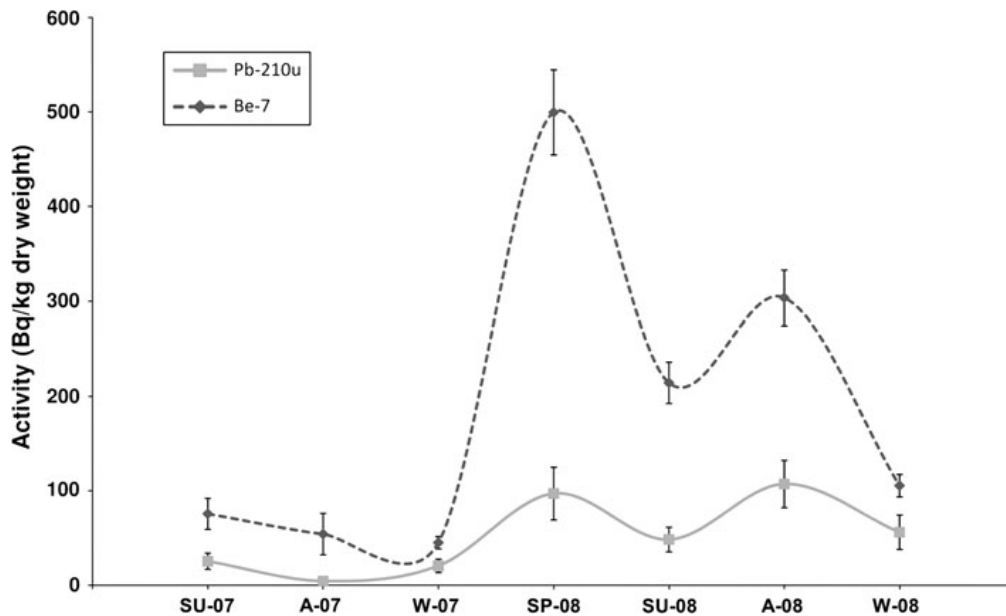
Figure. 5.9. Seasonal variation of ^{7}Be and ^{210}Pb$_u$ in sludge from WWTP-1.

As regards chemical characteristics, we found that ^{40}K, ^{238}U and ^{232}Th were all positively correlated with sludge pH, which suggested that high pH stimulated the accumulation of these radionuclides. Similar conclusion was obtained in drinking water treatment plants where the influence of the pH of the coagulation was study in order to know the removal of uranium and radium (Baeza et al., 2006) from liquids samples.

No significant correlations were found between manmade radionuclides ^{131}I and ^{137}Cs and other natural radionuclides and they were not correlated with each other due to the different sources of these radionuclides.

5.4   Preliminary study of radioactivity levels at Waukesha WWTP (WI, USA)

Water samples and one sludge sample were collected from a municipal conventional full scale WWTP located in Midwest of the United States (Waukesha-Wisconsin) during the period 5/16/12 to 5/23/12 in order to carry out a preliminary study of the radioactivity levels and their behavior in the WWTP.

The State of Wisconsin is known to have many public waterworks using groundwater in which they are in violation of the current radiological standards mainly due to Radium isotopes. Therefore, it was considering interesting to study the radionuclide's behavior in a WWTP which receives groundwater containing radium isotopes.

5.4.1 Plant characteristics and sampling collection

The current liquid treatment facilities include raw wastewater screening and grit removal, influent pumping, primary clarification, primary effluent pumping, activated sludge treatment, secondary clarification, chemical phosphorus removal with coagulation, dual media filtration, and UV disinfection. Biosolids treatment includes waste activated sludge (WAS) thickening by dissolved air flotation, anaerobic digestion of primary solids and WAS, liquid sludge storage, belt filter press dewatering, and cake storage. Biogas generated during anaerobic digestion is utilized to fire steam boilers that provide heat to the digestion process and several buildings.

The facilities were designed for a daily average flow of 53000 m^3/day. Figure 5.10 shows a process flow diagram and the points where the liquid samples were taken are also indicated by a star.

Five sampling collection days were carried out over the period 5/16/12 to 5/23/12. 25 samples including influent (raw water), primary effluent, secondary effluent, phosphorus removal effluent and final effluent were sampled. A sewage sludge that corresponds to a mix of primary, secondary and Phosphorus removal sludges was also sampled.

The liquid samples were collected in sterile polyethylene containers with a capacity of 5 L. After collection, the samples were immediately transported to the WSLH where they were acidified with nitric acid 1/1000 to pH < 2 and filtered through 0.45 μm pore cellulose nitrate filters. The dehydrated sludge sample was collected in a clean plastic bag container (200 mg).

For the liquid samples, gross alpha activity by co-precipitation method (Appendix A) and gross beta activity by evaporation method were tested. Uranium and radium isotopes were assayed using radiochemical separation and alpha spectrometry. Radium isotopes were also determined by gamma spectrometry. Potassium content was also assayed (see Appendix B for methods and instrumentation).

The sludge sample collected was analyzed to determine gross alpha, gross beta and gamma activities.
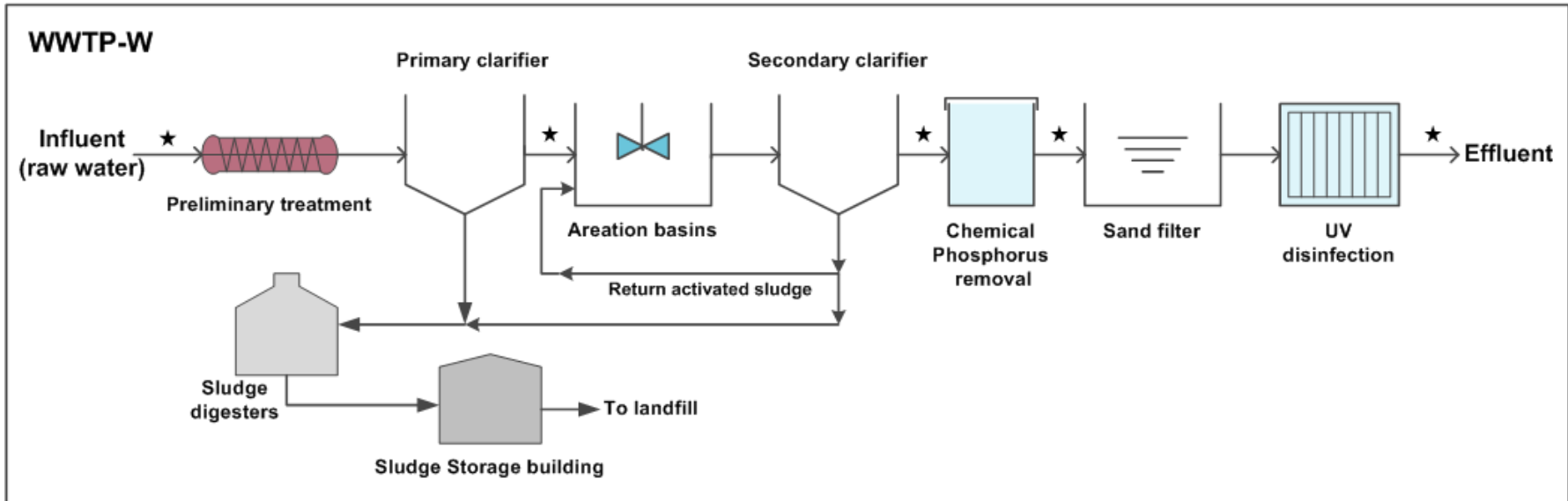
Figure 5.10. Schematic diagram of the Waukesha WWTP. The points where the liwuid samples were taken from the WWTP are indicated by star.

5.4.2 Results and discussion

Gross Alpha and Beta activities in liquid samples

Figs. 5.11 and 5.12 show gross alpha and beta activities respectively measured in liquid samples for the different sampling days at different sampling points within the treatment.

In the influent wastewater gross alpha activity ranged between 0.3 and 0.7 Bq/L. After the treatment, gross alpha activity ranged between 0.05 and 0.10 Bq/L. Consequently, a significant reduction of the gross alpha activity was achieved during the treatment process. This reduction basically occurred after the primary and secondary treatments.
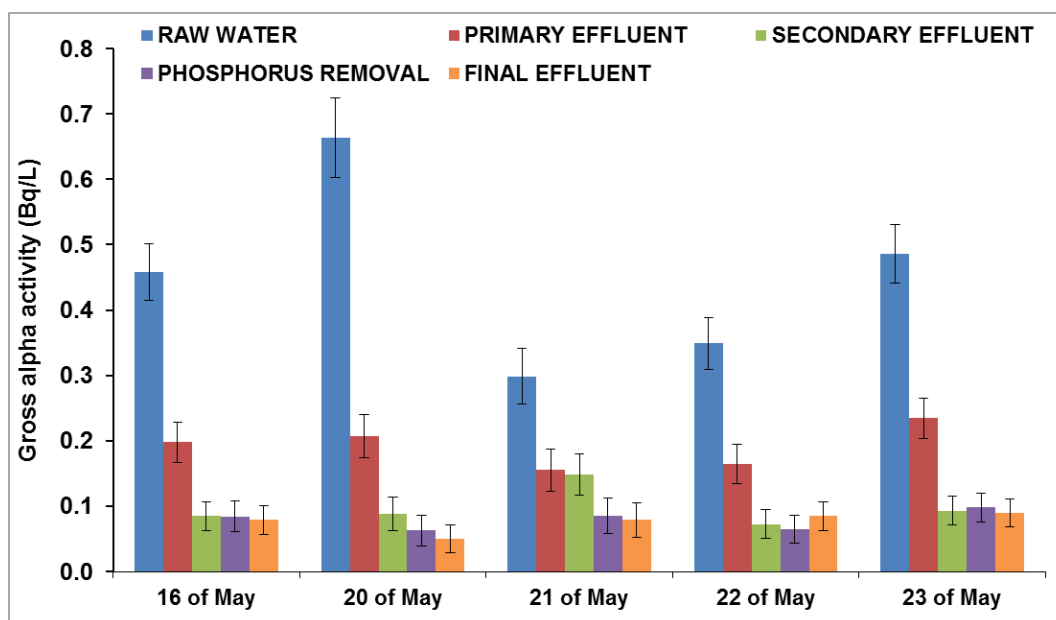
Figure 5.11. Gross alpha activity in liquid samples from Waukesha WWTP. Error bars are the overall uncertainty (*k=2*).

It should be noted that, despite the short period of time studied (one week), a significant variation was obtained in gross alpha activity in liquid samples with relative standard deviation (RSD) of 28% (influent samples) and 21% (effluent samples). One reason for the variation in gross alpha may be the source water. This wastewater treatment plant receives the backwash water periodically from the drinking water treatment plant located in the same city, increasing the Radium contribution. This information was not available and therefore we couldn't allocate

this variation due to this contribution. On the other hand, the sample collection protocols were not done taking into account the retention time and, therefore effluent water sample (after treatment) was not fully representative of the influent water sample (raw water) as well as the intermediate effluents sampled.
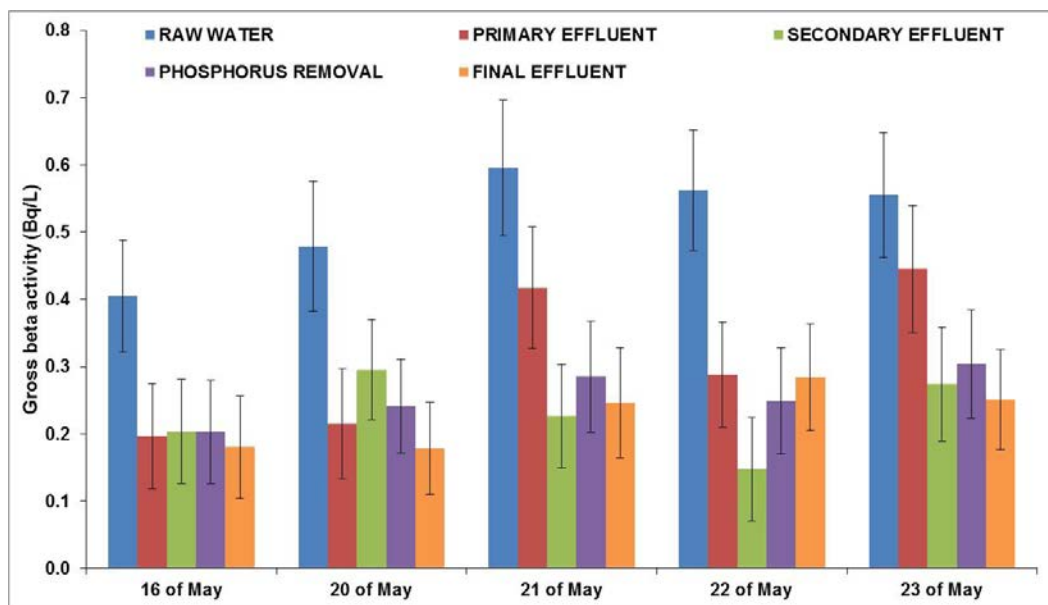
Figure 5.12. Gross beta activity in liquid samples from Waukesha WWTP. Error bars are the overall uncertainty (*k=2*).

Gross beta (including ^{40}K) in raw water ranged between 0.4 and 0.6 Bq/L. The potassium content was determined in order to know its contribution in the gross beta activity and the activity mean value of ^{40}K was 0.34 ± 0.04 (RSD=11%). The results indicate that, after the primary treatment, gross beta activity was mainly due to ^{40}K. Nevertheless, raw water contained other beta emitters different to ^{40}K which were removed during the primary treatment. Probably this gross beta excluding ^{40}K contribution could be due to the presence of ^{228}Ra and its beta progeny (^{228}Ac, ^{212}Pb and ^{212}Bi).

Characterization of alpha activity contributors

To identify which radionuclide produced the gross alpha activity, uranium (^{238}U, ^{234}U and ^{235}U) and Radium (^{224}Ra, ^{226}Ra and ^{228}Ra) isotopes were analyzed in all liquid samples. Table 5.12 shows total uranium, ^{226}Ra and ^{228}Ra activities.

From Table 5.12 it can be seen that the contribution of alpha emitters differs significantly according to sampling collection day. It was observed that ^{226}Ra content remains constant during the different sampling collection days, while uranium content varied in each sampling collection day being the main contributor in two of five days (22th and 23th of May).

Samples that contained ^{228}Ra also contained a comparable activity of ^{224}Ra at the collection time (^{224}Ra supported), but if the sample contains ^{224}Ra unsupported, ^{228}Ra content will not be the same as the ^{224}Ra content. According to results previously reported in the literature related to the radioactivity in water samples from Wisconsin (Arndt and West 2004), it was found that, in general, ^{224}Ra activity exceeds the ^{228}Ra activity. Consequently, it was of interest determining the amount of ^{224}Ra in order to know its contribution. The ^{224}Ra content was intended to be determined directly by gamma spectrometry through its progeny ^{212}Pb and ^{212}Bi using one liter of water sample. However, the results obtained were below MDA and consequently ^{224}Ra content was not determined. ^{226}Ra and ^{228}Ra were also determined by gamma spectroscopy giving non satisfactory results (values below MDA).

Table 5.12. Total uranium, [226]Ra and [228]Ra activities (mBq/L) at different steps into the Waukesha WWTP. Overall uncertainty at the 95 percent confidence level ($k=2$).

	Sampling collection date	RAW WATER	PRIMARY EFFLUENT	SECONDARY EFFLUENT	PHOSPHORUS REMOVAL	FINAL EFFLUENT
Total uranium [1]	16th of May 2012	31 ± 20	9 ± 3	9 ± 4	<30	34 ± 8
	20th of May 2012	<16	<20	34 ± 9	30 ± 11	<22
	21th of May 2012	18 ± 10	15 ± 8	8 ± 5	<27	45 ± 16
	22th of May 2012	265 ± 31	226 ± 30	30 ± 11	105 ± 18	<28
	23th of May 2012	216 ± 28	34 ± 12	8 ± 5	36 ± 17	<27
[226]Ra [1]	16th of May 2012	108 ± 20	<24	15 ± 10	18 ± 10	13 ± 9
	20th of May 2012	67 ± 10	24 ± 7	28 ± 7	13 ± 4	11 ± 6
	21th of May 2012	65 ± 10	39 ± 9	15 ± 7	<13	10 ± 6
	22th of May 2012	47 ± 10	40 ± 10	40 ± 10	13 ± 8	12 ± 5
	23th of May 2012	61 ± 13	27 ± 9	22 ± 11	<14	17 ± 11
[228]Ra [1]	16th of May 2012	119 ± 30	57 ± 23	46 ± 21	38 ± 24	78 ± 27
	20th of May 2012	<48	<45	<42	<56	<46
	21th of May 2012	106 ± 31	98 ± 30	<44	69 ± 29	77 ± 31
	22th of May 2012	<40	<36	<34	<30	<33
	23th of May 2012	<38	<36	<35	<42	<38

[1] Total uncertainty, $k=2$.

In order to know if there was a ^{224}Ra unsupported contribution, raw water samples were measured over time between 0 days and about 10 days after sample preparation.

Figure 5.13 shows gross alpha activity in raw water measured within 0 and 20 days after sample collection. The elapsed time presented in the plot corresponds to an average elapsed time between collection and measurement of each raw water sample, being the range of days when 1st, 2nd and 3rd measurements were performed [3-4], [6-12] and [13-20] respectively.
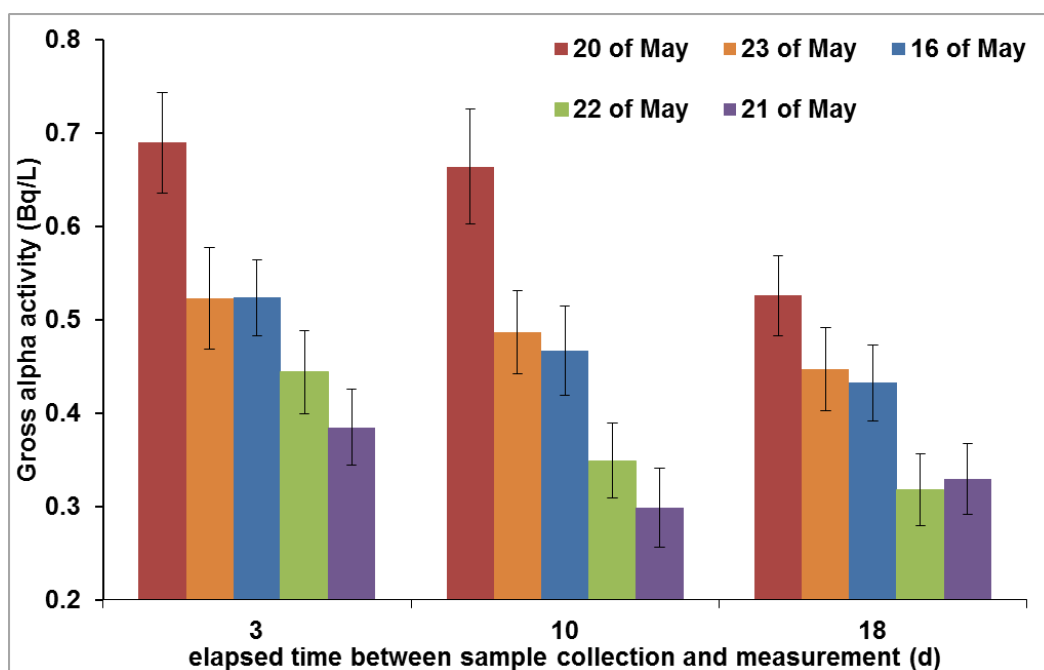
Figure 5.13. Temporal evolution of the gross alpha activity in the raw water from Waukesha WWTP. Error bars are the overall uncertainty (*k=2*).

As we can see, gross alpha activity decreased over time for some of raw water samples. This is probably due the presence of ^{224}Ra unsupported in the sample (half life 3.6 days). Based on this temporal evolution, the disintegration time was determined. The value obtained (8 days) did not agree with the ^{224}Ra disintegration time, probably due to the ^{226}Ra presence which its progeny provide an increase to the gross alpha activity over time.

For one of the sampling collection days (16th of May), two preparations were made in order to see if gross alpha activity decreased over time indicating a ^{224}Ra contribution. The differences between both replicates were the elapsed time between sample collection time and their

preparation. Figure 5.14 shows the gross alpha activity temporal evolution of these two replicates.
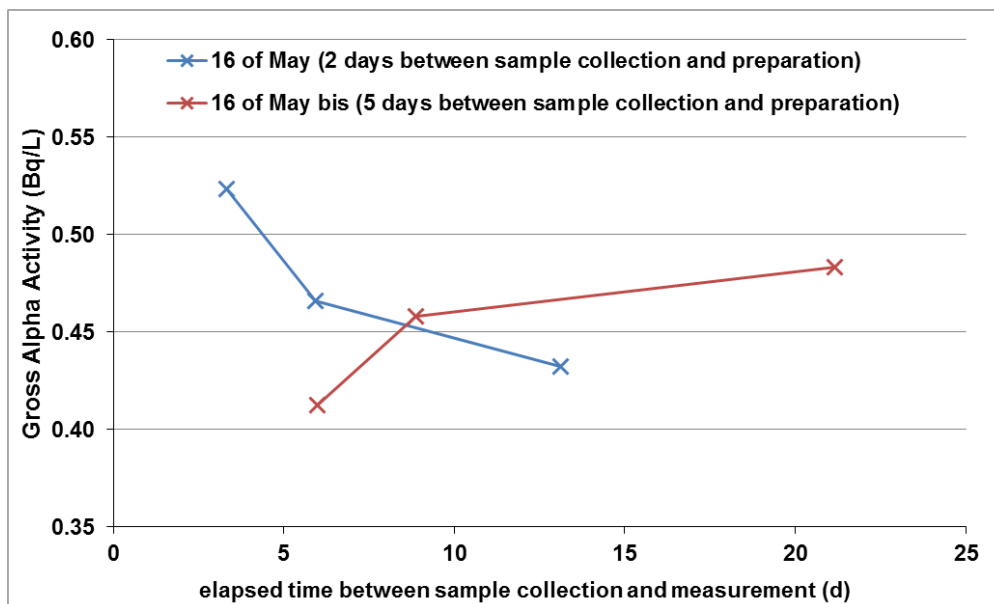
Figure 5.14. Gross alpha activity in the raw water from WWTP in two different sampling points.

As we can see, the gross alpha activity decreased over time if the elapsed time between sample collection and measurement was less than three days as it is observed in the previous Figure 5.13. When sample is prepared after more than five days, ^{224}Ra decayed (would remain 38% of the initial activity) and, in this case, the GAA increased due to the presence ^{226}Ra in this sample.

Removal rate calculation

In this study we employed the removal rate in order to determine alpha and beta activity removal during wastewater treatment. Removal rates (RE) were calculated by comparing the load of each parameter (gross alpha and beta activities) in influent and effluent waste using the equation 5.1 (section 5.3.2).

Positive removals in liquids for gross alpha and beta activity indicated in Figs. 5.15 and 5.16, respectively, varied from rather low (for gross beta activity) to high rate values (for gross alpha

activity). For gross alpha activity, the removal rate varied from 74 to 92% and for gross beta activity, the removal rate varied from 50 to 63%.

Removal rates confirm that the treatment applied in the WWTP scan efficiently remove a high percentage of alpha and beta emitters, specially the radium isotopes (^{226}Ra and ^{224}Ra: alpha emitters and ^{228}Ra: beta emitter) from wastewater.
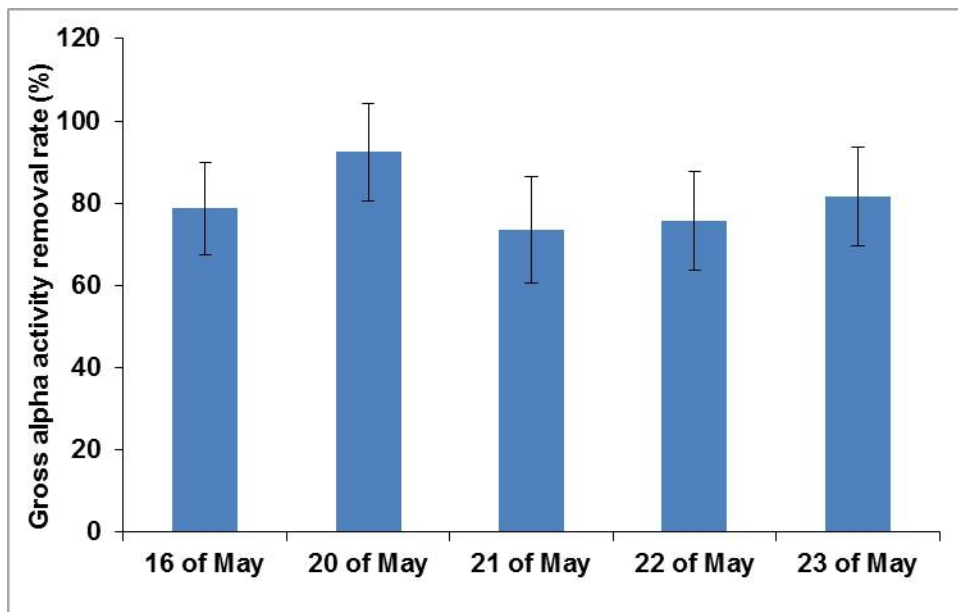
Figure 5.15. Gross alpha activity removal rate. Overall uncertainty at the 95 percent confidence level (*k=2*).
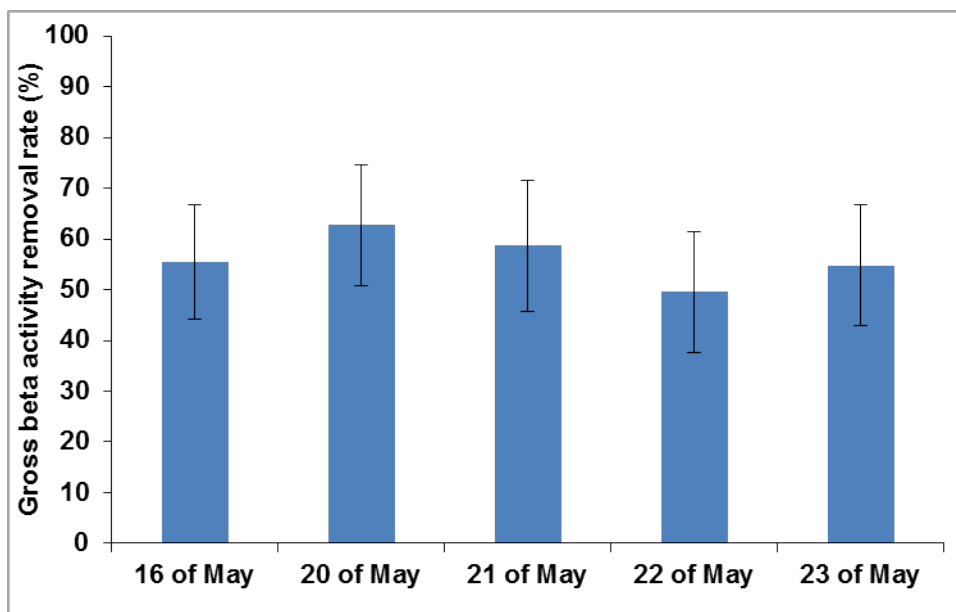
Figure 5.16. Gross beta activity removal rate. Overall uncertainty at the 95 percent confidence level (*k=2*).

Activity in the sludge sample

Gross alpha and beta radioactivity and the activity of gamma emitting radionuclides in the sludge from Waukesha WWTP are given in Table 5.13. Gross alpha and beta concentrations in the sludge were 363 ± 39 and 251 ± 13 Bq/kg respectively. These values were in the range of activities measured in the national survey carried out in the U.S. (Bastian, et al., 2005) as well as similar than those obtained in the Spanish WWTPs.

Related to gamma emitting radionuclides, naturally gamma emitters from the natural ^{238}U series (such as ^{214}Pb, ^{214}Bi), the ^{232}Th series (such as ^{228}Ac, ^{212}Pb, ^{212}Bi and ^{208}Tl) and ^{40}K were detected. ^{226}Ra and ^{232}Th activities were established indirectly by their decay products. In the case of ^{226}Ra, its daughter ^{214}Pb was used since ^{222}Rn and its progeny (^{214}Pb and ^{214}Bi) were in secular equilibrium with ^{226}Ra after 20 days of sample sealing. Furthermore, we found that ^{214}Pb and ^{214}Bi were present with similar values which agreed with the secular equilibrium that existed among them. For ^{232}Th activities, we used ^{228}Ac as a daughter of ^{228}Ra and ^{212}Pb as a daughter of ^{224}Ra. We also checked that ^{224}Ra daughters reached equilibrium because ^{212}Pb and ^{208}Tl activities were within theoretical values (^{208}Tl activity was about 0.36 ^{212}Pb activity due to the ^{212}Bi branching ratio).

Table 5.13. Gross alpha and beta activities and activity of gamma radionuclides in sludge from Waukesha WWTP.

Radionuclide	Activity ± uncertainty ($k=2$) [1]
Gross alpha	363 ± 39
Gross beta	251 ± 13
^{238}**U series**	
^{234}**Th**	n.a.
^{214}**Pb**	882 ± 49
^{214}**Bi**	814 ± 37
^{210}**Pb**	< 76
^{232}**Th series**	
^{228}**Ac**	1090 ± 129
^{212}**Pb**	151 ± 19
^{212}**Bi**	252 ± 41
^{208}**Tl**	52 ± 4
^{7}**Be**	<59
^{40}**K**	112 ± 26
^{131}**I**	693 ± 254
^{137}**Cs**	< 1.9

[1] Activity expressed in Bq/kg dry weight.
n.a.: data not available.

According to the results presented in section 5.2, the main contribution from natural gamma radionuclides was produced by ^{7}Be or ^{40}K. Rather, in the sludge from Waukesha WWTP the main contribution to natural gamma radioisotopes was made by ^{228}Ac (1090 ± 129 Bq/kg).

^{7}Be was not detected since this radionuclide has an atmospheric origin. In this case the treatment steps were done inside the building.

In the case of man-made radionuclides an important amount of ^{131}I was detected which is used in nuclear medicine (693 Bq/kg). There are many studies on the presence of ^{131}I in sludge from WWTPs when sewerage from health centers is treated (Martin and Fenner, 1997; Puhakainen M., 1998; Jimenéz et al., 2011).

In general, the results obtained are quite similar to those found by Bastian et al. (2005) in the same country and the treatment applied does remove efficiently the Radium from water.

Finally, it is worth mentioning that Radium values obtained in the Waukesha WWTP were higher compared to those found in the Spanish WWTPs. On the other hand, the ^{40}K content was below than those detected in the Spanish ones.

5.5 Summary

5.5.1 Screening study of the presence of radionuclides in wastewater treatment plants in Spain

As main conclusions from the screening study, Gross alpha (3 to 119 mBq/L) and beta (150 to 1422 mBq/L) activities in liquid samples showed huge variations among the considered plants. This may be due to the differences, between the various plants, in both the geological zones.

As regards the results obtained for the determination of gross alpha activity in liquid waste, the co-precipitation method provides a lower MDA and alpha activity is detected. Evaporation determination does not seem to be appropriate for the determination of low levels of alpha activity in wastewater.

Removal rates obtained confirm that conventional treatment applied in some of the 11 WWTPs scan efficiently remove a high percentage of alpha emitters from wastewater. However, no influence in gross beta activity when was produced by the radionuclide ^{40}K was observed.

Alpha, beta and gamma activity is concentrated in sewage sludge during the wastewater treatment, as in the case of solids and metals. WWTPs can be therefore an important treatment barrier for their removal.

The main contribution to the radioactivity in the sludge samples was from natural sources (^{40}K and ^{7}Be), whereas the contribution from artificial radionuclides was lower than 1% with the exception of ^{131}I from medical treatments.

It has to be stated that none of the treated wastewater showed activity levels that exceed the maximum annual intake values for members of the public, according to current regulatory standards.

The results indicate that the radiological characteristics of the effluents and sludge do not present a significant radiological risk and thus make them suitable for future applications. However, more exhaustive studies need to be carried out to evaluate possible effects on workers and also on the population in general when such sludge samples are re-used for different applications such as landfills or building materials.

5.5.2 Temporal evolution of radionuclides in wastewater treatment plants

The major findings that we can draw from the studies related to the temporal evolution in water and sludge samples are summarized as follows.

Gross alpha activity in effluent was below the screening level of 0.1 Bq/L in most of the samples, and none of them presented 'rest beta' activity above the screening level of 1 Bq/L for drinking water.

The treatment applied at these WWTPs did not influence gross beta activity (produced by the ^{40}K activity), but increased gross alpha activity. Gross alpha activity in liquids at the studied WWTPs was associated to uranium isotopes (^{234}U, ^{235}U, ^{238}U). In waters, all the members of the uranium series are not present due to their different solubility. In fact, in the studied liquids ^{226}Ra was not detected, and thus, we can suggest that beta emitters from the U series (^{230}Th or ^{234}Th) are not soluble in the studied conditions. For this reason, gross beta activity did not increase. This increase was produced after secondary treatment, which suggests that uranium isotopes are the radionuclides that are dissolved or desorbed during the secondary treatment.

The inflow or hydraulic retention time of the wastewater in the WWTP greatly influenced gross alpha behavior. These results show the importance of considering the retention time of the liquids in the WWTP.

Particularly with regard to sludge samples, naturally gamma emitters from the natural ^{238}U series (such as ^{234}Th, ^{214}Pb, ^{214}Bi, ^{210}Pb), the ^{232}Th series (such as ^{228}Ac, ^{212}Pb, ^{212}Bi and ^{208}Tl) and other natural gamma emitters such as ^{7}Be, ^{210}Pb$_u$ or ^{40}K were detected. The activities were similar to other published values and the main contribution was produced by the ^{7}Be and the ^{40}K activities (mean values higher than 150 Bq/kg dry weight). Correlations were found between radionuclides with the same origin. For example, the natural ^{238}U and ^{232}Th series were correlated and other radionuclides associated with surface particulate matter such as ^{7}Be and ^{210}Pb$_u$ were also correlated. However, no correlation between radionuclides with different sources was encountered.

The ^{238}U and ^{232}Th series were present as low activities (mean values lower than 40 Bq/kg dry weight) and the high uncertainties associated to these activities didn't allow to finding any seasonal variation in the studied period. ^{7}Be and ^{210}Pb$_u$ behave similarly and their seasonal variation was explained by the monthly rainfall.

5.5.3 Preliminary study of radioactivity levels at Waukesha WWTP (WI, USA)

In this study it was found a significant variation in the gross alpha activity probably due to the source water which could contain backwash water with large amounts of Radium isotopes from the Waukesha DWTP.

Nevertheless, removal rates confirm that the treatment applied in the WWTP scan efficiently remove a high percentage of alpha and beta emitters, specially the Radium isotopes from wastewater.

Related to gamma emitting radionuclides found in the sludge, the main contribution to natural gamma radioisotopes was made by ^{228}Ac. Related to the artificial radionuclides, a significant amount of ^{131}I was detected.

Compared with the other WWTPs studied, Radium values obtained in the Waukesha WWTP were higher compared to those found in the Spanish WWTPs. On the other hand, the ^{40}K content was below than those detected in the Spanish ones.

Chapter 6

Evaluation of radiological hazard effects of sludge samples from water treatment plants

6.1   Introduction and motivation

Radiation in the environment from natural sources is the major source of radiation exposure to man. Radiation exposure results from the naturally-occurring radionuclides in the environment (terrestrial radiation) and direct cosmic (extra-terrestial) radiation (UNSCEAR, 2000). Only radionuclides with half-lives comparable with the age of the earth or they corresponding decay products existing in terrestrial material such as ^{232}Th, ^{238}U and ^{40}K are of great interest. Another minor source is the radioactive decay of ^{235}U isotope, but this is very rate in the earth's crust (only 0.72% compared with 99.3% of ^{238}U of its total uranium content) (Aksoy, et al., 2002). Gamma radiation from these represents the main external source of irradiation to the human body.

Some sources of natural radiation have been enhanced (concentrated) by human technological activities and include wastes from mineral ores and the petroleum industry, sludge and scale from water treatments plants (WTPs). The occurrence of natural radionuclides in water treatment processes poses a problem of health hazard.

Based on what is known about the potential for reconcentration at WTPs, possible sources of radiation exposure would be at sludge processing or handling areas at the WTPs and at off-site locations where the sewage sludge is disposed or used. People most likely to be exposed to elevated levels of radioactive materials would be sewage sludge handling personnel at the WTPs or members of the public near disposal or land application sites (EC, 2000).. Three primary ways for these people to be exposed to radiation associated with WTP operations are inhalation, ingestion, and direct exposure (see Figure 6.1).

The common practice of dispersing sewage sludge onto agricultural land can lead to the accumulation of radionuclides in the soils and eventually their uptake into crops. Sludge containing NORM is also disposed in sanitary landfills, discharged to sewers or incorporated into building materials. Furthermore, measuring terrestrial gamma doses rates is essential since gamma radiation provides information concerning excess life time cancer risk.
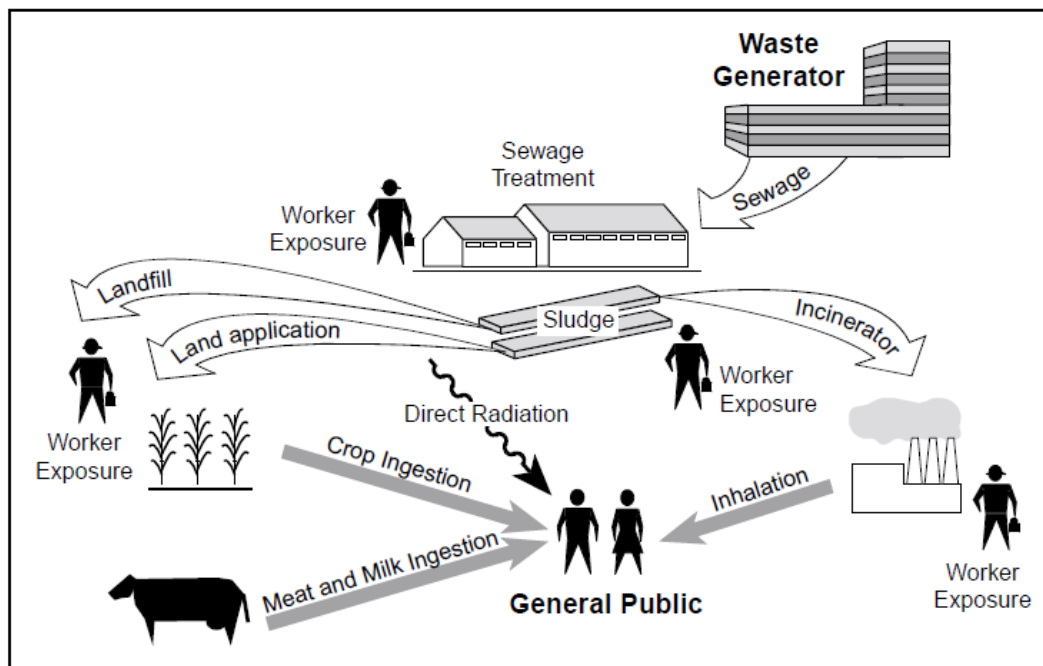

Figure 6.1. Primary pathways for radiation exposure due to sludge from WTPs. Source: Interagency Steering Committee on Radiation Standards (EPA, 2004).

There are no specific regulations that limit the levels of radioactive material in sludge from WTPs but, a number of countries have established concentration levels at which NORM must be controlled as mentioned earlier in the introduction.

For these reasons and, since very little is known about the natural radioactivity of sludge from Spanish WTPs we have considered important to evaluate the radiological impact of these sludge, because depending on the concentration levels found in the sludge, special considerations may need to be given to the re-use or disposal of this waste in order to avoid an additional radiation exposure.

This chapter is organized as follows. In section 6.2, sludge samples from 13 Spanish WTPs and one sludge sample from US were evaluated their possible consideration as NORM. Section 6.3 consist on an evaluation of the environmental outdoor gamma dose rates and an evaluation of radiological hazard effects of the sludge samples previously studied in chapters 4 and 5. In order to conduct these evaluations, the radioactivity sludge values from the different WTPs presented above in chapters 4 and 5 were used. In sludge samples from DWTP-1, DWTP-2, WWTP-1, WWTP-2 and WWTP-3, the radiological hazard effects were evaluated taking into account both maximum and mean activity values obtained from the temporal evolution studies (Sections 4.5 and 5.4.4). Part of this study was published in the Journal of Radioanalitical Nuclear Chemistry (Camacho et al., 2013).

6.2   Evaluation of NORM

Radioactive materials are an ever-present component of the natural environment and are also produced through some human activities. Generally, the presence of radioactive materials is a concern only when concentrations become sufficiently elevated above background levels to potentially pose a health risk (effective dose world average value: 2.4 mSv/y; source: UNSCEAR, 2000).

WTPs can receive naturally occurring radioactive material (NORM) or man-made radionuclides from many sources (Table 6.1). Grounds and surface water, as well as food and plants, can contain elevated levels of NORM. Levels of NORM can be enhanced by human activity and by technologies associated with extraction processes, thus producing technologically enhanced naturally occurring radioactive materials (TENORM). The TENORM can be introduced to the sewerage system from potential industrial discharges (e.g., water treatment plants, mining and petroleum industries, fertilizers, electronics, ceramics and pulp and paper mills). Therefore, disposal or reuse of such materials may be significant with regard to public exposure.

Table 6.1. Sources and potential pathways for radioactive materials to reach water treatment works. [1]

Discharges to Water treatment plants
Drinking water and their residuals that contain naturally occurring radioactive material (NORM)
Sewage with radioactive materials from food and medical procedures
Wastewater from industries handling or processing materials containing NORM
Exempt or unlicensed radioactive materials
Surface waters runoff containing NORM or fallout
Infiltrating groundwater containing NORM, including radon gas
Agents used in composting sewage sludge

[1] Source: Interagency Steering Committee on Radiation Standards (EPA, 2004).

In Europe, the exemption values of NORM are given in Table 6.2 as it reports in the Radiation Protection report nº 122 (RP 122, 2001). These values are the same than values reported by the Spanish Nuclear Safety Council (CSN) in the instruction IS-II (CSN, 2012).

In general it is assumed that inside the NORM residues the radionuclides of the natural decay chains are in secular equilibrium since the activity members of the same series are similar.

The radioactive equilibrium of ^{232}Th and ^{238}U between their daughter products could be disturbed in materials which have undergone chemical treatment. Possible cases of disequilibrium were checked by recounting the suspected samples after a period of one or more years. No changes in measured activity were observed for sludges from DWTPs. Instead, disequilibriums in ^{238}U series were mainly found in sludges from WWTPs.

According to the Radiation Protection report nº 122, the data on activity concentrations of the nuclide with the highest individual activity must be used when the equilibrium between nuclides of one decay chain is disturbed. As clearance levels, the first value presented for each series in Table 6.2 are the values that should be used since not all radionuclides belonging to both series were detected (these values are displayed in bold text). Considering these clearance values, the results obtained will be the most restrictive.

Table 6.2. Rounded General Clearance Levels in Bq/kg.

Nuclide	All materials
^{238}U sec	**500**
^{nat}U	5000
^{230}Th	10000
^{226}Ra+	500
^{210}Pb+	5000
^{210}Po	5000
^{235}U sec	**1000**
^{235}U+	5000
^{231}Pa	5000
^{227}Ac+	1000
^{232}Th sec	**500**
^{232}Th	5000
^{228}Ra+	1000
^{228}Th+	500
^{40}K	50000

(+) radionuclides in secular equilibrium with their short-lived daughters.

In nearly all practical cases more than one radionuclide is involved. For instance, in sludge samples both ^{238}U and ^{232}Th series and ^{40}K are present. To determine if a mixture of radionuclides is below the clearance level a simple summation formula can be used:

$$\sum_{i=1}^{n} \frac{C_i}{C_{Li}} \leq 1.0 \qquad\qquad (6.1)$$

where

C_i is the total activity in the structure per unit mass of radionuclide i (Bq/kg),

C_{Li} is the clearance level of radionuclide i (Bq/kg),

n is the number of radionuclides in the mixture.

In the above expression, the ratio of the highest concentration activity of the radionuclide of each series to the clearance level is summed over all radionuclides in the mixture. If this sum is less than one the sludge complies with the clearance requirements.

The activity concentrations of ^{40}K, the highest activity found in ^{238}U and ^{232}Th series and their weighted sum in the sludge samples from different WTPs are presented in Table 6.3. This table

also presents the maximum and average activity values obtained in sludge samples from WTP studied as temporal evolution in Chapter 4 and 5 (DWTP-1, DWTP-2, WWTP-1, WWTP-2 and WWTP-3).

From the table it could be observed that none of the sludge samples studied located in Spain exceeds the clearance level, and therefore any of the sludge samples cannot be considered as a NORM. The levels of radioactive materials found in sludge samples are low and the associated radiation exposure to workers and general public is very low, and not likely to be of concern. Radioactivity concentrations of sludge produced in these Spanish WTPs are consistent with those reported by Palomo et al. (2010b) located at the same geological area (north east of Spain).

On the other hand, sludge sample from Waukesha exceeds four times the clearance level and therefore this sludge must be controlled being investigated in more detail to evaluate the possible effects on workers in contact with this sludge and also on the general population when this sludge is reused for different applications such as landfill, as a fertilizer or as building materials.

Table 6.3. Concentration of ^{40}K, the maximum value found in ^{238}U and ^{232}Th series and their sumation in the sludge from water treatment plants.

Water treatment plant	^{40}K (Bq/kg)	^{238}U series (Bq/kg)	^{232}Th series (Bq/kg)	Σ
DWTP-1 (ave)[1]	598	45	40	0.3
(max)[2]	728	88	44	0.4
DWTP-2 (ave)[1]	539	87	47	0.4
(max)[2]	773	129	65	0.5
WWTP-1 (ave)[1]	122	66	15	0.2
(max)[2]	157	124	22	0.3
WWTP-2 (ave)[1]	214	64	23	0.2
(max)[2]	497	141	33	0.4
WWTP-3 (ave)[1]	179	55	18	0.2
(max)[2]	213	103	23	0.3
WWTP-4	478	387	73	1.0
WWTP-5	221	156	43	0.4
WWTP-6	325	80	45	0.3
WWTP-7	308	111	39	0.4
WWTP-8	347	225	77	0.7
WWTP-9	369	73	30	0.3
WWTP-10	313	119	28	0.3
WWTP-11	151	88	21	0.2
Waukesha	112	882	1090	4.0

[1]Ave = average values obtained in the temporal evolution study made in DWTP-1, DWTP-2, WWTP-1, WWTP-2 and WWTP-3

[2]Max = maximum value obtained in the temporal evolution study made in DWTP-1, DWTP-2, WWTP-1, WWTP-2 and WWTP-3.

6.3   Evaluation of radiological hazard effects

Radioactive materials that emit gamma radiation are of concern because the gamma rays pose an external radiation exposure hazard. Because gamma rays can pass through common construction materials, the distance between the radioactive material and the person is a factor in the amount of exposure the person receives. WTPs workers most likely to receive direct exposure are workers that handle sludge. Farmers and other members of the public who use sewage sludge products as fertilizer or soil conditioners could receive direct exposure to gamma radiation if these materials are present.

As the main uses of the sludge are as fertilizer or as building materials, their potential hazard was evaluated by the indices used in the radiological assessment of soil and building materials, such as radium-equivalent activity, external radiation hazard and the gamma index. Moreover, the derived outdoor an indoor dose rates, the annual effective dose equivalent and the excess lifetime cancer risk were determined to establish the radiation background database. The values for these radiation hazard parameters are presented in Table 6.4.

Radium equivalent (Ra$_{eq}$)

The radium equivalent activity can be used as a common index to compare the specific activities of sediment samples containing different concentrations of ^{226}Ra, ^{232}Th (^{228}Ra) and ^{40}K. Radium equivalent gives the useful guideline in the regulation of the safety standards on radiation protection for general public. It was defined on the assumption that 10Bq/kg of ^{226}Ra, 7 Bq/kg of ^{232}Th and 130 Bq/kg of ^{40}K produce the same gamma dose rate (Jibiri et al., 2009) and it was calculated through the equation (8.2) given by Beretka and Mathew (1985):

$$Ra_{eq} = 0.077C_K + C_{Ra} + 1.43C_{Th} \qquad (6.2)$$

where C_K, C_{Ra} and C_{Th} are the activity concentrations of ^{40}K, ^{226}Ra and ^{232}Th in Bq/kg respectively.

From the safety limit point of view, the maximum value of the radium equivalent for a material to be used in building construction is Ra$_{eq}$ ≤ 370 Bq/kg (Beretka and Mathew, 1985).

In this study, the values of Ra$_{eq}$ for the Spanish sludge samples varied from 46 to 272 and were lower than the recommended maximum value of 370 Bq/ kg (OECD, 1979) which corresponds to the dose limit of 1mSv for the general population. The Ra values obtained in the sludge from Spanish WTPs were below to the world average for soils samples which is equal to 89 Bq/kg

(UNSCEAR, 2000) except in the case of WWTP-4 where the Ra value was 131 Bq/kg. The Ra_{eq} value for the sludge sample from Waukesha instead, was around 7 times higher (2449 Bq/kg) than the recommended maximum value. Therefore this sludge shouldn't be reused in order to avoid radiation hazards.

*** External hazard index (H_{ex}) ***

The external hazard index is an important parameter in order to estimate the radiological suitability of a material used for building. The external hazard index due to gamma radiation was calculated using the criterion formula (Beretka and Mathew, 1985) as follows:

$$H_{ex} = \frac{C_K}{4810} + \frac{C_{Ra}}{370} + \frac{C_{Th}}{259} \qquad (6.3)$$

According to the UNSCEAR (2000), the upper limit for the annual external dose is 1.5 mGy. Therefore the radiation hazard to be negligible, the external hazard index must be in conformity with the criterion of $H_{ex} \leq 1$.

H_{ex} results for the Spanish WTPs ranged from 0.13 to 0.73 and were less than 1, and consequently the annual external dose was less than 1.5mGy. But in the case of Waukesha WWTP, this value exceeds 6.62 times the recommended limit producing a significant increase of the annual external dose.

Table 6.4. Radium equivalent (Ra_{eq}), external hazard index (H_{ex}) and gamma index ($I\gamma$) for sludge samples.

Water treatment plant	^{40}K	^{226}Ra	^{232}Th	Ra_{eq}	H_{ex}	I_g	D outdoor (nGy/h)	D indoor (nGy/h)	AEDE outdoor (mSv/y)	AEDE indoor (mSv/y)	AEDE total (mSv/y)
DWTP-1 (ave)[1]	598	32	37	132	0.36	0.49	62.3	74.8	0.08	0.37	0.44
(max)[2]	728	35	43	154	0.42	0.58	73.0	87.6	0.09	0.43	0.52
DWTP-2 (ave)[1]	539	27	42	129	0.35	0.48	60.5	72.7	0.07	0.36	0.43
(max)[2]	773	36	50	167	0.45	0.63	79.1	94.9	0.10	0.47	0.56
WWTP-1 (ave)[1]	122	14	15	46	0.12	0.17	21.1	25.3	0.03	0.12	0.15
(max)[2]	157	28	22	72	0.19	0.26	32.8	39.4	0.04	0.19	0.23
WWTP-2 (ave)[1]	214	12	23	62	0.17	0.23	28.6	34.3	0.04	0.17	0.20
(max)[2]	497	25	33	111	0.30	0.41	52.3	62.7	0.06	0.31	0.37
WWTP-3 (ave)[1]	179	11	18	51	0.14	0.19	23.5	28.2	0.03	0.14	0.17
(max)[2]	213	16	22	64	0.17	0.23	29.5	35.4	0.04	0.17	0.21
WWTP-4	478	132	73	273	0.74	0.96	125.0	150.0	0.15	0.74	0.89
WWTP-5	221	56	43	135	0.36	0.48	61.1	73.3	0.07	0.36	0.43
WWTP-6	325	22	45	111	0.30	0.41	50.9	61.1	0.06	0.30	0.36
WWTP-7	308	29	39	108	0.29	0.39	49.8	59.8	0.06	0.29	0.35
WWTP-8	347	64	77	201	0.54	0.71	90.5	108.7	0.11	0.53	0.64
WWTP-9	369	20	29	90	0.24	0.33	42.1	50.6	0.05	0.25	0.30
WWTP-10	313	16	28	80	0.22	0.30	37.4	44.8	0.05	0.22	0.27
WWTP-11	151	17	21	59	0.16	0.21	26.8	32.2	0.03	0.37	0.19
Waukesha	112	882	1090	2449	6.62	8.43	1071	1285	1.31	6.31	7.62
Concrete	400	40	30	114	0.31	0.42	53.3	63.9	0.07	0.31	0.38
Gypsum	80	10	10	30	0.08	0.11	14.0	16.8	0.02	0.08	0.10
World Average	370	25	25	89	0.30	0.66	55	70	0.07	0.34	0.41

[1]Ave = average values obtained in the temporal evolution study made in DWTP-1, DWTP-2, WWTP-1, WWTP-2 and WWTP-3

[2]Max = maximum value obtained in the temporal evolution study made in DWTP-1, DWTP-2, WWTP-1, WWTP-2 and WWTP-3.

Gamma Index (I_γ)

Another radiation hazard index is the gamma index which is used to estimate the level of gamma radiation hazard associated with the natural radionuclides in the sample. It is used only as a screening tool for correlating the annual dose rate due to the excess external gamma radiation caused by superficial materials (Jibiri and Okeyode, 2012). In this study, the gamma index was calculated as proposed by the European Commission of Radiation Protection (RP, 1999):

$$I_\gamma = \frac{C_K}{3000} + \frac{C_{Ra}}{300} + \frac{C_{Th}}{200} \tag{6.4}$$

where C_K, C_{Ra} and C_{Th} were the activities of [40]K, [226]Ra and [232]Th in Bq/kg. Values of Iγ≤1 correspond to an annual effective dose of less than or equal to 1mSv, while Iγ≤ 0.5 corresponds to an annual effective dose less or equal to 0.3 mSv.

The gamma indices for the Spanish WTPs sludge samples were lower than 1 so these samples did not exceed the dose criteria limit of 1mSv/y given by the European Commission Report 112 (RP, 1999). However the gamma index obtained for the Waukesha WWTP sludge sample was higher than 1Bq/kg (8.43 Bq/kg).

As the overall result of these radiological hazard indices, all the Spanish samples are safe and do not present a significant radiological risk. Thus, these samples are within the recommended safety limit when used as building raw materials and products. On the other hand, the sludge sample from Waukesha WWTP can present a significant radiological risk if it is reused.

Absorbed Gamma Dose Rate (D)

The absorbed dose rate in air from radioactivity in sludge which may form part of soils or fertilizers was also determined. Absorbed dose rate in air is the dose that is received in the open air from the radiation emitted from the radionuclides present in the ground. The outdoor absorbed dose rate in air were calculated from [226]Ra, [232]Th and [40]K concentration values assuming that the other radionuclides, such as ^{137}Cs, ^{90}Sr, and the [235]U series can be neglected as they contribute very little to the total dose from environmental background. It was calculated at a height of 1 m above the surface of the ground based on guidelines provided by UNSCEAR (2000). The conversions factor used to compute outdoor absorbed gamma dose rate ($D_{outdoor}$) in air per unit activity concentration in Bq/kg (dry weight) corresponds to 0.427 nGy/h for [226]Ra,

0.66 nGy/h for ^{232}Th and 0.0432 nGy/h for ^{40}K. Therefore D can be calculated as follows (UNSCEAR, 2000):

$$D_{outdoor} = 0.427C_{Ra} + 0.66C_{Th} + 0.0432C_K \qquad (6.5)$$

where C_{Ra}, C_{Th} and C_K are the concentration in Bq/Kg of radium, thorium and potassium respectively.

The indoor contribution is assumed to be 1.2 times higher than the outdoor dose (UNSCEAR, 2000):

$$D_{indoor} = D_{outdoor} \; x \; 1.2 \qquad (6.6)$$

Table 6.4 gives the results for adsorbed dose rate in air for samples under investigation. Outdoor and indoor absorbed dose rate for all water treatment plants ranged from 21 to 1071 nGy/h and 25 to 1285 nGy/h respectively, where the highest value was in WWTP from Waukesha while the lowest value was in WWTP-11. The large variations in the dose rate are due to large variations in the activity concentrations of different primordial radionuclides in the sludge samples, which vary from sludge to sludge. A comparison of absorbed dose rate in air found in the present study with values reported in literature for some other countries is shown in Table 6.5.

According to the data from Table 6.5, the outdoor absorbed doses rate in air of the Spanish WTPs studies are in agreement with those in Spain reported by UNSCEAR (2000).

Table 6.5. Comparison of outdoor absorbed doses rates in air obtained in this study with other countries as given in UNSCEAR (2000).

Location	Minimum	Maximum	Average
	(nGy/h)		
China	2	340	62
Hong Kong	51	120	87
India	20	1100	56
Egypt	20	133	32
Japan	21	77	53
Korea	18	200	79
Belgium	13	180	43
Denmark	35	70	52
Switzerland	15	120	45
Poland	18	97	45
Norway	20	1200	73
United States	14	118	47
Spain	40	120	76
Present study (Spanish WTPs)	**21**	**125**	**52**

Annual Effective Dose equivalent

In order to estimate the annual effective doses from outdoor and indoor terrestrial gamma radiation, one has to take into account the conversion coefficient from adsorbed dose in air to effective dose and the indoor occupancy factor. A value of 0.7 Sv/Gy was used for the conversion coefficient from adsorbed dose in air to effective dose received by adults, and 0.8 for the indoor occupancy factor, implying that 20% of time is spent outdoors, on average, around the world. The annual effective dose rate outdoors in units of μSv/y is calculated by the following formula (Saito, et al., 1990):

$$Annual\ Effective\ Dose\ equivalent\ (AEDE)_{outdoor} = D_{outdoor}\ x\ T_{outdoor}\ x\ F\ x\ 10^{-6} \quad (\textbf{6.7})$$

Where D is the calculated dose rate in nGy/h, $T_{outdoor}$ is the outdoor occupancy time (0.2 x 8760 h/y), F is the conversion factor (0.7 Sv/Gy) and 10^{-6} is the conversion factor between nano and mili.

For indoor exposure, using an occupancy factor of 0.8 (T_{indoor} = 0.8 x 8760 h/y), the annual effective dose equivalent is:

$$AEDE_{indoor} = D_{indoor} \; x \; T_{indoor} \; x \; F \; x \; 10^{-6} \qquad\qquad (6.8)$$

The annual effective dose equivalent for the sludge samples determined in the present study has been also summarized in Table 8.4. The annual effective dose equivalent from outdoor terrestrial gamma radiation ranged from 0.03 to 1.31 mSv/y with a mean value of 0.13 mSv/y. For indoor exposure, the annual effective dose equivalent had a range from 0.12 to 6.31 mSv/y with a mean value of 0.63 mSv/y. The total (outdoor plus indoor) annual effective dose equivalent from terrestrial radiation ranged from 0.15 to 0.89 (mean: 0.37) for the Spanish samples and the corresponding world average value for soils is 0.41mSv/ of which 0.34 mSv/y corresponds to indoor and 0.07mSv/y from outdoor (UNSCEAR, 2000).

In the case of the Waukesha sludge sample, as a result of the elevated Radium and Thorium concentrations, the total annual effective dose equivalent exceeds 19 times the world average value for soils.

6.4   Summary

In the present study, radioactivity in sludge samples from different WTPs were studied as NORM and evaluated their potential hazard by the indices used in the assessment of soil and building materials.

With all the results from the total inventory of the sludge samples analyzed, the concentrations of radionuclides found in Spanish sludge samples were nominal and do not pose any potential health hazard to the general public. These results are in good agreement with those obtained in the radiological assessment of soil and building materials study. The Ra_{eq} activity was found to be less than 370 Bq/kg and internal and external hazard indices were found to be less than acceptable limit of unity, except in the case of Waukesha sludge sample.

In the case of Waukesha sludge sample, ^{232}Th was present in relatively somewhat higher concentration than world average and exceeded the hazard indices for the radiological assessment of soil and building materials.

Given that, especially when sludge samples exceed the clearance level, more exhaustive studies to evaluate the possible effects on workers must be carried out.

These results may provide a general background level for the sludges studied and may also serve as a guideline for future assessment of radionuclides in WTPs.

Part III

Conclusions

Chapter 7

Conclusions and future works

Part I

This part of the thesis has provided a systematic analysis of many of the major factors that affect a water sample's gross alpha activity as determined by co-precipitation methods using gas proportional counting and, to a lesser extent, ZnS(Ag) scintillation counting.

Since discrepancies among co-precipitation procedure versions were found, it was necessary to analyze some steps of that procedure. An optimized co-precipitation procedure for gross alpha activity determination has been proposed and is going to be published by CSN. This optimization has shown that paper pulp and detergent diluted additions are not necessary in order to achieve good yields. Furthermore, an innovative aspect of this thesis has been the morphological study of the precipitate showing that the different salts were evenly distributed onto the filter.

The studies presented related to the calibration of the method have been shown that mass efficiency curves constructed with different radionuclides shifted upward as the alpha emitter energy increases showing that the higher.energy alpha emitters contribute more to the gross alpha activity than the lower-energy ones. The mass-efficiency curves of the [226]Ra progeny and the two sets of progeny in the [224]Ra decay series showed that their contributions to the gross alpha activity significantly exceeded their actual alpha activities.

Through extensive validation experiments, we have proved that both standard of calibration chosen, [241]Am and [230]Th, are suitable to determine the gross alpha activity of a water sample

achieving accurate results bearing in mind the significance of this taking into account the meaning of this measurement.

Another subject certainly deserving further interest is the elapsed time between sample preparation and measurement. Since radiological laboratories can process a large number of samples in a small window of time, gross alpha measurements ought to be carried out after two days and preferably before five days after sample preparation in order to obtain accurate results, especially in waters in which the main contributor is ^{226}Ra. Measurements before two days after sample preparation are not recommended since high values of alpha counts are detected in the blank.

Results pertaining to the comparison of the three stablished methods have been that the precision of the method increased in the order: evaporation < co-precipitation < total evaporation by liquid scintillation counting and the bias decreased in the order evaporation > co-precipitation > total evaporation by liquid scintillation counting.

Future research regarding the co-precipitation method should involve its validation as a gross beta determination excluding ^{40}K contribution. In addition, the modeling of the gross alpha activity through all alpha emitters' contribution by co-precipitation method is a subject certainly deserving further research.

Part II

In this part, we have presented a set of results related to the radionuclide's behavior in water treatment plants for treating drinking and wastewater.

The amounts of radionuclides encountered during the investigations correspond to the respective geology of the areas. The highest alpha activity concentrations have been detected at the wastewater treatment plant in the city of Waukesha, Wisconsin, USA, mainly due to the presence of high levels of Radium. Instead, for the Spanish water treatment plants studied, gross alpha activity has been mainly associated to uranium isotopes being below the screening level of 0.1 Bq/L in most of the samples.

In particular, the treatment applied in some Spanish wastewater treatment plants has shown an increase in gross alpha activity. This increase was produced after the secondary treatment, suggesting that uranium isotopes were dissolved or desorbed during the secondary treatment. Furthermore, these results have demonstrated that hydraulic retention time in the water treatment plant greatly influences gross alpha behavior and its importance is to be considered in the sampling protocol.

For the drinking water treatment plants studied, and comparing gross alpha activity values between raw water and treated water, it has been difficult to assess a radioactivity diminution in both conventional plants and therefore, conventional treatments have not been suitable to remove gross alpha activity (due to uranium). Instead, membranebased technologies can reduce gross alpha and gross beta activities. UF has not significantly reduced gross alpha and gross beta activities, while RO has shown great efficiency in doing so.

Another valuable result of this project has been the fact that wastes from water treatment could be contaminated with long-lived natural radioisotopes, such as uranium and radium. With all the results from the total inventory of the sludge samples analyzed, the concentrations of radionuclides found in Spanish sludge samples have been nominal, constant over time and have not presented a significant radiological risk, thereby making them suitable for future applications. However, more exhaustive studies need to be carried out to evaluate possible effects on workers and also on the population in general for the sludge of Waukesha, where it is re-used for different applications such as landfills, as the screening study conducted indicated high concentration of ^{232}Th in the sludge sample collected.

We encourage carrying out more studies to evaluate to a larger extent the radium isotopes behaviour in water treatment plants. These studies could be complemented by investigating other wastes generated in water treatment processes.

Appendix A

Co-precipitation method for gross alpha activity determination in water

A.1. Scope of the analysis

The method described below, allows the determination of the GAA in water samples. This method can be used in samples containing low saline content (surface waters), high saline content (groundwater) as well as in wastewater samples.

This procedure is applicable to the alpha particle energy range between 4.1 and 5.5 MeV. This range includes the main alpha emitters most likely to be found in water samples.

A.2. Apparatus

a) Hot plate/magnetic stirrer and stirring bars.

b) Glassware.

c) Filter membranes of cellulose nitrate, 47 mm of diameter 0.45 µm pore size.

d) Planchets, stainless steel, 51 mm of diameter.

e) Retaining rings.

f) Temperature-controlled drying oven.

A.3. Reagents

a) Ammonium hydroxide, NH_4OH, 6N: dilute 400 mL of concentrated NH_4OH solution (25%) to 1 L with distilled water.

b) Barium carrier, 5 mg Ba^{2+}/mL: dissolve 0.4806 g $BaNO_3$ (99%) in 50 mL of 0.1N HNO_3 solution.

c) Iron carrier, 5mg Fe^{3+}/mL: dissolve 1.808 g $Fe(NO_3)_3x9H_2O$ in 50 mL distilled water.

d) Bromocresol purple, 0.1%: dissolve 100 mg water soluble reagent in 100 mL distilled water.

e) Nitric acid, 16M. 65% HNO_3 reagent.

f)   Sulfuric acid, 1M: dilute 55 mL of the 96% reagent grade H_2SO_4 to 1 L with distilled water.

A.4. Procedure

1) Use a 500 mL aliquot of water sample. If the sample is less than 500 mL dilute with distilled water.

2) Add a magnetic stir bar to the sample.

3) Measure the pH of the sample and adjust to 7.0 ± 0.5.

4) Place the sample on a magnetic stirrer/hot plate and, while stirring, gently add 20 mL of 1M H_2SO_4 and boil for 5 minutes to flush carbon dioxide from carbonates and bicarbonates and radon from the sample.

5) Lower the hot plate temperature to approximately 50 ºC.

6) Add 1 mL of barium carrier solution.

7) Continue stirring for 30 min.

8) Add 1mL of iron carrier and 1 mL of bromocresol purple indicator solution.

9) Continue stirring and add 6N NH_4OH dropwise to the sample until there is a distinct color change (yellow to purple) and the precipitate is produced. Stop warming and continue stirring for 30 min.

10) Cool on an ice-water bath. Remove the stir bar and allow the combined precipitates settling (about 15 min).

11) Filter and collect the combined precipitates on a 0.45 µm pre-weighted filter using a vacuum filtration system. Wash the precipitate with 25 mL of distilled water. At this point, it is important to consider a good filtration takes at least 10 min to ensure that the precipitate is collected perfectly by removing the maximum amount of water and to avoid losing precipitate.

12) Place the filter with the precipitate onto the planchet and secure with a retaining ring.

13) Dry in an oven at 105 ºC for 1 h. It is recommended not warming at higher temperatures since the filter could be damaged.

14) Cool the planchet at room temperature inside a desiccator for 15 min.

15) Weight the planchet and store in a desiccator for two days before counting on a ZnS(Ag) scintillation detector, using a thin plastic screen of ZnS(Ag) placed on the planchet, or counted directly on a gas-flow proportional counter.

16) Prepare a reagent blank precipitate to determine alpha activity background.

A.5. Calibration

Add at least 2 Bq/L standard alpha pure emitter (^{241}Am or ^{230}Th) to 500 mL portions of distilled water in separate beakers. Determine counting efficiency (cpm/dps) for the alpha emitter by taking these known additions by following the procedure described below. In order to obtain a gross alpha efficiency curve (efficiency vs. residue mass), the amount of barium and iron carriers are proportionally increased in the procedure (1 to 2 mL of each carrier, obtaining 6 residues when increasing 0.2 mL of each carrier gradually). Make at least three replicates determinations for each residue.

A.6. Calculations and expression of results

a) **Gross alpha activity (GAA)**

The gross alpha activity is calculated using the following expression:

$$GAA \left(^{Bq}/_L\right) = \frac{C_s - C_b}{60 \cdot E \cdot V} \qquad (A.1)$$

where

E = counter efficiency, cps/dps

V = volume analyzed (L)

C_s = samples counts per minute, cpm, and

C_b = blanks counts per minute, cpm.

b) **Minimum Detectable Activity (MDA)**

At 95% confidence level, the MDA is calculated using the following expression:

$$MDA \left(^{Bq}/_L\right) = \frac{2k \cdot \sqrt{\dfrac{C_b}{t(s)} + \dfrac{C_b}{t(b)}} + k^2 \cdot \left(\dfrac{1}{t(s)} + \dfrac{1}{t(b)}\right)}{60 \cdot E_i \cdot V} \qquad (A.2)$$

where

$k = 1{,}645$

C_b = blank counts per minute, cpm

$t(s)$ = sample measurement time, in minutes

$t(b)$ = blank measurement time, in minutes

E = counter efficiency, cps/dps, and

V = volume analyzed (L)

For a sample volume of 0.5 L and a counting time of 1400 min, the MDA achieved is about 0.003 Bq/L, measured in a gas flow proportional detector and zinc sulfide solid scintillation detector.

c) **Uncertainty (U)**

The uncertainty calculated in this section only corresponds to the uncertainty associated with sample counting. At the 68% confidence level ($k=1$), the uncertainty is calculated using the following expression:

$$u_c \left(Bq/_L \right) = \sqrt{\frac{C_s}{t(s)} + \frac{C_b}{t(b)}} \qquad (A.3)$$

where

C_s = sample counts per minute, cpm, and

C_b = blank counts per minute, cpm

$t(s)$ = sample measurement time, in minutes, and

$t(b)$ = blank measurement time, in minutes

d) **Expression of results**

The results are expressed as follows:

- **When GAA ≥ MDA:**
  The results is reported as GAA ± U (indicating the confidence level used)

  where,

  U is the expanded uncertainty in Bq/L and is given by the following expression:

$$U = k \cdot u_c \qquad\qquad (\boldsymbol{A}.\boldsymbol{4})$$

where,

k = coverage factor

u_c = combined uncertainty of the entire analysis process, which is calculated from various contributions using the following expression:

$$\frac{u_c}{GAA} = \sqrt{\left(\frac{u_V}{V}\right)^2 + \left(\frac{u_E}{E}\right)^2 + \left(\frac{u_N}{N}\right)^2 + (u_R)^2} \qquad\qquad (\boldsymbol{A}.\boldsymbol{5})$$

where,

u_V is the uncertainty associated to the volume of the analyzed sample

u_E is the uncertainty associated to the alpha efficiency

u_N is the uncertainty associated to the sample counting. This is calculated according to the expression included in section c.

u_R is the uncertainty associated to the repeatability or reproducibility of the assay

V = volume analyzed (L)

E = counter efficiency (cps/dps) corresponding to the sample residue,

N is the net alpha particle count rate of the sample, in counts per minute (C_s). It is calculated substracting the alpha particle count rate of the blank (C_b).

- **When GAA < MDA:**
  The results is reported as < MDA specifying the MDA value obtained.

A.7. Check list of the method

	Done (✓)
SAMPLE REFERENCE	
SAMPLE COLLECTION DATE	
START DATE	
SAMPLE VOLUME (0,5 L)	
PRECIPITATION OF SULFATES AND HYDROXIDES	
• pH adjustment: 7,0 ± 0,5	
• While stirring, add 20 mL de H_2SO_4 1 M	
• Heat until the samples begin to boil (5 min.)	
• Lower the temperature around 50ºC.	
• Add 1 mL of barium carrier solution (5 mg·mL^{-1})	
• Stir for 30 minutes. (50ºC aproximately)	
• Add 1mL of iron carrier solution (5 mg·mL^{-1}) and 1mL of the bromocresol purple indicator	
• Add dropwise NH_4OH 6 M until there is a distinct color change (yellow to purple)	
• Stop the heater and continue stirring for 30 minutes	
• Cool on an ice-water bath	
FILTRATION (celulose nitrate membrane, 0.45 μm)	
• Planchet identification	
• Weigh the planchet+ filter and ring (**ENTER the weight P$_1$,in** g)	
• Filter and wash with 25-50 mL of water	
RESIDUE MASS	
• Place the filter onto the planchet and adjust with the ring	
• Dry the whole to 105ºC, for at least one hour	
• Allow to cool in the desiccator to room temperature (15 min)	
• Weigh the whole (**ENTER the weight P2, in g**)	
• (**ENTER the residue mass P$_2$-P$_1$, in g**)	
SAMPLE MEASUREMENT	
• Let sit for 2days to allow for the decay of any radon progeny	
DATE AND TIME OF THE FINAL PREPARATION	
COMMENTS	

Appendix B

Test methods and instrumentation

The following annex is a summary of the methodologies used in this thesis which have been carried out in the "Laboratori d'Analisis de Radioactivitat" (LARA) of the Institute of Energy Technologies-Universitat Politecnica de Catalunya (UPC) and in the "Wisconsin State Laboratory of Hygiene" (WSLH)-University of Wisconsin, U.S.A.

Methods used at LARA have been accredited under the ISO/IEC 17025 standard since 2002. Furthermore, we periodically participate in both national and international proficiency/inter-comparison exercises with the aim of improving and ensuring the quality of the results of all the procedures carried out at our laboratory.

The Wisconsin State Laboratory of Hygiene (WSLH) is NELAC (National Environmental Laboratory Accreditation Conference) certified to perform Safe Drinking Water Act analyses using EPA approved methods. The WSLH participates in both national and international proficiency/ inter-comparison exercise with the aim of improving and ensuring the quality of the results of all the procedures carried out at this laboratory.

B.1. Water samples

In order to preserve the liquid samples prior to radioanalysis water samples were acidified with concentrated nitric acid (at pH 2). Moreover, wastewater samples were filtered through 1-mm glass fiber filters followed by 0.45 μm membrane filters. Therefore it should be highlighted that wastewater sample results refer to dissolved radioactivity levels according to the pre-treatment.

a) Gross alpha and gross beta activities

The analytical procedures used to determine the gross alpha activity level were the 'evaporation method' (EPA, 1980) and the 'co-precipitation method' (Appendix A).

For sample prepared in Spain the method followed was the standard method UNE 73311-4:2002 for determining the gross beta activity in non-saline water. This method is basically the same as the EPA 900.0 method (EPA, 1980) which is used to determine gross alpha and beta activities in samples analyzed in the U.S. The basis of this method is firstly a mild reducing evaporation of a given volume of water sample. Subsequently, when the volume has been reduced to about 5 to 8 mL, the sample is transferred to a stainless steel planchet of 4.7 cm diameter and oven-dried at 105º C. The optimal mass density of the residue for determining the gross alpha activity is about 5 mg/cm^2. Both the steel planchet and the deposit are weighed and stored in a desiccator. Finally, the sample is measured after two days.

The analytical preparation for gross beta activity was also the evaporation method (EPA, 1980).

For samples analyzed in Spain, the rest beta activity was calculated by subtracting the ^{40}K activity from gross beta activity. The potassium content was analyzed by flame photometry and the ^{40}K content was calculated using the potassium content and the percentage of ^{40}K that contains natural potassium (UNE, 2002).

b) Total evaporation/LSC method

A 100-mL aliquot of a water sample was evaporated to dryness. When the precipitate obtained was cooled to room temperature, it was then dissolved in 10 mL of deionized water acidified by HCl to pH = 1.5. Some samples with a high salt content needed more acidic solution to be completely dissolved. The solution was then stirred for 5 minutes in order to ensure that the entire residue was dissolved. With this treatment ^{222}Rn and all its short-lived decay daughters were eliminated in the sample. An 8-mL aliquot of the evaporated sample was mixed with 12 mL of the scintillation cocktail Ultima Gold AB (Perkin Elmer LifeScience, Boston, MA, USA) in a low diffusion scintillator vial. Under these conditions the sample remained homogenous and chemically stable for some months. The vial was counted in a liquid scintillation counter which could discriminate between alpha and beta pulses. The Pulse Shape Analyzer (PSA) level optimized value obtained using ^{236}U and ^{40}K calibration standards was 100 (Zapata-García et al., 2012). The alpha window was set from channel 500 to 800; the beta window from 250 to 1024 (CSN, 2011).

c) Radiochemical procedures for specific alpha emitter determinations

Procedures used at LARA (Spain)

Uranium and Thorium

To determine the uranium and thorium content in the water samples, $^{232}U/^{228}Th$ in secular equilibrium was added as tracers. The uranium and thorium content was then co-precipitated with $Fe(OH)_3$. The precipitate was dissolved and separated in a Dowex resin AG1X8. The uranium and thorium were retained in the column and subsequently eluted. A detailed description of the experimental procedure has been reported in Vallés (1994). Finally, the alpha sources were electrodeposited onto stainless steel planchets (Hallstadius, 1984).

Radium

Radium isotopes (^{226}Ra and ^{224}Ra) were determined by co-precipitation from a 1-L sample with barium and lead carriers adding 9M H_2SO_4. The solution was then purified by barium sulfate

precipitation at pH 5-5.3 in the presence of EDTA. A detailed description of the procedure has been reported in Vallés (1994).

Polonium

[210]Po was determined by spontaneous deposition onto a silver planchet. [209]Po was used as a tracer. The water sample was previously concentrated by evaporation at 90ºC to a volume of 25 mL. The solution was transferred to a 40 mL Teflon cell, and 5 mL of 20% hydrochloride hydroxylamine, 2 mL of 25% sodium citrate and 1mL of Bi^{3+}carrier were added and stirred. Finally, the polonium was deposited for 3 hours at a temperature of 90-95ºC, with agitation of the solution (Vallés, 1994).

Procedures used at WSLH (United States)

Radium

The [226]Ra and [228]Ra activities were determined using EPA Methods 903.1 and 904.0 (1980), respectively. In method 904.0 [228]Ac is allowed to come to secular equilibrium with its parent, [228]Ra; then the beta activity of [228]Ac is measured and is used to determine the activity of [228]Ra in the sample. The determination of the [226]Ra activity is based on the emanation and scintillation alpha counting of its progeny, [222]Rn.

For samples analyzed by this procedure, it was assumed that [224]Ra was in secular equilibrium at the time of sample collection with [228]Ra and therefore the [228]Ra activity determined was the [224]Ra activity of the sample.

The radium isotopes [224]Ra, [226]Ra and [228]Ra were also measured through their gamma-ray emitting decay products, [212]Pb, [214]Pb (and/or [212]Pb), and [228]Ac, respectively using 1L of sample in marinelli beaker geometry. The beaker containing samples were sealed avoiding losses of [222]Rn. Because of the short life of [224]Ra the sample should be counted within four days of the sample collection date. The counting is repeated after about 21 days to ensure the [226]Ra progeny are in equilibrium with their parent. At this point, the [228]Ac equilibration with its [228]Ra parent is already established.

Polonium

The [210]Po activity was determined using a modified version of Procedure Po-02-RC, the Environmental Measurements Laboratory, United States Department of Energy (1990). To prevent the formation of silica gel, the acidified water samples were digested with hydrofluoric

acid. A water sample was reduced in volume to about 200 mL, and transferred to a 400-mL Teflon beaker. Then 10 mL of 48% hydrofluoric acid was added to the beaker, and the contents of the beaker were evaporated to dryness. An acidic boric acid solution was added to the beaker, which dissolved the sample and reacted with any fluoride ion that was left. The acidic boric acid solution usually contained a small amount of insoluble white matter, so the solution was filtered, and the polonium in the filtered solution was deposited on a nickel disc, as in the original procedure.

Uranium

The activities of the uranium isotopes were determined using alpha spectroscopy. The samples were prepared for analysis using Eichrom Method ACW02 (2001) and employing ^{232}U as the tracer.

d) Other determinations

The dry residue, indicated in mg/L, which corresponds to the total quantity of salts in the water, was obtained by evaporating the liquid samples and later drying them at a temperature of 180°C.

pH in water samples was measured by using a glass electrode pHmeter from CRISON.

B.2. Sludge samples

These samples were prepared using the Spanish standard method for soil samples (UNE 73311-5, 2002). Wet sludge samples were transferred to a tray and dried in a stove at a temperature of 130ºC to constant weight. Subsequently, the sample was crushed in a ball mill and sifted in a 2-mm sieve.

For the sludge sampled at Waukesha WWTP, this was dried in an oven set at 75 ºC and then ground and homogenized.

a) Gross alpha and gross beta activities

To determine gross alpha and gross beta activity in sludge samples, approximately 0.05 g of dried, sieved sludge was uniformly deposited on a 20 cm^2 stainless steel planchet with 0.002 L of distilled water.

b) Gamma emitting isotopes determination

Between 23 and 98 g of the sample was sealed using Teflon tape in 50 or 100-mL polyethylene jars, depending on the quantity of sample, for a minimum of 20 days (to allow radium series decay progeny to reach secular equilibrium) before counting (Quindos et al., 1994).

For the sludge sampled at Waukesha WWTP, 34 g were placed in an ointment can and sealed with epoxy. Telfon tape was placed around the edge of the container after being sealed with epoxy. The container was storage for a minimum of 30 days before counting.

c) pH determination

pH in sludge was determined by using 5 g of sieved sludge mixed with 45 mL of distilled water and stirred vigorously for 5 min. The sludge was left to stand for 10 min and the pH was measured by using a glass electrode pHmeter from CRISON.

B.3- Instrumentation

a) Visible light microscopy

A visible light microscope was used; model Stemi 2000-C (Carl Zeiss), to study the morphology of the co-precipitation residue. Images were recorded electronically with a digital camera connected directly to the optical microscope. The Buehler Omnimet software, version 5.30 build 07, was used to obtain the equivalent diameter of the precipitate fragments in three samples with different residue mass.

b) Scanning electron microscopy

A section of the residue was imaged using a scanning electron microscope (SEM) with an energy-dispersive X-ray spectroscopy system (EDX), model JSM-6400, JEOL Technics, Tokyo, Japan. The samples were coated with a thin layer of gold to ensure electron conductivity. This was used to determine the height of the residue, the distribution and to identify barium sulphate and ferric hydroxide salts.

c) Measurement of gross alpha and beta activity

For samples analyzed in Spain, the gross alpha measurements were carried out in 4 ZnS(Ag) scintillation alpha detectors (photomultiplier tube and base preamplifier, Canberra model 2007

P) calibrated with an [241]Am and [230]Th sources. The thin-layer plastic ZnS(Ag) scintillator used is distributed by TECNASA (Spain) (model EJ-440, 49 mm in diameter).

Gross beta measurements were carried out in a 10-detector, low-background gas-flow proportional counting system (Berthold, model LB770-2) calibrated with a ^{90}Sr/^{90}Y source (UNE, 2002).

In the comparative study among different methods to determine gross alpha activity, measurements were also carried out in a liquid scintillation counter (Wallac 1220 Quantulus, Perkin Elmer LifeScience, Boston, MA, USA).

For samples analyzed and the experiments made in the U.S.A, both measurements (alpha and beta) were carried out in a 3 4-detector low-background gas-flow proportional counting system (Protean model MPC 9604) calibrated with a [230]Th and ^{137}Cs sources.

All the calculations were done using the appropriate density thickness corrections for efficiencies to convert the gross alpha and gross beta measurements to specific activities. Since the levels of radioactivity found in environmental samples were low, long counting times, of approximately 1400 minutes per sample, were necessary.

In general, for gross alpha activity, the Minimum Detectable Activity (MDA) was in the range of 20-80 mBq/L for the evaporation method and 4 mBq/L for the co-precipitation method. For gross beta activity, the MDA was in the range of 32-178 mBq/L.

d) Measurement of radium isotopes activities

For samples analyzed in Spain, radium isotopes activities ([226]Ra and [224]Ra) were measured using a ZnS (Ag) scintillation counter (photomultiplier tube and base preamplifier, Canberra model 2007 P) making two counting of the planchets at two and twenty-one days after the separation of Radium. The MDA for this method was 2.5 mBq/L.

For samples analyzed in the U.S.A., [226]Ra was determined by alpha scintillation counting of [222]Rn progeny emanation in Ludlum scintillation cell counter (Model 182 Radon Flask Counter). Beta activity of [228]Ac is measured using a low-background gas-flow proportional counting system (Protean model MPC 9604) calibrated with a ^{89}Sr in order to determine [228]Ra activity. A MDA of 4 mBq/L for [226]Ra 40 mBq/L for [228]Ra can be readily obtained.

e) Determination by alpha spectrometry

For water samples analyzed in Spain, uranium isotope activities (^{234}U, ^{235}U and ^{238}U), ^{232}Th and ^{210}Po were determined by alpha spectrometry using PIPS detectors with a 450 mm^2 active area (Canberra). The detectors were energy-calibrated using a NIST traceable mixed standard alpha source containing ^{239}Pu, ^{241}Am and ^{244}Cm. The energy slope of the spectrum was about 4 keV per channel, and the region of observation selected was from 4 to 8 MeV. The counting efficiency of the detectors was 30%. The activity concentration was calculated using Genie 2000 software. The samples were generally measured about 5 mm from the detectors and during 250,000 s in order to achieve adequate minimum detectable activities (MDA) of 0.1 mBq/L (U), 0.1 mBq/L (Th), 0.4 mBq/L (Po).

For water samples analyzed in the U.S.A., uranium isotope activities (^{234}U, ^{235}U and ^{238}U) and ^{210}Po were determined by alpha spectrometry using eight PIPS detectors with a 600 mm^2 active area (EG & ORTEC company). The detectors were energy-calibrated using a mixed standard alpha disc containing ^{239}Pu, ^{241}Am and ^{244}Cm from Eckert and Ziegler Analytics. The energy slope of the spectrum was about 5 keV per channel, and the region of observation selected was from 3 to 8 MeV. The counting efficiency of the detectors was 28%. The activity concentration was calculated using Alpha Vision v5.3 software. In this case the MDA achieved were 0.1 and 0.3 mBq/L for Uranium and Polonium measurements respectively.

f) Determination by gamma spectrometry

At LARA for the measurements of sludge samples, Canberra HPGe coaxial detectors model GX3020 and GX4020 were used. Their nominal efficiencies relative to a 3 in. x 3 in. NaI(Tl) detector are 33 and 41 % respectively, and the resolutions 1.77 and 1.86 keV at 1.33 MeV of ^{60}Co. Detectors are mounted in cubic low-background Fe and Pb shield with a wall thickness of 14 and 10 cm respectively. All detectors are located inside a room with one metre thick walls and constant flux of fresh air to avoid high levels of radon inside the facility. Genie 2000 software (Canberra Industries, Meriden, USA) was used to acquire and subsequently analyze the information provided by the gamma spectra.

The activities of the detected radionuclides are dependent on count rate, efficiency of the detector and sample mass. These factors were also selected as sources of uncertainty and they were used to calculate the combined uncertainty. The range (minima and maximum values) for the reported uncertainties (for a level of confidence of 95%, *k=2*) and the mean Minimum Detectable Activity (MDA) are shown in Table B.1. MDA were calculated by the Currie equation (Currie, 1968).

It is worth mentioning that the activities of the detected radionuclides in sludge from WWTPs were different than those detected in the sludge studied in Chapter 4 (from DWTPs). Therefore, the range (minima and maximum values) for the reported uncertainties (for a level of confidence of 95%, *k=2*) and the mean Minimum Detectable Activity (MDA) are shown below in Table B.2. In general, MDA values for gross alpha and gross beta as well as gamma-emitters were similar, but in this case ^{131}I activities were detected in this type of sludge.

At WSLH for the measurements of [133]Ba and [228]Ac yields, [224]Ra activity determination through its progeny and the sludge and water samples from Waukesha WWTP, Canberra HPGe coaxial detectors model GC8021, GC4519, GC4020 and Canberra HPGe semiplanar detector model GL2020R were used. For the coaxial detectors, their nominal efficiencies relative to a 3 in. x 3 in. NaI(Tl) detector are 80, 45, and 45 % respectively, and the resolutions 2.1, 1.9 and 2.0 keV at 1.33 MeV of [60]Co. For the planar detector, the resolution is 0.34 keV at 6.4 keV of [57]Co. Genie 2000 software (Canberra Industries, Meriden, USA) was used to acquire and subsequently analyze the information provided by the gamma spectra.

Table B.1. Minimum Detectable Activity (MDA) and uncertainties in percentage (coverage factor *k=2*) in sludge from the studied DWTPs.

Radionuclide	MDA [1]	Uncertainty (%)	
	Mean	Minimum	Maximum
Gross alpha	40	26.7	30.7
Gross beta	49	14.3	16.2
[238]U series			
[234]Th	18	12.1	53.7
[214]Pb	4.2	5.4	43.6
[214]Bi	4.1	5.4	38.1
[214]Pb$_d$	23	17.9	39.9
[232]Th series			
[228]Ac	6.9	7.0	43.1
[212]Pb	3.4	3.8	40.1
[212]Bi	14	17.3	39.6
[208]Tl	1.5	7.2	70.3
[7]Be	17	9.1	38.7
[40]K	25	3.9	17.7
[137]Cs	1.0	14.8	49.2

[1]Activity expressed in Bq/kg dry weight.

Table B.2. Minimum Detectable Activity (MDA) and uncertainties in percentage (coverage factor *k=2*) in sludge from the studied WWTPs.

Radionuclide	MDA [1]	Uncertainty (%)	
	Mean	Minimum	Maximum
Gross alpha	40	32.8	63.2
Gross beta	50	15.6	35.8
^{238}**U series**			
^{234}**Th**	16	6.7	35.9
^{214}**Pb**	2.5	16.5	48.5
^{214}**Bi**	2.2	8.3	55.5
^{214}**Pb$_d$**	18	16.0	46.6
^{232}**Th series**			
^{228}**Ac**	3.6	9.8	29.6
^{212}**Pb**	1.6	14.5	39.4
^{212}**Bi**	11.9	30.7	71.8
^{208}**Tl**	1.1	12.1	68.8
^{7}**Be**	17	9.0	40.5
^{40}**K**	13	7.6	19.3
^{137}**Cs**	1.0	59.5	78.2
^{131}**I**	67	17.7	68.8

[1] Activity expressed in Bq/kg dry weight.

Appendix C

Radioactive standard solutions

Table C.1. List of radioactive standard solutions used for the accomplishment of the different investigations presented in this thesis. For all investigations diluted solutions from the stock solution (concentrated) were prepared.

Radionuclide	Institution	Activity of the stock solution (Bq/g) and reference date [4]	standard media	Uses	manuscript section	Country
^{133}Ba	Eckert & Ziegler	759 ± 13 (25-03-2008)	0.1 M HCl	^{226}Ra and BaSO$_4$ yields calculation by gamma spectrometr	1.2 2.4	U.S.A.
^{230}Th	Eckert & Ziegler	785 ± 14 (12-12-2011)	0.5 M HNO$_3$	Paper pulp study, alpha particle mass efficiency curve, ^{230}Th recovery checking	1.2 2.4	U.S.A.
^{230}Th	NIST [1]	40.83 ± 0.16 (1-04-2007)	1M HNO$_3$	alpha particle mass efficiency curve, energy dependence of the efficiency	2.3	Spain
^{241}Am	CIEMAT [2]	329 ± 2 (21-04-1999)	1M HNO$_3$	alpha particle mass efficiency curve, energy dependence of the efficiency	2.3	Spain
^{nat}U	Eckert & Ziegler	957 ± 19 (01-05-2010)	1M HNO$_3$	alpha particle mass efficiency curve, synthetic samples preparation	1.4 2.3	Spain
^{236}U	Eckert & Ziegler	761 ± 16 (15-12-2008)	1M HNO$_3$	energy dependence of the efficiency	2.3	Spain
^{228}Ra	Eckert & Ziegler	753 ± 30 (7-01-2008)	0.1 M HCl	^{228}Ac gamma efficiency curve, ^{224}Ra activity determination, ^{224}Ra and its progeny alpha particle mass efficiency curve	2.4	U.S.A.
^{226}Ra	NIST [1]	31.0 ± 0.4 (9-10-1991)	1M HCl	^{226}Ra and its progeny mass efficiency curve	2.4	U.S.A.
^{226}Ra	CIEMAT [2]	176 ± 2	1M HNO$_3$	synthetic samples preparation, ^{226}Ra contribution estimation	3.3.1	Spain
^{210}Pb	DKD [3]	213 ± 3 (1-01-2003)	1.2 M HNO$_3$	^{210}Pb, ^{210}Bi and ^{210}Po recovery checking.	2.4	U.S.A
^{210}Pb	CIEMAT [2]	232 ± 4 (20-05-1991)	1M HNO$_3$	synthetic samples preparation	3.3.1	Spain

[1] National Institute of Standards & Technology (U.S.A.).
[2] Centro de Investigaciones Energéticas, Medioambientales y Tecnológicas (Spain).
[3] Deutscher Kalibrierdienst (Germany).
[4] Expanded uncertaitny coverage factor $k=2$, providing a level of confidence of 95%

Appendix D

Thesis scientific production

D.1. Journal articles

- Montaña, M., Camacho, A., Devesa, R., Vallés, I., Céspedes, R., Serrano, I., Blázquez, S., Barjola, V. 2011. ***The presence of radionuclides in wastewater treatment plants in Spain and their effect on human health.*** J. Clean. Prod. doi:10.1016/j.jclepro.2011.07.007.

- Camacho A, Montaña M, Vallés I, Devesa R, Céspedes-Sánchez R, Serrano I, Blázquez S, Barjola V. 2012. ***Behavior of natural radionuclides in wastewater treatment plants.*** J Environ Radioact 109, 76-83.

- Montaña M., Camacho A., Serrano I., Vallés I., 2012. ***Experimental analysis of the mass efficiency curve for gross alpha activity and morphological study of the residue obtained by the co-precipitation method.*** Appl. Radiat. Isotopes 70, 1541-1548.

- Camacho A., Montaña M., Vallés I., Devesa R., Céspedes-Sánchez R., Serrano I. 2013. ***Temporal evolution of radionuclides in sludge from wastewater treatment plants.*** J Radioanal Nucl Chem. 295, 297-306.

- Montaña M., Fons J., Corbacho J.A., Camacho A., Zapata-García D., Guillén J., Serrano I., Tent J., Baeza A., Llauradó M, Vallés I. 2013. ***A comparative experimental study of gross alpha methods in natural waters.*** J Environ Radioact. 118, 1-8.

- Montaña M., Camacho A, Serrano I, Devesa R, Matia L, Valles I. 2013. ***Removal of radionuclides in drinking water by membrane treatment using ultrafiltration, reverse osmosis and electrodialysis reversal.*** J Environ Radioact. doi: 10.1016/j.jenvrad.2013.01.010.

D.2. Conference posters and presentations

- **SOSTAQUA Project: Technical and Science Conference 2008. Torre Agbar, Barcelona, Spain, 10 April**. *'Radiological Impact of water and wastes from water treatment plants. Health risk evaluation'*. (*"Impacto radiológico ambiental de los subproductos relativos al tratamiento y depuración del agua. Evaluación del riesgo a consecuencia de los componentes radiactivos"*). A.Camacho, I.Vallés, M.Montaña.

- **XVII Congreso "Sociedad Española de Física Médica" y XII Sociedad Española de Protección Radiológica", Alicante, Valencia, Spain, 2-5 June 2009.** *"Resultados del índice de actividad alfa total en aguas potables en función del método de preparación radioquímica y de medida"*. A. Camacho, I.Vallés, I.Serrano, M.Montaña, S.Blazquez, V.Barjola, X.Ortega.

- **SOSTAQUA Project: Technical and Science Conference 2009. Museu Agbar-Can Serra, Cornellà, Spain, 22 April and 16-17 November.** *'Radiological Impact of water and wastes from water treatment plants. Health risk evaluation'*. A.Camacho, I.Vallés, M.Montaña.

- **SOSTAQUA Project: Technical and Science Conference 2010. Museu Agbar-Can Serra, Cornellà, España, 29 April and 18 November.** *'Radiological Impact of water and wastes from water treatment plants. Health risk evaluation'*. A.Camacho, I.Vallés, M.Montaña.

- **VI Jornadas sobre calidad en el control de la radiactividad ambiental, Cáceres, Spain, 20-23 September 2010.** *'Preliminary study of some factors affecting the gross alpha activity in drinking water by co-precipitation method'*. M.Montaña, A.Camacho, I.Vallés.

- **Environmental Radioactivity, Rome, 25-27th October 2010.** *'Behavior of radionuclides in wastewater treatment plants'*. M. Montaña, A. Camacho, I. Vallés, R. Devesa, R. Céspedes, I. Serrano, S. Blàzquez, V. Barjola. M. Montaña.

- **SOSTAQUA Project: Final Evaluation Conference.** Museu Agbar-Can Serra, Cornellà, Spain, 24 February. *'Radiological Impact of water and wastes from water treatment plants. Health risk evaluation'. Evaluación del riesgo a consecuencia de los componentes radiactivos").* A.Camacho, I.Vallés, M.Montaña.

- **INSINUME'12. 6th International Symposium On In Situ Nuclear Metrology As A Tool For Radioecology. Brussels (Belgium), 11-15th June 2012.**

  'Removal of radionuclides in drinking water by membrane treatment using ultrafiltration, reverse osmosis and electrodialysis reversal.' M. Montaña, A. Camacho, I. Serrano, R. Devesa, R. Matia, I. Vallés.

  'A comparative experimental study of gross alpha methods in natural waters. M. Montaña, J. Fons, J.A. Corbacho, A. Camacho, D. Zapata-García, J. Guillen, I. Serrano, J. Tent, A. Baeza, M. Llauradó, I. Vallés.

- **III Congreso conjunto "Sociedad Española de Física Médica" y Sociedad Española de Protección Radiológica", Cáceres, Spain, 18-21 June 2013.** *"Estudio sobre los niveles de actividad de radionúclidos en productos sólidos de plantas de potabilización de aguas catalanas".* M. Montaña, A.Camacho, R. Céspedes, R. Devesa, I. Serrano, MA. Duch, I. Vallés.

D.3. Other publications

- A.Camacho, I.Vallés, I. Serrano, M. Montaña, S. Blazquez, V. Barjola, X Ortega. ***Resultados del índice de actividad alfa total en aguas potables en función del método de preparación radioquímica y de medida.*** Sociedad Española de protección radiológica, resumen en la Memoria del congreso conjunto SEFM y SEPR, Alicante 2009. Full paper on www.sefmsepralicante2009.es; (last accessed 12-07-11).

- A. Camacho, M. Montaña, I. Serrano, I. Vallés, Fons, J., Llauradó, M., Zapata-García, D., Tent, J., Baeza, A., Corbacho, J.A., Guillén, J.***Estudio de la problemática existente en la determinación del índice de actividad alfa total en aguas potables. Propuesta de procedimientos. Acuerdo específico de colaboración entre el Consejo de Seguridad Nuclear y la Universidad de Extremadura. Universidades participantes: Universidad de Extremadura, Universitat de Barcelona y Universitat Politècnica de Catalunya.*** Next publication as 'Colección Informes Técnicos', CSN, 2013.

- M. Montaña, A. Camacho, I. Serrano, I. Vallés. ***Procedimiento para la determinación del índice de actividad alfa total en aguas potables mediante el método de coprecipitación y medida en detectores de centelleo de ZnS o en contador proporcional***. Next publication as 'Serie Vigilancia Radiológica Ambiental. Procedimientos, Int-04-07, procedimiento 1.17', CSN, 2013.

D.4. Internal Reports

Within the framework of SOSTAQUA Project, different reports (deliverable) were made and are listed in the following table.

Table D.1. Deliverable documents drafted related to the SOSTAQUA Project.

YEAR	Deliverable Title
2007	Informe Técnico de Progreso L10. Tarea 10G (1r. Semestre-07)
2007	Informe Técnico Anual 2007. Tarea 10G.
2007	Informe Anual L10. Tarea 10G 2007
2008	Informe Técnico de Progreso L10. Tarea 10G (1r. Semestre-08)
2008	Informe Científico anual. Tarea 10G (2008)
2008	Informe Técnico anual. Tarea 10G (2008)
2009	Informe Técnico de Progreso L10. Tarea 10G (1r. Semestre-09)
2009	Informe Científico anual. Tarea 10G (2009)
2009	Informe Técnico anual. Tarea 10G (2009)
2010	Informe Técnico de Progreso L10. Tarea 10G (1r. Semestre-10)
2010	Informe Científico anual. Tarea 10G (2010)
2010	Informe Técnico anual. Tarea 10G (2010)
2010	Contenido radiológico de muestras de agua de distribución españolas. Cumplimiento con el RD 140/2003.
2010	Evolución temporal de radiactividad en líquidos y subproductos sólidos de plantas ETAP.

Bibliography

Aksoy, A., Ahmed, M., Matterm, W.S.A., El-Naggar, Z.R. 2002. Gamma-ray spectroscopic and PIXE analysis of selected samples from the phosporite deposits of Northwestern Saudi Arabia. Radioanal. Nucl. Chem., 253, 3, 517-521.

APHA. 1998. Standard Methods for the Examination of Water and Wastewater, 20th Ed. 7110 C. Coprecipitation method for gross alpha radioactivity in drinking water. Denver, CO: American Public Health Association, the American Water Works Association, and the Water Environment Federation.

Arndt M.F., West, L.E. 2004. A Study of the Factors Affecting the Gross Alpha Measurement, and a Radiochemical Analysis of some Groundwater Samples from the State of Wisconsin Exhibiting an Elevated Gross Alpha Activity. 51st Annual Radiobioassay & Radiochemical Measurements Conference, Cincinnati, Oct 30 - Nov 4.

Arndt MF, West LE. 2007. An experimental analysis of some of the factors affecting gross alpha-particle activity with an emphasis on ^{226}Ra and its progeny. Health Phys 92, 148-156.

Arndt MF, West LE. 2008. An experimental analysis of some of the contribution of ^{224}Ra and ^{226}Ra and progeny to the gross alpha-particle activity of water samples. Health Phys 94, 459-470.

Ardnt, M.F. 2010. Evaluation of gross alpha and uranium measurements for MCL compliance. Water Research Foundation.

ASTM (American Society for testing and materials). Standard test methods for alpha-particle radioactivity of water. Method: D1 943-996.

Baeza, A., Del Rio, L.M., Jimenez, A., Miro, C., Paniagua, J.M., 1995. Factors determining the radioactivity levels of waters in the province of Cáceres (Spain). Appl. Radiat. Isotopes. 46, 1053-1059.

Baeza A., Fernández M., Herranz M., Legarda F., Miró C., Salas A. 2004. Elimination of man-made radionuclides from natural waters by applying a standard coagulation-flocculation process. J. Radioanal. Nucl. Chem. 260, 2, 321-326.

Baeza A., Fernández M., Herranz M., Legarda F., Miró C., Salas A. 2006. Removing uranium and radium from natural water. Water, Air and Soil Pollution, 173, 57-69.

Baeza A., Salas A., Legarda F. 2008. Determining factors in the elimination of uranium and radium from groundwaters during a standard potabilization process. Sci. Total Environ. 406, 24-34.

Bastian, R.K., Bachmaier, J.T., Schmidt, D.W., Salomon, S.N, Jones, A., Chiu, W.A, Setlow, L.W., Wolbarst, A.B, Goodman, C.Yu., Lenhart, T., 2005. Radioactive materials in biosolids: National Survey, Dose Modeling, and Publicly Owned Treatment Works (POTW) Guidance. J. Environ. Qual. 34, 64-74.

Beretka, J. and Mathew, PJ. 1985. Natural Radioactivity in Australian Building Materials, Industrial Waste and By-Products. Health Phys. 48, 87-95.

Caillet S, Arpagaus P, Monna F, Dominik J. 2001. Factors controlling ^{7}Be and ^{210}Pb atmospheric deposition as revealed by sampling individual rain events in the región of Geneva, Switzerland. J Environ. Radioac 53:241-256

Camacho A., Devesa R., Vallés I., Serrano I., Soler J., Blázquez S., Ortega X., Matia L., 2010. Distribution of uranium isotopes in surface water of the Llobregat river basin (Northeast Spain). J. Environ. Radioact. 101, 1048-1054.

Camacho A, Montaña M, Vallés I, Devesa R, Céspedes-Sánchez R, Serrano I, Blázquez S, Barjola V. 2012. Behavior of natural radionuclides in wastewater treatment plants. J Environ Radioac 109, 76-83.

Camacho A., Montaña M., Vallés I., Devesa R., Céspedes-Sánchez R., Serrano I. 2013. Temporal evolution of radionuclides in sludge from wastewater treatment plants. J Radioanal Nucl Chem. 295, 297-306.

Casacuberta N., Masqué P., Garcia-Orellana J., Bruach JM., Anguita M., Gasa J., Villa M., Hurtado S., García-Tenorio R. 2009. Journal of Hazardous Materials, 170, 814-823.

Coleman S.J., Coronado, P.R., Maxwell, R.M., Reynolds, J.G. 2003. Granulated Activated Carbon Modified with Hydrophobic Silica Aerogel-Potential Composite Materials for the Removal of Uranium from Aqueous Solutions. Environ. Sci. Technol. 37, 2286-2290.

Coll, A. 2005. Aplicacio de la distribució i migració de radionuclids naturals i artificials a l'estudi dels procesos erosius en conques hidrologiques catalanes. Tesis Doctoral. Universitat Politècnica de Catalunya (in Catalan).

CSN (Consejo de Seguridad Nuclear). 2005. Llauradó M., Vallés I., Abelairas A., Alonso A., Díaz MF., García R, de Lucas MJ., Suárez JA., Procedimientos para la determinación del índice

de actividad alfa total en muestras de agua. Métodos de coprecipitación y evaporación, Colección Informes Técnicos 11.2005, Serie Vigilancia Radiológica Ambiental (in Spanish).

CSN (Consejo de Seguridad Nuclear). 2011. Intercomparacion CSN/CIEMAT 2011. Determinación de radionúclidos naturales y artificiales en agua.

CSN (Consejo de Seguridad Nuclear). 2012. Instrucción IS-33, sobre criterios radiológicos para la protección frente a la exposición a la radiación natural (in Spanish). www.csn.es

CSN (Consejo de Seguridad Nuclear), 2012. Acuerdo específico de colaboración entre el consejo de seguridad nuclear y la universidad de Extremadura para el estudio de la problemática existente en la determinación del índice de actividad alfa total en aguas potables. Propuesta de procedimientos. Internal report (in Spanish).

Cothern CR. and Rebers PA. 1990. Radon, Radium and Uranium in Drinking Water, Lewis Publishers, Chelsea, MI.

Currie L.A. 1968. Limits for qualitative detection and quantitative determination. Application to radiochemistry. Analytica Chemistry, 40, 586-593.

Devesa R., García V., Matía Ll. 2010.Water flavour improvement by membrane (RO and EDR) treatment. Desalination 250, 113-117.

EC (European commission). Sewage Sludge, Directorate General for the Environment, EC, Brussels, http://europa.eu.int/comm/environment/sludge/index.htm. http://ec.europa.eu. (last updated: 18/09/2012).

EC (European commission). 1999. Report on radiological protection principles concerning the natural radioactivity of building materials. Radiat. Prot., vol. 112.

EC (European commission). 2000. Radiological Impact due to wastes containing radionuclides from use and treatment of water. Report EUR 19255.

EC (European commission). 2001. Practical Use of the Concepts of Clearance and Exemption-Part II. Application of the Concepts of Exemption and Clearance to Natural Radiation Sources. Radiat. Prot., vol. 122. ISBN 92-894-3315-9.

EC (European commission). 2012. Interlaboratory comparison on gross alpha/beta activity measurement in drinking waters.

Ehmann W. D. and Vance D. E. 1991. Radiochemistry and Nuclear Methods of Analysis, Wiley, New York.

Eichrom (Eichrom Technologies, LLC). 2001. Method ACW02, Rev. 1.3: Uranium in Water. 8205 S. Cass Ave., Suite 106, Darien, IL 60561.

EPA U.S. (Environmental Protection Agency) 600/4-80-032. 1980. Prescribed procedures for measurement of radioactivity in drinking water. Gross alpha and gross beta radioactivity in drinking water, Method 900.0, Environmental Protection Agency.

EPA U.S. (Environmental Protection Agency) 520/5-84-006,00-02. 1984. Radiochemistry procedures manual. Radiochemical determination of gross alpha activity in drinking water by co-precipitation. Montgomery, AL: Eastern Environmental Radiation Facility.

EPA U.S. (Environmental Protection Agency). 1990. Suggested Guidelines for the Disposal of Drinking Water Treatment Wastes Containing Naturally-occurring Radionuclides, USEPA,Washington, DC.

EPA U.S. (Environmental Protection Agency). 1994., Radioactive Waste Disposal. An Environmental Perspective, Rep. EPA-402-K-94-001, USEPA,Washington, DC.

EPA U.S. (Environmental Protection Agency). 1997. National Primary Drinking Water Regulations: Analytical Methods for Radionuclides; Final Rule and Proposed Rule. 40 CFR Part 141. FR 62, 10168–10175.

EPA U.S. (Environmental Protection Agency). 1998. Small System Compliance Technology List for the Non-Microbial Contaminants Regulated Before 1996. EPA 815-R-98-002.

EPA U.S. (Environmental Protection Agency). 2000. National drinking water regulations: Radionuclides. Final Rule. Federal Register, 65 FR, 76708-76753.

EPA U.S. (Environmental Protection Agency). 2004. ISCORS Assessment of Radioactivity in Sewage Sludge: Recommendations on Management of Radioactive Materials in Sewage Sludge and Ash at Publicly Owned Treatment Works. EPA 832-R-03-002B.

Erlandsson, B., Ingemansson, T., Mattsson, S., 1983. Comparative studies of radionuclides from global fallout and local sources in ground level air and sewage sludge. Water, air, soil Poll. 20, 331-346.

Erlandsson B., Bjurman B. and Mattsson S. 1989. Calculation of radionuclide ground deposition by means of measurements on sewage. Water, Air, & Soil Pollution. 45, 3-4, 329-344.

EURACHEM. 1998. The Fitness for Purpose of Analytical Methods. A Laboratory Guide to Method Validation and Related Topics.

European Council Directive 96/29, 13-May 1996. "Laying down basic safety standards for the protection of the health of workers and the general public against the dangers arising from ionizing radiation".

Favre-Réguillon A., Lebuzit G., Murat D., Foos J., Mansour C. and Draye M. 2008. Selective removal of dissolved uranium in drinking water by nanofiltration. Water Research, 42, 1160-1166.

Fernández-Turiel, JL., Llorens JF., Roig, A., Carnicero, M., Valero, F. 2000. Monitoring of drinking water treatment plants using ICP-MS. Toxicol. Environ. Chem. 74, 87-103.

Gäfvert T., Ellmark C., Holm E. 2002. Removal of radionuclides at a waterworks. J. Environ. Radioact. 63, 105-115.

Goldin AS. 1961. Determination of dissolved radium. Anal Chem. 33:406-409.

González-Gómez C., Azahra M., López-Peñalver J.J., Camacho A., Bardouni T.El., Boukhal H. 2006. Seasonal variability

Hallstadius, L. 1984. A method for the electrodeposition of actinides. Nuclear Instruments and Methods in Nuclear Research 223, 266-267.

Hansen C. 2004. Uranium removal vital to public health. Environmental Science and Engineering Magazine. (http:/www.esemag.com/0904/uranium.html, last accessed: 27/12/2011).

Hofmann J., Leicht R., Wingender HJ., Wörner J. 2000. Radiological impact due to wastes containing radionuclides from the use and treatment of drinking water, Directorate General Environment, Rep. EUR 19255, European Commission, Luxembourg, 88 pp.

Huikuri P., Salonen L., Raff, O. 1998. Removal of natural radionuclides from drinking water by point of entry reverse osmosis. Desalination 119, 235-239.

IAEA (International Atomic Energy Agency). 2003 Technical Reports Series No.419. Extent of environmental contamination by naturally occurring radioactive material (NORM) and technological options for mitigation. Vienna, Austria.

IAEA (International Atomic Energy Agency).. 2008. IAEA-CU-2008-03, world-wide open proficiency test on the determination of natural radionuclides in phosphogypsum and spiked water and spiked water. http://nucleus.iaea.org/rpst/.

IAEA (International Atomic Energy Agency). 2010. IAEA-CU-2010-03, 2010.World-wide Open Proficiency Test on the Determination of Natural Radionuclides inWater and Ra-226 in Soil. http://nucleus.iaea.org/rpst/.

Imhoff KR., Koppe P., Dietz F., 1988. Investigations on the concentration of radionuclides in sewage sludges of Ruhrverband wastewater treatment plants 1960 through to 1986. Water. Res. 22, 8, 1059-1067.

INSINUME 2012. 6th International symposium on in situ nuclear metrology as a tool for radioecology. Brussels, Belgium. www.insinume2012.com

Ioannidou A., Papastefanou C. 2006. Precipitation scavenging of [7]Be and ^{137}Cs radionuclides in air. J. Environmental Radioactivity 85, 121-136.

Ipek, U., Arslan, E.I., Aslan, S., Drogu, M., Baykara, O., 2004. Radioactivity in Municipal Wastewater and Its behavior in Biological Treatment. B. Environ. Contam. Tox.72, 319-325.

ISO/IEC 8402. 1994. Quality management and quality assurance. Vocabulary. International organization for Standardization.

ISO/IEC 17025, 2005. General Requirements for the Competence of Testing and Calibration Laboratories. International organization for Standardization.

Jelic A., Gros M., Ginebreda A., Cespedes-Sanchez R., Ventura F., Petrovic M., Barcelo D., 2011. Occurrence, partition and removal of pharmaceuticals in sewage water and sludge during wastewater treatment. Water Res. 45, 1165-1176.

Jibiri NN., Alausa SK., Farai IP. 2009. Radiological hazard indices due to activity concentrations of natural radionuclides in farm soils from two high background radiation areas in Nigeria. Int JLow Radiat. 6(2), 79-95.

Jibiri, N.N., Okeyode I.C. 2012. Evaluation of radiological hazards in the sediments of Ogun river, south-Western Nigeria. Radiation Physics and Chemistry, 81, 103-112.

Jiménez A., De la Montaña Rufo M. 2002. Effect of water purification on its radioactive content. Water Research 36, 1715-1724.

Jiménez F., Deban L., Pardo R., López R., García-Talavera M., 2011. Levels of ^{131}I and six natural radionuclides in sludge from the sewage treatment plant of Valladolid, Spain. Water, air, soil, pollut. 217, 515-521.

Jobbágy V., Wätjen U., Meresova J., 2010. Current status of gross alpha/beta activity analysis in water samples: a short overview of methods. J. Radioanalytical Nucl. Chem. 286, 393-399.

Jury Ayub J., Di Gregorio D.E., Velasco H., Huck H., Rizzotto M., Lohaiza F. 2009. Short-term seasonal variability in ^{7}Be deposition in a semiarid ecosystem of central Argentina. Journal of Environmental Radioactivity, 100, 977-981.

Khan Hasan M., Ismail M., Khan Khalid, Akhter Perveen. 2011. Measurement of radionuclides and gamma-ray dose rate in soil and transfer of radionuclides from soil to vegetation, vegetable of some Northern area of Pakistan using gamma-ray spectrometry. Water Air Soil Pollut. 219, 129-142.

Kleinschmidt R., Akber R. 2008. Naturally occurring radionuclides in materials derived from urban water treatment plants in sout-heast Queensland, Australia Journal of Environmental Radioactivity, 99, 607-620.

Kryvoruchko A.P., Yurlova L.Y., Atamanenko I.D., Kornilovich B.Y. 2004 Ultrafiltration removal of U(VI) from contaminated water. Desalination. 162, 229-236.

Landa ER, Le AH, Luck RL, Yeich PJ. 1995. Sorption and coprecipitation of trace concentrations of thorium with various minerals under conditions simulating an acid uranium mill effluent environment. Inorg Chim Acta 229;1/2:247–252.

Llauradó, M. 1990. Estudi per espectrometria gamma d'alta resolució de l'effecte de l'accident de la central nuclear de Txernòbil a Catalunya. Tesi Doctoral. Universitat de Barcelona (in Catalan).

Martin J. E., Fenner F. D., 1997. Radioactivity in municipal sewage and sludge. Public Health Rep. Jul–Aug; 112, 4, 308–318.

Martín Sánchez A., Sáenz García G., Jurado Vargas M. 2009. Study of self-absorption for the determination of gross alpha and beta activities in water and soil samples. Appl. Radiat. Isot. 67, 817-820.

Miller, W., Kuzne F., Banerji, S., Yu-Chu Li, Graham, C., 1996. The determination of radioisotope levels in municipal sewage sludge. Health Phys. 71, 3, 286-289.

Montaña M., Camacho A., Devesa R., Vallés I., Céspedes R., Serrano I., Blázquez S., Barjola V., 2011. The presence of radionuclides in wastewater treatment plants in Spain and their effect on human health. J. Cle. Pro. doi: 10.1016/j.jclepro.2011.07.007.

Montaña M., Camacho A., Serrano I., Vallés I. 2012. Experimental analysis of the mass efficiency curve for gross alpha activity and morphological study of the residue obtained by the co-precipitation method. Appl. Radiat. Isot. 70, 1541-1548.

Montaña M., Fons J., Corbacho J.A., Camacho A., Zapata-García D., Guillén J., Serrano I., Tent J., Baeza A., Llauradó M, Vallés I. 2013a. A comparative experimental study of gross alpha methods in natural waters. J Environ Radioact. 118, 1-8.

Montaña M., Camacho A, Serrano I, Devesa R, Matia L, Valles I. 2013b. Removal of radionuclides in drinking water by membrane treatment using ultrafiltration, reverse osmosis and electrodialysis reversal. J Environ Radioact. doi: 10.1016/j.jenvrad.2013.01.010.

OECD Nuclear Energy Agency. 1979. Exposure to Radiation from Natural Radioactivity in Building Materials. Report by NEA Group of Experts (Paris: OECD).

Ortega X., Vallés I., Serrano I. 1996. Natural radioactivity in drinking water in Catalonia (SPAIN). Environmental International, 22 (1), S347-S354.

Outola I., Nour S., Kurosaki H., Inn K., La Rosa J., Lucas L., Volkovitsky P. and Koepenick K. 2008. Investigation of radioactivity in selected drinking water samples from Maryland. Journal of Radioanalytical and Nuclear Chemistry, 277 (1), 155-159.

Palomo M., Peñalver A., Aguilar C., Borrull F., 2010a. Radioactivity evaluation of Ebro river water and sludge treated in a potable water treatment plant located in the South of Catalonia (Spain). Applied Radiation and Isotopes 68, 474-480.

Palomo, M., Peñalver, A., Aguilar, C., Borrull, F., 2010b. Presence of naturally occurring radioactive materials in sludge samples from several Spanish water treatment plants. J.Hazard. Mater. 181, 716-721.

Parsa B, Nemeth WK, Obed RN. 2000. The role of radon progenies in influencing gross alpha-particle determination in drinking water. Radioact Radiochem 11, 11–22.

Parsa B., Obed RN., Nemeth,WK., Suozzo GP. 2005. Determination of gross alpha, Ra-224, Ra-226 and Ra-228 activities in drinking water using a single sample preparation procedure. Health Phys. 89 (6), 660-666.

Parsa B., Henitz J.B., Carter JA. 2011. Rapid screening and analysis of alpha and gamma emiting radionuclides in liquids using a single sample preparation procedure. Health Phys. 100 (2), 152-159.

Puhakainen, M., 1998. Detection of radionuclides in sewage water and sludge. Radiochemistry. 40, 529-533.

Quindós LS, Fernández PL, Soto J, Ródenas C, Gómez J. 1994. Natural radioactivity in Spanish soils. Health Physics, 66 (2):194-200.

Raff, O., Wilken, R.-D., 1999. Removal of dissolved uranium by nanofiltration. Desalination 122, 147–150.

Real Decreto (Royal Decree) 783/2001 de 6 de julio, 2001. Reglamento sobre protección sanitaria contra radiaciones ionizantes. B.O.E., Boletin Oficial del Estado (Official Bulletin of the State) 178, 27284e27393. Madrid, Spain.

Real Decreto (Royal Decree) 140/2003 de 7 de febrero, 2003. Criterios sanitarios de la calidad del agua de consumo humano. B.O.E., Boletin Oficial del Estado (Official Bulletin of the State) 45, 7228e7245. Madrid, Spain.

Real Decreto (Royal Decree) 1439/2010 de 5 de noviembre, 2010. Modificación del Reglamento sobre protección sanitaria contra radiaciones ionizantes, aprobado por el Real Decreto 783/2001 de 6 de Julio. B.O.E., Boletin Oficial del Estado (Official Bulletin of the State) 279, 96395e96398. Madrid, Spain.

Retallack, M.M.T., Hart, W., Gagnon, G., 2007. Life cycle management on onsite wastewater treatment contaminants of concern: a case study review. In Proc. of IWA Specialist Conference: Moving Forward Wastewater Biosolids Sustainability: Technical, Managerial, and Public Synergy, June 24-27, Moncton, New Brunswick, Canada, 981-987.

Rodriguez C., Devine B., Cook A., Weinstein P., Buynder P. van, 2009. Gross alpha and gross beta particle activity in recycled water for augmentation of drinking water supplies. J. Water Sup.: Research and Technology-AQUA 58.3 191-202.

Ruberu, Shiyamalie R., Liu Yun-Gang, Perera S Kusum. 2005. Occurrence of Ra-224, Ra-226 and Ra-228, Gross alpha, and uranium in California groundwater. Health Physics, 89 (6):667-678.

Salas, A. 2005. Estudio de la eficiencia de eliminación de radionúclidos naturals en procesos compatibles con el de potablilización de aguas. Doctoral Thesis. Universidad de Extremadura, Cáceres (in Spanish).

Saito, K., N. Petoussi, M. Zanki, 1990. Calculation of organ doses from environmental gamma rays using human phantoms and Monte Carlo methods. Part 1. Monoenergetic sources of natural radionuclides in the ground, GSF-B2/90.

Salonen L. 2006. Alpha/Beta Liquid Scintillation Spectrometry in Surveying Finnish Groundwater Samples. Radiochemistry, 48, 6, 606–612.

Semkow TM., Bari A., Parekh PP., Haines DK., Gao H., Bolden AN., Dahms K.S., Thern RE., Velazquez S. 2004. Experimental investigation of mass efficiency curve for alpha radioactivity counting using a gas-proportional detector. Applied Radiation and Isotopes, 60, 879-886.

Sill CW., Williams RL. 1969. Radiochemical determination of uranium and transuranium elements in process solutions and environmental samples. Anal Chem 41, 1624-1632.

Smith, J.T. Voitsekhovitch, O.V.; Hakanson, L. and Hilton, J. 2001. A critical review of measures to reduce radioactive doses from drinking water and consumption of freshwater foodstuffs. J. Environ. Radioactiv. 56, 11-32.

Sorg, TJ., 1990. Removal of uranium from drinking water by conventional treatment methods. in: Cothern, C.R., Rebers, P.A. (Eds.), Radon, radium and uranium in drinking water.. Lewis Publishers, Chelsea, MI. pp. 173-191.

Stetar EA, Boston, HL., Larsen, IL., Mobley, MH., 1993. The removal of radioactive cobalt, cesium, and iodine in a conventional municipal wastewater treatment plant. Water Environ Res. 65, 5, 630-639.

Suárez-Navarro JA., Pujol Ll., de Pablo MA., 2002. Rapid determination of gross alpha-activity in sea water by co-precipitation. J. Radioanalytical Nucl. Chem. 253 (1), 47-52.

Suárez-Navarro J.A. 2009. Investigación y procedimientos radioquímicos para la determinación de los principales emisores alfa en agua para su implementación en una red de vigilancia radiológica ambiental. Doctoral Thesis (in Spanish).

Sundell-Bergman, S., de la Cruz, I., Avila, R., Hasselblad, S., 2008. A new approach to assessment and management of the impact from medical liquid radioactive waste. J. Environ. Radioactiv. 99, 1572-1577.

Teijón G., Candela L., Tamoh K., Molina-Díaz A., Fernández-Alba A.R., 2010. Occurrence of emerging contaminants, priority substances (2008/10//CE) and heavy metals in treated wastewater and groundwater at Depurbaix. Sci. Total Environ. 408, 3584-3595.

UNE 73311-4:2002 (Spanish standard). 2002. Determination of the total beta activity index in water by means of a proportional meter.

UNE 73340-2: 2003 (Spanish standard). Determination of the Beta Rest in water by proportional counter (in Spanish).

UNSCEAR, United nations Scientific Committee on Effects of Atomic radiation (UNSCEAR). 2000. Sources and effects of ionizing radiation, United Nations, New York.

U.S. Department of Energy. Method Po-02-RC, Polonium in Water Vegetation, Soil, and Air Filters, Environmental Measurements Laboratory Procedures Manual, 27 ed., vol. 1, Environmental Measurements Laboratory, U.S. Department of Energy, 376 Hudson St., New York, NY.

Vallés, I. 1994. Development of the analytical procedures to measure the radioactivity in waters and its application to drinking water. Doctoral thesis, pp. 52-84 (in Spanish). University of Barcelona. Barcelona, Spain.

Vallés I, Devesa R, Ortega X, Matía L, Serrano I, Camacho A. 2007. Estudio de la radioactividad en las aguas de abastecimiento de Barcelona en el periodo 1995 a 2005. Radioproteccion, 53, XIV, 282-286. Número especial - XI Congreso Nacional de la Sociedad Española de Protección Radiológica.

Van der Bruggen B. and Van der Casteele C., 2003. Removal of pollutants from surface water and groundwater by nanofiltration overview of possible applications in the drinking water industry. Environ. Pollut. 122, 435–445.

WHO (World Health Organization). 2011. Chapter 9: Radiological aspects. In: Guidelines for Drinking-Water Quality, 4th edition. ISBN 978 92 4 154815 1.

Weast RC. 1976. CRC Handbook of Chemistry and Physics, 57th ed. CRC Press, Boca Raton, Florida.

Whitaker EL. 1986. Project Summary: Test Procedure for Gross Alpha particle Activity in Drinking water: Interlaboratory Collaborative Study. EPA/600/S4-86/027.

Wisser, S. 2003. Balancing Natural Radionuclides in Drinking Water Supply. Doctoral Thesis. Johannes Gutenberg-University, Mainz, Germany.

Zapata-García, D., Llauradó, M., Rauret, G., 2012. The implications of particle energy and acidic media on gross alpha and gross beta determination using liquid scintillation. Appl. Radiat. Isotopes, 70, 705–711.